

# Signaling Pathways in Cancer: a Matter of Dosage

Cláudia  
Gaspar



# Signaling Pathways in Cancer: a Matter of Dosage

Signaal transductie in kanker: een kwestie van dosering

## Thesis

to obtain the degree of Doctor from the  
Erasmus University Rotterdam  
by command of the  
rector magnificus

Prof.dr. S.W.J. Lamberts

and in accordance with the decision of the Doctorate Board

The public defence shall be held on

thursday 26 february 2009 at 13.30 hrs

by

Cláudia Sofia Cardoso Gaspar  
born in Lisbon, Portugal



## Doctoral Committee

**Promotor:** Prof.dr. Riccardo Fodde

**Other members:** Dr.ir. G.W. Jenster  
Prof.dr. C.P. Verrijzer  
Prof.dr. J.P.T.M. van Leeuwen

These studies were supported by grants from:

Dutch Cancer Society (KWF)  
Netherlands Organization for Scientific Research (NWO)  
BSIK Innovation programme “Stem Cells in Development and Disease” (SCDD, BSIK 03038).  
EUFP6 Migrating Cancer Stem Cells program (MCSCs)  
Association for International Cancer Research (AICR)

## Financial Support by:

SCDD for the publication of this thesis is gratefully acknowledged;  
ErasmusMC;  
Josephine Nefkens Institute.



## Signaling Pathways in Cancer: a Matter of Dosage

**Author:** Cláudia Gaspar  
**Printed:** Ipskamp Drukkers  
**Layout:** Luís Martins

**ISBN/EAN:** 978-90-9023985-9



# Contents

<b>Aims and Outline</b>	<b>7</b>
<b>Chapter 1</b>	<b>9</b>
APC dosage effects in tumorigenesis and stem cell differentiation. Int J Dev Biol. 2004;48(5-6):377-86.	
<b>Chapter 2</b>	<b>21</b>
Apc modulates embryonic stem-cell differentiation by controlling the dosage of beta-catenin signaling. Nat Genet. 2002 Dec;32(4):594-605.	
<b>Chapter 3</b>	<b>35</b>
Wnt dosage-dependent transcriptional responses in embryonic stem cells. Manuscript in preparation.	
<b>Chapter 4</b>	<b>51</b>
A Specific $\beta$ -catenin signaling dosage underlies cancer stemness and metastatic behavior in Apc-driven tumorigenesis. Manuscript in preparation.	
<b>Chapter 5</b>	<b>93</b>
Cross-species comparison of human and mouse intestinal polyps reveals conserved mechanisms in adenomatous polyposis coli (APC)-driven tumorigenesis. Am J Pathol. 2008 May;172(5):1363-80.	
<b>Chapter 6</b>	<b>113</b>
Smad4 haploinsufficiency: a matter of dosage. Pathogenetics. 2008 Nov 3;1(1):2.	
<b>Chapter 7</b>	<b>131</b>
Discussion	
<b>Summary and Samenvatting</b>	<b>149</b>
Summary Samenvatting	
<b>Acknowledgements</b>	<b>155</b>
<b>Curriculum Vitae</b>	<b>159</b>
<b>PhD Portfolio</b>	<b>165</b>



## Outline of the thesis

The main issue addressed in this thesis is how different levels of signaling activity of the Wnt and TGF- $\beta$ /BMP pathways can affect transcriptional responses in particular relevant for self-renewal and differentiation both in homeostasis and in cancer.

**Chapter 1** presents an overview of the existent literature leading to the formulation of the hypothesis that Apc/Wnt pathway acts in a dosage-dependent manner both in normal and neoplastic tissues.

In **Chapter 2** we employ a series of embryonic stem cells carrying homozygous and compound heterozygous hypomorphic mutations at the *Apc* locus resulting into a range of different levels of Wnt signaling activity. We report the dosage-dependent correlation between Wnt signaling and cellular differentiation. Expression profiling was used to characterize the molecular events underlying the differentiation defects and to establish a dose dependent transcriptional response. In **Chapter 3**, a similar analysis of undifferentiated embryonic stem cells reveals the same trend in dose dependent transcriptional effect.

A newly targeted mutation in the *Apc* tumor suppressor gene obtained by introducing a stop cassette at codon 1572 is described in **Chapter 4**. The intermediate level of Wnt activity encoded by this allele and its milder differentiation defect is addressed by the analysis of *Apc*<sup>1572I/1572I</sup> homozygous embryonic stem cells. Unexpectedly, *Apc*<sup>+/1572I</sup> mice show no predisposition to intestinal tumorigenesis but are characterized by the development of mammary adenocarcinomas that spontaneously metastasize to the lungs. The isolation and characterization of cancer stem cells (CSCs) from *Apc*<sup>+/1572I</sup> mammary adenocarcinomas reveals a role for the intracellular accumulation of  $\beta$ -catenin in tumor initiation and malignant behavior. Genome-wide expression analysis of mammary CSCs compared with their normal counterparts lay the basis for the elucidation of the molecular mechanisms underlying stemness in homeostasis and cancer in the mouse mammary gland.

In man, familial adenomatous polyposis (FAP) and most of the sporadic forms of colon cancer are caused by mutations in the *APC* gene resulting in the constitutive activation of the Wnt signaling pathway. In **Chapter 5** we address the transcriptional response

underlying this initial and rate-limiting event in intestinal tumorigenesis by using a large cohort of human colonic adenomatous polyps from FAP patients with germline *APC* mutations. Cross-species comparison between human and mouse (*Apc*<sup>+/1638N</sup>) intestinal tumors identifies evolutionary conserved genes thought to be relevant for tumorigenesis. The validity of the newly generated cross-species signature is further demonstrated by its ability to resolve FAP adenomas from those caused by germline mutations in the *MYH* gene (MAP, *MYH* associated polyposis).

Germline mutations in the tumor suppressor *SMAD4*, an integral component of the TGF- $\beta$  and BMP signaling pathways, are associated with juvenile polyposis syndrome (JPS). In **Chapter 6**, we show that haploinsufficiency at the *SMAD4* locus earmarks polyp formation in a proportion of JPS patients as shown by the retention of the wild type allele in the nascent polyps. The molecular effects elicited by haploinsufficiency are evaluated in a set of embryonic stem cells homozygous and heterozygous for the *Smad4*<sup>Sad</sup> allele. We report a reduction in expression of the Smad4 protein accompanied by decrease in TGF- $\beta$  and BMP signaling transduction pathways. Expression profiling reveals a set of dosage-dependent target genes whose regulation is further confirmed on mouse intestinal tissues from *Smad4*<sup>+/Sad</sup> mice further highlighting their relevance in the initial steps of the tumorigenic process.



***APC* dosage effects in tumorigenesis  
and stem cell differentiation**

# Chapter 1

Claudia Gaspar and Riccardo Fodde

■ Int J Dev Biol. 2004;48(5-6):377-86.



# APC dosage effects in tumorigenesis and stem cell differentiation

CLAUDIA GASPAR and RICCARDO FODDE\*

Dept. of Pathology, Josephine Nefkens Institute, Erasmus University Medical Center, Rotterdam, The Netherlands

**ABSTRACT** It is well established that concentration gradients of signaling molecules (the so-called "morphogens") organize and pattern tissues in developing animals. In particular, studies in *Drosophila* and different vertebrates have shown that gradients of the Wnt, Hedgehog (Hh) and transforming growth factor-beta (TGF- $\beta$ ) families of morphogens play critical roles in limb patterning. Morphogens are often expressed in organizing centres and can act over a long range to coordinate the patterning of an entire field of cells. These observations imply that exposure to different concentrations of these diffusible factors may trigger differential cellular responses. In order to study these dosage-dependent Wnt/ $\beta$ -catenin signaling effects, we have generated several hypomorphic mutant alleles at the mouse *Apc* locus and studied their cellular and phenotypic outcomes in stem cell renewal and differentiation, and in tumorigenesis. The results clearly show that *Apc* mutations differentially affect the capacity of stem cells to differentiate in a dosage-dependent fashion. Likewise, different *Apc* mutations (and the corresponding Wnt signaling dosages) confer different degrees of susceptibility to tumorigenesis in the corresponding mouse models. These results have implications for the understanding of the molecular and cellular basis of tumor initiation by defects in the Wnt pathway. We propose a model in which adult somatic stem cell compartments are characterized by tissue-specific  $\beta$ -catenin threshold levels for cell proliferation, differentiation and apoptosis. Different *APC* mutations will result in different levels of  $\beta$ -catenin signaling, thus conferring different degrees of tumor susceptibility in different tissues. Hence,  $\beta$ -catenin dosage - dependent effects may not only explain how a single pathway is involved in the development and homeostasis of different tissues, but also its pleiotrophic role in tumorigenesis.

**KEY WORDS:** *Wnt*, *APC*, development, differentiation, colorectal tumorigenesis, dosage

## APC, Wnt signalling and colorectal cancer

In 1991 different research laboratories in the US and Japan isolated the adenomatous polyposis coli (*APC*) gene on chromosome 5q22 and identified *APC* germline mutations in patients affected by Familial Adenomatous Polyposis (FAP), an hereditary colorectal cancer syndrome characterized by the presence of hundreds to thousands of polyps in the colon and rectum (Grodén *et al.*, 1991, Joslyn *et al.*, 1991, Kinzler *et al.*, 1991, Nishisho *et al.*, 1991). Even more importantly, *APC* was subsequently found to be mutated in the majority of sporadic colorectal cancers notwithstanding the histological stage of the neoplastic lesions analyzed (Miyoshi *et al.*, 1992, Powell *et al.*, 1992, Smith *et al.*, 1993). Thus, *APC* mutations represent one of the earliest event in the adenoma carcinoma sequence (Kinzler and Vogelstein 1996). Mutation analysis of the *APC* gene in sporadic and FAP polyps showed that both alleles are mutated in the majority of the cases (Ichii *et al.*, 1993, Levy *et al.*, 1994), in

agreement with Knudson's two hit model of tumorigenesis for tumor suppressor genes (Knudson 1971).

During the last decade, several functional studies have been conducted on the *APC* gene and its protein product, especially aimed at the identification of its main tumor suppressing function (Polakis 2000, Fodde *et al.*, 2001). Notably, these studies have shown APC's involvement in a wide variety of cellular processes such as cell cycle regulation, apoptosis, cell adhesion and migration, microtubule assembly, cell fate determination and chromosomal stability (Fodde 2003). This multi-functionality is reflected by the presence of a large number of specific motifs and domains along the 312 kDa APC protein (Fig. 1). However, biochemical and genetic evidence was provided showing that APC's main suppressor

*Abbreviations used in this paper:* APC, Adenomatous Polyposis Coli; CRC, Colorectal Cancer; ES, Embryonic Stem; FAP, Familial Adenomatous Polyposis; Hh, hedgehog gene; TGF, transforming growth factor.

\*Address correspondence to: Dr. Riccardo Fodde. Dept. of Pathology, Josephine Nefkens Institute, Erasmus University Medical Center, P.O. Box 1738, 3000 DR Rotterdam, The Netherlands. Fax: +31-10-408-8450. e-mail: r.fodde@erasmusmc.nl



activity resides in its ability to bind to and down-regulate  $\beta$ -catenin (Korinek *et al.*, 1997, Morin *et al.*, 1997, Smits *et al.*, 1999).  $\beta$ -catenin is a key player in the formation of adherens junctions of mammalian epithelia through its binding with the cell adhesion molecule E-cadherin. Moreover, it represents the central signaling molecule within the WNT signal transduction pathway.

Three different functional domains within APC allows it to regulate  $\beta$ -catenin in the cell: three 15 a.a. repeats bind  $\beta$ -catenin, whereas seven 20 a.a. motifs and three SAMP repeats (Ser-Ala-Met-Pro) trigger its down-regulation through the formation of the so-called destruction complex together with the scaffold proteins axin and conductin, and the glycogen synthase kinase  $3\beta$  (GSK3 $\beta$ ) (Rubinfeld *et al.*, 1993, Su *et al.*, 1993, Behrens *et al.*, 1998). In the absence of the WNT signal, the destruction complex is assembled and GSK3 $\beta$  phosphorylates four critical Ser/Thr residues in  $\beta$ -catenin. This targets  $\beta$ -catenin for ubiquitination and subsequent proteasomal degradation (Rubinfeld *et al.*, 1996, Aberle *et al.*, 1997, Behrens *et al.*, 1998, Hart *et al.*, 1998). Extracellular ligands of the WNT family bind to the transmembrane receptor frizzled and the co-receptor lipoprotein-related proteins 5 and 6 (LRP-5/6) thus inactivating GSK3 $\beta$  in the destruction complex. This inactivation process is not well understood but involves the intracellular protein Dishevelled. As a consequence,  $\beta$ -catenin becomes stabilized, accumulates in the cytoplasm and is eventually shuttled to the nucleus where it binds to DNA-binding proteins of the T-cell factor (TCF/LEF) family, to serve as an essential co-activator of transcription (Behrens *et al.*, 1996, Molenaar *et al.*, 1996).

WNT signaling is tightly controlled by a number of regulators at different steps of the signal transduction cascade. Dickkopf1 and dickkopf2 have been identified as extracellular proteins that modulate the pathway in a positive and negative fashion, respectively (Wu *et al.*, 2000, Semenov *et al.*, 2001). Also, the activity of TCF is tightly controlled at the nuclear level, as TCFs can complex with co repressors such as groucho and chibby (Cavallo *et al.*, 1998, Takemaru *et al.*, 2003).

The WNT pathway is nowadays recognized to function in a variety of critical biological processes such as embryonic development, cell polarity and cell fate specification (Cadigan and Nusse 1997). Moreover, a large body of experimental evidence collected over the past decades clearly pinpoints its role in tumorigenesis. Loss of *APC* function or oncogenic  $\beta$ -catenin

activation (Morin *et al.*, 1997, Sparks *et al.*, 1998) results in uncontrolled signaling and activation of downstream target genes. The first two identified downstream target genes of the APC/ $\beta$ -catenin pathway, *c-MYC* and cyclin D1, are clearly relevant in tumor formation because of their role in proliferation, apoptosis and cell-cycle progression (He *et al.*, 1998, Shtutman *et al.*, 1999, Tetsu and McCormick 1999). Changes in the normal expression pattern of these genes are likely to increase the overall proliferation rate. Other WNT target genes, such as matrilysin (Brabletz *et al.*, 1999, Crawford *et al.*, 1999), *CD44* (Wielenga *et al.*, 1999), and *MYC* itself (Brabletz *et al.*, 2000), appear more likely to play a role in tumor promotion rather than initiation.

(see also <http://www.stanford.edu/~russe/pathways/targets.html>).

Here, rather than presenting a comprehensive overview of the different members of the WNT pathway and the WNT downstream target genes thought to play key roles in homeostasis and cancer, we will discuss the issue of dosage of APC/ $\beta$ -catenin signaling and how it can affect stem cell renewal and differentiation during development and tumorigenesis. Though well known to cause not only developmental defects in model organisms but also inherited disorders in man, gene dosage effects have been overlooked in tumor biology. Cell proliferation, differentiation and apoptosis are modulated by gradients of WNT morphogens during development and in the adult organism. Hypomorphic alleles at tumor suppressor genes like *APC* are likely to cause WNT signaling dosage fluctuations below tissue-specific thresholds thus interfering with the control of fundamental cellular processes which either directly trigger tumorigenesis or modify the cellular environment so that additional mutations and/or epigenetic changes at other genes can successfully promote tumor growth.

### APC dosage effects in tumorigenesis

As mentioned above, familial adenomatous polyposis is due to germline APC mutations that predict the truncation of the protein. A large number of different nonsense, frameshift, and splice site mutations spread throughout the *APC* gene have been characterized among FAP patients. This broad mutation spectrum is reflected by the clinical heterogeneity of the FAP phenotype: large variability of age of onset, polyp multiplicity and distribution along the GI tract, number and type of extra-colonic manifestations

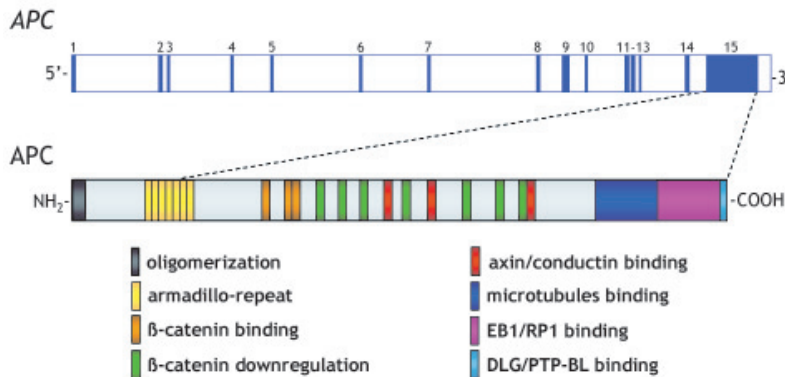
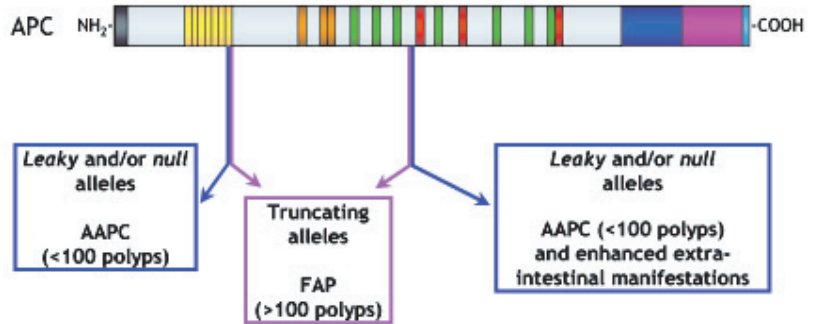


**Fig. 1. Schematic representation of the APC tumor suppressor.** Upper bar shows the APC gene characterized by 15 exons. Exon 15 is the largest (6.6 kb) and encodes most of the protein's main functional domains. Along the APC protein (lower bar), conserved regions, such as the armadillo repeats, and regions that interact with other proteins, including tubulin, the microtubule-associated protein EB1, discs large (DLG),  $\beta$ -catenin and axin/conductin, are shown.

**Fig. 2. Human genotype-phenotype correlations at the APC gene.**

Summary of the relationship between site of the APC mutations, their consequences for the stability of the corresponding truncated proteins, and the FAP clinical features (polyp multiplicity and extra-colonic manifestations). In general, mutations located close to the 5' end and in the 3' half of the gene (beyond codon 1600) result in unstable mRNAs and/or polypeptides, and a mild and variable FAP phenotype, termed attenuated adenomatous polyposis coli (AAPC). Consistent correlations between germline mutations at the 3' half of the APC gene and FAP extra-intestinal manifestations such as desmoid tumors, CHRPE's and osteomas have also been reported (Fodde and Khan, 1995). Mutations in the central part of the gene (codon 450-1450) result in *in vivo* stably truncated APC proteins and in classical FAP phenotypes characterized by early onset and high polyp multiplicity (>100 and up to several thousands) in the large bowel (Fodde and Khan 1995, Fodde et al., 1999).



has been reported among different FAP families. This combination of genetic and phenotypic heterogeneity has allowed the establishment of genotype-phenotype correlations (Fodde and Khan 1995) (Fig. 2). In general, mutations that lead to the expression of an *in vivo* stably truncated APC protein result in classical FAP phenotypes characterized by early onset and high polyp multiplicity (>100 and up to several thousands) in the large bowel. On the other hand, truncating APC mutations which, due to the instability of the corresponding mRNAs and/or proteins, do not lead to the expression of stably truncated polypeptides are often associated with atypical or attenuated forms of FAP often characterized by delayed age of onset, lower tumor multiplicity and enhanced extra-colonic manifestations (Fodde and Khan 1995). However, the observed FAP intra-familial phenotypic variability, presumably due to genetic and environmental modifiers, does not allow the establishment of more precise cause-effect correlations between different dosages of WNT signaling and their phenotypic outcomes. The generation and analysis of mouse models carrying different *Apc* mutations in the same inbred genetic background and in controlled environmental (dietary) conditions, have been instrumental to our understanding of the mechanisms underlying multi-organ tumorigenesis due to uncontrolled WNT signaling (Fodde and Smits 2001) (Fig. 3).

The *Apc<sup>Min</sup>* mouse model is due to an A to T transversion resulting in a nonsense mutation at codon 850. Heterozygous *Apc<sup>+/Min</sup>* mice display a severe intestinal phenotype with more than 100 upper GI tumors in the C57BL/6J (B6) genetic background (Su et al., 1992). The wild-type *Apc* allele is lost together with the entire chromosome 18 in almost 100% of the lesions (Levy et al., 1994). Furthermore, *Apc<sup>+/Min</sup>* mice have a low penetrance of extracolonic-manifestations such as mammary tumors, desmoids or cysts (Moser et al., 1993, Smits et al., 1998, Halberg et al., 2000). Homozygosity for this mutation leads to embryonic lethality at very early stages of gestation (6.5 dpc) (Moser et al., 1995). Accordingly, a similar mouse model, *Apc<sup>Δ716</sup>*, carrying a targeted truncation mutation at codon 716 is also characterized by multiple intestinal tumors and no extra-intestinal manifestations (Oshima et al., 1995). Both *Apc<sup>Min</sup>* and *Apc<sup>Δ716</sup>* mutations result in stable truncated Apc proteins retaining the N-terminal oligodimerization and Arm domains but are deprived of all the β-catenin binding and down-regulation domains.

In the past years, our laboratory has generated different FAP mouse models due to hypomorphic *Apc* mutations (Fodde et al., 1994, Smits et al., 1998, Smits et al., 1999). Two of them, *Apc<sup>1638N</sup>* and *Apc<sup>1638T</sup>* carry similar targeted mutations at codon 1638 which differ in their ability to express the corresponding 182 kDa truncated protein encompassing all 3 β-catenin binding domains, three of the 7 β-catenin down-regulating repeats, and only one of the 3 SAMP axin/conductin binding motifs. Whereas the *Apc<sup>1638T</sup>* mutation does express the expected 182 kDa truncated protein at normal levels readily detected by western analysis, residual (1-2%) amounts of the same protein are detectable in *Apc<sup>1638N</sup>* only after immunoprecipitation assays (Smits et al., 1999, Kielman et al., 2002). Notably, *Apc<sup>+/1638T</sup>* mice are tumor free and homozygous *Apc<sup>1638T/1638T</sup>* animals are viable though with growth retardation and specific developmental defects (Smits et al., 1999).

*Apc<sup>+/1638N</sup>* mice do develop intestinal tumours though significantly fewer (5-6) when compared with *Apc<sup>Min</sup>* and *Apc<sup>Δ716</sup>*. Apart from its attenuated intestinal tumor phenotype, the *Apc<sup>+/1638N</sup>* mouse model is characterized by a wide spectrum of extra-intestinal manifestations ranging from desmoid tumors, epidermal cysts, mammary tumors, abnormalities of the retinal pigment epithelium, gastric tumors and osteomas (Fodde et al., 1994, Marcus et al., 1997, van der Hoven van Oordt et al., 1997, Smits et al., 1998, Smits et al., 2000b). *Apc<sup>1638N/1638N</sup>* homozygous animals are embryonic lethal and die during gastrulation at 7.5 dpc (Kielman et al., in preparation).

More recently, we have generated the *Apc<sup>1572T</sup>* mouse model by targeting a nonsense codon at residue 1572 (Smits et al., 1999) (Gaspar et al., in preparation). The *Apc<sup>1572T</sup>* mutation results in a stable truncated protein encompassing all the β-catenin binding domains, 3 of the 7 β-catenin downregulating repeats, but, unlike *Apc<sup>1638T</sup>*, none of the SAMP axin/conductin binding motifs. Surprisingly, *Apc<sup>+/1572T</sup>* mice develop invasive and metastasizing mammary cancer, desmoids, epidermal cysts, and hepatic tumors, but no intestinal adenomas. An overview of the above *Apc* mouse models, their intestinal and extra-intestinal phenotype, and their corresponding truncated proteins is depicted in Fig. 3.

The striking phenotypic differences among *Apc* mouse models strongly correlates with specific dosages of transcriptionally active nuclear β-catenin (and thus of WNT signal transduction) measured

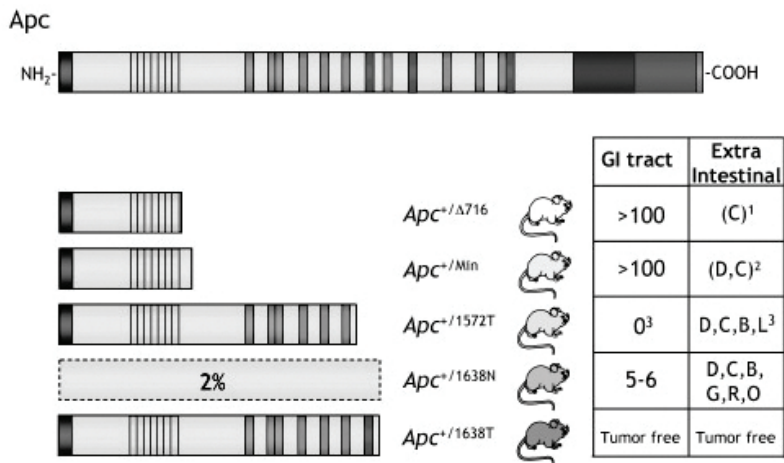


**Fig. 3. Mouse genotype-phenotype correlations at the *Apc* gene.** Pre-clinical mouse models for FAP. The full-length APC protein is shown with the major functional domains characterized to date (see key in Fig. 1). The main five models are depicted next to the truncated APC proteins they encode. Please note that *Apc*<sup>1638N</sup> and *Apc*<sup>1638T</sup> truncated proteins are virtually identical as far as the position of the termination codon is concerned. However, whereas *Apc*<sup>1638T</sup> is present in a 1:1 ratio with wild-type *Apc*, in *Apc*<sup>1638N</sup> only 'leaky' amounts (1–2%) of the predicted protein are generated. Tumor multiplicity in the gastro-intestinal tract and elsewhere are listed in the table. These phenotypic data have been obtained from inbred C57BL/6J mice. Abbreviations: C, cysts; D, desmoids; B, breast tumors; L, liver tumors; O, osteomas; R, abnormalities of the retinal pigment epithelium; G,

gastric tumors. Notes: <sup>1</sup>Apart from the rare occurrence of epidermal cysts (1 in 200 mice), extra-intestinal manifestations have not been reported for the *Apc*<sup>Δ716</sup> mouse model (Dr. M. Taketo, personal communication). <sup>2</sup>*Apc*<sup>Min</sup> mice develop on average less than a single desmoid tumor per animal and 1-2 cutaneous cysts invariably located in the skin covering the neck region (Smits *et al.*, 1998, Halberg *et al.*, 2000). <sup>3</sup>Gaspar *et al.*, manuscript in preparation.

by the TOPFLASH reporter assay (Korinek *et al.*, 1997) in ES cells carrying the *Apc*<sup>Min</sup>, *Apc*<sup>1638N</sup>, *Apc*<sup>1638T</sup>, and *Apc*<sup>1572T</sup> targeted mutations in various genetic combinations (Smits *et al.*, 1999, Kielman *et al.*, 2002). We observed an increasing gradient of  $\beta$ -catenin regulatory activity among the different genotypes with *Apc*<sup>Min/Min</sup> and *Apc*<sup>1638N/1638N</sup> ES cells showing the highest reporter activity, followed by *Apc*<sup>1638N/1572T</sup>, *Apc*<sup>1638N/1638T</sup>, and *Apc*<sup>1638T/1638T</sup>, the latter being comparable to wild type cells (Fig. 4).

A clear trend in the correlation between WNT signaling and tumor phenotype is visible: severe truncation of the  $\beta$ -catenin regulating domains as in the case of *Apc*<sup>Min</sup>, results in high dosages of transcriptionally active  $\beta$ -catenin and in the highest tumor multiplicity in the GI tract. In the case of more hypomorphic alleles as *Apc*<sup>1638N</sup>, *Apc*<sup>1638T</sup> and *Apc*<sup>1572T</sup>, the decrease in  $\beta$ -catenin signaling is accompanied by a lower polyp incidence in the intestine. On the other hand, the type and incidence of extra intestinal manifestations seems to be inversely correlated with WNT activity and the severity of the intestinal phenotype. Desmoid tumors and cysts, virtually absent in *Apc*<sup>Min</sup> (Smits *et al.*, 1998, Halberg *et al.*, 2000), are common in both *Apc*<sup>1638N</sup> and *Apc*<sup>1572T</sup>, while the latter is also characterized by spontaneous and aggressive mammary adenocarcinomas unique to this strain (Gaspar *et al.*, in preparation) (Fig. 3).

A possible explanation for these genotype-phenotype correlations can be found in the central role of the APC/ $\beta$ -catenin signalling in stem cell renewal and differentiation during development and in adult tissues (Ridanpaa *et al.*, 2001, Battle *et al.*, 2002, Kielman *et al.*, 2002, van de Wetering *et al.*, 2002). We hypothesize that homeostasis of several adult stem cell niches is regulated by tissue-specific WNT signaling levels. Specific  $\beta$ -catenin activity levels resulting from different *APC* mutations may affect proliferation, differentiation and apoptosis in a tissue-specific fashion, thus triggering tumorigenesis in a subset of organs throughout the body.

Notably, the absence of tumors and the post-natal viability characteristic of mice homozygous for the *Apc*<sup>1638T</sup> allele allow us to delineate the critical domains of the APC protein involved in tumorigenesis and development: a truncated protein encompassing three of the seven 20 amino acid repeats and one SAMP motif, but missing all of the carboxy-terminal domains previously thought to be associated with tumorigenesis, is sufficient to ensure in utero development and prevent tumorigenesis in the adult (Smits *et al.*, 1999). A gene dosage effect is the cause of the phenotypic differences between *Apc*<sup>1638T</sup> and *Apc*<sup>1638N</sup> mouse models. Although these two alleles encode for the same truncated protein, whereas in *Apc*<sup>1638T</sup> expression levels are comparable to those of the full-length protein and sufficient to prevent tumor formation, in *Apc*<sup>1638N</sup> the presence of only residual amounts (1-2%) of this otherwise functional truncated protein underlies this model's susceptibility to multi-organ tumorigenesis.

A different example of the relevance of Wnt dosage effects in tumorigenesis came from the analysis of germline (1<sup>st</sup> hit) and somatic mutations (2<sup>nd</sup> hit) at the *APC* gene from FAP intestinal adenomas. Lamlum *et al.*, (1999) showed that polyps originating from patients with germline mutations around codon 1300 are characterized by allelic loss as the preferred second hit mechanism. On the other hand, polyps from patients harboring germline mutations outside this region show preferentially somatic point mutations and only very rare allelic losses as second hit mechanism (Lamlum *et al.*, 1999). In our laboratory, a similar approach was applied to both mouse and human polyps. *Apc*<sup>1638N</sup> or *Apc*<sup>Min</sup> mice when bred in a mismatch repair (Msh2) deficient background undergo somatic inactivation of the wild type *Apc* allele by point mutation rather than by complete chromosomal loss as observed in the majority of tumors from *Apc* mutant mouse models. Somatic mutations at the *Apc* gene in the *Apc*<sup>+/+</sup>*Msh2*<sup>-/-</sup> mice are predominantly dinucleotide deletions at simple sequence repeats

leading to truncated Apc polypeptides that partially retain some of the 20 a.a. beta-catenin downregulating motifs. In the presence of a germline *Apc* mutation (*Apc<sup>+/+</sup>/Msh2<sup>-/-</sup>* mice) the spectrum of somatic *Apc* mutations is shifted to the 5' end, thereby completely inactivating Apc's beta-catenin downregulating activity (Smits *et al.*, 2000a). These results indicate that somatic *Apc* mutations are selected during intestinal tumorigenesis and that specific combination of *Apc* alleles encoding for specific dosages of  $\beta$ -catenin signaling represent the main selective factor. Also, analysis of the type and distribution of 2<sup>nd</sup> hit mutations in polyps from FAP patients revealed a clear interdependence between germline and somatic mutations (Albuquerque *et al.*, 2002). Germline mutations that do not retain any of the  $\beta$ -catenin downregulating domains are usually associated with somatic point mutations encompassing one or less frequently two downregulating motifs. In contrast, the majority of polyps from FAP patients with germline mutations retaining one downregulating motif are characterized by somatic loss of the wild type *Apc* allele, though few point mutations that remove all the downregulating motifs were also observed. Accordingly, among tumors where the germline defect retained 2 downregulating domains, the most common somatic hits are point mutations that remove all 20 a.a. domains, or, less frequently, allelic losses. It should be noted that most truncated APC proteins retaining one or more of the 20 a.a. repeats, as found in colorectal tumors, do not represent null alleles and encode for residual  $\beta$ -catenin regulating activity (Albuquerque *et al.*, 2002).

According to the "just-right" signaling model (Albuquerque *et al.*, 2002), APC regulation of Wnt/ $\beta$ -catenin signal transduction must be impaired at specific levels to successfully trigger tumorigenesis. A too low signal will not provide sufficient transcriptional response and selective advantage to allow clonal expansion, whereas a too strong signaling activity might trigger an apoptotic response (Kim *et al.*, 2000).

Another model has been suggested to describe the interdependence between 1<sup>st</sup> and 2<sup>nd</sup> hit in APC-driven tumorigenesis. According to the "loose fit" model, although the majority of the cases seem to retain at least two downregulating domains, margins of variation in the number of remaining functional domains exist (Crabtree *et al.*, 2003). Additional studies on tumors other than those of the colon-rectum, revealed tissue-specific thresholds of  $\beta$ -catenin mediated signaling. In desmoid tumours the majority of somatic mutations retain two or three downregulation domains (Miyaki *et al.*, 1993, Palmirotta *et al.*, 1995, Giarola *et al.*, 1998). Upper gastrointestinal tumours also seem to follow the same trend (Groves *et al.*, 2002).

### APC dosage effects on differentiation

As mentioned before the Wnt pathway is better known for its role in differentiation and cell fate determination in a wide range of organisms, from *Drosophila* to mammals (Cadigan and Nusse 1997). In the early mouse embryo Wnt signaling is involved in the differentiation of pluripotent embryonic stem (ES) cells present in the inner cell mass into the three main germ layers: ectoderm, mesoderm and definitive endoderm. ES differentiation is not exclusively regulated by WNT but also by other factors like BMP's, FGF's, Smad's and Mixl1. Complex co-activation and interactions among these signaling pathways give rise to the different lineages (Loebel *et al.*, 2003).

Gene dosage effects are well known to control differentiation and cell fate. Lack of expression of the transcription factor OCT4 (Pou5f1) results in trophoblast ES cell differentiation; its increased expression induces endodermal and mesodermal differentiation whereas intermediate expression levels are needed for maintenance of ES cells pluripotency (Niwa *et al.*, 2000).

Different dosages of Apc/ $\beta$ -catenin signalling modulate stem cell renewal and differentiation. Mouse embryonic stem cells can easily be genetically manipulated and cultured *in vitro* without affecting their differentiation potential. There are several possibilities to assess the ability of these cells to differentiate: *in vitro* assays where culture conditions are modulated to induce ES differentiation into specific cell types or lineages, and teratoma formation assays where ES cells are injected in isogenic mice to allow *in vivo* differentiation and formation of benign teratomas.

Our collection of *Apc*-mutant ES cell lines shows a gradient of  $\beta$ -catenin regulatory activity and represents therefore a unique tool to study Wnt dosage-dependent consequences on stem cell differentiation (Fig. 4). We have therefore investigated the effect of different *Apc* dosages on the differentiation potential of mouse ES cells by teratoma formation and microarray expression profiling (Kielman *et al.*, 2002). We have provided genetic and molecular evidence that the ability and sensitivity of ES cells to differentiate into the three germ layers is inhibited by increasing dosages of  $\beta$ -catenin signaling ranging from a severe differentiation blockade in severely truncated *Apc* alleles, to more specific neuroectodermal, dorsal mesodermal and endodermal defects in more hypomorphic alleles. Accordingly, a targeted oncogenic mutation in the  $\beta$ -catenin gene recapitulates the differentiation defects observed in *Apc* mutant ES cells (Kielman *et al.*, 2002). From these results we

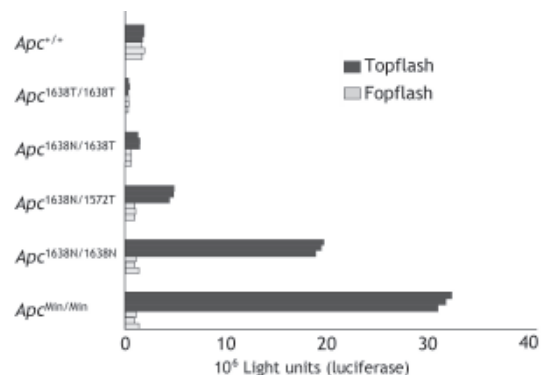


**Fig. 4. Wnt ( $\beta$ -catenin/Tcf) reporter assay analysis of the *Apc* allelic series.** Embryonic stem cells carrying different allelic combinations of targeted *Apc* mutations were tested by the TOP-Flash reporter assay (Korinek *et al.*, 1997) for their ability to activate luciferase expression under the control of TCF binding sites, (TOP, dark gray bars). Baseline expression of the vector was tested using mutated TCF binding sites (FOP, light gray bars). Measurements are the average of triplicate measurements of three independent experiments. All ES cell lines here employed are inbred 129/Ola, with the only exception of *Apc<sup>Min/Min</sup>* (C57BL/6J). Please note that this figure represents a composition derived from two different sets of previously reported assays (Smits *et al.*, 1999, Kielman *et al.*, 2002).



can conclude that specific levels of Apc/ $\beta$ -catenin signaling differentially affect stem cell differentiation.

Differentiation into paraxial mesoderm requires a higher induction of Wnt signalling while differentiation into neuroectoderm and endoderm require lower levels or even inhibition of the Wnt signal (Loebel *et al.*, 2003). These results are in agreement with experiments in Wnt3a null mouse models where the epiblast cells of homozygous embryos divert into neuroectodermal differentiation instead of differentiating into mesodermal cells (Yoshikawa *et al.*, 1997). Moreover, mouse models lacking both Lef1 and Tcf1 are also defective in paraxial mesoderm differentiation (Galceran *et al.*, 1999). Sfrp2, an antagonist of Wnt signalling, promotes *in vitro* neuronal differentiation when transfected into ES cells (Aubert *et al.*, 2002).

Expression profiling of wild type and Apc-mutant teratomas supports the differentiation defects at the molecular level and pinpoints a large number of downstream structural and regulating genes. Hierarchical clustering analysis correctly clustered the Apc-mutant teratomas according to  $\beta$ -catenin signalling dosage and to differentiation potential, even in those cases histologically indistinguishable from wild type teratomas. Notably, the distribution between up and downregulated genes in the ES-derived teratomas is approximately 50-50. The latter observation indicates that Wnt/ $\beta$ -catenin activity is not exclusively associated with transcriptional activation of target genes but also with their repression (Kielman *et al.*, 2002). More recently, microarray analysis of undifferentiated ES cells revealed that the expression profile of wild type stem cells is distinguishable from that of Apc mutant cells even before differentiation is induced (unpublished data). Thus, differential transcriptional regulation of Wnt/ $\beta$ -catenin downstream targets precedes the differentiation defect.

During development, the organism is able to accommodate stem cells in specific niches that preserve and restrict their renewal and differentiation. Although thought to be derived from ES cells through a progressive restriction of their pluripotency during development, adult stem cells still possess ample cell-renewal capacity and differentiation potential (Jiang *et al.*, 2002). They play an important role in the homeostasis of several self-renewing tissues like bone marrow, gut and skin. The dosage effects mentioned for ES cells also seem to hold true for adult stem cells. Mesodermal stem cells have the capability of differentiating among others to adipocytes and myocytes; Ross and colleagues have elegantly shown that activation of the Wnt pathway inhibits adipogenesis by downregulating the expression of transcription factors like C/EBP $\alpha$  and PPAR $\gamma$ . On the other hand, constitutive Wnt signaling is essential for myocyte differentiation since withdrawal of the Wnt signal by a dnTCF4 triggers the trans-differentiation of myoblasts into adipocytes (Ross *et al.*, 2000). Hence, Wnt signalling seems to control the differentiation program of mesenchymal adult stem cells in a dosage dependent way.

Another classic example of adult stem cell is located in the intestinal crypts of Lieberkhu. The intestinal mucosa is specialized for absorption of nutrients and consists of a simple columnar epithelium the surface area of which is vastly increased via evaginating villi and invaginating crypts. Throughout the intestine, large numbers of cells are daily shed into the lumen and must be replaced by new cells differentiating from multipotent stem cells. These stem cells have the ability to differentiate into five different intestinal types: columnar absorptive enterocytes, mucus-secreting

Goblet cells, hormone-secreting enteroendocrine cells, the antimicrobial peptide producing Paneth cells, and the M cell. The first three cell types can be found throughout the whole intestine, Paneth cells are restricted to the small intestine, and M cells can only be found in the crypts adjacent to the Peyer's patches (Marshman *et al.*, 2002).

A consistent body of experimental evidence supports a role for Wnt signaling in the regulation of intestinal stem cell differentiation. First, Tcf4<sup>-/-</sup> mice cannot sustain an intestinal stem cell compartment due to premature onset of differentiation, strongly suggesting that activation of Wnt downstream targets are required to maintain proliferative capacity (Korinek *et al.*, 1998). Thus, Wnt signaling is needed for the maintenance of the intestinal stem cell compartment. Further evidence was provided with the colon cancer cell line Caco-2 as a model. *In vitro* differentiation of Caco-2 cells along the absorptive cell lineage coincides with downregulation of Wnt signaling (Mariadason *et al.*, 2001). More recently, it was shown that inhibition of  $\beta$ -catenin/TCF-4 transcriptional activity induces a rapid G1 arrest and interferes with the physiological proliferation program active in the lower third of the colon crypt (van de Wetering *et al.*, 2002). Coincidentally, an intestinal differentiation program is triggered. The Wnt target gene *c-MYC* plays a central role in this switch by direct repression of p21(CIP1/WAF1). Following disruption of  $\beta$ -catenin/TCF-4 activity, the decreased expression of c-MYC releases p21(CIP1/WAF1) transcription, which in turn mediates G1 arrest and differentiation (van de Wetering *et al.*, 2002). Thus, the  $\beta$ -catenin/TCF-4 complex seems to represent the master switch that controls the equilibrium between proliferation and differentiation in the intestinal epithelium.

In the small intestine, the progeny of stem cells follow specific differentiation patterns. Absorptive, enteroendocrine, and goblet cells migrate upwards toward the villus while Paneth cells occupy the bottom of the crypts. Battle *et al.*, showed that  $\beta$ -catenin and TCF couple proliferation and differentiation to the sorting of cell populations in the intestinal epithelium by controlling the expression levels of the EphB receptors and their ligand ephrin-B along the crypt-villus axis (Battle *et al.*, 2002). Accordingly, in the intestine of EphB-null mice the proliferative and differentiated populations intermingle, and Paneth cells do not follow their downward migratory path, but are scattered along crypt and villus.

### A model for Wnt-mediated regulation of intestinal homeostasis and its consequences for tumour initiation and progression

Different observations from our and other laboratories are indicative of a central role of the Wnt signal transduction pathway in controlling the renewal and differentiation of stem cell compartments both during development and in the adult organism (Korinek *et al.*, 1998, Battle *et al.*, 2002, Kielman *et al.*, 2002, van de Wetering *et al.*, 2002). Cell renewal and differentiation are regulated by  $\beta$ -catenin in a dosage-dependent fashion. It is now well established that concentration gradients of signaling molecules known as morphogens organize and pattern tissues in developing animals. In particular, studies of patterning of Drosophila and vertebrate limbs have demonstrated the critical roles of gradients of the Wnt, Hedgehog (Hh) and transforming growth factor-beta (TGF- $\beta$ ) families of morphogens. These molecules are often expressed in organizing centres, and can act over a long range to

coordinate the patterning of an entire field of cells. Importantly, their transcriptional and cellular effects are, as in the case of  $\beta$ -catenin, dose-dependent, which identifies them as the 'morphogens' first postulated in 1924 (Spemann and Mangold 2001, Kielman *et al.*, 2002). The latter nicely fits in a model where a Wnt organizing centre is located in the stroma underlying the intestinal epithelial lining that generates a gradient of Wnt activity along crypt-villus axis. Due to the organization of the intestinal epithelium in invaginations in the stroma (crypts) and protrusions into the lumen (villi), the stem cell niche at the bottom of the crypt is located at the shortest physical distance from a putative source of Wnt diffusible ligands. Accordingly, in the colon nuclear  $\beta$ -catenin localization has been shown in normal intestinal cells located at the bottom of the crypt (Battlle *et al.*, 2002, van de Wetering *et al.*, 2002) (Fig. 5). In the small intestine, Paneth cells migrate downwards and share the lower third of the crypt with the putative stem cells. Both Paneth cells and other intestinal cells located in the bottom third of the crypt are characterized by nuclear  $\beta$ -catenin. Therefore, physiological  $\beta$ -catenin signaling occurs in lower crypt cells including the Paneth cells (Battlle *et al.*, 2002). The downward migration pattern of Paneth cells results from the presence of the EphB3 receptor as shown in EphB3<sup>-/-</sup> mice where Paneth cells are scattered along crypt and villus. Notably, Paneth cells can correctly differentiate when positioned outside the bottom third of the crypt but fail to show nuclear  $\beta$ -catenin (Battlle *et al.*, 2002). Thus, while induction of  $\beta$ -catenin nuclear translocation appears to result from a cell non-autonomous process and depends on the position of the epithelial cells along the crypt-villus axis, the differentiation program of Paneth cells occurs independently of Wnt signalling. Accordingly, several Paneth-specific cryptdin/defensin-related genes were found to be upregulated in a dosage-specific fashion in teratomas derived from *Apc*-mutant ES cells (Kielman *et al.*, 2002).

In the progenitor intestinal stem cells, Wnt/ $\beta$ -catenin signaling activates a genetic program of cell proliferation by c-MYC activation and p21(CIP1/WAF1) repression, and consequent 'stemness', i.e. the maintenance of multi-potency, by a broad range of downstream effectors. Moving upward along the crypt-villus axis, the exposure to the Wnt ligands will progressively decrease thus triggering p21-mediated growth arrest and terminal differentiation (Battlle *et al.*, 2002, Kielman *et al.*, 2002).

APC expression along the crypt villus also shows an inverse gradient suggesting an increased level of expression with maturation (Smith *et al.*, 1993, Midgley *et al.*, 1997). However, how this expression gradient is determined is still unclear. A similar regional organization of  $\beta$ -catenin expression and intracellular localization has been observed in the hair follicle (Ridnappa *et al.*, 2001) and is likely to apply to a broad spectrum of adult stem cell compartments.

Enhanced  $\beta$ -catenin/TCF4 activity is common to normal intestinal stem cell compartments and colorectal cancer. This indicates that colorectal tumors may result from excessive proliferation and/or lack of differentiation within the stem cell compartment. Computer simulations of proliferation, migration and differentiation rates in the colonic crypt showed that only an enlargement of the stem cell compartment efficiently predicts polyp formation (Boman *et al.*, 2001). These observations well agree both with a model where tumor formation occurs in the crypt, but also with a top-down mechanism where well-differentiated cells in the villi may acquire *APC* or  $\beta$ -catenin mutations leading to Wnt deregulation, trans-differentiation and regression to a more proliferative, progenitor

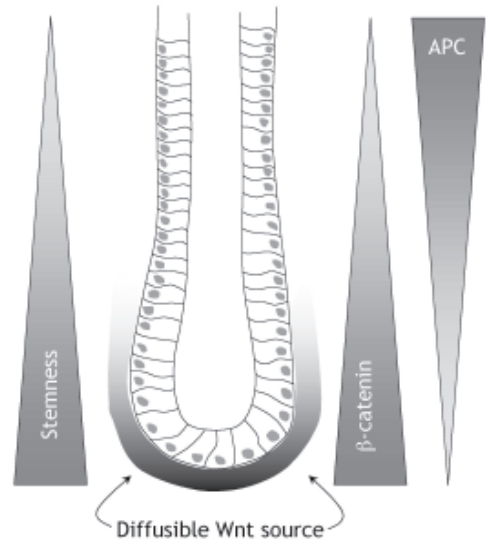


**Fig. 5. Wnt mediated control of intestinal stem cell renewal and differentiation along the crypt-villus axis.** The putative presence of a source of Wnt ligands within the stroma compartment underlying the intestinal mucosa generates a concentration gradient of Wnt morphogens reflected by the gradient of  $\beta$ -catenin expression (nuclear at the bottom of the crypt, more membrane-associated when moving towards the lumen (Battlle *et al.*, 2002)) and by a gradient of 'stemness', i.e. the pluripotency of intestinal progenitor cells. APC expression along the crypt villus shows an inverse gradient (Smith *et al.*, 1993, Midgley *et al.*, 1997) suggesting an increased level of expression with maturation. However, how this expression gradient is determined is still unclear.

17

cell-like phenotype (Shih *et al.*, 2001). This central role of Wnt-mediated 'stemness' in tumor formation is also in agreement with the observation according to which specific degrees of  $\beta$ -catenin signaling are selected during polyp formation (Albuquerque *et al.*, 2002). These tumor-selected signaling dosages will promote stem cell proliferation, inhibition of differentiation, and/or trans-differentiation in already committed cell types, as shown by the epithelial-mesenchymal transitions characteristic of colorectal cancer cells with nuclear  $\beta$ -catenin localization (Kirchner and Brabletz 2000). Tissue-specific thresholds in Wnt signaling dosages may exist among different stem cell niches, as indicated by the mammary and desmoid tumor phenotype of *Apc*<sup>1572T</sup> and *Apc*<sup>1638N</sup> mice (Smits *et al.*, 1998) (Gaspar *et al.*, manuscript in preparation). Accordingly, the Wnt pathway has been involved in a broad spectrum of tumor types arising from all three embryonic lineages in gene-specific (*APC*,  $\beta$ -catenin, *Axin*, *Pin1*) (Polakis 2000, Ryo *et al.*, 2001), and dosage-specific fashions (Smits *et al.*, 1999, Fodde and Smits 2001, Kielman *et al.*, 2002). It is likely that different mutations in a subset of Wnt-related genes confer specific signaling dosages to allow tumor formation in specific tissues by uncontrolled expansion of the corresponding stem cell compartment.

Notably, although *APC* (or  $\beta$ -catenin) mutations predict the nuclear accumulation of  $\beta$ -catenin throughout colorectal tumors, only

a subset of the cancer cells are positive after immunohistochemistry (Kirchner and Brabletz 2000). This 'active' subset of alleged cancer stem cells increases with tumor size but not with the grade of dysplasia of the colon adenoma (Brabletz *et al.*, 2000). Presumably, *APC* mutations alone are not sufficient for nuclear translocation of  $\beta$ -catenin and other synergistic factors trigger constitutive Wnt signaling in more advanced stages of colorectal cancer. Further studies are needed to understand the molecular mechanisms underlying the dose-dependent transcriptional response in Wnt signaling, its primary downstream targets, and the likely cross-talk with other signal transduction pathways and cellular functions in homeostasis and in tumor formation and progression.

#### Acknowledgements

The authors are grateful to Dr. Ron Smits, for his critical reading of the manuscript. This study was supported by grant no. 99-109 from AIRC to C.G. and by VICI-grant 918.36.636 from the Dutch Research Council (NWO).

#### References

- ABERLE, H., A. BAUER, J. STAPPERT, A. KISPERS, and R. KEMLER. 1997. beta-catenin is a target for the ubiquitin-proteasome pathway. *EMBO J* 16: 3797-804.
- ALBUQUERQUE, C., C. BREUKEL, R. VAN DER LUIJT, P. FIDALGO, P. LAGE, F. J. SLOORS, C. N. LEITAO, R. FODDE, and R. SMITS. 2002. The just-right' signaling model: APC somatic mutations are selected based on a specific level of activation of the beta-catenin signaling cascade. *Hum Mol Genet* 11: 1549-60.
- AUBERT, J., H. DUNSTAN, I. CHAMBERS, and A. SMITH. 2002. Functional gene screening in embryonic stem cells implicates Wnt antagonism in neural differentiation. *Nat Biotechnol* 20: 1240-5.
- BATLLE, E., J. T. HENDERSON, H. BEGHTLE, M. M. VAN DEN BORN, E. SANCHO, G. HULS, J. MEELDIJK, J. ROBERTSON, M. VAN DE WETERING, T. PAWSON, and H. CLEVERS. 2002. Beta-catenin and TCF mediate cell positioning in the intestinal epithelium by controlling the expression of EphB/ephrinB. *Cell* 111: 251-63.
- BEHRENS, J., B. A. JERCHOW, M. WURTELE, J. GRIMM, C. ASBRAND, R. WIRTZ, M. KÜHL, D. WEDLICH, and W. BIRCHMEIER. 1998. Functional interaction of an axin homolog, conductin, with beta-catenin, APC, and GSK3beta. *Science* 280: 596-9.
- BEHRENS, J., J. P. VON KRIES, M. KÜHL, L. BRUHN, D. WEDLICH, R. GROSSCHEDL, and W. BIRCHMEIER. 1996. Functional interaction of beta-catenin with the transcription factor LEF-1. *Nature* 382: 638-42.
- BOMAN, B. M., J. Z. FIELDS, O. BONHAM-CARTER, and O. A. RUNQUIST. 2001. Computer modeling implicates stem cell overproduction in colon cancer initiation. *Cancer Res* 61: 8408-11.
- BRABLETZ, T., K. HERRMANN, A. JUNG, G. FALLER, and T. KIRCHNER. 2000. Expression of nuclear beta-catenin and c-myc is correlated with tumor size but not with proliferative activity of colorectal adenomas. *Am J Pathol* 156: 865-70.
- BRABLETZ, T., A. JUNG, S. DAG, F. HUBEK, and T. KIRCHNER. 1999. beta-catenin regulates the expression of the matrix metalloproteinase-7 in human colorectal cancer. *Am J Pathol* 155: 1033-8.
- CADIGAN, K. M., and R. NUSSE. 1997. Wnt signaling: a common theme in animal development. *Genes Dev* 11: 3286-305.
- CAVALLO, R. A., R. T. COX, M. M. MOLINE, J. ROOSE, G. A. POLEVOY, H. CLEVERS, M. PEIFER, and A. BEJSOVEC. 1998. Drosophila Tcf and Groucho interact to repress Wingless signalling activity. *Nature* 395: 604-8.
- CRABTREE, M., O. M. SIEBER, L. LIPTON, S. V. HODGSON, H. LAMLUM, H. J. THOMAS, K. NEALE, R. K. PHILLIPS, K. HEINIMANN, and I. P. TOMLINSON. 2003. Refining the relation between 'first hits' and 'second hits' at the APC locus: the 'loose fit' model and evidence for differences in somatic mutation spectra among patients. *Oncogene* 22: 4257-65.
- CRAWFORD, H. C., B. M. FINGLETON, L. A. RUDOLPH-OWEN, K. J. GOSS, B. RUBINFELD, P. POLAKIS, and L. M. MATRISIAN. 1999. The metalloproteinase matrilysin is a target of beta-catenin transactivation in intestinal tumors. *Oncogene* 18: 2883-91.
- FODDE, R. 2003. The multiple functions of tumour suppressors: it's all in APC. *Nat Cell Biol* 5: 190-2.
- FODDE, R., W. EDELMANN, K. YANG, C. VAN LEEUWEN, C. CARLSON, B. RENAULT, C. BREUKEL, E. ALT, M. LIPKIN, P. M. KHAN, and *ET AL.*, 1994. A targeted chain-termination mutation in the mouse Apc gene results in multiple intestinal tumors. *Proc Natl Acad Sci USA* 91: 8969-73.
- FODDE, R., and P. M. KHAN. 1995. Genotype-phenotype correlations at the adenomatous polyposis coli (APC) gene. *Crit Rev Oncog* 6: 291-303.
- FODDE, R., and R. SMITS. 2001. Disease model: familial adenomatous polyposis. *Trends Mol Med* 7: 369-73.
- FODDE, R., R. SMITS, and H. CLEVERS. 2001. APC, signal transduction and genetic instability in colorectal cancer. *Nat Rev Cancer* 1: 55-67.
- FODDE, R., R. SMITS, N. HOFLAND, M. KIELMAN, and P. MEERA KHAN. 1999. Mechanisms of APC-driven tumorigenesis: lessons from mouse models. *Cytogenet Cell Genet* 86: 105-11.
- GALCERAN, J., I. FARINAS, M. J. DEPEW, H. CLEVERS, and R. GROSSCHEDL. 1999. Wnt3a-/- like phenotype and limb deficiency in Lef1(-/-)Tcf1(-/-) mice. *Genes Dev* 13: 709-17.
- GIAROLA, M., D. WELLS, P. MONDINI, S. PILOTTI, P. SALA, A. AZZARELLI, L. BERTARIO, M. A. PIEROTTI, J. D. DELHANTY, and P. RADICE. 1998. Mutations of adenomatous polyposis coli (APC) gene are uncommon in sporadic desmoid tumours. *Br J Cancer* 78: 582-7.
- GRODEN, J., A. THLIVERIS, W. SAMOWITZ, M. CARLSON, L. GELBERT, H. ALBERTSEN, G. JOSLYN, J. STEVENS, L. SPIRO, M. ROBERTSON, and *ET AL.*, 1991. Identification and characterization of the familial adenomatous polyposis coli gene. *Cell* 66: 589-600.
- GROVES, C., H. LAMLUM, M. CRABTREE, J. WILLIAMSON, C. TAYLOR, S. BASS, D. CUTHBERT-HEAVENS, S. HODGSON, R. PHILLIPS, and I. TOMLINSON. 2002. Mutation cluster region, association between germline and somatic mutations and genotype-phenotype correlation in upper gastrointestinal familial adenomatous polyposis. *Am J Pathol* 160: 2055-61.
- HALBERG, R. B., D. S. KATZUNG, P. D. HOFF, A. R. MOSER, C. E. COLE, R. A. LUBET, L. A. DONEHOWER, R. F. JACOBY, and W. F. DOVE. 2000. Tumorigenesis in the multiple intestinal neoplasia mouse: redundancy of negative regulators and specificity of modifiers. *Proc Natl Acad Sci USA* 97: 3461-6.
- HART, M. J., R. DELOS SANTOS, I. N. ALBERT, B. RUBINFELD, and P. POLAKIS. 1998. Downregulation of beta-catenin by human Axin and its association with the APC tumor suppressor, beta-catenin and GSK3 beta. *Curr Biol* 8: 573-81.
- HE, T. C., A. B. SPARKS, C. RAGO, H. HERMEKING, L. ZAWEL, L. T. DA COSTA, P. J. MORIN, B. VOGELSTEIN, and K. W. KINZLER. 1998. Identification of c-MYC as a target of the APC pathway. *Science* 281: 1509-12.
- ICHII, S., S. TAKEDA, A. HORII, S. NAKATSURU, Y. MIYOSHI, M. EMI, Y. FUJIWARA, K. KOYAMA, J. FURUYAMA, J. UTSUNOMIYA, and *ET AL.*, 1993. Detailed analysis of genetic alterations in colorectal tumors from patients with and without familial adenomatous polyposis (FAP). *Oncogene* 8: 2399-405.
- JIANG, Y., B. N. JAHAGIRDAR, R. L. REINHARDT, R. E. SCHWARTZ, C. D. KEENE, X. R. ORTIZ-GONZALEZ, M. REYES, T. LENVIK, T. LUND, M. BLACKSTAD, J. DU, S. ALDRICH, A. LISBERG, W. C. LOW, D. A. LARGAESPADA, and C. M. VERFAILLIE. 2002. Pluripotency of mesenchymal stem cells derived from adult marrow. *Nature* 418: 41-9.
- JOSLYN, G., M. CARLSON, A. THLIVERIS, H. ALBERTSEN, L. GELBERT, W. SAMOWITZ, J. GRODEN, J. STEVENS, L. SPIRO, M. ROBERTSON, and *ET AL.*, 1991. Identification of deletion mutations and three new genes at the familial polyposis locus. *Cell* 66: 601-13.
- KIELMAN, M. F., M. RINDAPAA, C. GASPAR, N. VAN POPPEL, C. BREUKEL, S. VAN LEEUWEN, M. M. TAKETO, S. ROBERTS, R. SMITS, and R. FODDE. 2002. Apc modulates embryonic stem-cell differentiation by controlling the dosage of beta-catenin signaling. *Nat Genet* 32: 594-605.
- KIM, K., K. M. PANG, M. EVANS, and E. D. HAY. 2000. Overexpression of beta-catenin induces apoptosis independent of its transactivation function with LEF-1 or the involvement of major G1 cell cycle regulators. *Mol Biol Cell* 11: 3509-23.
- KINZLER, K. W., M. C. NILBERT, L. K. SU, B. VOGELSTEIN, T. M. BRYAN, D. B. LEVY, K. J. SMITH, A. C. PREISINGER, P. HEDGE, D. MCKECHNIE, and *ET AL.*, 1991. Identification of FAP locus genes from chromosome 5q21. *Science* 253: 661-5.



- KINZLER, K. W., and B. VOGELSTEIN. 1996. Lessons from hereditary colorectal cancer. *Cell* 87: 159-70.
- KIRCHNER, T., and T. BRABLETZ. 2000. Patterning and nuclear beta-catenin expression in the colonic adenoma-carcinoma sequence. Analogies with embryonic gastrulation. *Am J Pathol* 157: 1113-21.
- KNUDSON, A. G., JR. 1971. Mutation and cancer: statistical study of retinoblastoma. *Proc Natl Acad Sci USA* 68: 820-3.
- KORINEK, V., N. BARKER, P. MOERER, E. VAN DONSELAAR, G. HULS, P. J. PETERS, and H. CLEVERS. 1998. Depletion of epithelial stem-cell compartments in the small intestine of mice lacking Tcf-4. *Nat Genet* 19: 379-83.
- KORINEK, V., N. BARKER, P. J. MORIN, D. VAN WICHEN, R. DE WEGER, K. W. KINZLER, B. VOGELSTEIN, and H. CLEVERS. 1997. Constitutive transcriptional activation by a beta-catenin-Tcf complex in APC-/- colon carcinoma. *Science* 275: 1784-7.
- LAMLUM, H., M. ILYAS, A. ROWAN, S. CLARK, V. JOHNSON, J. BELL, I. FRAYLING, J. EFSTATHIOU, K. PACK, S. PAYNE, R. ROYLANCE, P. GORMAN, D. SHEER, K. NEALE, R. PHILLIPS, I. TALBOT, W. BODMER, and I. TOMLINSON. 1999. The type of somatic mutation at APC in familial adenomatous polyposis is determined by the site of the germline mutation: a new facet to Knudson's 'two-hit' hypothesis. *Nat Med* 5: 1071-5.
- LEVY, D. B., K. J. SMITH, Y. BEAZER-BARCLAY, S. R. HAMILTON, B. VOGELSTEIN, and K. W. KINZLER. 1994. Inactivation of both APC alleles in human and mouse tumors. *Cancer Res* 54: 5953-8.
- LOEBEL, D. A., C. M. WATSON, R. A. DE YOUNG, and P. P. TAM. 2003. Lineage choice and differentiation in mouse embryos and embryonic stem cells. *Dev Biol* 264: 1-14.
- MARCUS, D. M., A. K. RUSTGI, D. DEFOE, S. E. BROOKS, R. S. MCCORMICK, T. P. THOMPSON, W. EDELMANN, R. KUCHERLAPATI, and S. SMITH. 1997. Retinal pigment epithelium abnormalities in mice with adenomatous polyposis coli gene disruption. *Arch Ophthalmol* 115: 645-50.
- MARIADASON, J. M., M. BORDONARO, F. ASLAM, L. SHI, M. KURAGUCHI, A. VELCICH, and L. H. AUGENLICHT. 2001. Down-regulation of beta-catenin TCF signaling is linked to colonic epithelial cell differentiation. *Cancer Res* 61: 3465-71.
- MARSHMAN, E., C. BOOTH, and C. S. POTTEN. 2002. The intestinal epithelial stem cell. *Bioessays* 24: 91-8.
- MIDGLEY, C. A., S. WHITE, R. HOWITT, V. SAVE, M. G. DUNLOP, P. A. HALL, D. P. LANE, A. H. WYLLIE, and V. J. BUBB. 1997. APC expression in normal human tissues. *J Pathol* 181: 426-33.
- MIYAKI, M., M. KONISHI, R. KIKUCHI-YANOSHITA, M. ENOMOTO, K. TANAKA, H. TAKAHASHI, M. MURAOKA, T. MORI, F. KONISHI, and T. IWAMA. 1993. Coexistence of somatic and germ-line mutations of APC gene in desmoid tumors from patients with familial adenomatous polyposis. *Cancer Res* 53: 5079-82.
- MIYOSHI, Y., H. NAGASE, H. ANDO, A. HORII, S. ICHII, S. NAKATSURU, T. AOKI, Y. MIKI, T. MORI, and Y. NAKAMURA. 1992. Somatic mutations of the APC gene in colorectal tumors: mutation cluster region in the APC gene. *Hum Mol Genet* 1: 229-33.
- MOLENAAR, M., M. VAN DE WETERING, M. OOSTERWEGEL, J. PETERSON-MADURO, S. GODSAVE, V. KORINEK, J. ROOSE, O. DESTREE, and H. CLEVERS. 1996. XTCF-3 transcription factor mediates beta-catenin-induced axis formation in *Xenopus* embryos. *Cell* 86: 391-9.
- MORIN, P. J., A. B. SPARKS, V. KORINEK, N. BARKER, H. CLEVERS, B. VOGELSTEIN, and K. W. KINZLER. 1997. Activation of beta-catenin-Tcf signaling in colon cancer by mutations in beta-catenin or APC. *Science* 275: 1787-90.
- MOSER, A. R., E. M. MATTES, W. F. DOVE, M. J. LINDSTROM, J. D. HAAG, and M. N. GOULD. 1993. ApCmin, a mutation in the murine Apc gene, predisposes to mammary carcinomas and focal alveolar hyperplasias. *Proc Natl Acad Sci USA* 90: 8977-81.
- MOSER, A. R., A. R. SHOEMAKER, C. S. CONNELLY, L. CLIPSON, K. A. GOULD, C. LUONGO, W. F. DOVE, P. H. SIGGERS, and R. L. GARDNER. 1995. Homozygosity for the Min allele of Apc results in disruption of mouse development prior to gastrulation. *Dev Dyn* 203: 422-33.
- NISHISHIO, I., Y. NAKAMURA, Y. MIYOSHI, Y. MIKI, H. ANDO, A. HORII, K. KOYAMA, J. UTSUNOMIYA, S. BABA, and P. HEDGE. 1991. Mutations of chromosome 5q21 genes in FAP and colorectal cancer patients. *Science* 253: 665-9.
- NIWA, H., J. MIYAZAKI, and A. G. SMITH. 2000. Quantitative expression of Oct-3/4 defines differentiation, dedifferentiation or self-renewal of ES cells. *Nat Genet* 24: 372-6.
- OSHIMA, M., H. OSHIMA, K. KITAGAWA, M. KOBAYASHI, C. ITAKURA, and M. TAKETO. 1995. Loss of Apc heterozygosity and abnormal tissue building in nascent intestinal polyps in mice carrying a truncated Apc gene. *Proc Natl Acad Sci USA* 92: 4482-6.
- PALMIROTTA, R., M. C. CURIA, D. L. ESPOSITO, R. VALANZANO, L. MESSERINI, F. FICARI, M. L. BRANDI, F. TONELLI, R. MARIANI-COSTANTINI, P. BATTISTA, and ETAL. 1995. Novel mutations and inactivation of both alleles of the APC gene in desmoid tumors. *Hum Mol Genet* 4: 1979-81.
- POLAKIS, P. 2000. Wnt signaling and cancer. *Genes Dev* 14: 1837-51.
- POWELL, S. M., N. ZILZ, Y. BEAZER-BARCLAY, T. M. BRYAN, S. R. HAMILTON, S. N. THIBODEAU, B. VOGELSTEIN, and K. W. KINZLER. 1992. APC mutations occur early during colorectal tumorigenesis. *Nature* 359: 235-7.
- RIDANPAA, M., R. FODDE, and M. KIELMAN. 2001. Dynamic expression and nuclear accumulation of beta-catenin during the development of hair follicle-derived structures. *Mech Dev* 109: 173-81.
- ROSS, S. E., N. HEMATI, K. A. LONGO, C. N. BENNETT, P. C. LUCAS, R. L. ERICKSON, and O. A. MACDOUGALD. 2000. Inhibition of adipogenesis by Wnt signaling. *Science* 289: 950-3.
- RUBINFELD, B., I. ALBERT, E. PORFIRI, C. FIOL, S. MUNEMITSU, and P. POLAKIS. 1996. Binding of GSK3beta to the APC-beta-catenin complex and regulation of complex assembly. *Science* 272: 1023-6.
- RUBINFELD, B., B. SOUZA, I. ALBERT, O. MULLER, S. H. CHAMBERLAIN, F. R. MASIAZ, S. MUNEMITSU, and P. POLAKIS. 1993. Association of the APC gene product with beta-catenin. *Science* 262: 1731-4.
- RYO, A., M. NAKAMURA, G. WULF, Y. C. LIU, and K. P. LU. 2001. Pin1 regulates turnover and subcellular localization of beta-catenin by inhibiting its interaction with APC. *Nat Cell Biol* 3: 793-801.
- SEMEONOV, M. V., K. TAMAI, B. K. BROTT, M. KUHL, S. SOKOL, and X. HE. 2001. Head inducer Dickkopf-1 is a ligand for Wnt coreceptor LRP6. *Curr Biol* 11: 951-61.
- SHIH, I. M., T. L. WANG, G. TRAVERSO, K. ROMANS, S. R. HAMILTON, S. BEN-SASSON, K. W. KINZLER, and B. VOGELSTEIN. 2001. Top-down morphogenesis of colorectal tumors. *Proc Natl Acad Sci USA* 98: 2640-5.
- SHTUTMAN, M., J. ZHURINSKY, I. SIMCHA, C. ALBANESE, M. D'AMICO, R. PESTELL, and A. BEN-ZE'EV. 1999. The cyclin D1 gene is a target of the beta-catenin/LEF-1 pathway. *Proc Natl Acad Sci USA* 96: 5522-7.
- SMITH, K. J., K. A. JOHNSON, T. M. BRYAN, D. E. HILL, S. MARKOWITZ, J. K. WILLSON, C. PARASKEVA, G. M. PETERSEN, S. R. HAMILTON, B. VOGELSTEIN, and ETAL. 1993. The APC gene product in normal and tumor cells. *Proc Natl Acad Sci USA* 90: 2846-50.
- SMITS, R., N. HOFLAND, W. EDELMANN, M. GEUGIEN, S. JAGMOHAN-CHANGUR, C. ALBUQUERQUE, C. BREUKEL, R. KUCHERLAPATI, M. F. KIELMAN, and R. FODDE. 2000a. Somatic Apc mutations are selected upon their capacity to inactivate the beta-catenin downregulating activity. *Genes Chrom. Cancer* 29: 229-39.
- SMITS, R., M. F. KIELMAN, C. BREUKEL, C. ZURCHER, K. NEUFELD, S. JAGMOHAN-CHANGUR, N. HOFLAND, J. VAN DIJK, R. WHITE, W. EDELMANN, R. KUCHERLAPATI, P. M. KHAN, and R. FODDE. 1999. Apc1638T: a mouse model delineating critical domains of the adenomatous polyposis coli protein involved in tumorigenesis and development. *Genes Dev* 13: 1309-21.
- SMITS, R., P. RUIZ, S. DIAZ-CANO, A. LUZ, S. JAGMOHAN-CHANGUR, C. BREUKEL, C. BIRCHMEIER, W. BIRCHMEIER, and R. FODDE. 2000b. E-cadherin and adenomatous polyposis coli mutations are synergistic in intestinal tumor initiation in mice. *Gastroenterology* 119: 1045-53.
- SMITS, R., W. VAN DER HOVEN VAN OORDT, A. LUZ, C. ZURCHER, S. JAGMOHAN-CHANGUR, C. BREUKEL, P. M. KHAN, and R. FODDE. 1998. Apc1638N: a mouse model for familial adenomatous polyposis-associated desmoid tumors and cutaneous cysts. *Gastroenterology* 114: 275-83.
- SPARKS, A. B., P. J. MORIN, B. VOGELSTEIN, and K. W. KINZLER. 1998. Mutational analysis of the APC/beta-catenin/Tcf pathway in colorectal cancer. *Cancer Res* 58: 1130-4.
- SPEMANN, H., and H. MANGOLD. (2001). Induction of embryonic primordia by implantation of organizers from a different species. 1923. *Int J Dev Biol* 45: 13-38.

- SU, L. K., K. W. KINZLER, B. VOGELSTEIN, A. C. PREISINGER, A. R. MOSER, C. LUONGO, K. A. GOULD, and W. F. DOVE. 1992. Multiple intestinal neoplasia caused by a mutation in the murine homolog of the APC gene. *Science* 256: 668-70.
- SU, L. K., B. VOGELSTEIN, and K. W. KINZLER. 1993. Association of the APC tumor suppressor protein with catenins. *Science* 262: 1734-7.
- TAKEMARU, K., S. YAMAGUCHI, Y. S. LEE, Y. ZHANG, R. W. CARTHEW, and R. T. MOON. 2003. Chibby, a nuclear beta-catenin-associated antagonist of the Wnt/Wingless pathway. *Nature* 422: 905-9.
- TETSU, O., and F. MCCORMICK. 1999. Beta-catenin regulates expression of cyclin D1 in colon carcinoma cells. *Nature* 398: 422-6.
- VAN DE WETERING, M., E. SANCHO, C. VERWEIJ, W. DE LAU, I. OVIING, A. HURLSTONE, K. VANDERHORN, E. BATLLE, D. COUDREUSE, A. P. HARAMIS, M. TJON-PON-FONG, P. MOERER, M. VAN DEN BORN, G. SOETE, S. PALS, M. EILERS, R. MEDEMA, and H. CLEVERS. 2002. The beta-catenin/TCF-4 complex imposes a crypt progenitor phenotype on colorectal cancer cells. *Cell* 111: 241-50.
- VAN DER HOUVEN VAN OORDT, C. W., R. SMITS, S. L. WILLIAMSON, A. LUZ, P. M. KHAN, R. FODDE, A. J. VANDEREB, and M. L. BREUER. 1997. Intestinal and extra-intestinal tumor multiplicities in the Apc1638N mouse model after exposure to X-rays. *Carcinogenesis* 18: 2197-203.
- WIELENGA, V. J., R. SMITS, V. KORINEK, L. SMIT, M. KIELMAN, R. FODDE, H. CLEVERS, and S. T. PALS. 1999. Expression of CD44 in Apc and Tcf mutant mice implies regulation by the WNT pathway. *Am J Pathol* 154: 515-23.
- WU, W., A. GLINKA, H. DELIUS, and C. NIEHRS. 2000. Mutual antagonism between dickkopf1 and dickopf2 regulates Wnt/beta-catenin signalling. *Curr Biol* 10: 1611-4.
- YOSHIKAWA, Y., T. FUJIMORI, A. P. MCMAHON, and S. TAKADA. 1997. Evidence that absence of Wnt-3a signaling promotes neuralization instead of paraxial mesoderm development in the mouse. *Dev Biol* 183: 234-42.

# Chapter 2

***Apc* modulates embryonic stem-cell differentiation by controlling the dosage of  $\beta$ -catenin signaling**

Menno F. Kielman, Maaret Rindapää, Claudia Gaspar,  
Nicole van Poppel, Cor Breukel, Sandra van Leeuwen,  
Makoto Mark Taketo, Scott Roberts,  
Ron Smits and Riccardo Fodde



# Apc modulates embryonic stem-cell differentiation by controlling the dosage of $\beta$ -catenin signaling

Menno F. Kielman<sup>1</sup>, Maaret Rindapää<sup>1\*</sup>, Claudia Gaspar<sup>1\*</sup>, Nicole van Poppel<sup>1</sup>, Cor Breukel<sup>1</sup>, Sandra van Leeuwen<sup>1</sup>, Makoto Mark Taketo<sup>2</sup>, Scott Roberts<sup>3</sup>, Ron Smits<sup>1</sup> & Riccardo Fodde<sup>1</sup>

\*These authors contributed equally to this work.

Published online 11 November 2002; doi:10.1038/ng1045

**The Wnt signal-transduction pathway induces the nuclear translocation of membrane-bound  $\beta$ -catenin (Catnb) and has a key role in cell-fate determination. Tight somatic regulation of this signal is essential, as uncontrolled nuclear accumulation of  $\beta$ -catenin can cause developmental defects and tumorigenesis in the adult organism. The adenomatous polyposis coli gene (APC) is a major controller of the Wnt pathway and is essential to prevent tumorigenesis in a variety of tissues and organs. Here, we have investigated the effect of different mutations in *Apc* on the differentiation potential of mouse embryonic stem (ES) cells. We provide genetic and molecular evidence that the ability and sensitivity of ES cells to differentiate into the three germ layers is inhibited by increased doses of  $\beta$ -catenin by specific *Apc* mutations. These range from a severe differentiation blockade in *Apc* alleles completely deficient in  $\beta$ -catenin regulation to more specific neuroectodermal, dorsal mesodermal and endodermal defects in more hypomorphic alleles. Accordingly, a targeted oncogenic mutation in *Catnb* also affects the differentiation potential of ES cells. Expression profiling of wildtype and *Apc*-mutated teratomas supports the differentiation defects at the molecular level and pinpoints a large number of downstream structural and regulating genes. Chimeric experiments showed that this effect is cell-autonomous. Our results imply that constitutive activation of the *Apc*/ $\beta$ -catenin signaling pathway results in differentiation defects in tissue homeostasis, and possibly underlies tumorigenesis in the colon and other self-renewing tissues.**

23

## Introduction

Wnt signalling induces nuclear translocation of transcriptionally active  $\beta$ -catenin through interference with a multi-protein complex (composed of glycogen synthase kinase 3 $\beta$  (GSK3B), axin 1, axin 2 and APC) capable of earmarking free cytoplasmic  $\beta$ -catenin for degradation through the ubiquitin/proteasome pathway<sup>1,2</sup>. One of the key components of this complex is the APC tumor suppressor, which serves as the scaffold to which  $\beta$ -catenin, axin 1 and axin 2 bind<sup>3</sup>. Mutations in *APC* are responsible for familial adenomatous polyposis (FAP), an autosomal dominant predisposition to the development of hundreds to thousands of adenomatous polyps in the colon and rectum<sup>4</sup>. Moreover, mutations in *APC* initiate the majority of sporadic colorectal cancers<sup>3,5</sup>.

Several mutated alleles of the mouse *Apc* gene have been generated (Fig. 1a). Notably, they result in different developmental defects and different degrees of tumor predisposition and incidence<sup>6</sup>. The *Apc*<sup>Min</sup> allele encodes a stable truncated protein of 850 amino acids lacking all the  $\beta$ -catenin binding and downregu-

lating motifs. Heterozygous *Apc*<sup>+/Min</sup> mice develop multiple intestinal tumors, whereas *Apc*<sup>Min/Min</sup> embryos die at very early developmental stages<sup>7,8</sup>. Two different *Apc* mouse models, *Apc*<sup>1638T</sup> and *Apc*<sup>1638N</sup>, were generated in our laboratory by introducing a selection cassette at codon 1638 of the endogenous *Apc* gene in the sense and anti-sense transcriptional orientation, respectively<sup>9</sup>. Heterozygous *Apc*<sup>+/1638N</sup> mice develop approximately 5–6 intestinal polyps in addition to a broad spectrum of extra-intestinal manifestations including desmoids, epidermal cysts, pilomatricomas and breast tumors<sup>10,11</sup>. Homozygosity with respect to the *Apc*<sup>1638N</sup> allele is embryonic lethal<sup>10,11</sup>. In contrast, *Apc*<sup>1638T/1638T</sup> mice are viable and tumor-free<sup>9</sup>.

Similar genotype–phenotype correlations have been established in humans between mutations in *APC* and the degree of severity of the corresponding FAP phenotype<sup>12</sup>. But the molecular and cellular mechanisms underlying these phenotypic differences are not understood. In fact, owing to the high complexity and turnover of the intestinal epithelium as a biological system, little is known regarding the cancer-causing cellular mechanisms

<sup>1</sup>Center for Human and Clinical Genetics, Leiden University Medical Center, Sylvius Laboratory, Wassenaarseweg 72, 2333 RA Leiden, The Netherlands.

<sup>2</sup>Department of Pharmacology, Kyoto University Graduate School of Medicine, Kyoto, Japan. <sup>3</sup>Rosetta Inpharmatics, Kirkland, Washington, USA. Correspondence should be addressed to R.F. (e-mail: r.fodde@lumc.nl).



triggered by loss of APC function. Alterations in rates of proliferation, apoptosis, cell migration and differentiation have been postulated to be involved. The observation that loss of function of transcription factor 4 (Tcf4) in mice leads to the depletion of intestinal stem cells indicates a role of the Wnt/ $\beta$ -catenin signal-transduction pathway in epithelial stem-cell maintenance<sup>13</sup>. More recently, computer modeling studies implicated crypt stem-cell overproduction in tumor initiation in the colon<sup>14</sup>.

Here, we analyzed the capacity of pluripotent stem cells carrying different *Apc* and *Catnb* alleles to differentiate into specialized cell lineages.

## Results

### Characterization of ES-cell lines with mutations in *Apc*

To elucidate the molecular basis of the phenotypic consequences of different mutations in *Apc* and to evaluate their effect on stem-cell differentiation, we generated different ES-cell lines carrying four mutated *Apc* alleles (Fig. 1a) in different combinations, and analyzed their expression level and  $\beta$ -catenin-driven transcriptional activity. ES-cell lines were generated either by two rounds of gene targeting<sup>9</sup> or by direct isolation from pre-implantation blastocysts. We also analyzed *Apc*<sup>1527T</sup>, a new allele obtained by deleting 197 nucleotides from the 3' end of the orig-

inal *Apc*<sup>1638T</sup> targeting construct, thereby removing the only residual SAMP repeat (the axin-binding domain; ref. 9; Fig. 1a). Western-blot analysis showed that all the alleles except for *Apc*<sup>1638N</sup> stably expressed the predicted truncated protein at a 1:1 ratio with the full-length wildtype protein (Fig. 1b). In contrast, no truncated protein was detected in heterozygous *Apc*<sup>+/1638N</sup> mice or ES cells (Fig. 1b).

To determine whether the *Apc*<sup>1638N</sup> mutation represents a true null allele, we attempted to identify minimal amounts of the truncated protein in homozygous *Apc*<sup>1638N</sup> cells by immunoprecipitation analysis (Fig. 1c). We observed a weak band of 182 kD (the size of the *Apc*<sup>1638T</sup> truncated protein). We then quantified the truncated *Apc* protein relative to its full-length equivalent by competition immunoprecipitation assays, which indicated that the *Apc*<sup>1638N</sup> allele expressed the mutant protein at approximately 2% of the endogenous level in ES cells (Fig. 1c). Therefore, the *Apc*<sup>1638N</sup> mutation represents a leaky hypomorphic variant of the *Apc*<sup>1638T</sup> allele.

The differences in expression levels of truncated *Apc* proteins were reflected by the corresponding levels of transcriptionally active nuclear  $\beta$ -catenin measured by the TCF/ $\beta$ -catenin responsive reporter assay TOPFLASH<sup>15</sup>. Previous analysis showed an increasing gradient of  $\beta$ -catenin regulatory activity among the

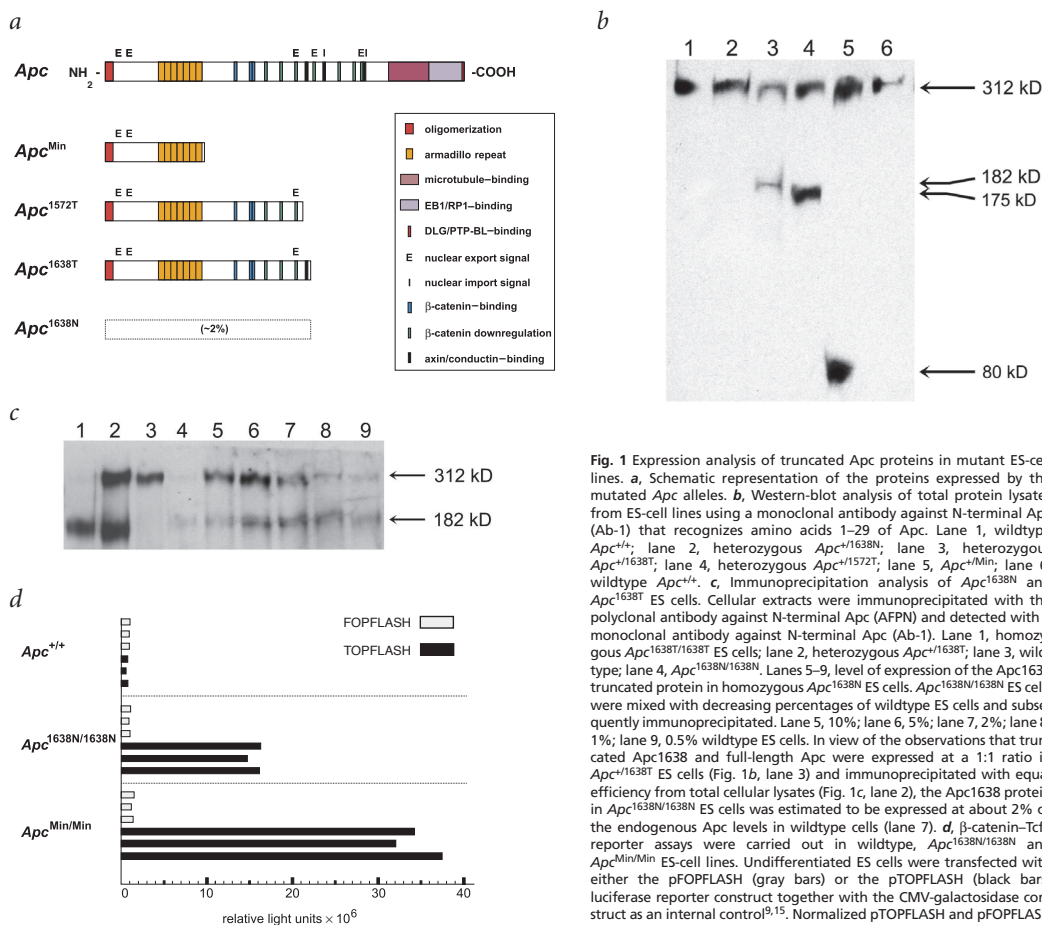


**Fig. 1** Expression analysis of truncated *Apc* proteins in mutant ES-cell lines. **a**, Schematic representation of the proteins expressed by the mutated *Apc* alleles. **b**, Western-blot analysis of total protein lysates from ES-cell lines using a monoclonal antibody against N-terminal *Apc* (Ab-1) that recognizes amino acids 1–29 of *Apc*. Lane 1, wildtype *Apc*<sup>+/+</sup>; lane 2, heterozygous *Apc*<sup>+/1638N</sup>; lane 3, heterozygous *Apc*<sup>+/1638T</sup>; lane 4, heterozygous *Apc*<sup>+/1572T</sup>; lane 5, *Apc*<sup>+/Min</sup>; lane 6, wildtype *Apc*<sup>+/+</sup>. **c**, Immunoprecipitation analysis of *Apc*<sup>1638N</sup> and *Apc*<sup>1638T</sup> ES cells. Cellular extracts were immunoprecipitated with the polyclonal antibody against N-terminal *Apc* (AFPN) and detected with a monoclonal antibody against N-terminal *Apc* (Ab-1). Lane 1, homozygous *Apc*<sup>1638T/1638T</sup> ES cells; lane 2, heterozygous *Apc*<sup>+/1638T</sup>; lane 3, wildtype; lane 4, *Apc*<sup>1638N/1638N</sup>. Lanes 5–9, level of expression of the *Apc*<sup>1638T</sup> truncated protein in homozygous *Apc*<sup>1638N</sup> ES cells. *Apc*<sup>1638N/1638N</sup> ES cells were mixed with decreasing percentages of wildtype ES cells and subsequently immunoprecipitated. Lane 5, 10%; lane 6, 5%; lane 7, 2%; lane 8, 1%; lane 9, 0.5% wildtype ES cells. In view of the observations that truncated *Apc*<sup>1638T</sup> and full-length *Apc* were expressed at a 1:1 ratio in *Apc*<sup>+/1638T</sup> ES cells (Fig. 1b, lane 3) and immunoprecipitated with equal efficiency from total cellular lysates (Fig. 1c, lane 2), the *Apc*<sup>1638N</sup> protein in *Apc*<sup>1638N/1638N</sup> ES cells was estimated to be expressed at about 2% of the endogenous *Apc* levels in wildtype cells (lane 7). **d**,  $\beta$ -catenin–Tcf4 reporter assays were carried out in wildtype, *Apc*<sup>1638N/1638N</sup> and *Apc*<sup>Min/Min</sup> ES-cell lines. Undifferentiated ES cells were transfected with either the pFOPFLASH (gray bars) or the pTOPFLASH (black bars) luciferase reporter construct together with the CMV-galactosidase construct as an internal control<sup>9,15</sup>. Normalized pTOPFLASH and pFOPFLASH levels are indicated for each cell line in triplicate transfections.



different genotypes. *Apc*<sup>1638N/1638N</sup> ES cells showed the highest reporter activity, followed by *Apc*<sup>1638N/1572T</sup>, *Apc*<sup>1638N/1638T</sup> and *Apc*<sup>1638T/1638T</sup>, the latter having reporter activity comparable to that of wildtype ES cells<sup>9</sup>. As the initial analysis did not include *Apc*<sup>Min</sup>, we isolated both *Apc*<sup>Min/Min</sup> and *Apc*<sup>1638N/1638N</sup> ES-cell lines directly from blastocysts of mixed genetic background C57BL/6J. Although direct comparison between the former (using 129-Ola ES-cell lines) and the latter reporter assays is not feasible owing to the different genetic backgrounds, *Apc*<sup>Min/Min</sup> ES cells showed considerably higher (twofold) TOPFLASH reporter levels than did *Apc*<sup>1638N/1638N</sup> ES cells (Fig. 1d).

Hence, our collection of ES-cell lines with mutations in *Apc* show a gradient of  $\beta$ -catenin regulatory activity that may be useful in studying its dose-dependent consequences on different cellular functions.

#### **In vivo differentiation analysis of ES-cell lines with mutations in *Apc* by teratoma formation**

To evaluate the differentiation potential of the cell lines with mutations in *Apc* in an *in vivo* assay, we injected undifferentiated ES cells subcutaneously into syngenic mice to induce formation

of teratomas. These are benign tumors derived from pluripotent stem cells and composed of well differentiated tissues of ecto-, meso- and endodermal origin<sup>16</sup>. Differentiation profiles of the resulting teratomas were investigated by histological and immunohistochemical analysis, and compared with those obtained with wildtype (*Apc*<sup>+/+</sup>) ES cells (Fig. 2a).

Teratomas derived from independent *Apc*<sup>1638N/1638N</sup> ES-cell lines either obtained by two rounds of gene targeting or derived from blastocysts showed severe differentiation defects (Fig. 2b,c). Several differentiation types were absent, namely neural, bone, cartilage and ciliated epithelia. As neural differentiation is sometimes difficult to recognize using morphological criteria, we used four different neural markers to identify neuroectodermal cellular types, specifically neurons, astrocytes, Schwann cells (detected with neural cell adhesion molecule (NCAM) and glial fibrillary acidic protein (GFAP)), neurofilaments and synaptic vesicles. These antibodies did not stain homozygous *Apc*<sup>1638N</sup> sections, in contrast with wildtype teratomas in which approximately 50–75% of the cells were positively stained (Fig. 2g–j,l–o). Differentiation to striated muscle (detected with adult myosin) was also severely affected and detectable in only a minority of the sections (data not shown). In contrast, smooth-muscle cellular types (detected with smooth muscle actin, 1A4) were abundant in *Apc*<sup>1638N</sup> teratomas (Fig. 2k,p). Other cell types and tissues that we positively identified in the *Apc*<sup>1638N</sup> teratomas included simple non-ciliated epithelia, keratinized epithelia and non-

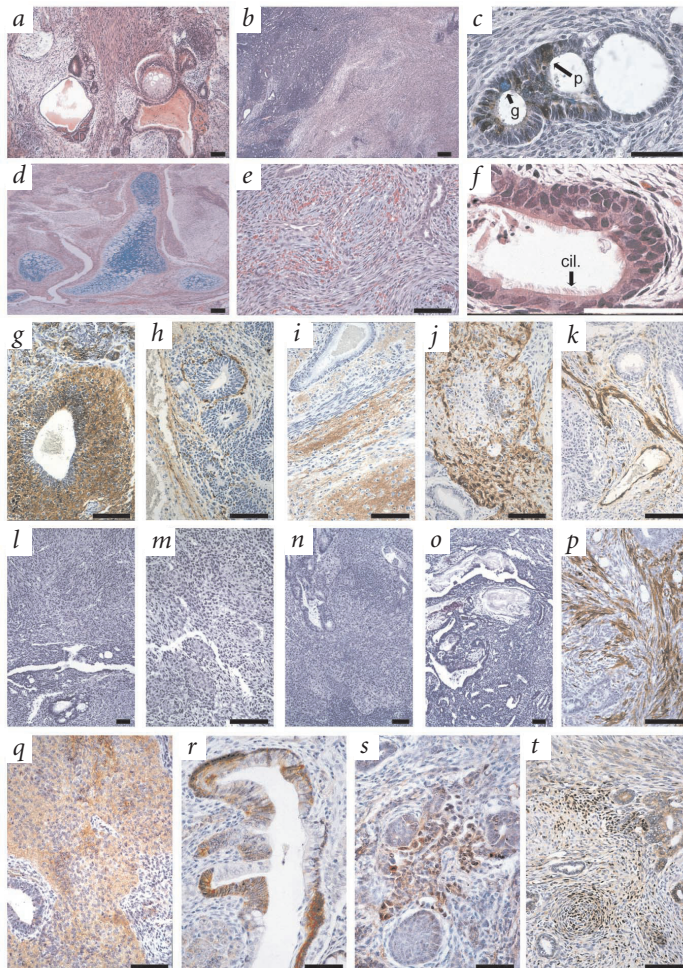


**Fig. 2** *In vivo* differentiation analysis of teratomas derived from wildtype and mutant ES cells. Low-magnification view of histological sections stained with hematoxylin and eosin shows the heterogeneous differentiation profile of teratomas derived from wildtype ES cells (a) compared with the more homogeneous and undifferentiated histological features of teratomas derived from homozygous *Apc*<sup>1638N</sup> ES cells (b). c, Detail of homozygous *Apc*<sup>1638N</sup> teratomas stained with an antibody against lysozyme identifying Paneth cells (p) within a non-ciliated secretory epithelium, and teratomas stained with Alcian blue identifying secretory goblet cells (g), both indicative of intestinal differentiation. d, Histological section of a homozygous *Apc*<sup>1638T</sup> teratoma stained with Alcian blue and hematoxylin shows cartilage/bone (blue) differentiation. Sections of compound heterozygous *Apc*<sup>1638N/1572T</sup> teratomas stained with hematoxylin and eosin showed a high degree of vascularization (e) and a ciliated secretory epithelium (cil; f) that were absent in *Apc*<sup>1638N/1638N</sup> teratomas. Immunohistochemical staining of paraffin sections from wildtype (g–k) and homozygous *Apc*<sup>1638N/1638N</sup> (l–p) teratomas with neural markers NCAM (g,l), neurofilament (h,m), synaptic vesicles (i,n), GFAP (j,o) and smooth muscle (k,p). The slides were lightly counterstained with hematoxylin. q–t, Expression and subcellular localization of  $\beta$ -catenin in teratomas derived from ES cells with mutations in *Apc*. Paraffin sections were stained for  $\beta$ -catenin by immunohistochemistry and counterstained with hematoxylin. q, Wildtype teratomas showed mainly cytoplasmic and membranous  $\beta$ -catenin staining. r, *Apc*<sup>1638N/1638T</sup> teratomas showed a clear increase and heterogeneity of intracellular  $\beta$ -catenin. s, *Apc*<sup>1638N/1572T</sup> teratomas showed moderate nuclear  $\beta$ -catenin staining. t, *Apc*<sup>1638N/1638N</sup> teratomas showed strong nuclear  $\beta$ -catenin staining in cells undergoing mesenchymal condensation and epithelial differentiation. Scale bars = 0.1 mm.

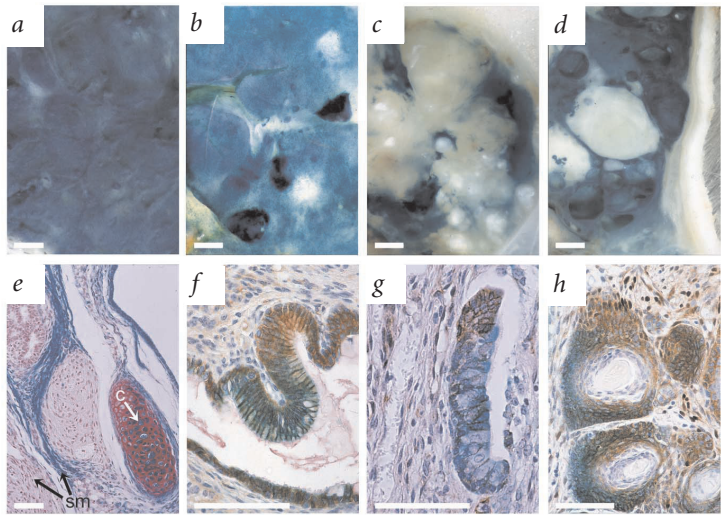


Table 1 • Tissue-specific gene expression profiles in teratomas with mutations in *Apc*

Unigene	Gene symbol and name	Factor of difference relative to wildtype			
		<i>Apc</i> <sup>1638N/1638N</sup>	<i>Apc</i> <sup>1638N/1572T</sup>	<i>Apc</i> <sup>1638N/1638T</sup>	<i>Apc</i> <sup>1638T/1638T</sup>
Neural-specific genes					
Mm.1287	<i>Mapt*</i> (microtubule-associated protein $\tau$ )	-100	-100	-2.3	1.1
Mm.1287	<i>Mapt*</i> (microtubule-associated protein $\tau$ )	-95.5	-100	-2.6	-1.1
Mm.3304	<i>Nsg2</i> (neuron-specific gene family member 2)	-74.1	-64.6	-4.5	-1.5
Mm.4599	<i>Astn1</i> (astrotactin 1)	-53.7	-30.2	-3.4	-1.4
Mm.40615	<i>Kcnaq2</i> (potassium voltage-gated channel subfamily Q member 2)	-52.5	-25.1	-5.1	-2.2
Mm.2496	<i>Ina</i> ( $\alpha$ internexin neuronal intermediate filament protein)	-100	-69.2	-2.7	-1.1
Mm.1419	<i>Aqp4*</i> (aquaporin 4)	-45.7	-20.4	-1.3	2.4
Mm.1419	<i>Aqp4*</i> (aquaporin 4)	-18.2	-8.1	-1.4	2.2
Mm.34637	<i>Catna2*</i> (catenin $\alpha$ 2)	-39.8	-36.3	-5.6	-1.7
Mm.34637	<i>Catna2*</i> (catenin $\alpha$ 2)	-8.3	-3.5	-2.6	1.1
Mm.34637	<i>Catna2*</i> (catenin $\alpha$ 2)	-6.8	-10.5	-2.4	-1
Mm.5309	<i>Gabrg2</i> ( $\gamma$ -aminobutyric acid A receptor subunit $\gamma$ 2)	-37.2	-24.5	-4.7	-1.3
Mm.5101	<i>Syt1</i> (synaptotagmin 1)	-27.5	-14.5	-12.3	-12.3
Mm.2991	<i>Oprl</i> (opioid receptor-like)	-18.2	-8.5	-7.4	-1.7
Mm.57194	<i>L1cam</i> (L1 cell adhesion molecule)	-18.2	-11.2	-8.3	-10.2
Mm.28562	<i>Syt9</i> (synaptotagmin 9)	-17.8	-17.8	-3	-1.2
Mm.2419	<i>Cdh4</i> (cadherin 4)	-17.4	-6.6	-2.3	1
Mm.1239	<i>Gfap</i> (glial fibrillary acidic protein)	-13.8	-4.8	-1.7	2
Mm.20892	<i>Syn2</i> (synapsin II)	-8.3	-5.8	-1.7	-1
Mm.4974	<i>Ncam1</i> (neural cell adhesion molecule 1)	-7.6	-7.6	-2.5	-1.5
Mm.4921	<i>Gria2</i> (glutamate receptor ionotropic AMPA2 $\alpha$ 2)	-7.2	-23.4	-4.7	-1.5
Mm.180868	<i>Syt11</i> (synaptotagmin 11)	-6.6	-6.5	-3.3	-3.4
Mm.4920	<i>Gria1</i> (glutamate receptor ionotropic AMPA1 $\alpha$ 1)	-6.2	-10.7	-3.4	-1.5
Mm.10696	<i>Nrg1</i> (neuregulin 1)	-5	-1.2	-1.4	1.2
Bone- and cartilage-specific genes					
Mm.4987	<i>Ibsp</i> (integrin-binding sialoprotein)	-4.4	-19.1	-2	-1.4
Mm.4778	<i>Cspg3</i> (chondroitin sulfate proteoglycan 3)	-10	-4.4	-7.2	-3
Mm.2759	<i>Agc1</i> (aggrecan 1)	-4.4	-5.2	1.5	-2.9
Mm.5091	<i>Spock1</i> (sparc/osteonectin cwcv and kazal-like domains proteoglycan 1)	-2.3	-3.7	-2.5	-2
Mm.7964	<i>Cdrap</i> (cartilage-derived retinoic acid-sensitive protein)	-10.7	-3.8	-1.3	1
Muscle-specific genes					
Mm.1529	<i>Mylpc</i> (myosin light chain phosphorylatable cardiac ventricles)	-34.7	-16.2	2.9	1.1
Mm.46514	<i>Mylc2a</i> (myosin light chain regulatory A)	-13.2	-9.1	4.7	1.3
Mm.16528	<i>Myog</i> (myogenin)	-1.6	4.2	2.1	1.8
Mm.3153	<i>Myh11</i> (myosin heavy chain 11 smooth muscle)	2.2	1.6	5.1	2.2
Mm.36850	<i>Smtn</i> (smoothelin)	19.1	13.5	9.5	-2.2
Intestine-specific genes					
Mm.15621	<i>Cftr</i> (cystic fibrosis transmembrane conductance regulator homolog)	5.6	3.8	1.4	2.3
Mm.10805	<i>Col13a1</i> (procollagen type XIII $\alpha$ 1)	6.6	6.6	-1.1	1.5
Mm.4010	<i>Vil</i> (villin)	8.7	4.2	2.3	1.6
Mm.27830	<i>Slc7a8</i> (solute carrier family 7, cationic a a. transporter, $y^+$ system, member 8)	12.3	2.8	-1.1	1.9
Mm.57132	<i>Defcr-ps1</i> (defensin-related cryptdin pseudogene 1)	16.6	4	-1.1	1.3
Mm.157909	<i>Defcr-rs1</i> (defensin-related sequence cryptdin peptide paneth cells)	32.4	7.2	1.2	1.3
Mm.140173	<i>Defcr5</i> (defensin-related cryptdin 5)	47.9	8.7	-1.3	2.7
Mm.14271	<i>Defcr-rs2</i> (defensin-related cryptdin related sequence 2)	60.3	4.4	3	1.8
Lung-specific genes					
Mm.7420	<i>Tubb4</i> (tubulin $\beta$ 4)	-16.6	-47.9	-2.6	-1.1
Mm.10414	<i>Mlf1</i> (myeloid leukemia factor 1)	-10	-4.6	-2.4	1.1
Mm.42257	<i>Tekt1</i> (tektin 1)	-6.8	-3.7	-2	1.3
Globin genes					
Mm.2308	<i>Hbb-bh1*</i> (hemoglobin Z $\beta$ -like embryonic chain)	4.9	11	4.7	3.2
Mm.2308	<i>Hbb-bh1*</i> (hemoglobin Z $\beta$ -like embryonic chain)	26.9	18.6	4.5	-1.7
Mm.141758	<i>Hba-x</i> (hemoglobin X $\alpha$ -like embryonic chain in Hba complex)	15.8	28.8	7.2	-1.1
Mm.35830	<i>Hbb-y</i> (hemoglobin Y $\beta$ -like embryonic chain)	100	81.3	16.2	-1.3

Genes whose expression patterns were validated by immunohistochemistry are indicated in bold. The listed entries were selected based on their tissue-specific expression from the unsupervised agglomerative cluster analysis by the error model in Rosetta Resolver v3.0 Gene Expression Data Analysis System. A total of 1,484 genes were included that differed by a factor of 2 with  $P < 0.01$  when compared with the wild type (*Apc*<sup>+/+</sup>). Some genes (marked with an asterisk and listed next to each other in the table) have multiple independent entries in the Affymetrix microarray that we used. As expected, variations in the corresponding factor of difference were observed, although the general trend of differential expression was concordant.

**Fig. 3** Analysis of chimeric teratomas showed the cell-autonomous nature of the differentiation defect of ES cells with mutations in *Apc*. **a**, Stereomicroscopic view of a wildtype *Apc* teratoma solely composed of ES cells targeted with a Rosa26- $\beta$ -geo construct showing uniform lacZ expression (blue). **b**, Stereomicroscopic view of a chimeric teratoma composed of wildtype Rosa26- $\beta$ -geo (blue) and non-tagged (white) wildtype ES cells showing uniform amalgamation of the two cell types, resulting in a light blue appearance with small patches of unicellular contribution. **c**, Stereomicroscopic view of a chimeric teratoma composed of tagged wildtype (blue) and *Apc*<sup>1638N/1638N</sup> (white) ES cells showing a non-uniform distribution of the two cell types. **d**, Stereomicroscopic view of a chimeric teratoma composed of tagged wildtype (blue) and *Apc*<sup>1638N/1572T</sup> (white) ES cells showing the same sorting mechanism as in **c**. **e**, Histological section of chimeric Rosa26- $\beta$ -geo-*Apc*<sup>+/+</sup> (blue) and *Apc*<sup>1638N/1638N</sup> (red) ES cells stained for  $\beta$ -galactosidase activity (turquoise blue) and counterstained with basic fuchsin (red nuclei), showing contribution of both cell types in smooth muscle (sm) and of exclusively Rosa26- $\beta$ -geo cells in cartilage (c). **f–h**, Histological sections of chimeric Rosa26- $\beta$ -geo-*Apc*<sup>+/+</sup>/non-tagged *Apc*<sup>+/+</sup> ES teratomas (**f**) and of Rosa26- $\beta$ -geo-*Apc*<sup>+/+</sup>/non-tagged *Apc*<sup>1638N/1638N</sup> teratomas (**g** and **h**) stained for  $\beta$ -galactosidase activity (turquoise blue cytoplasm), immunostained against  $\beta$ -catenin (brown) and counterstained with hematoxylin (blue nuclei).  $\beta$ -catenin was homogeneously expressed in the chimeric epithelium composed of the same cell type (**f**). The mutant epithelium expressed high levels of  $\beta$ -catenin and had differentiated to non-ciliated epithelium (g, white arrowhead), whereas the wildtype part containing relatively low levels of  $\beta$ -catenin had differentiated to ciliated epithelium (g, black arrowhead). This nicely demonstrates the correlation between the *Apc* defect, increased  $\beta$ -catenin dose and differentiation. **h**, Nuclear translocation of  $\beta$ -catenin in mutant cells was not prevented by surrounding wildtype cells. White bar = 1 mm; black bar = 0.1 mm.



ciliated secretory epithelia including Paneth cells, which are indicative of intestinal differentiation (Fig. 2c). Hence, homozygous *Apc*<sup>1638N</sup> ES cells showed severe differentiation defects that affected the neuroectodermal, dorsal mesodermal and endodermal lineages. In contrast, teratomas derived from homozygous *Apc*<sup>1638T/1638T</sup> or from compound *Apc*<sup>1638N/1638T</sup> ES cells were indistinguishable from wildtype teratomas at both the immunohistochemical and histological levels (Fig. 2d and data not shown), indicating that the differentiation defects observed in the *Apc*<sup>1638N/1638N</sup> teratomas were directly correlated to the quantitative expression of the 182-kD truncated protein.

We analyzed  $\beta$ -catenin expression in the teratomas by immunohistochemistry (Fig. 2q–t) and observed intense and abundant nuclear staining in the *Apc*<sup>1638N/1638N</sup> teratomas. The nuclear staining was not observed in every cell, but was clearly present in structures undergoing mesenchymal condensation and epithelial differentiation, a process known to be mediated by Wnt signaling<sup>17</sup> (Fig. 2t). Notably, compound heterozygous *Apc*<sup>1638N/1638T</sup> teratomas in which the *Apc*<sup>1638</sup> protein was expressed at approximately 50% of the level observed in homozygous *Apc*<sup>1638T</sup> cells did not show clear nuclear  $\beta$ -catenin accumulation but showed differences in  $\beta$ -catenin cytoplasmic staining patterns between flanking epithelial sheets, suggesting a more subtle defect of its downregulation by *Apc* (Fig. 2r). These abnormal staining patterns were never observed in *Apc*<sup>1638T/1638T</sup> or wildtype teratomas. The low dose (2%) of the *Apc*<sup>1638</sup> protein in homozygous *Apc*<sup>1638N</sup> teratomas seemed, therefore, to be insufficient to prevent nuclear accumulation of  $\beta$ -catenin during differentiation. On the other hand, a 50% increase in the dose of this truncated protein, as expressed by the *Apc*<sup>1638N/1638T</sup> teratomas, was sufficient to prevent  $\beta$ -catenin nuclear accumulation.

These results point to a direct relationship between nuclear accumulation of  $\beta$ -catenin and differentiation. To test this hypothesis, we analyzed the differentiation potential of *Apc*<sup>1572T</sup>, a truncated *Apc* protein almost identical to

*Apc*<sup>1638T</sup> except for the deletion of the last residual SAMP repeat (axin-binding domain; ref. 9; Fig. 1a). The *Apc*<sup>1572T</sup> protein was stably expressed (Fig. 1b), but its ability to downregulate  $\beta$ -catenin was impaired owing to its failure to bind axin. The *Apc*<sup>1572T</sup> mutation was targeted in ES cells in both the heterozygous (*Apc*<sup>+/1572T</sup>) and compound *Apc*<sup>1638N/1572T</sup> forms to allow comparison with *Apc*<sup>1638N/1638T</sup> and *Apc*<sup>1638N/1638N</sup> cells. Teratomas derived from *Apc*<sup>+/1572T</sup> ES cells had normal differentiation profiles whereas those derived from compound heterozygous *Apc*<sup>1638N/1572T</sup> ES cells had much lower differentiation potential than *Apc*<sup>1638N/1638T</sup> and wildtype counterparts. The differentiation defects of *Apc*<sup>1638N/1572T</sup> ES cells closely resembled those observed in *Apc*<sup>1638N/1638N</sup> teratomas, except that they maintained their capacity to differentiate into ciliated epithelia (Fig. 2e,f). Nuclear translocation of  $\beta$ -catenin was also evident, although the frequency and intensity were somewhat lower than those observed in the homozygous *Apc*<sup>1638N</sup> teratomas (Fig. 2s). Thus, removal of the only axin-binding motif in the *Apc*<sup>1638T</sup> protein resulted in nuclear translocation of  $\beta$ -catenin and in considerably lower differentiation potential.

#### Expression profiling of teratomas with mutations in *Apc* by oligonucleotide microarrays

The differentiation defect that we observed in teratomas with mutations in *Apc* by immunohistochemical analysis probably resulted from profound changes in gene expression patterns. We analyzed the teratomas by oligonucleotide microarrays encompassing probes for approximately 12,000 mouse genes and expressed sequence tags. Poly(A)<sup>+</sup> RNA was isolated from teratomas derived from wildtype (*Apc*<sup>+/+</sup>), *Apc*<sup>1638N/1638N</sup>, *Apc*<sup>1638N/1638T</sup>, *Apc*<sup>1638N/1572T</sup> and *Apc*<sup>1638T/1638T</sup> ES-cell lines and hybridized to the oligonucleotide microarrays. We used the gene expression profiles from the mutant teratomas to select for tissue-specific genes that were up- or downregulated relative to wildtype tumors.

We observed a strong correlation between the morphological and immunohistochemical characterization of the mutant teratomas and their tissue-specific expression profiles (Table 1). In particular, a large collection of neuroectodermal-specific probes were shown to be consistently downregulated among the teratomas with mutations in *Apc* (Table 1), in agreement with previous histological and immunohistochemical observations (Fig. 2). Mesoderm-derived lineages such as bone and cartilage were also absent in mutant teratomas. Accordingly, bone- and cartilage-specific genes were considerably downregulated (Table 1). Other mesodermal lineages such as smooth and striated muscle were present and absent, respectively, in the mutant teratomas, as also shown by the differential up- and downregulation of the specific gene markers (Table 1). Specific endodermal lineages were also differentially represented in mutant teratomas: whereas non-ciliated epithelia of intestinal type were present (Fig. 2), ciliated epithelia such as those of the respiratory tract were under-represented or absent. Microarray analysis confirmed the upregulation of several intestinal markers (for example, defensin-related cryptidins), whereas lung-specific genes were downregulated (Table 1). Notably, we observed upregulation by a factor of up to 100 of embryonic  $\alpha$ - and  $\beta$ -like globin genes in the mutant tissues (Table 1).

### The *Apc* differentiation defect is cell-autonomous

To investigate the cellular nature of the differentiation defect that results from loss of *Apc* function, we generated chimeric teratomas composed of either *Apc*<sup>1638N/1638N</sup> or *Apc*<sup>1638N/1572T</sup> cells mixed with *Apc*<sup>+/+</sup> ES cells, the latter tagged with a constitutively expressed  $\beta$ -galactosidase gene (*Rosa26- $\beta$ -geo*)<sup>18</sup>. We generated chimeric teratomas with wildtype ES cells mixed with their *Rosa26- $\beta$ -geo*-targeted counterpart. This resulted in a homogeneous mixture of blue and unstained cells with a light blue macroscopic appearance when compared with teratomas made exclusively of wildtype *Rosa26- $\beta$ -geo* ES cells (Fig. 3*a,b*). When wildtype *Rosa26- $\beta$ -geo* ES cells were used together with ES cells with mutations in *Apc* to generate teratomas, we found all differentiated cell lineages in the resulting chimeric tumors, indicating that the homozygous *Apc*<sup>1638N</sup> and compound *Apc*<sup>1638N/1572T</sup> ES cells did not affect the differentiation potential of wildtype ES cells (Fig. 3).

In chimeric teratomas, the wildtype cells differentiated into tissues otherwise never observed in teratomas derived from *Apc*<sup>1638N/1638N</sup> and *Apc*<sup>1638N/1572T</sup> cells only, whereas other tissues contained both mutant and wildtype cells, showing that the *Apc* differentiation defect is cell-autonomous. Accordingly,  $\beta$ -catenin staining was markedly elevated and often nuclear in homozygous *Apc*<sup>1638N</sup> cells, but was cytoplasmic and membrane-bound in

wildtype cells, even in chimeric epithelia where mutant and wildtype cells were in direct contact with each other (Fig. 3*e-h*). Thus, the *Apc* mutation is cell-autonomous with respect to both differentiation and  $\beta$ -catenin downregulation capacity.

Notably, we observed cell sorting when we analyzed the chimeric teratomas macroscopically (Fig. 3*c,d*). We observed this non-uniform distribution of wildtype and mutant cells with both the homozygous *Apc*<sup>1638N</sup> and compound *Apc*<sup>1638N/1572T</sup> ES-cell lines. The cell sorting was probably due to homotypic cell-cell recognition. Further studies will elucidate the molecular and cellular mechanisms underlying this phenomenon.

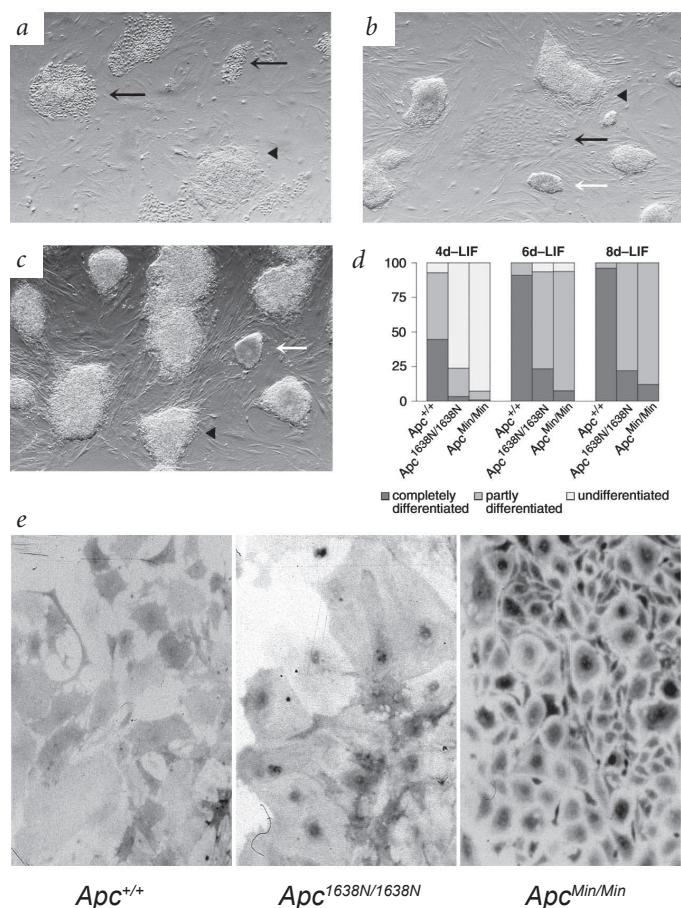
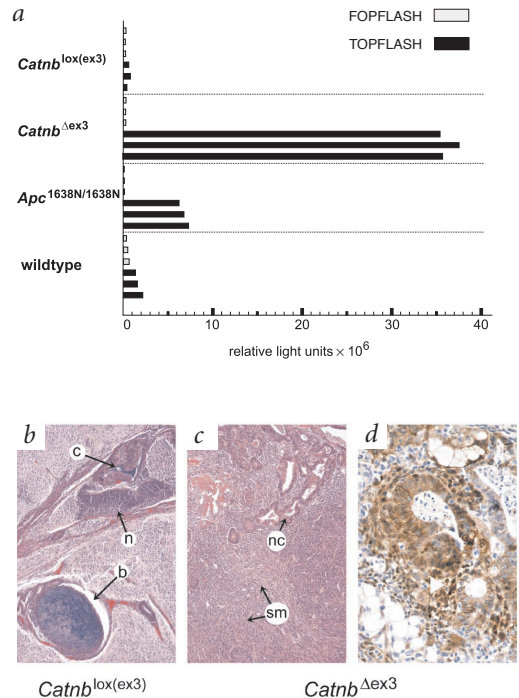


**Fig. 4** *In vitro* differentiation analysis of *Apc*<sup>Min</sup> and *Apc*<sup>1638N</sup> ES cells. Wildtype (*a*), homozygous *Apc*<sup>1638N/1638N</sup> (*b*) and *Apc*<sup>Min/Min</sup> (*c*) ES cells were cultured for 2 d with LIF. LIF was then withdrawn so that differentiation could occur, and colonies were monitored at 4, 6 and 8 d after the start of the cultures. Data shown is from 8 d of culture. The colonies were subdivided in three categories: completely undifferentiated with no mesenchymal cells protruding from the edge of the ES colony (white arrows); partly differentiated with mesenchymal cells surrounding a core of undifferentiated cells (black arrowheads); and completely differentiated, composed exclusively of mesenchymal cells (black arrows). *d*, Number (percentage of total) of completely undifferentiated (white bars), partly differentiated (gray bars) and completely differentiated (black bars) wildtype and mutant ES colonies after 4, 6 and 8 d of culture in absence of LIF. The value for each bar was determined from counting over 200 colonies from independently cultured plates and randomly selected stereomicroscopic fields. Results were confirmed by two independent experiments. *e*,  $\beta$ -catenin immunohistochemical staining of colonies differentiated *in vitro* showed absent, moderate and strong  $\beta$ -catenin nuclear accumulation in wildtype, *Apc*<sup>1638N/1638N</sup> and *Apc*<sup>Min/Min</sup> ES cells, respectively.



**Fig. 5** Biochemical and immunohistochemical analysis of teratomas with mutations in *Catnb*. **a**,  $\beta$ -catenin-Tcf reporter assays were carried out in wildtype (*Apc*<sup>+/+</sup> *Catnb*<sup>+/+</sup>), *Apc*<sup>1638N/1638N</sup> *Catnb*<sup>lox(ex3)</sup> (equivalent to wildtype) and *Catnb*<sup>Δex3</sup> (mutated) ES-cell lines. Undifferentiated ES cells were transfected with either the pTOPFLASH (black bars) or the pFOPFLASH (gray bars) luciferase reporter construct, together with the *R. reniformis* luciferase construct as an internal control<sup>19,15</sup>. Normalized pTOPFLASH and pFOPFLASH levels are indicated for each cell line from triplicate transfections. **b, c**, Differentiation profiles of teratomas with mutations in *Catnb*. Hematoxylin and eosin staining of paraffin-embedded sections of teratomas derived from generated *Catnb*<sup>lox(ex3)</sup> (**b**) and *Catnb*<sup>Δex3</sup> (**c**) ES cells. **d**, Expression and subcellular distribution of  $\beta$ -catenin in teratomas derived from *Catnb*<sup>Δex3</sup> ES cells. Paraffin sections were stained for  $\beta$ -catenin by immunohistochemistry and counterstained with hematoxylin. Overexpression and nuclear localization of  $\beta$ -catenin was observed in mesenchymal cell types (white arrowhead), among others. c, ciliated epithelium; n, neural lineages; b, bone; nc, non-ciliated epithelium; sm, smooth muscle.



### *Apc*<sup>Min/Min</sup> ES cells did not form teratomas

The above results are indicative of a dose-dependent defect in *Apc* in ES-cell differentiation, possibly owing to partial loss of  $\beta$ -catenin regulation. The *Apc*<sup>Min</sup> allele encodes a short truncated protein lacking all the  $\beta$ -catenin binding and downregulating domains and, therefore, is unable to control Wnt/ $\beta$ -catenin signaling. We attempted teratoma formation using independent blastocyst-derived *Apc*<sup>Min/Min</sup> ES-cell lines together with ES-cell lines derived from *Apc*<sup>+/+</sup> and *Apc*<sup>+/Min</sup> littermates as controls. Notably, all attempts to generate teratomas with *Apc*<sup>Min/Min</sup> ES-cell lines failed in our *in vivo* assay, whereas their *Apc*<sup>+/+</sup> and *Apc*<sup>+/Min</sup> counterparts gave rise to teratomas with normal differentiation patterns.

### *In vitro* differentiation analysis of *Apc*<sup>Min/Min</sup> and *Apc*<sup>1638N/1638N</sup> ES cells

The inability of *Apc*<sup>Min/Min</sup> ES-cell lines to form teratomas indicates a severe differentiation defect that may be due to the complete loss of  $\beta$ -catenin downregulating activity in this allele. To study in more detail the cellular nature of the most severe *Apc* differentiation defects, we carried out *in vitro* differentiation analysis of *Apc*<sup>Min/Min</sup> and *Apc*<sup>1638N/1638N</sup> ES-cell lines by simply withdrawing leukemia inhibiting factor (LIF) from the culture medium and by analyzing cell morphology at different time intervals when compared with wildtype cells (Fig. 4). In general, *Apc*<sup>Min/Min</sup> and *Apc*<sup>1638N/1638N</sup> ES cells differentiated at a much lower rate than their wildtype counterparts (eight days and two days, respectively). Although we eventually observed differentiation in both *Apc*<sup>Min/Min</sup> and *Apc*<sup>1638N/1638N</sup> ES cells, they seemed to maintain their undifferentiated state in culture for a considerably longer period than wildtype and heterozygous controls.

To identify the cell types formed after differentiation, we analyzed ES-cell colonies by immunohistochemical staining with different lineage-specific antibodies. Similar to teratomas, *Apc*<sup>1638N/1638N</sup> colonies formed massive amounts of smooth muscle but did not form neuroectodermal derivatives. *Apc*<sup>Min/Min</sup> colonies formed large amounts of visceral and parietal endoderm (identified by morphology and by antibodies against  $\alpha$ -fetoprotein and vimentin, respectively) but did not differentiate into smooth muscle cells or nerve cells. Notably, after prolonged culture of *Apc*<sup>Min</sup> cells, only extensive epithelial sheets of parietal endoderm were present (data not shown).

Next, we tried to modulate *in vitro* differentiation of the *Apc*<sup>Min</sup> and *Apc*<sup>1638N</sup> ES cells towards neuroectodermal, mesodermal and trophectodermal lineages by complementing the culture medium with retinoic acid, dimethyl sulfoxide and fibroblast growth factor 4, respectively<sup>19,20</sup>. Compared with the wildtype ES-cell line, neither *Apc*<sup>Min/Min</sup> nor *Apc*<sup>1638N/1638N</sup> ES cells responded to these stimuli, as we observed no change in their morphology or expression of tissue-specific markers (data not shown). This indicates that the differentiation defects cannot be rescued by external factors.

We also stained *Apc*<sup>Min</sup> and *Apc*<sup>1638N</sup> ES clones differentiated *in vitro* for  $\beta$ -catenin and compared them to *Apc*<sup>+/+</sup> ES cells (Fig. 4e). An intense nuclear signal was present in most *Apc*<sup>Min/Min</sup> cells. *Apc*<sup>1638N/1638N</sup> cells also had nuclear  $\beta$ -catenin, although the signal intensity was considerably weaker and less abundant than in the *Apc*<sup>Min</sup> clones. Wildtype ES cells did not show any nuclear accumulation of  $\beta$ -catenin. Excessive  $\beta$ -catenin accumulation in the nucleus has been shown to result in programmed cell death<sup>21</sup>, which may explain the inability of *Apc*<sup>Min/Min</sup> to form teratomas.

### Impaired differentiation in ES cells with mutations in *Catnb*

We confirmed that the differentiation defect observed in ES cells with mutations in *Apc* was due to the loss of the  $\beta$ -catenin regulating function by repeating the teratoma differentiation assay with ES cells carrying a Cre-*loxP* mediated deletion of exon 3 of  $\beta$ -catenin (ref. 22). This exon encompasses all serine/threonine residues of  $\beta$ -catenin, which are phosphorylation targets that earmark  $\beta$ -catenin for ubiquitination and proteolytic degradation. We used two ES-cell lines: *Catnb*<sup>lox(ex3)</sup>, in which exon 3 of the  $\beta$ -catenin gene is flanked by *loxP* sites without compromising functionality of the corresponding allele, and *Catnb*<sup>Δex3</sup>, which was obtained by Cre-mediated deletion of exon 3 (ref. 22). The two ES-cell lines were first analyzed by TOPFLASH reporter assay and compared with wildtype and *Apc*<sup>1638N/1638N</sup> ES-cell lines (Fig. 5a). *Catnb*<sup>Δex3</sup> ES cells had approximately three times higher reporter levels than did *Apc*<sup>1638N/1638N</sup> ES cells. Direct comparison between *Catnb*<sup>Δex3</sup> and *Apc*<sup>Min/Min</sup> ES cells was not feasible, as these lines were only available in different genetic backgrounds. TOPFLASH reporter levels in *Catnb*<sup>lox(ex3)</sup> were indistinguishable from those observed in wildtype cells.

Next, *Catnb*<sup>lox(ex3)</sup> and *Catnb*<sup>ex3</sup> ES cells were assayed for their differentiation potential by teratoma formation. Teratomas were successfully derived from both cell lines. *Catnb*<sup>lox(ex3)</sup> differentiation profiles were indistinguishable from those obtained with wildtype ES cells, whereas *Catnb*<sup>ex3</sup> cells formed teratomas with limited differentiation patterns, similar to those observed in *Apc*<sup>1638N/1638N</sup>. In particular, ectoderm-derived cell lineages were absent, whereas an abundance of smooth muscle and non-ciliated epithelia was observed (Fig. 5b). Nuclear  $\beta$ -catenin localization (Fig. 5b) and other immunohistochemical observations obtained with the same set of antibodies that we used to analyze teratomas with mutations in *Apc* (data not shown) confirmed these aberrant differentiation patterns in the *Catnb*<sup>ex3</sup> teratomas.

These data confirm that the differentiation defect observed in ES cells with mutations in *Apc* was due to improper  $\beta$ -catenin regulation. Moreover, different doses of residual  $\beta$ -catenin directly correlated with differences in differentiation potential and with the intensity and frequency of nuclear accumulation of  $\beta$ -catenin. Taken together, the data point to a dose-response

effect between *Apc* mutations affecting the  $\beta$ -catenin downregulating function, the increase in  $\beta$ -catenin-mediated transcriptional activity and the differentiation defects in ES cells.

### Expression profiling and data mining

Loss of  $\beta$ -catenin regulation may cause multiple changes in the transcription of several genes downstream in the Wnt pathway. To investigate the changes in gene expression that accompany the differentiation of wildtype and *Apc*-mutated ES cells, and to pinpoint potential key regulatory genes, we analyzed the teratomas with mutations in *Apc* by Affymetrix microarray technology. We compared expression data from the mutant teratomas with the wildtype tumors by an unsupervised, hierarchical clustering algorithm. This analysis correctly clustered the mutant teratomas characterized by aberrant differentiation (*Apc*<sup>1638N/1638N</sup> and *Apc*<sup>1638N/1572T</sup>) apart from those that were indistinguishable from the wildtype tumors at the immunohistochemical level (*Apc*<sup>1638N/1638T</sup> and *Apc*<sup>1638T/1638T</sup>; Fig. 6a). The majority of genes up- or downregulated in *Apc*<sup>1638N/1638N</sup>, *Apc*<sup>1638N/1572T</sup>

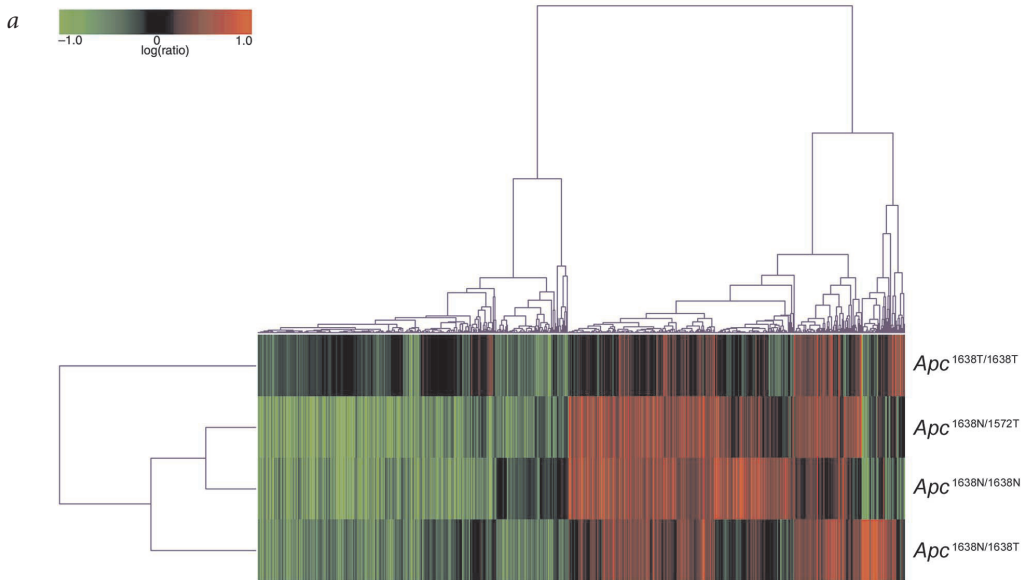
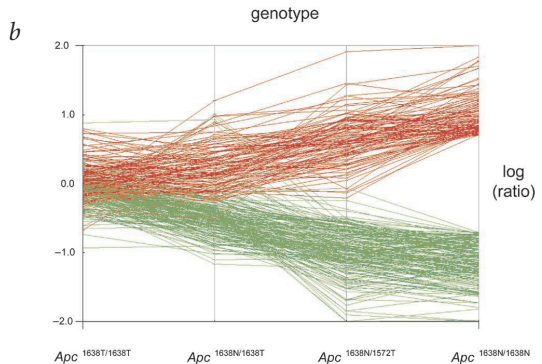


**Fig. 6** Expression profiling analysis of teratomas with mutations in *Apc*. **a**, Two-dimensional agglomerative cluster analysis of mutant teratomas compared with wildtype (*Apc*<sup>+/+</sup>). A total of 1,484 genes showed expression that differed by a factor of 2 with  $P < 0.01$ . Each row represents a specific genotype/teratoma and each column a single gene. As shown in the colored bar, red indicates upregulation, green downregulation and black no change. **b**, Expression analysis of a selected group ( $n = 300$ ) of differentially expressed genes in the four different mutated *Apc* genotypes. For this analysis, genes differentially expressed by a factor of  $\pm 5$  and  $P = 0.01$  between the *Apc*<sup>1638N/1638N</sup> and *Apc*<sup>+/+</sup> arrays are shown. Genes differentially expressed between the *Apc*<sup>1638T/1638T</sup> and *Apc*<sup>+/+</sup> arrays by a factor of  $\pm 2$  and  $P = 0.01$  were excluded from this analysis. The rationale for this exclusion is that the *Apc*<sup>1638T/1638T</sup> and *Apc*<sup>+/+</sup> genotypes do not differ both in terms of signaling activity (as measured by TOPFLASH) and differentiation (as measured by teratoma assay). Hence, genes differentially expressed between these two ES-cell lines are not likely to contribute to the differentiation defect due to Wnt signaling activation and could be excluded to reduce background noise.



and, to a lesser extent, *Apc*<sup>1638N/1638T</sup> teratomas were, in general, not changed in *Apc*<sup>1638T/1638T</sup> teratomas (Fig. 6a). This confirms that the mutated *Apc* genotypes that result in constitutive activation of Wnt signaling are characterized by distinct gene expression profiles when compared with teratomas derived from Wnt-proficient ES-cell lines (as judged by TOPFLASH reporter assays).

Among the differentially expressed entries, both structural tissue-specific (Table 1) and regulatory (Table 2) genes were identified. The latter belong to well-known signal-transduction pathways such as Wnt, transforming growth factor  $\beta$ , fibroblast growth factor and retinoic acid (Table 2). Although the elucidation of the signal-transduction pathways underlying the stem-cell differentiation caused by mutations in *Apc* is beyond the scope of the present study, the pattern of differential expression among these genes seems to agree with the differentiation defects observed in the mutant teratomas. For example, the upregulation of the bone morphogenetic proteins 2 and 4 (encoded by *Bmp2* and *Bmp4*; Table 2) may explain

some of the observed differentiation defects. Bmp proteins are morphogenetic signaling proteins belonging to the Tgfb superfamily originally isolated for their capacity to induce ectopic bone formation<sup>23,24</sup>. Bmp proteins signal through heteromeric complexes of type I and type II transmembrane Ser/Thr kinase receptors, triggering the expression of downstream target genes. Among the latter, the homeobox genes *Msx1* and *Msx2* have been previously reported to be induced by *Bmp2* and *Bmp4* (ref. 25) and are accordingly upregulated in teratomas with mutations in *Apc* (Table 2). Expression of *Msx1* (and *Msx2*) is known to interfere with the differentiation process by blocking cell-cycle exit through upregulation of cyclin D1 (ref. 26). Though the gene encoding cyclin D1 was not upregulated in our data set, the homolog cyclin D3 was (Table 2). The gene T-box 2 (*Tbx2*), a known modulator (both activator and repressor) of bone development whose activity largely depends on the cellular context, was also upregulated in teratomas with mutations in *Apc*<sup>27</sup> (Table 2). *Tbx2* expression is induced by *Bmp2* (ref. 28).

**Table 2 • Signal-transduction gene expression profiles in teratomas with mutations in *Apc*.**

Unigene	Gene symbol and name	Factor of difference relative to wildtype			
		<i>Apc</i> <sup>1638N/1638N</sup>	<i>Apc</i> <sup>1638N/1572T</sup>	<i>Apc</i> <sup>1638N/1638T</sup>	<i>Apc</i> <sup>1638T/1638T</sup>
Wnt pathway genes					
Mm.20355	<i>Wnt4</i> (wingless-related MMTV integration site 4)	18.6	3.9	5.6	5.2
Mm.22182	<i>Wnt11</i> (wingless-related MMTV integration site 11)	10.5	5.4	9.1	1
Mm.2438	<i>Wnt6</i> (wingless-related MMTV integration site 6)	8.1	1.9	-1.3	1.4
Mm.32207	<i>Wnt5a</i> (wingless-related MMTV integration site 5A)	7.1	3.2	-1.1	1
Mm.5130	<i>Wnt10a</i> (wingless-related MMTV integration site 10a)	6	1.3	1	1.9
Mm.45050	<i>Fzd1</i> (frizzled homolog 1 <i>Drosophila</i> )	3.3	1.7	-2.2	-3.9
Mm.103593	<i>Dkk2</i> (dickkopf 2)	21.9	14.1	1.9	-1.3
Mm.7960	<i>Dkk1</i> (dickkopf homolog 1 <i>Xenopus laevis</i> )	11.5	8.3	3.7	1.4
Mm.2029	<i>Lef1</i> (lymphoid enhancer binding factor 1)	2	1.3	-1.8	1.1
Mm.5080	<i>Sox17</i> (SRY-box containing gene 17)	4.8	4.2	3.5	1.9
Mm.2580	<i>Sdc1</i> (syndecan 1)	18.6	6.5	2.2	-1.1
Mm.4272	<i>Snai2</i> (snail homolog 2 <i>Drosophila</i> )	6.8	5.2	2.1	2
Mm.6813	<i>Bmp4</i> * (bone morphogenetic protein 4)	3.9	2.3	1.4	-1.1
Mm.13828	<i>Wisp2</i> (WNT1 inducible signaling pathway protein 2)	5.1	2.8	1.9	1.5
Mm.7417	<i>Ccnd3</i> (cyclin D3)	2.6	3.2	2.1	-1.2
Mm.16234	<i>Itga5</i> (integrin $\alpha$ 5 fibronectin receptor $\alpha$ )	10.6	5	4.8	2.3
Mm.5039	<i>Six2</i> (sine oculis-related homeobox 2 homolog <i>Drosophila</i> )	7.9	8.7	1.9	-1.3
Tgfb pathway genes					
Mm.57216	<i>Bmp2</i> (bone morphogenetic protein 2)	13	2.3	1.9	-1.2
Mm.6813	<i>Bmp4</i> * (bone morphogenetic protein 4)	6.3	4.3	1.4	-1.4
Mm.9154	<i>Tgfb1</i> (transforming growth factor $\beta$ 1)	5.5	2.8	-1.6	-3
Mm.18213	<i>Tgfb2</i> (transforming growth factor $\beta$ 2)	4.1	2.4	-1.5	-1.4
Mm.8042	<i>Inhba</i> (inhibin $\beta$ -A)	7.8	1.4	-1.7	1.2
Mm.9404	<i>Nbl1</i> (neuroblastoma suppression of tumorigenicity 1)	6.2	6.1	3	2.5
Mm.19307	<i>Ltbp1</i> (latent transforming growth factor $\beta$ binding protein 1)	6.1	9.2	2	1.3
Mm.1763	<i>Msx2</i> (homeo box msh-like 2)	69.2	8.5	2.8	2.3
Mm.870	<i>Msx1</i> (homeo box msh-like 1)	5.3	2	-1.1	1.1
Mm.5194	<i>Dlx3</i> (distal-less homeobox 3)	17	4.1	1.4	-1.5
Mm.23467	<i>D5Ert189e</i> (DNA segment Chr 5 ERATO Doi 189 expressed)	11.2	8.9	1.3	1.4
Mm.4605	<i>Tbx2</i> (T-box 2)	4.8	4.6	1.3	1.6
Mm.4509	<i>Runx2</i> (runt-related transcription factor 2)	8.7	2.6	-1	-1.8
Fgf pathway genes					
Mm.4912	<i>Fgfr4</i> (fibroblast growth factor receptor 4)	13.8	3.2	-1.3	-1.5
Mm.16340	<i>Fgfr2</i> * (fibroblast growth factor receptor 2)	3.5	1.7	1	-6
Mm.3157	<i>Fgfr1</i> (fibroblast growth factor receptor 1)	3.2	1.9	1.2	1.3
Mm.16340	<i>Fgfr2</i> * (fibroblast growth factor receptor 2)	2.5	1	-1	-2.5
Mm.2580	<i>Sdc1</i> (syndecan 1)	18.6	6.5	2.2	-1.1
Mm.67919	<i>Maib</i> (v-maf musculoaponeurotic fibrosarcoma oncogene family protein B)	11.5	2.3	1.7	1.1
Retinoic acid pathway genes					
Mm.1273	<i>Rarg</i> (retinoic acid receptor $\gamma$ )	46.8	10.7	2.8	-2
Mm.34797	<i>Crabp1</i> (cellular retinoic acid-binding protein I)	9.8	6.6	3.3	5.4
Mm.4757	<i>Crabp2</i> (cellular retinoic acid-binding protein II)	3.2	3.3	1.4	1.9

The listed entries were derived from the unsupervised agglomerative cluster analysis by the error model in Rosetta Resolver v3.0 Gene Expression Data Analysis System (1,484 genes included that differed by a factor of 2 with  $P < 0.01$  when compared with the wild type (*Apc*<sup>+/+</sup>)) and classified into the different signaling pathways based on the information provided by the Affymetrix Gene Ontology annotations. Some genes (marked with an asterisk) have multiple entries in the Affymetrix microarrays that we used.

Notably, we also found that dickkopf genes (*Dkk1* and *Dkk2*) were upregulated in teratomas with mutations in *Apc* (Table 2). *Dkk1* and *Dkk2* encode secreted proteins that act as potent inhibitors of Wnt signaling, are involved in head induction in *Xenopus laevis* embryogenesis and are highly expressed during mouse development in mesodermal tissues that mediate epithelial–mesenchyme transitions<sup>29</sup>. The upregulation of the *Dkk1* and *Dkk2* inhibitors is in apparent contradiction to the similar behavior of several Wnt-related genes, including inducers/ligands (Wnt-ligands), receptors (frizzled), transcription factors (lymphoid enhancer binding factor 1) and downstream targets (WNT1-inducible signaling pathway proteins, cyclins and others; Table 2). The complexity and tissue heterogeneity of the teratomas are confounding factors, however, as we cannot ascertain which tissues contribute to which differential gene expression patterns.

To visualize the Apc– $\beta$ -catenin dose-dependent control of gene expression, we selected a subset of 300 highly differentially expressed genes in *Apc*<sup>1638N/1638N</sup> teratomas (that is, those that differed by a factor of >5 or <–5). We subtracted those that were differentially expressed in *Apc*<sup>1638T/1638T</sup> relative to wildtype teratomas (those that differed by a factor of >2 or <–2) and followed their behavior in the four genotypes (Fig. 6b). We observed a clear gradient of transcriptional response starting from the Wnt-proficient alleles (*Apc*<sup>1638T/1638T</sup>) and gradually increasing (or decreasing) in more severely affected genotypes (*Apc*<sup>1638N/1638T</sup>, *Apc*<sup>1638N/1572T</sup>, *Apc*<sup>1638N/1638N</sup>). This clearly indicates that different doses of  $\beta$ -catenin made available for Wnt signaling by specific *Apc* defects resulted in different target-gene expression responses and, consequently, in different degrees of ES-cell differentiation.

The rationale for our data mining approach (Fig. 6b) was the observation that the *Apc*<sup>1638T/1638T</sup> ES cells were shown to be Wnt- and differentiation-proficient by TOPFLASH reporter and by teratoma assays, respectively<sup>9</sup>. Hence, the differential expression in *Apc*<sup>1638T/1638T</sup> relative to wildtype teratomas was probably caused by  $\beta$ -catenin-independent effects. The recently characterized chromosomal instability of the ES-cell lines with mutations in *Apc* that we used<sup>30</sup> may partly account for this differential gene expression. Loss of this function of *Apc* in mitosis cannot possibly account for the differentiation defects reported here, however, as *Apc*<sup>1638T/1638T</sup> ES cells were shown to be chromosomally unstable but differentiation-proficient.

## Discussion

In this study, we show that mutations in *Apc* affect the differentiation capacity of mouse ES cells in a quantitative and qualitative fashion depending on the dose of  $\beta$ -catenin signaling. This direct correlation between differentiation and Apc/ $\beta$ -catenin signal transduction has implications for understanding the cellular mechanism underlying *Apc*-driven tumorigenesis. Although it is generally accepted that the tumor-suppressor function of *Apc* resides in its ability to downregulate  $\beta$ -catenin<sup>9,15,31–33</sup>, the tissue-specific downstream targets responsible for the broad tumor spectrum observed both in individuals affected with FAP<sup>12</sup> and *Apc*-mutated mouse models<sup>6</sup> are still largely unknown.

Our results are in agreement with the role of  $\beta$ -catenin signaling in maintaining stem-cell properties in the intestine, as also illustrated by the inability of mice that lack Tcf4 to form crypt stem cells<sup>13</sup>. In these mice, the neonatal epithelium is composed entirely of differentiated cells. Thus, the genetic program controlled by  $\beta$ -catenin signaling and executed by Tcf4 maintains the crypt stem cells of the small intestine and, on the basis of the data presented here, modulates differentiation. In the colonic

epithelium, mitotic cell rates equal terminal differentiation and cell loss rates. Intestinal tumors are the result of an increase in this gain:loss ratio. In view of the present data, this increase may be the consequence of a differentiation defect resulting from the constitutive activation of  $\beta$ -catenin signaling by mutations in *Apc*. This may retard or inhibit differentiation and ultimately result in an enlargement of the stem-cell compartment, the target cell population that undergoes additional mutations eventually leading to tumor formation.

In an alternative but analogous scenario, a differentiated colonic epithelial cell undergoes *Apc* (or *Catnb*) mutation, thus triggering a process of de-differentiation and, again, enlargement of the stem-cell compartment within the crypt. This would agree with the recently postulated 'top-down' model of colorectal tumorigenesis in which neoplastic transformation is initiated in a fully differentiated cell that becomes dysplastic, spreads laterally and progressively replaces the normal crypt cells<sup>34</sup>. In general, colorectal tumors do show a high proportion of undifferentiated crypt-like cells with high numbers of dividing cells, although all differentiated cell types are still present<sup>22,35</sup>. The same correlation between activation of Wnt/ $\beta$ -catenin signaling and stem-cell maintenance may also apply to other tumor types, as it represents an effective way to sustain tumor growth in a broad spectrum of self-renewing tissues. Accordingly, a large number of tumor types are characterized by  $\beta$ -catenin overexpression and/or nuclear localization. Recently, it was shown that overexpression of *Pin1* is responsible for the frequently observed  $\beta$ -catenin upregulation in breast cancer, a tumor type in which mutations in *APC* or *CATNB* are not common<sup>36</sup>. Different mutation types in different members of the Wnt pathway will result in different signaling doses associated with specific tumors in susceptible tissues.

In conclusion, we report that mutations in *Apc* and *Catnb* affect the capacity of embryonic stem cells to differentiate into the three germ layers in a  $\beta$ -catenin dose-dependent fashion. These results have implications for understanding the molecular and cellular basis of tumor initiation by defects in the Wnt pathway. We propose a model in which adult somatic stem-cell compartments are characterized by tissue-specific  $\beta$ -catenin threshold levels for cell proliferation, differentiation and apoptosis. Different mutations in *Apc* will result in different levels of intracellular  $\beta$ -catenin and will confer different degrees of tumor susceptibility in different tissues. Hence,  $\beta$ -catenin dose-dependent differentiation may explain not only how a single pathway is involved in the development of different tissues, but also its pleiotropic role in tumorigenesis.

## Methods

**Mice.** The experiments on mice were approved by the local animal experimental committee of the Leiden University and by the Commission Biotechnology in Animals of the Dutch Ministry of Agriculture (permission number VVA/BD 01.168).

**Constructs.** The gene-targeting Rosa26- $\beta$ -geo construct used to tag wild-type ES cells by homologous recombination fused the ubiquitously expressed protein encoded by the endogenous Rosa26 locus with a hybrid  $\beta$ -galactosidase–neomycin-resistance protein ( $\beta$ -geo). The construct was a derivative of the gene trap construct previously employed<sup>18</sup> and was constructed and kindly provided by J.-H. Dannenberg and H. te Riele.

**ES cell lines.** We mated heterozygous *Apc*<sup>+/1638N</sup> and *Apc*<sup>+/Min</sup> mice on a mixed C57BL/6J  $\times$  CD1 background and harvested blastocysts 3.5 d after fertilization. We plated the flushed pre-implantation blastocysts in 96-well dishes coated with mouse embryonic fibroblasts and cultured them to isolate undifferentiated ES-cell lines according to previously reported methods<sup>20</sup>. We obtained six independently isolated *Apc*<sup>Min/Min</sup>,



four *Apc*<sup>1638N/1638N</sup>, four littermate *Apc*<sup>+/Min</sup> and two wildtype *Apc*<sup>+/+</sup> ES-cell lines, which we used in the differentiation experiments. Only early passage (p4–p5) embryo-derived ES-cell lines were used. All remaining cell lines (*Apc*<sup>1638N/1638N</sup>, *Apc*<sup>1638N/1638T</sup>, *Apc*<sup>1572T/1638N</sup>, *Apc*<sup>1638T/1638T</sup>) were derived by gene targeting in the E14 ES-cell line (129/Ola), as previously described<sup>9</sup>. These cell lines were previously established and are therefore characterized by higher passage numbers (roughly p20). To exclude that the observed defects result from mutations acquired *in vitro*, at least two independently generated clones for each genotype were used in the teratoma assays.

We generated the *Catnb*<sup>lox(ex3)</sup> and *Catnb*<sup>ex3</sup> ES-cell lines by *loxP* gene targeting and by Cre-mediated deletion of exon 3 as previously described<sup>22</sup>.

**Generation of teratomas.** We prepared single-cell suspensions from semi-confluent undifferentiated ES-cell cultures grown on 9-cm culture dishes coated with mouse embryonic fibroblasts using 1× trypsin/EDTA (Life Technologies). We washed cells three times with a large volume of phosphate-buffered saline (PBS) and then injected subcutaneously a total of 4 × 10<sup>6</sup> cells in 200  $\mu$ l PBS into the flank of a syngenic mouse, C57BL/6J × CD1 recipient mice were used for the blastocyst-derived ES-cell lines (*Apc*<sup>1638N</sup> and *Apc*<sup>Min</sup>). We injected ES cells with mutations in *Apc* or *Catnb* derived by gene targeting in the E14 ES-cell line<sup>9,22</sup> into 129/Ola recipient mice. Chimeric teratomas were induced by mixing 2 × 10<sup>6</sup> cells of each cell line shortly before injection. After 3 wk, the mice were killed and teratomas were removed, washed with PBS, fixed overnight in 4% paraformaldehyde and processed for paraffin-based histology using standard techniques.

**Western-blot and immunoprecipitation analyses.** To detect the various mutant Apc proteins by western-blot analysis, we derived total protein lysates and immunoprecipitates from freshly cultured ES-cell lines and resolved them on agarose gels as described previously<sup>9</sup>. We quantified residual amounts of the Apc1638 protein by mixing homozygous *Apc*<sup>1638N</sup> ES cells with given percentages of wildtype ES cells before immunoprecipitation with the polyclonal antibody to N-terminal Apc (AFPN; ref. 9), immunoblotting and detecting product with a monoclonal antibody against Apc (Ab-1, Oncogene Research Products) recognizing amino acids 1–29 of Apc.

**In vitro differentiation of ES cells.** We plated 10<sup>4</sup> ES cells per well on 12-well tissue culture plates and cultured them in ES culture medium containing LIF (Life Technologies) for 2 d. Spontaneous differentiation was allowed by keeping the ES clones in culture for 2 d in the presence and for 6 d in the absence of LIF without passaging. We induced differentiation by plating 2-d-old embryoid bodies on gelatin-coated 12-well culture plates and withdrawing LIF. We achieved differentiation to mesodermal, neuroectodermal and trophoderm lineages by adding dimethyl sulfoxide (0.05%, 0.1%, 0.5%, 1% or 2%), retinoic acid (0.1 and 0.5  $\mu$ M, Sigma) and fibroblast growth factor 4 (25 ng ml<sup>-1</sup>), respectively, as previously described<sup>19,20</sup>.

**Immunohistochemical analysis of ES-cell colonies differentiated in vitro.** Differentiated embryoid bodies attached to 12-well dishes were fixed with 1% paraformaldehyde for 10 min, washed for 5 min in PBS, dehydrated in methanol and stored at -20 °C until use. For immunohistochemistry, plates were re-hydrated in PBS and blocked in 5% non-fat dried milk (NFDm) in PBS for 2 h at room temperature. The primary antibody was diluted in 5% NFDm 2 h before use. We incubated samples with the primary antibody at 4 °C overnight under gentle shaking. The next day, we washed the plates five times for 30 min at room temperature with PBS containing 0.1% Tween-20 (PBT), after which the plates were incubated overnight with the secondary antibody diluted in PBS containing 5% NFDm. The following day we washed the plates thoroughly with PBT, equilibrated them in alkaline phosphatase buffer for 15 min and stained them with 5-bromo-4-chloro-3-indolyl phosphate and nitro blue tetrazolium according to the manufacturer's recommendations (Roche).

**Antibodies.** The primary antibodies used for immunohistochemistry were: mouse antibody against  $\beta$ -catenin (Transduction Laboratories), antibody against AFP (Novocastra), antibody against NCAM (5B8, from

Developmental Studies Hybridoma Bank (DSHB)), antibody against neurofilament (2H3, DSHB), antibody against synaptic vesicles (SV-2, DSHB), antibody against GFAP (DAKO), antibody against smooth muscle actin (clone 1A4, Neomarkers Ab-1), antibody against striated muscle (A4.1025, DSHB), antibody against vimentin (NCL-VIM, Novocastra) and antibody against  $\alpha$ -fetoprotein (AFP 08-0055, Zymed Labs). The polyclonal antibody against AFPN was previously described<sup>9</sup>.

For conventional immunohistochemistry and western-blot analysis, we used a goat antibody against mouse IgG/IgM conjugated with peroxidase. We used a goat antibody against mouse IgG/IgM conjugated with alkaline phosphatase as the secondary antibody for the immunohistochemical analysis of ES cells differentiated *in vitro*. All secondary antibodies were purchased from Jackson ImmunoResearch Laboratories.

**TOPFLASH and FOPFLASH reporter assays.** Twenty hours before transfection, we plated 10<sup>5</sup> cells per well on 12-well tissue culture plates coated by a feeder cell layer. We transfected cells in each well with 500 ng pTOPFLASH or pFOPFLASH vector (kindly provided by H. Clevers) and 500 ng *lacZ* vector (or 25 ng luciferase from *Renilla reniformis*) using Lipofectamine 2000 (Life Technologies) as recommended by the manufacturer. After 24 h, we measured luciferase activities in a luminometer (Lumat LB 9507) and normalized the data for the transfection efficiency by either measuring the  $\beta$ -galactosidase activity as described previously<sup>9</sup> or using the Dual Luciferase Reporter Assay system (Promega) according to the manufacturer's instruction.

**Expression profiling by oligonucleotide microarray and data analysis.** We extracted total RNA (200  $\mu$ g) from snap-frozen teratomas by standard procedures. We isolated the poly(A)<sup>+</sup> fraction (roughly 2  $\mu$ g) by Dynabeads biomagnetic separation (DynaBeads) and used them to directly probe the GeneChip Murine Genome U74A Set microarray (Affymetrix) according to the manufacturer's protocol.

We analyzed the microarray data using the Rosetta Resolver v3.0 Gene Expression Data Analysis System. The input data for the system were the CEL files generated by Affymetrix GeneChip. The CEL files contained the 75th percentile pixel intensity of a given feature as well as the standard deviation (s.d.) of the pixels and the number of pixels of a given feature. The Affymetrix array contained perfect match (PM) and corresponding mismatch probes (MM), which were used to control for background and non-specific hybridization. The arrays generally contained 16 probe pairs per probe set.

We processed the data by an error model in Rosetta Resolver v3.0 Gene Expression Data Analysis System. The error-weighted PM/MM differences were considered outliers and not used for computation if they were more than 3 s.d. from the mean of the PM/MM intensity difference for a given probe set.

If a probe pair was excluded on one array, then it was also excluded from the differential calculation between two arrays. We determined differential expression by correcting for intra-array gain adjustment, normalizing between arrays and correcting for non-linearity. The intra-array gain adjustment was calculated by dividing the array into 64 sectors and providing gain adjustments for each sector. For differential expression between two arrays, the sectors of the two arrays were normalized sector-by-sector. Then we detected a set of invariant probe sets by calculating the error-weighted log ratio between the two arrays. We used these probe sets, whose probe pairs exhibited a log<sub>10</sub> ratio closest to zero, for the non-linearity adjustment. We calculated a *P* value for each probe set using the error-normalized differential expression between arrays. The error model assumed that the log ratio statistic followed a normal distribution. We used a probability density function of the error-normalized differential with the null hypothesis that the sequence was not differentially expressed.

We used the agglomerative clustering algorithm for clustering genes and arrays into a hierarchical structure. The error-weighted correlation without mean subtraction, based on log ratio, was used as the similarity measure. When merging the two closest objects, we used a heuristic criterion of average linkage to redefine the between-cluster similarity measure. Only sequences that had a factor of change = 2 and *P* < 0.01 were used for clustering. The color displays in Fig. 6a represent the log<sub>10</sub> ratio between the two arrays, red when the sequence was upregulated relative to the control, green when downregulated and black when the expression was close to zero.

# Acknowledgments

We thank J. Boer and collaborators from the Leiden Genome Technology Center for their assistance with the Affymetrix equipment and G.J.B. van Ommen for his continued support. This study was made possible by a grant to R.F. from the Dutch Research Council. M.R. was supported by grants from the Academy of Finland and the Finnish Cultural Foundation.

# Competing interests statement

The authors declare that they have no competing financial interests.

Received 9 July; accepted 19 September 2002.

1. Cadigan, K.M. & Nusse, R. Wnt signaling: a common theme in animal development. *Genes Dev.* **11**, 3286–3305 (1997).
2. Seidenficker, M.J. & Behrens, J. Biochemical interactions in the wnt pathway. *Biochim. Biophys. Acta* **1495**, 168–182 (2000).
3. Polakis, P. Wnt signaling and cancer. *Genes Dev.* **14**, 1837–1851 (2000).
4. Kinzler, K.W. & Vogelstein, B. Lessons from hereditary colorectal cancer. *Cell* **87**, 159–170 (1996).
5. Fodde, R., Smits, R. & Clevers, H. APC, signal transduction and genetic instability in colorectal cancer. *Nature Rev. Cancer* **1**, 55–67 (2001).
6. Fodde, R. & Smits, R. Disease model: familial adenomatous polyposis. *Trends Mol. Med.* **7**, 369–373 (2001).
7. Su, L.K. et al. Multiple intestinal neoplasia caused by a mutation in the murine homolog of the APC gene. *Science* **256**, 668–670 (1992).
8. Moser, A.R. et al. Homozygosity for the Min allele of *Apc* results in disruption of mouse development prior to gastrulation. *Dev. Dyn.* **203**, 422–433 (1995).
9. Smits, R. et al. Apc1638T: a mouse model delineating critical domains of the adenomatous polyposis coli protein involved in tumorigenesis and development. *Genes Dev.* **13**, 1309–1321 (1999).
10. Fodde, R. et al. A targeted chain-termination mutation in the mouse *Apc* gene results in multiple intestinal tumors. *Proc. Natl Acad. Sci. USA* **91**, 8969–8973 (1994).
11. Smits, R. et al. Apc1638N: a mouse model for familial adenomatous polyposis-associated desmoid tumors and cutaneous cysts. *Gastroenterology* **114**, 275–283 (1998).
12. Fodde, R. & Khan, P.M. Genotype-phenotype correlations at the adenomatous polyposis coli (APC) gene. *Crit. Rev. Oncog.* **6**, 291–303 (1995).
13. Korinek, V. et al. Depletion of epithelial stem-cell compartments in the small intestine of mice lacking Tcf-4. *Nature Genet.* **19**, 379–383 (1998).
14. Boman, B.M., Fields, J.Z., Bonham-Carter, O. & Runquist, O.A. Computer modeling implicates stem cell overproduction in colon cancer initiation. *Cancer Res.* **61**, 8408–8411 (2001).
15. Korinek, V. et al. Constitutive transcriptional activation by a  $\beta$ -catenin-Tcf complex in APC<sup>-/-</sup> colon carcinoma. *Science* **275**, 1784–1787 (1997).
16. Stevens, L.C. The biology of teratomas. *Adv. Morphog.* **6**, 1–31 (1967).
17. Hay, E.D. & Zuk, A. Transformations between epithelium and mesenchyme: normal, pathological, and experimentally induced. *Am. J. Kidney Dis.* **26**, 678–690 (1995).
18. Friedrich, G. & Soriano, P. Promoter traps in embryonic stem cells: a genetic screen to identify and mutate developmental genes in mice. *Genes Dev.* **5**, 1513–1523 (1991).
19. Tanaka, S., Kunath, T., Hadjantonakis, A.K., Nagy, A. & Rossant, J. Promotion of trophoblast stem cell proliferation by FGF4. *Science* **282**, 2072–2075 (1998).
20. Rudnicki, M.A. & McBurney, M.W. Cell culture methods and induction of differentiation of embryonal carcinoma cell lines. in *Teratocarcinomas and Embryonic Stem Cells: A Practical Approach* (ed. Robertson, E.) 19–50 (IRL, Oxford, UK, 1987).
21. Kim, K., Pang, K.M., Evans, M. & Hay, E.D. Overexpression of  $\beta$ -catenin induces apoptosis independent of its transactivation function with LEF-1 or the involvement of major G1 cell cycle regulators. *Mol. Biol. Cell* **11**, 3509–3523 (2000).
22. Harada, N. et al. Intestinal polyposis in mice with a dominant stable mutation of the  $\beta$ -catenin gene. *EMBO J.* **18**, 5931–5942 (1999).
23. Urist, M.R. Bone: formation by autoinduction. *Science* **150**, 893–899 (1965).
24. Wozney, J.M. et al. Novel regulators of bone formation: molecular clones and activities. *Science* **242**, 1528–1534 (1988).
25. Hollnagel, A., Oehlmann, V., Heymer, J., Ruther, U. & Nordheim, A. Id genes are direct targets of bone morphogenetic protein induction in embryonic stem cells. *J. Biol. Chem.* **274**, 19838–19845 (1999).
26. Hu, G., Lee, H., Price, S.M., Shen, M.M. & Abate-Shen, C. *Msx* homeobox genes inhibit differentiation through upregulation of cyclin D1. *Development* **128**, 2373–2384 (2001).
27. Chen, J. et al. Microarray analysis of Tbx2-directed gene expression: a possible role in osteogenesis. *Mol. Cell. Endocrinol.* **177**, 43–54 (2001).
28. Yamada, M., Revelli, J.P., Eichele, G., Barron, M. & Schwartz, R.J. Expression of chick *Tbx-2*, *Tbx-3*, and *Tbx-5* genes during early heart development: evidence for BMP2 induction of Tbx2. *Dev. Biol.* **228**, 95–105 (2000).
29. Monaghan, A.P. et al. Dickkopf genes are co-ordinately expressed in mesodermal lineages. *Mech. Dev.* **87**, 45–56 (1999).
30. Fodde, R. et al. Mutations in the APC tumour suppressor gene cause chromosomal instability. *Nature Cell Biol.* **3**, 433–438 (2001).
31. Morin, P.J. et al. Activation of  $\beta$ -catenin-Tcf signaling in colon cancer by mutations in  $\beta$ -catenin or APC. *Science* **275**, 1787–1790 (1997).
32. Lamlum, H. et al. The type of somatic mutation at APC in familial adenomatous polyposis is determined by the site of the germline mutation: a new facet to Knudson's 'two-hit' hypothesis. *Nature Med.* **5**, 1071–1075 (1999).
33. Smits, R. et al. Somatic APC mutations are selected upon their capacity to inactivate the  $\beta$ -catenin downregulating activity. *Genes Chromosomes Cancer* **29**, 229–239 (2000).
34. Shih, I.M. et al. Top-down morphogenesis of colorectal tumors. *Proc. Natl Acad. Sci. USA* **98**, 2640–2645 (2001).
35. Moser, A.R., Dove, W.F., Roth, K.A. & Gordon, J.I. The Min (multiple intestinal neoplasia) mutation: its effect on gut epithelial cell differentiation and interaction with a modifier system. *J. Cell Biol.* **116**, 1517–1526 (1992).
36. Ryo, A., Nakamura, M., Wulf, G., Liou, Y.C. & Lu, K.P. Pin1 regulates turnover and subcellular localization of  $\beta$ -catenin by inhibiting its interaction with APC. *Nature Cell Biol.* **3**, 793–801 (2001).

**Wnt dosage-dependent transcriptional  
responses in embryonic stem cells**

# Chapter 3

Claudia Gaspar, Patrick Franken, Cor Breukel,  
Renée X. de Menezes and Riccardo Fodde

■ Manuscript in preparation





# Chapter 4

**A specific  $\beta$ -catenin signaling dosage underlies cancer stemness and metastatic behavior in Apc-driven mammary tumorigenesis.**

Claudia Gaspar, Patrick Franken, Joana Monteiro,  
Lia Molenaar, Cor Breukel, Martin van der Valk, Ron Smits,  
and Riccardo Fodde



■ Manuscript in preparation.







**Cross-Species Comparison of Human and  
Mouse Intestinal Polyps Reveals Conserved  
Mechanisms in Adenomatous Polyposis Coli  
(APC)-Driven Tumorigenesis**

# Chapter 5

Claudia Gaspar, Joana Cardoso, Patrick Franken,  
Lia Molenaar, Hans Morreau, Gabriela Möslin, Julian Sampson,  
Judith M. Boer, Renée X. de Menezes and Riccardo Fodde



*Tumorigenesis and Neoplastic Progression*

# Cross-Species Comparison of Human and Mouse Intestinal Polyps Reveals Conserved Mechanisms in Adenomatous Polyposis Coli (APC)-Driven Tumorigenesis

Claudia Gaspar,\* Joana Cardoso,\*<sup>†</sup>  
Patrick Franken,\* Lia Molenaar,\* Hans Morreau,<sup>§</sup>  
Gabriela Möslein,<sup>¶</sup> Julian Sampson,<sup>||</sup>  
Judith M. Boer,<sup>‡</sup> Renée X. de Menezes,<sup>††</sup>  
and Riccardo Fodde\*

From the Department of Pathology,\* Josephine Nefkens Institute, and Department of Pediatric Oncology,<sup>†</sup> Erasmus Medical Center, Rotterdam, The Netherlands; Center for Human & Clinical Genetics,<sup>‡</sup> and Department of Pathology,<sup>§</sup> Leiden University Medical Center, Leiden, The Netherlands; St. Josephs-Hospital Bochum-Linden,<sup>¶</sup> Bochum, Germany; and Institute of Medical Genetics,<sup>||</sup> Cardiff University, Cardiff, United Kingdom

**Expression profiling is a well established tool for the genome-wide analysis of human cancers. However, the high sensitivity of this approach combined with the well known cellular and molecular heterogeneity of cancer often result in extremely complex expression signatures that are difficult to interpret functionally. The majority of sporadic colorectal cancers are triggered by mutations in the adenomatous polyposis coli (APC) tumor suppressor gene, leading to the constitutive activation of the Wnt/ $\beta$ -catenin signaling pathway and formation of adenomas. Despite this common genetic basis, colorectal cancers are very heterogeneous in their degree of differentiation, growth rate, and malignancy potential. Here, we applied a cross-species comparison of expression profiles of intestinal polyps derived from hereditary colorectal cancer patients carrying APC germline mutations and from mice carrying a targeted inactivating mutation in the mouse homologue Apc. This comparative approach resulted in the establishment of a conserved signature of 166 genes that were differentially expressed between adenomas and normal intestinal mucosa in both species. Functional analyses of the conserved genes revealed a general increase in cell proliferation and the activation of the Wnt/ $\beta$ -catenin**

**signaling pathway. Moreover, the conserved signature was able to resolve expression profiles from hereditary polyposis patients carrying APC germline mutations from those with bi-allelic inactivation of the MYH gene, supporting the usefulness of such comparisons to discriminate among patients with distinct genetic defects. (Am J Pathol 2008, 172:1363–1380; DOI: 10.2353/ajpath.2008.070851)**

Colorectal cancer (CRC) is one of the major causes of morbidity and mortality among Western societies. Although the vast majority of CRC cases are sporadic, a considerable fraction has been attributed to hereditary and familial factors.<sup>1</sup> Hereditary CRC syndromes have served as unique models to elucidate the molecular and cellular mechanisms underlying colorectal tumor initiation and progression to malignancy, as the same genes mutated in the germline of affected individuals are also known to play rate-limiting roles in the majority of the sporadic cases.<sup>2</sup> This is certainly the case of the adenomatous polyposis coli (APC) tumor suppressor gene, known to be mutated in the germline of individuals affected by familial adenomatous polyposis (FAP)<sup>3–6</sup> and in the majority of the sporadic CRC cases.<sup>7–9</sup> In fact, loss of APC function appears to play a rate-limiting and initiating role in the adenoma-carcinoma sequence.<sup>10</sup> Among the multiple functional domains characterized in its coding

These studies were supported by grants from the Dutch Cancer Society (EMCR 2001-2482), The Netherlands Organisation for Scientific Research (NWO/Vici 016.036.636), the BSIK program of the Dutch Government grant 03038, the EU FP6 (MCSCs), "Deutsche Krebshilfe, Verbundprojekt familiärer Darmkrebs", and the Centre for Medical Systems Biology (CMSB).

C.G. and J.C. equally contributed to the study.

Accepted for publication January 17, 2008.

Supplemental material for this article can be found on <http://ajp.amjpathol.org>.

Address reprint requests to Riccardo Fodde, Ph.D., Dept. of Pathology, Erasmus MC, PO Box 2040, 3000CA Rotterdam, The Netherlands. E-mail: [r.fodde@erasmusmc.nl](mailto:r.fodde@erasmusmc.nl).

sequence, APC's ability to bind and down-regulate  $\beta$ -catenin, the main signaling molecule in the canonical Wnt pathway, is generally regarded as its main tumor-suppressing activity.<sup>10</sup> Loss of APC function or oncogenic activation of  $\beta$ -catenin, as observed in the vast majority of the sporadic CRC cases, leads to intracellular accumulation of  $\beta$ -catenin and its translocation to the nucleus, where it binds to transcription factors of the T cell factor/lymphoid enhancer-binding factor (TCF/LEF) family and modulates transcription of a broad spectrum of downstream target genes.<sup>11,12</sup> The vast majority (70 to 90%) of FAP patients have been shown to carry germline APC mutations.<sup>13</sup> More recently, biallelic mutations in the base excision repair gene *MYH* were found in a subset of polyposis families with attenuated clinical presentation and an autosomal recessive inheritance pattern, often referred to as MAP (*MYH*-associated polyposis).<sup>14</sup>

In view of its initiating role in intestinal cancer, several preclinical models carrying germline mutations in the endogenous mouse *Apc* tumor suppressor gene have been generated, and their phenotype has been characterized.<sup>15</sup> The predisposition of these mouse models to multiple intestinal adenomas closely resembles the FAP phenotype at the molecular, cellular, and phenotypic level.<sup>15</sup> One exception to the latter is represented by the proximal localization and distribution of adenomas along the gastrointestinal (GI) tract of *Apc*-mutant mouse models when compared with the colorectal clustering of polyps among FAP patients.<sup>15</sup>

Expression profiling by cDNA and oligonucleotide microarrays represents a powerful tool for genome-wide transcriptional analysis. Several studies in the literature have reported on the comparison of expression profiles from colorectal tumors and normal intestinal mucosa in an attempt to identify differentially expressed genes, predict, whenever feasible, clinical outcome, and elucidate the molecular and cellular mechanisms underlying colorectal tumorigenesis.<sup>16</sup> However, the different lists of genes differentially expressed in CRC are often very extensive and only partially overlapping among independent studies, possibly reflecting differences in the methodologies and in cohorts used.<sup>16</sup> To pinpoint conserved and functionally relevant genes differentially expressed between normal and malignant tissues, cross-species comparison have been successfully applied by comparing expression signatures of hepatocellular carcinoma, and prostate and lung cancer derived from human patients and mouse models.<sup>17–20</sup>

Here, we report the cross-species comparison of expression profiles of intestinal adenomas from FAP patients with established APC germline mutations and from *Apc*<sup>+/1638N</sup>, a mouse model for familial polyposis previously developed in our laboratory and characterized by the development of an average of five tumors in the upper GI tract, together with other extra-intestinal manifestations characteristic of FAP patients, such as epidermal cysts and desmoids.<sup>21,22</sup> A total of 166 genes were found to be highly conserved between the two species and are likely to play important roles in the cellular and molecular mechanisms underlying adenoma formation in the gastrointestinal tract. Among these, several Wnt downstream

target genes are included, as also expected from the selection of APC-mutant mouse and human adenomas. Notably, the conserved APC signature also made it possible to distinguish FAP tumors from MAP ones in an unsupervised fashion.

## Materials and Methods

### Patients and Tumor Samples

Colorectal adenomatous polyps were obtained from a total of 13 patients from the Department of Surgery, Heinrich Heine University (Düsseldorf, Germany); the Institute of Medical Genetics, Cardiff University (Cardiff, UK); the Department of Pathology, Leiden University Medical Center (Leiden, The Netherlands); and the Department of Surgery, Erasmus Medical Center (Rotterdam, The Netherlands). Of the 13 polyposis patients, 8 carried truncating APC mutations, whereas 5 were found to carry biallelic MYH mutations. Detailed characterization of the polyposis patients carrying biallelic MYH or monoallelic APC germline mutations and of the corresponding tumor samples used in the present study has been reported elsewhere.<sup>23</sup> Normal epithelial mucosa from 3 healthy individuals was also collected (control samples NC1 to NC3). All tissue samples were snap-frozen, embedded in OCT medium, and stored at  $-80^{\circ}\text{C}$ . Detailed sample processing procedures were as previously described.<sup>24</sup> All of the analyzed adenomatous lesions were matched for histology (low-grade dysplasia) and anatomical location (left-sided colon or rectum). Two to six polyps were analyzed for each individual patient.

### Mouse Strains and Material

All wild-type and *Apc*<sup>+/1638N</sup> mice used in this study were inbred C57BL6/J, maintained under SPF conditions and fed *ad libitum*. Duodenal adenomas and normal mucosa samples were collected from 9-month-old males, briefly washed in PBS, and snap-frozen in OCT medium. Hematoxylin and eosin (H&E) staining of all tissues was performed to determine histology and tumor content.

### Laser Capture Microdissection and RNA Isolation

Sample preparation and laser capture microdissection (LCM) were performed as previously described using a PALM MicroBeam microscope system (P.A.L.M. Micro-laser Technologies, Bernried, Germany).<sup>23</sup> In short, 10- $\mu\text{m}$  cryosections were mounted on microscope slides with a polyethylene naphthalate membrane and stained by H&E to allow histological identification of the desired normal and tumor cells. Approximately 1000 to 2000 cells, corresponding to 600,000 (human samples)- and 1,200,000 (mouse specimens)- $\mu\text{m}^2$  areas, were microdissected.

RNA was isolated from the LCM samples by Mini RNeasy columns (QIAGEN, Valencia, CA), according to

# Cross-Species Comparison of Human and Mouse Intestinal Polyps Reveals Conserved Mechanisms in Adenomatous Polyposis Coli (*Apc*)-Driven Tumorigenesis

Conserved Mechanisms in *APC*-Mutant Tumors 1365  
*AJP* May 2008, Vol. 172, No. 5

the manufacturer's instructions, including a DNase step on the column. Quality of the isolated RNA was checked with RNA 6000 Pico LabChip kit (Agilent Technologies, Palo Alto, CA).

## Expression Profiling and Data Analysis

### Human Adenoma Samples

Each RNA sample that passed the quality controls was linearly amplified with two rounds of amplification using the MessageAmp kit (Ambion, Huntingdon, UK), according to the manufacturer's protocol. Quality and quantity of each amplified RNA sample was again evaluated by Nano Lab-on-Chip (Agilent Technologies). One- $\mu$ g aliquots of target and reference amplified RNA were labeled with Cy5-dUTP and Cy3-dUTP, respectively (Amersham Biosciences, Amersham, UK) by reverse transcription using the CyScribe First Strand cDNA Labeling kit (Amersham Biosciences). Each labeling reaction was further purified with the CyScribe GFX purification kit (Amersham Biosciences). Subsequently, both labeled cDNAs were hybridized on a human 18K cDNA microarray encompassing 19,200 spots (representing 18,432 independent cDNAs) produced and obtained from The Netherlands Cancer Institute Microarray Facility (Amsterdam, The Netherlands). The cDNAs spotted in this array platform were PCR-amplified from a clone set purchased from Research Genetics (Huntsville, AL). Hybridization and washing procedures were performed according to the manufacturer's (The Netherlands Cancer Institute Microarray Facility) protocol. Sixteen-bit fluorescent images from the expression arrays were acquired with an Agilent DNA Microarray Scanner (Agilent Technologies), and the resulting TIFF images were analyzed with the software GenePix Pro 4.0 (Axon Instruments, Union City, CA). For each array, a GenePix results file (.gpr) with the extracted Cy3 and Cy5 spot and background raw intensities was generated.

Expression data analysis was performed with a set of functions implemented in R (<http://www.R-project.org/>)<sup>25</sup>. Briefly, .gpr files from the array platforms were directly loaded into the R environment using the marray package to extract the background-corrected Cy3 and Cy5 median raw intensity per spot. Intensity data from both platforms were normalized with the variance stabilization and normalization function implemented in the vsn package.<sup>26</sup>

To find genes that could better characterize the histological and mutational status of the analyzed samples, we have used "mixed-effects" regression models. Briefly, we fitted the following model:  $Y(i) = \alpha + \beta * \text{histology} + \gamma * \text{mutation} + \delta * \text{patient} + \text{error}(i)$ , where  $Y$  represents the log-ratio of the expression value for clone  $i$ ; *histology* and *mutation* are categorical variables represented as stages (normal or adenoma) and (APC or MYH), respectively, whereas  $\alpha$  represents the baseline expression level of clone  $i$ . A patient effect must be included in the model to correctly handle multiple samples derived from the same patient. Although both histology and mutation are assumed to have fixed effects, the patient effect is assumed to be random, as the patients included in this study

represent the heterogeneous (outbred) population of familial CRC patients. This model was fitted to the data using the MAANOVA package.<sup>27</sup> Moderated  $F$ -test statistics, which take advantage of the large number of genes being analyzed simultaneously to yield more reliable variance estimates, were extracted corresponding to histology and mutation effects. Their  $P$  values were subsequently corrected for multiple testing using Benjamini and Hochberg's false discovery rate (FDR) method.<sup>28</sup>

### Mouse Adenoma Samples

RNA samples were submitted to a double round of amplification according to the Small Sample Labeling Protocol vII (Affymetrix, Inc, Santa Clara, CA). Quality of synthesized cRNA was checked using the RNA 6000 Nano LabChip kit (Agilent Technologies). Labeled cRNA products were hybridized to mouse arrays MOE430A (Affymetrix, Inc) according to the manufacturer's instructions. Data analysis was performed using R Statistical Computing software v2.4.1<sup>25</sup> complemented with BioConductor Packages *affy*,<sup>29</sup> *limma*,<sup>30,31</sup> and *vsn*.<sup>26</sup> Cel files were uploaded and summarized using the *affy* package and normalized with *vsn* at the probe level. Using an empirical-Bayesian linear model (implemented in the package *limma*), we identified genes that were differentially expressed, with multiple testing correction performed using Benjamini and Hochberg's FDR step-up method.<sup>28</sup> Hierarchical clustering (Euclidean similarity measure) was performed on *vsn*-normalized data for all probe identifications (IDs) using Spotfire DecisionSite 9.0. (<http://www.spotfire.com>).

To test and/or confirm that a set of genes yielded a differential expression signature between groups of samples, the globaltest<sup>32</sup> of *vsn*-normalized data was performed using R Statistical Computing software v2.4.1<sup>25</sup> complemented with the BioConductor Package globaltest.<sup>32</sup>

## Functional Annotation Analysis

GenBank accession numbers or Affymetrix probe set IDs were assigned to biological process using the GO (Gene Ontology) chart feature offered by the Database for Annotation Visualization and Integrated Discovery (DAVID) 2006 (<http://david.abcc.ncifcrf.gov/home.jsp>). Individual genes from selected expression signatures were also placed in the context of their molecular and functional interactions by using Ingenuity Pathways Analysis (IPA) tools according to the manufacturer's instructions (Ingenuity Systems, Redwood City, CA).

## Data Integration

The cross-species comparison was performed using the Sequence Retrieval System (SRS).<sup>33</sup> Both sets were first annotated using Unigene; next, the SRS system was used to pair the two species' Unigene entries based on Homologene. The MOE430A array includes a total of 22,626 probes, whereas the human cDNA array encom-

passes 19,200 probes. Of the 22,626 mouse probes in the mouse Affymetrix platform, the SRS system retrieved a total of 12,083 homologous genes encompassed by the human array. Due to probe multiplicity in both platforms, the total overlap between the platforms consists of 18,369 entries.

From the two original data sets (mouse adenomas versus normal mucosa and human adenomas versus normal mucosa), probe sets with the same direction of differential expression were selected, adding to a total of 9495 probes. Further selection was applied based on the statistical significance according to the following thresholds: mouse data FDR <5% and human data FDR <0.5% ( $n = 234$  probes). To exclude the possibility that the observed overlap resulted by sheer chance, we have performed a  $\chi^2$  test with the selected probes and reached a highly significant  $P$  value ( $P = 0.007$ ).

### Immunohistochemistry

Immunohistochemistry of mouse and human normal and adenomatous intestinal sections was performed according to standard protocols. The following antibodies were used and optimized for human and mouse tissues: MacMarcks (Calbiochem cat.442708; EMD Biosciences, San Diego, CA), CyclinA (cat.GTX27956; Genetex, San Antonio, TX), AnnexinI (cat.71-3400; Zymed, South San Francisco, CA). Signal detection of these antibodies was obtained by the Rabbit Envision+ System-HRP (cat.K4011; DakoCytomation, Carpinteria, CA). CD44 (cat.553131; BD Pharmingen, San Diego, CA) was detected using a secondary antibody goat anti-rat, HRP labeled.

### Results

The overall rationale and strategy of the present study was to attempt the comparative expression profiling of intestinal adenomas derived from FAP patients carrying *APC* germline mutations<sup>23</sup> and from the *Apc*<sup>+/-1638N</sup> mouse model.<sup>21,22</sup> In both cases, we aimed at using tumor samples in which the initiating and rate-limiting mutation event is represented by loss of *APC* tumor-suppressing function to gain insight into conserved molecular and cellular pathways relevant for intestinal tumor initiation. Furthermore, we explored the ability of the conserved gene signature to discriminate between adenomas from polyposis patients carrying germline *APC* mutations from those with different genetic defects.

### Expression Profiling Analysis of Familial Adenomatous Polypos

Colorectal adenomatous polyps ( $n = 42$ ) have been obtained from a total of eight unrelated FAP patients carrying previously identified germline *APC* mutations.<sup>23</sup> To obtain expression signatures exclusively derived from parenchymal cells and avoid the confounding effects of infiltrating and adjacent stromal cells, dysplastic tumor

cells were collected by laser capture microdissection (LCM). Control LCM samples were obtained from the intestinal mucosa of three individuals with no CRC history. RNA was extracted from the microdissected tumor and normal specimens and subsequently used for expression profiling by hybridization to human 18K cDNA arrays generated at The Netherlands Cancer Institute Microarray Facility (see Materials and Methods). The expression profiling data have been deposited at the National Center for Biotechnology Information Gene Expression Omnibus (<http://www.ncbi.nlm.nih.gov/geo>) and is accessible through GEO Series accession number GSE9689.

Two-dimensional hierarchical clustering was first applied to all 19,200 array probes to generate an overview, without any prior filtering, of the global gene expression differences among all samples (Figure 1a). Notably, the three normal colon mucosa specimens (NC1-3) do not cluster separately from the adenoma samples. Also, several samples from the same individual are often observed to cluster together, indicative of a patient effect. In view of the latter, a statistical approach using a mixed-effects regression model<sup>34</sup> was applied to all samples to determine whether specific patterns of gene expression could be associated with the adenomatous polyps. The linear mixed-effects model was fitted considering histology (adenoma versus normal mucosa) as having a fixed effect and patient as having a random effect. This procedure not only allowed us to calculate  $P$  values for all genes, but also to control the variance component associated with random patient-specific genetic variation, ie, the variability in gene expression related to the genetic background of each individual patient. With an FDR set to 0.5%, a total of 1859 probes appeared to be differentially expressed between normal colonic epithelium and adenomas (see Supplemental Tables S1 and S2 at <http://ajp.amjpathol.org>). The relatively high number of differentially expressed genes even under highly stringent conditions clearly illustrates the strong effect of histology on global gene expression. This is also further illustrated by the empirical cumulative  $P$  values distribution function, which is clearly distinct from what would be expected if no effect was detectable (Figure 1b). Of the 1859 probes, 839 (45%) and 1020 (55%) were, respectively, up- and down-regulated in tumor cells when compared with normal mucosa (see Supplemental Tables S1 and S2 at <http://ajp.amjpathol.org>).

To gain insight into the biological relevance of the newly generated list of genes differentially expressed in adenomatous polyps, we used the GO-based bioinformatics tool DAVID<sup>35</sup> (see Materials and Methods). An overview of the functional categories represented by the genes differentially expressed among *APC*-mutant adenomatous polyps when compared with normal colonic mucosa reveals a very broad spectrum of biological processes, ranging from different aspects of cellular metabolism to apoptosis, cell migration, and immune response (data not shown). The broadness of the transcriptional profiles of the colorectal polyps when compared with normal mucosa is likely to reflect the heterogeneity of these benign tumors even at this very early stage of the adenoma-carcinoma sequence.

# Cross-Species Comparison of Human and Mouse Intestinal Polyps Reveals Conserved Mechanisms in Adenomatous Polyposis Coli (*Apc*)-Driven Tumorigenesis

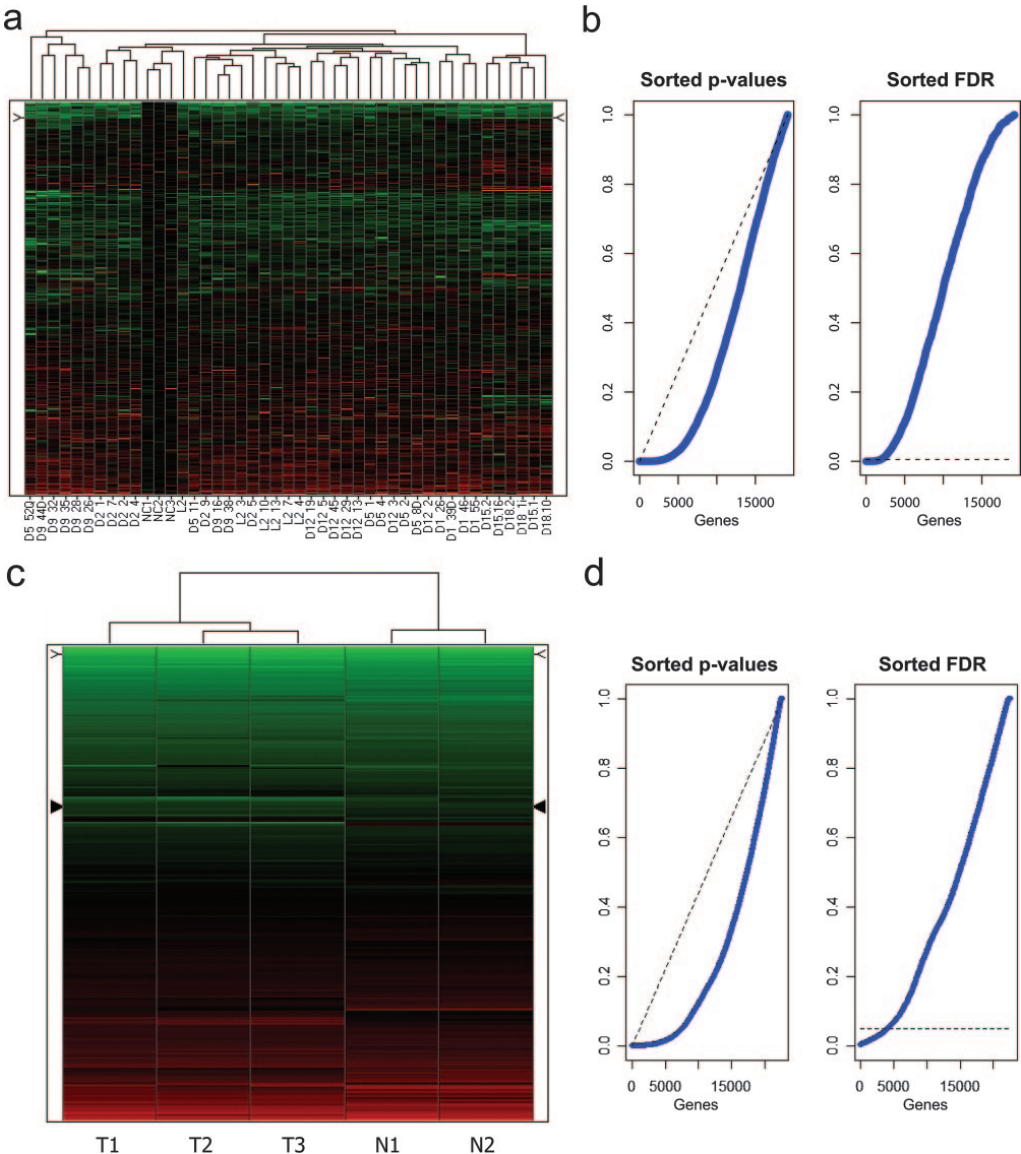


**Figure 1.** Unsupervised hierarchical cluster analysis of expression profiles from human and mouse intestinal polyps, without preliminary gene selection. Up- and down-regulated probes are depicted in red and green, respectively. **a:** Unsupervised hierarchical clustering analysis of 42 colorectal adenomatous polyps (obtained from eight unrelated FAP patients with previously identified germline *APC* mutations<sup>23</sup>) and 3 control normal mucosa samples (labeled as **NC1-3**) obtained from individuals with no history of CRC. **b:** Distribution of *P* values (left plot) relative to the comparison of patient-derived colorectal adenomas versus normal mucosa samples, sorted in ascending order (blue line). The dashed (black) line represents what would be expected if no effect was detectable. In the right plot, FDR-adjusted sorted *P* values are shown. The dashed line represents the FDR threshold used in our study to select the differentially expressed genes in the human set that led to the selection of 1859 probes. **c:** Unsupervised hierarchical clustering analysis of duodenal adenomas (*n* = 3, labeled **T1-T3**) and normal mucosa (*n* = 2, **N1-N2**) samples obtained from inbred C57BL6/J *Apc*<sup>+/-1638N</sup> and *Apc*<sup>+/+</sup> mice, respectively. **d:** Distribution of *P* values (left plot) relative to the comparison of mouse duodenal adenomas versus normal tissue samples, sorted in ascending order (blue line). The dashed (black) line represents what would be expected if no effect was detectable. In the right plot, FDR-adjusted sorted *P* values are shown. The dashed line represents the FDR threshold used in our study to select the differentially expressed genes in the mouse set that led to the selection of 4137 probes.



**Table 1.** The Cross-Species Conserved 166-Gene Signature: Up-Regulated Genes

Mouse			Human		
Probe ID	Unigene*	Gene symbol	Unigene†	Gene symbol	Gene description
1448213_at	Mm.248360	<i>Anxa1</i>	Hs.494173	<i>ANXA1</i>	Annexin A1
1424460_s_at	Mm.284649	<i>Aytl2</i>	Hs.368853	<i>AYTL2</i>	Acytransferase like 2
1424278_a_at	Mm.8552	<i>Birc5</i>	Hs.514527	<i>BIRC5</i>	Baculoviral IAP repeat-containing 5 (survivin)
1416815_s_at	Mm.927	<i>Bub3</i>	Hs.418533	<i>BUB3</i>	BUB3 budding uninhibited by benzimidazoles 3 homolog (yeast)
1455356_at	Mm.36834	<i>Camsap1</i>	Hs.522493	<i>CAMSAP1</i>	Calmodulin-regulated spectrin-associated protein 1
1416884_at	Mm.280968	<i>Cbx3</i>	Hs.381189	<i>CBX3</i>	Chromobox homolog 3 (HP1 gamma homolog, <i>Drosophila</i> )
1425616_a_at	Mm.36697	<i>Ccdc23</i>	Hs.113919	<i>CCDC23</i>	Coiled-coil domain containing 23
1427031_s_at	Mm.24035	<i>Ccdc52</i>	Hs.477144	<i>CCDC52</i>	Coiled-coil domain containing 52
1417911_at	Mm.4189	<i>Ccna2</i>	Hs.58974	<i>CCNA2</i>	Cyclin A2
1417419_at	Mm.273049	<i>Ccnd1</i>	Hs.523852	<i>CCND1</i>	Cyclin D1
1438560_x_at	Mm.296985	<i>Cct4</i>	Hs.421509	<i>CCT4</i>	Chaperonin containing TCP1, subunit 4 (delta)
1417258_at	Mm.282158	<i>Cct5</i>	Hs.1600	<i>CCT5</i>	Chaperonin containing TCP1, subunit 5 (epsilon)
1423760_at	Mm.423621	<i>Cd44</i>	Hs.502328	<i>CD44</i>	CD44 molecule (Indian blood group)
1452242_at	Mm.9916	<i>Cep55</i>	Hs.14559	<i>CEP55</i>	Centrosomal protein 55 kDa
1417457_at	Mm.222228	<i>Cks2</i>	Hs.83758	<i>CKS2</i>	CDC28 protein kinase regulatory subunit 2
1449300_at	Mm.200327	<i>Cttnbp2 nl</i>	Hs.485899	<i>CTTNBP2NL</i>	CTTNBP2 N-terminal like
1454268_a_at	Mm.271671	<i>Cyba</i>	Hs.513803	<i>CYBA</i>	Cytochrome b-245, alpha polypeptide
1419275_at	Mm.148693	<i>Dazap1</i>	Hs.222510	<i>DAZAP1</i>	DAZ associated protein 1
1424198_at	Mm.68971	<i>Dlg5</i>	Hs.500245	<i>DLG5</i>	Discs, large homolog 5 ( <i>Drosophila</i> )
1435122_x_at	Mm.128580	<i>Dnmt1</i>	Hs.202672	<i>DNMT1</i>	DNA (cytosine-5-)-methyltransferase 1
1452052_s_at	Mm.27695	<i>Eif3s1</i>	Hs.404056	<i>EIF3S1</i>	Eukaryotic translation initiation factor 3, subunit 1 alpha
1426674_at	Mm.21671	<i>Eif3s9</i>	Hs.371001	<i>EIF3S9</i>	Eukaryotic translation initiation factor 3, subunit 9 eta
1448797_at	Mm.4454	<i>Elk3</i>	Hs.591015	<i>ELK3</i>	ETS-domain protein (SRF accessory protein 2)
1437211_x_at	Mm.427018	<i>Elovl5</i>	Hs.520189	<i>ELOVL5</i>	ELOVL family member 5, elongation of long chain fatty acids (FEN1/Elo2, SUR4/Elo3-like, yeast)
1420965_a_at	Mm.241073	<i>Enc1</i>	Hs.104925	<i>ENC1</i>	Ectodermal-neural cortex (with BTB-like domain)
1451550_at	Mm.6972	<i>Ephb3</i>	Hs.2913	<i>EPHB3</i>	EPH receptor B3
1417301_at	Mm.4769	<i>Fzd6</i>	Hs.591863	<i>FZD6</i>	Frizzled homolog 6 ( <i>Drosophila</i> )
1419595_a_at	Mm.20461	<i>Ggh</i>	Hs.78619	<i>GGH</i>	Gamma-glutamyl hydrolase (conjugase, folylpolyglutamyldolase)
1419205_x_at	Mm.46029	<i>Gpatc4</i>	Hs.193832	<i>GPATC4</i>	G patch domain containing 4
1433736_at	Mm.248353	<i>Hcfc1</i>	Hs.83634	<i>HCFC1</i>	Host cell factor C1 (VP16-accessory protein)
1423051_at	Mm.426956	<i>Hnrpu</i>	Hs.166463	<i>HNRPU</i>	Heterogeneous nuclear ribonucleoprotein U (scaffold attachment factor A)
1426705_s_at	Mm.21118	<i>Iars</i>	Hs.445403	<i>IARS</i>	Isoleucine-tRNA synthetase
1422546_at	Mm.440026	<i>Ilf3</i>	Hs.465885	<i>ILF3</i>	Interleukin enhancer binding factor 3
1456097_s_at	Mm.257094	<i>Itgb3bp</i>	Hs.166539	<i>ITGB3BP</i>	Integrin beta 3 binding protein (beta3-endonexin)
1421344_a_at	Mm.100253	<i>Jub</i>	Hs.655832	<i>JUB</i>	ajuba homolog ( <i>Xenopus laevis</i> )
1452118_at	Mm.102761	<i>2600005C20Rik</i>	Hs.129621	<i>KIAA0179</i>	KIAA0179
1427080_at	Mm.29068	<i>2610036D13Rik</i>	Hs.370118	<i>KIAA0406</i>	KIAA0406
1448169_at	Mm.22479	<i>Krt18</i>	Hs.406013	<i>KRT18</i>	Keratin 18
1416621_at	Mm.285453	<i>Lgl1</i>	Hs.513983	<i>LLGL1</i>	Lethal giant larvae homolog 1 ( <i>Drosophila</i> )
1434210_s_at	Mm.245210	<i>Lrig1</i>	Hs.518055	<i>LRIG1</i>	Leucine-rich repeats and immunoglobulin-like domains 1
1417511_at	Mm.28560	<i>Lyar</i>	Hs.425427	<i>LYAR</i>	Hypothetical protein FLJ20425
1439426_x_at	Mm.177539	<i>Lzp-s</i>	Hs.524579	<i>LYZ</i>	Lysozyme (renal amyloidosis)
1455941_s_at	Mm.325746	<i>Map2k5</i>	Hs.114198	<i>MAP2K5</i>	Mitogen-activated protein kinase kinase 5
1437226_x_at	Mm.424974	<i>Marcks1</i>	Hs.75061	<i>MARCKSL1</i>	MARCKS-like 1
1439081_at	Mm.122725	<i>Mgea5</i>	Hs.500842	<i>MGEA5</i>	Meningioma expressed antigen 5 (hyaluronidase)
1424001_at	Mm.280311	<i>Mki67p</i>	Hs.367842	<i>MKI67IP</i>	MKI67 (FHA domain) interacting nucleolar phosphoprotein
1449478_at	Mm.4825	<i>Mmp7</i>	Hs.2256	<i>MMP7</i>	Matrix metalloproteinase 7 (matrilysin, uterine)
1455129_at	Mm.130883	<i>Mtdh</i>	Hs.377155	<i>MTDH</i>	Metadherin
1419254_at	Mm.443	<i>Mthfd2</i>	Hs.469030	<i>MTHFD2</i>	Methylenetetrahydrofolate dehydrogenase (NADP+ dependent) 2, methylenetetrahydrofolate cyclohydrolase
1452778_x_at	Mm.290407	<i>Nap11</i>	Hs.524599	<i>NAP1L1</i>	Nucleosome assembly protein 1-like 1
1423046_s_at	Mm.290027	<i>Ncbp2</i>	Hs.591671	<i>NCBP2</i>	Nuclear cap binding protein subunit 2
1455035_s_at	Mm.29363	<i>Nol5a</i>	Hs.376064	<i>NOL5A</i>	Nucleolar protein 5A (56 kDa with KKE/D repeat)
1416606_s_at	Mm.28203	<i>Nola2</i>	Hs.27222	<i>NOLA2</i>	Nucleolar protein family A, member 2 (H/ACA small nucleolar RNPs)
1449140_at	Mm.276504	<i>Nudcd2</i>	Hs.140443	<i>NUDCD2</i>	NudC domain containing 2
1428277_at	Mm.387724	<i>Otud6b</i>	Hs.30532	<i>OTUD6B</i>	OTU domain containing 6B

(table continues)

# Cross-Species Comparison of Human and Mouse Intestinal Polyps Reveals Conserved Mechanisms in Adenomatous Polyposis Coli (*Apc*)-Driven Tumorigenesis

Table 1. Continued

Mouse			Human		
Probe ID	Unigene*	Gene symbol	Unigene†	Gene symbol	Gene description
1435368_a_at	Mm.277779	<i>Parp1</i>	Hs.177766	<i>PARP1</i>	poly-(ADP-ribose) polymerase family, member 1
1452620_at	Mm.29856	<i>Pck2</i>	Hs.75812	<i>PCK2</i>	Phosphoenolpyruvate carboxykinase 2 (mitochondrial)
1426838_at	Mm.37562	<i>Pold3</i>	Hs.82502	<i>POLD3</i>	Polymerase (DNA-directed), delta 3, accessory subunit
1427094_at	Mm.9199	<i>Pole2</i>	Hs.162777	<i>POLE2</i>	Polymerase (DNA directed), epsilon 2 (p59 subunit)
1449648_s_at	Mm.3458	<i>Rpo1-1</i>	Hs.584839	<i>POLR1C</i>	polymerase (RNA) I polypeptide C
1433552_a_at	Mm.273217	<i>Polr2b</i>	Hs.602757	<i>POLR2B</i>	polymerase (RNA) II (DNA directed) polypeptide B
1436505_at	Mm.11815	<i>Ppig</i>	Hs.470544	<i>PPIG</i>	Peptidylprolyl isomerase G (cyclophilin G)
1428265_at	Mm.7726	<i>Ppp2r1b</i>	Hs.546276	<i>PPP2R1B</i>	protein phosphatase 2 (formerly 2A), regulatory subunit A, beta isoform
1423775_s_at	Mm.227274	<i>Prc1</i>	Hs.567385	<i>PRC1</i>	protein regulator of cytokinesis 1
1452032_at	Mm.30039	<i>Prkar1a</i>	Hs.280342	<i>PRKAR1A</i>	Protein kinase, cAMP-dependent, regulatory, type I, alpha (tissue-specific extinguisher 1)
1451576_at	Mm.71	<i>Prkdc</i>	Hs.491682	<i>PRKDC</i>	Protein kinase, DNA-activated, catalytic polypeptide
1435859_x_at	Mm.2462	<i>Psmc2</i>	Hs.437366	<i>PSMC2</i>	Proteasome (prosome, macropain) 26S subunit, ATPase, 2
1426631_at	Mm.58660	<i>Pus7</i>	Hs.520619	<i>PUS7</i>	Pseudouridylylate synthase 7 homolog ( <i>S. cerevisiae</i> )
1448899_s_at	Mm.204634	<i>Rad51ap1</i>	Hs.591046	<i>RAD51AP1</i>	RAD51-associated protein 1
1423700_at	Mm.12553	<i>Rfc3</i>	Hs.115474	<i>RFC3</i>	Replication factor C (activator 1) 3
1456375_x_at	Mm.314056	<i>Trim27</i>	Hs.440382	<i>RFP</i>	Tripartite motif-containing 27
1439403_x_at	Mm.435574	<i>Rnf12</i>	Hs.653288	<i>RNF12</i>	Ring finger protein 12
1437309_a_at	Mm.180734	<i>Rpa1</i>	Hs.461925	<i>RPA1</i>	Replication protein A1
1453362_x_at	Mm.16775	<i>Rps24</i>	Hs.356794	<i>RPS24</i>	Ribosomal protein S24
1416276_a_at	Mm.66	<i>Rps4x</i>	Hs.446628	<i>RPS4X</i>	Ribosomal protein S4, X-linked
1416120_at	Mm.99	<i>Rrm2</i>	Hs.226390	<i>RRM2</i>	Ribonucleotide reductase M2 polypeptide
1422864_at	Mm.4081	<i>Runx1</i>	Hs.149261	<i>RUNX1</i>	Runt-related transcription factor 1 (acute myeloid leukemia 1; aml1 oncogene)
1420824_at	Mm.33903	<i>Sema4 d</i>	Hs.655281	<i>SEMA4D</i>	Sema domain, immunoglobulin domain (Ig), transmembrane domain (TM) and short cytoplasmic domain, (semaphorin) 4D
1434972_x_at	Mm.391719	<i>Sfrs1</i>	Hs.68714	<i>SFRS1</i>	Splicing factor, arginine/serine-rich 1 (splicing factor 2, alternate splicing factor)
1417623_at	Mm.399997	<i>Slc12a2</i>	Hs.162585	<i>SLC12A2</i>	Solute carrier family 12 (sodium/potassium/chloride transporters), member 2
1418326_at	Mm.27943	<i>Slc7a5</i>	Hs.513797	<i>SLC7A5</i>	Solute carrier family 7 (cationic amino acid transporter, y+ system), member 5
1422771_at	Mm.325757	<i>Smad6</i>	Hs.153863	<i>SMAD6</i>	SMAD family member 6
1424206_at	Mm.246803	<i>Smarca5</i>	Hs.589489	<i>SMARCA5</i>	SWI/SNF-related, matrix-associated, actin-dependent regulator of chromatin, subfamily a, member 5
1452422_a_at	Mm.1323	<i>Snrbp2</i>	Hs.280378	<i>SNRBP2</i>	Small nuclear ribonucleoprotein polypeptide B
1419156_at	Mm.240627	<i>Sox4</i>	Hs.643910	<i>SOX4</i>	SRY (sex determining region Y)-box 4
1433502_s_at	Mm.220843	<i>Tsr1</i>	Hs.388170	<i>SRR</i>	TSR1, 20S rRNA accumulation, homolog ( <i>S. cerevisiae</i> )
1415849_s_at	Mm.378957	<i>Stmn1</i>	Hs.693592	<i>STMN1</i>	Stathmin 1/oncoprotein 18
1450743_s_at	Mm.260545	<i>Syncrip</i>	Hs.571177	<i>SYNCRIP</i>	Synaptotagmin binding, cytoplasmic RNA interacting protein
1423601_s_at	Mm.2215	<i>Tcof1</i>	Hs.519672	<i>TCOF1</i>	Treacher Collins-Franceschetti syndrome 1
1416358_at	Mm.34564	<i>0610009O03Rik</i>	Hs.632581	<i>TETRA</i>	Tetracycline transporter-like protein (TETRA)
1434317_s_at	Mm.272025	<i>Tex10</i>	Hs.494648	<i>TEX10</i>	Testis expressed sequence 10
1426397_at	Mm.172346	<i>Tgfbir2</i>	Hs.82028	<i>TGFBR2</i>	Transforming growth factor, beta receptor II
1424641_a_at	Mm.219648	<i>Thoc1</i>	Hs.654460	<i>THOC1</i>	THO complex 1
1427318_s_at	Mm.34674	<i>Fer1l3</i>	Hs.500572	<i>FER1L3</i>	Fer-1-like 3, myoferlin ( <i>C. elegans</i> )
1449041_a_at	Mm.27063	<i>Trip6</i>	Hs.534360	<i>TRIP6</i>	Thyroid hormone receptor interactor 6
1437906_x_at	Mm.19169	<i>Txn1l</i>	Hs.114412	<i>TXNL1</i>	Thioredoxin-like 1
1422842_at	Mm.3065	<i>Xrn2</i>	Hs.255932	<i>XRN2</i>	5'-3' exoribonuclease 2
1448363_at	Mm.221992	<i>Yap1</i>	Hs.503692	<i>YAP1</i>	Yes-associated protein 1
1427208_at	Mm.289103	<i>Zfp451</i>	Hs.485628	<i>ZNF451</i>	Zinc finger protein 451
1416757_at	Mm.335237	<i>Zwilch</i>	Hs.21331	<i>ZWILCH</i>	Zwilch, kinetochore associated, homolog ( <i>Drosophila</i> )

For simplicity, the gene description is only given for the human entry. \*Unigene build 163; †Unigene build 202.

*Expression Profiling Analysis of Apc<sup>+/-1638N</sup> Mouse Intestinal Adenomas*

Duodenal adenomas and normal mucosal samples from age- and sex-matched C57BL6/J *Apc<sup>+/-1638N</sup>* mice ( $n = 3$ ) and *Apc<sup>+/+</sup>* controls ( $n = 2$ ) were collected and snap-frozen as for the above human polyps. Histological analysis of these lesions confirmed their benign adenomatous nature (not shown). Also in these cases, dysplastic epithelial cells were collected by LCM. Control expression signatures were obtained from wild-type C57BL6/J epithelial cells microdissected from the same anatomical location. Total RNA was extracted from normal and tumor samples and hybridized to Affymetrix MOE430A arrays. The corresponding data have been deposited in National Center for Biotechnology Information's Gene Expression Omnibus and are accessible through GEO Series accession number GSE9580. Unsupervised two-dimensional hierarchical clustering was able to discriminate and correctly cluster tumor from normal samples (Figure 1c). Empirical-Bayesian linear regression analysis allowed the identification of statistically significant differences between normal and tumor samples.<sup>30,31</sup> Notwithstanding the admittedly limited sample size, a strong gene expression signature of the tumor samples is detected as illustrated by the empirical cumulative distribution function of the  $P$  values, which is clearly distinct from what would be expected if no effect was detectable (Figure 1d). Such a strong histology-specific gene expression signature, despite the small sample size, may result from the use of inbred animals in which genetic background is identical among unrelated tumor-bearing mice. An FDR threshold of 5% resulted in the identification of as many as 4137 probes differentially regulated between normal and tumor tissue, and 2163 (52%) and 1974 (48%) up- and down-regulated, respectively (see Supplemental Tables S3 and S4 at <http://ajp.amjpathol.org>). As for the human gene list, annotation analysis of the mouse genes by DAVID revealed a very broad and partially overlapping spectrum of cellular functions (data not shown).

*Cross-Species Comparison*

As shown above, expression profiling analysis of human and mouse intestinal adenomas and their normal tissue counterparts resulted in very extensive lists of differentially expressed genes even when stringent parameters were used. We postulated that the cross-species comparison of the genes differentially expressed between the two independent data sets would limit bystander and adaptation effects and help in narrowing down the list to conserved transcripts more likely to play relevant roles in the tumorigenic process. As the two profiling data sets were generated with different microarray platforms (cDNA and oligonucleotide arrays for the human and mouse tumors, respectively), the comparative analysis was performed exclusively on the probes present in both platforms (see Materials and Methods).

Conserved probes were selected by applying the following inclusion criteria: FDR <5% for the mouse set

( $n = 4137$  probes) and FDR <0.5% for the human set ( $n = 1859$  probes). Further filtering was performed to eliminate probes with discordant transcriptional directions (eg, up- vs. down-regulated probes) between the two species. Following this procedure, a total of 234 probes representative of 166 genes were selected, 100 and 66 of which were up- and down-regulated, respectively (Tables 1 and 2). In those cases in which a gene is represented by more than one probe in the array platform, the probe ID associated with the lowest FDR value was selected.

Bioinformatic analysis of the 166 genes was performed by assigning them to functional groups based on their GO classification in addition to other information from the scientific literature (Table 3). Overall, up-regulation of genes with functions related to cell division was observed: DNA replication and repair, cell cycle regulation, and the maintenance of genomic integrity. Also, the transcriptional and translational machinery was up-regulated when compared with normal tissues.

To map the conserved genes to existing signaling and cellular pathways, we used the web-based software application IPA (Ingenuity Systems). As expected from our selection of human and mouse intestinal tumors arising from *APC* mutations, IPA revealed several differentially expressed genes encoding for members of the Wnt signal transduction pathway (Figure 2). Of the other pathways included in the IPA database, only the extracellular signal-regulated kinase/mitogen-activated protein kinase signaling network encompassed more than two differentially expressed genes in the conserved signature, namely *PKA*, *PKC*, *PP1/PP2A*, and *ELK3* (not shown).

*Immunohistochemical Validation of Conserved Targets*

To validate the results of our comparative cross-species expression analysis, we have performed immunohistochemistry (IHC) on mouse and human intestinal tissues with antibodies directed against proteins encoded by differentially expressed genes from the list reported in Table 1. Enhanced expression of the cell surface glycoprotein CD44 is an early event in the adenoma-carcinoma sequence both in mouse and human,<sup>36,37</sup> and is thought to result from direct *CD44* transcriptional up-regulation by Wnt/ $\beta$ -catenin signaling.<sup>37</sup> Accordingly, *CD44* was found to be conserved in our cross-species analysis and was used as an internal positive control for the IHC analysis (Figure 3, m-p).

The annexin A1 (*ANXA1*) gene, up-regulated in both human and mouse *APC/Apc*-mutant adenomas (Table 1), encodes for annexin A1, an anti-inflammatory protein induced by glucocorticoids and overexpressed in colitis in both human and rat.<sup>38-40</sup> Annexin A1 IHC analysis reveals a distinct perinuclear localization in normal intestinal mucosa, possibly in association with the endoplasmic reticulum (Figure 3, a and b). In *Apc<sup>+/-1638N</sup>* and FAP intestinal tumors, cytoplasmic accumulation of annexin A1 is observed concomitantly with loss of the perinuclear localization (Figure 3, c and d). In distinct tumor areas, nuclear localization was also observed, possibly sugges-

# Cross-Species Comparison of Human and Mouse Intestinal Polyps Reveals Conserved Mechanisms in Adenomatous Polyposis Coli (*Apc*)-Driven Tumorigenesis

Conserved Mechanisms in APC-Mutant Tumors 1371  
AJP May 2008, Vol. 172, No. 5

**Table 2.** The Cross-Species Conserved 166-Gene Signature: Down-Regulated Genes

Mouse			Human		
Probe ID	Unigene*	Gene	Unigene†	Gene	Description
1424600_at	Mm.213898	<i>Abp1</i>	Hs.647097	<i>ABP1</i>	Amiloride binding protein 1 [amine oxidase (copper-containing)]
1427034_at	Mm.754	<i>Ace</i>	Hs.298469	<i>ACE</i>	Angiotensin I-converting enzyme (peptidyl dipeptidase A) 1
1418553_at	Mm.170461	<i>Arhgef18</i>	Hs.465761	<i>ARHGEF18</i>	Rho/rac guanine nucleotide exchange factor (GEF) 18
1459924_at	Mm.340818	<i>Atp6v0a1</i>	Hs.463074	<i>ATP6V0A1</i>	ATPase, H <sup>+</sup> transporting, lysosomal V0 subunit a1
1416582_a_at	Mm.4387	<i>Bad</i>	Hs.370254	<i>BAD</i>	BCL2-antagonist of cell death
1423635_at	Mm.103205	<i>Bmp2</i>	Hs.73853	<i>BMP2</i>	Bone morphogenetic protein 2
1456616_a_at	Mm.726	<i>Bsg</i>	Hs.591382	<i>BSG</i>	BSG: Basigin (Ok blood group)
1424226_at	Mm.218590	<i>9030617O03Rik</i>	Hs.309849	<i>C14orf159</i>	Chromosome 14 open reading frame 159
1427944_at	Mm.150568	<i>C1qdc1</i>	Hs.234355	<i>C1QDC1</i>	C1q domain containing 1
1449248_at	Mm.177761	<i>Clcn2</i>	Hs.436847	<i>CLCN2</i>	Chloride channel 2
1416565_at	Mm.400	<i>Cox6b1</i>	Hs.431668	<i>COX6B1</i>	Cytochrome c oxidase subunit Vib polypeptide 1 (ubiquitous)
1420617_at	Mm.339792	<i>Cpeb4</i>	Hs.127126	<i>CPEB4</i>	Cytoplasmic polyadenylation element binding protein 4
1415677_at	Mm.21623	<i>Dhrs1</i>	Hs.348350	<i>DHRS1</i>	Dehydrogenase/reductase (SDR family) member 1
1416697_at	Mm.1151	<i>Dpp4</i>	Hs.368912	<i>DPP4</i>	Dipeptidylpeptidase 4 (CD26, adenosine deaminase complexing protein 2)
1450314_at	Mm.140332	<i>Dqx1</i>	Hs.191705	<i>DQX1</i>	DEAQ box polypeptide 1 (RNA-dependent ATPase)
1421136_at	Mm.9478	<i>Edn3</i>	Hs.1408	<i>EDN3</i>	Endothelin 3
1423005_a_at	Mm.264215	<i>Espn</i>	Hs.147953	<i>ESPN</i>	Espin
1421969_a_at	Mm.256025	<i>Faah</i>	Hs.528334	<i>FAAH</i>	Fatty acid amide hydrolase
1452117_a_at	Mm.170905	<i>Fyb</i>	Hs.370503	<i>FYB</i>	FYN binding protein (FYB-120/130)
1436889_at	Mm.338713	<i>Gabra1</i>	Hs.175934	<i>GABRA1</i>	γ-Aminobutyric acid (GABA) A receptor, alpha 1
1423236_at	Mm.30249	<i>Galt1</i>	Hs.514806	<i>GALNT1</i>	UDP-N-acetyl-α-D-galactosamine:polypeptide N-acetyl-galactosaminyltransferase 1 (GalNAc-T1)
1418863_at	Mm.247669	<i>Gata4</i>	Hs.243987	<i>GATA4</i>	GATA binding protein 4
1429076_a_at	Mm.283495	<i>Gdpd2</i>	Hs.438712	<i>GDPD2</i>	Glycerophosphodiester phosphodiesterase domain containing 2
1449144_at	Mm.260925	<i>Gna11</i>	Hs.654784	<i>GNA11</i>	Guanine nucleotide binding protein (G protein), alpha 11 (Gq class)
1419371_s_at	Mm.195451	<i>Gosr2</i>	Hs.463278	<i>GOSR2</i>	Golgi SNAP receptor complex member 2
1416416_x_at	Mm.37199	<i>Gstm1</i>	Hs.75652	<i>GSTM5</i>	Glutathione S-transferase M5
1425343_at	Mm.41506	<i>Hdh3</i>	Hs.7739	<i>HDHD3</i>	Haloacid dehalogenase-like hydrolase domain containing 3
1422527_at	Mm.16373	<i>H2-DMA</i>	Hs.351279	<i>HLA-DMA</i>	HLA-DMA: Major histocompatibility complex, class II, DM alpha
1419455_at	Mm.4154	<i>Il10rb</i>	Hs.418291	<i>IL10RB</i>	Interleukin 10 receptor, beta
1418265_s_at	Mm.1149	<i>Irf2</i>	Hs.374097	<i>IRF2</i>	Interferon regulatory factor 2
1433775_at	Mm.331907	<i>C77080</i>	Hs.591502	<i>KIAA1522</i>	KIAA1522
1425547_a_at	Mm.279599	<i>Klc4</i>	Hs.408062	<i>KLC4</i>	Kinesin light chain 4
1451322_at	Mm.28108	<i>Cmb1</i>	Hs.192586	<i>CMBL</i>	Carboxymethylenebutenolidase homolog ( <i>Pseudomonas</i> )
1425780_a_at	Mm.241387	<i>Tmem167</i>	Hs.355606	<i>TMEM167</i>	Transmembrane protein 167
1425704_at	Mm.192213	<i>BC022224</i>	Hs.462859	<i>MGC4172</i>	Short-chain dehydrogenase/reductase
1425930_a_at	Mm.628	<i>Mlx</i>	Hs.383019	<i>MLX</i>	MAX-like protein X
1450376_at	Mm.2154	<i>Mxi1</i>	Hs.501023	<i>MXI1</i>	MAX interactor 1
1425230_at	Mm.31686	<i>Nags</i>	Hs.8876	<i>NAGS</i>	N-Acetylglutamate synthase
1448331_at	Mm.29683	<i>Ndufb7</i>	Hs.532853	<i>NDUFB7</i>	NADH dehydrogenase (ubiquinone) 1 beta subcomplex, 7
1415821_at	Mm.15125	<i>Nptn</i>	Hs.187866	<i>NPTN</i>	Neuroplastin
1451274_at	Mm.276348	<i>Ogdh</i>	Hs.488181	<i>OGDH</i>	Oxoglutarate (α-ketoglutarate) dehydrogenase (lipoamide)
1417677_at	Mm.32744	<i>Opn3</i>	Hs.534399	<i>OPN3</i>	Opsin 3
1449330_at	Mm.29872	<i>Pdzd3</i>	Hs.374726	<i>PDZD3</i>	PDZ domain containing 3
1435872_at	Mm.328931	<i>Pim1</i>	Hs.81170	<i>PIM1</i>	Pim-1 oncogene
1425542_a_at	Mm.240396	<i>Ppp2r5c</i>	Hs.368264	<i>PPP2R5C</i>	Protein phosphatase 2, regulatory subunit B', gamma isoform
1422847_a_at	Mm.2314	<i>Prkcd</i>	Hs.155342	<i>PRKCD</i>	Protein kinase C, delta
1424456_at	Mm.4341	<i>Pvrl2</i>	Hs.655455	<i>PVRL2</i>	Poliovirus receptor-related 2 (herpesvirus entry mediator B)
1430527_a_at	Mm.261818	<i>Rnf167</i>	Hs.7158	<i>RNF167</i>	Ring finger protein 167
1448704_s_at	Mm.22362	<i>H47</i>	Hs.32148	<i>SELS</i>	Selenoprotein S

(table continues)

**Table 2.** *Continued*

Mouse			Human		
Probe ID	Unigene*	Gene	Unigene <sup>†</sup>	Gene	Description
1448299_at	Mm.246670	<i>Slc1a1</i>	Hs.444915	<i>SLC1A1</i>	Solute carrier family 1 (neuronal/epithelial high affinity glutamate transporter, system Xag), member 1
1424441_at	Mm.330113	<i>Slc27a4</i>	Hs.656699	<i>SLC27A4</i>	Solute carrier family 27 (fatty acid transporter), member 4
1433595_at	Mm.281800	<i>Slc35d1</i>	Hs.213642	<i>SLC35D1</i>	Solute carrier family 35 (UDP-glucuronic acid/UDP-N-acetylgalactosamine dual transporter), member D1
1421225_a_at	Mm.41044	<i>Slc4a4</i>	Hs.5462	<i>SLC4A4</i>	Solute carrier family 4, sodium bicarbonate cotransporter, member 4
1448783_at	Mm.45874	<i>Slc7a9</i>	Hs.408567	<i>SLC7A9</i>	Solute carrier family 7 (cationic amino acid transporter, y+ system), member 9
1436797_a_at	Mm.300594	<i>Surf4</i>	Hs.512465	<i>SURF4</i>	Surfeit 4
1428095_a_at	Mm.33869	<i>Tmem24</i>	Hs.587176	<i>TMEM24</i>	Transmembrane protein 24
1417895_a_at	Mm.25295	<i>Tmem54</i>	Hs.534521	<i>TMEM54</i>	Transmembrane protein 54
1434553_at	Mm.26088	<i>Tmem56</i>	Hs.483512	<i>TMEM56</i>	Transmembrane protein 56
1420412_at	Mm.1062	<i>Tnfsf10</i>	Hs.478275	<i>TNFSF10</i>	Tumor necrosis factor (ligand) superfamily, member 10
1428327_at	Mm.305318	<i>Trak1</i>	Hs.535711	<i>TRAK1</i>	Trafficking protein, kinesin binding 1
1448737_at	Mm.18590	<i>Tspan7</i>	Hs.441664	<i>TSPAN7</i>	Tetraspanin 7
1448782_at	Mm.291015	<i>Txnbc11</i>	Hs.313847	<i>TXNDC11</i>	Thioredoxin domain containing 11
1435110_at	Mm.290433	<i>Unc5b</i>	Hs.585457	<i>UNC5B</i>	Unc-5 homolog B
1426399_at	Mm.26515	<i>Vwa1</i>	Hs.449009	<i>VWA1</i>	Von Willebrand factor A domain containing 1
1436953_at	Mm.223504	<i>Vipf1</i>	Hs.654521	<i>WASPIP</i>	WAS/WASL interacting protein family, member 1
1416545_at	Mm.240076	<i>Zdhhc7</i>	Hs.592065	<i>ZDHHC7</i>	Zinc finger, DHHC-type containing 7

For simplicity, the gene description is only given for the human entry. \*Unigene build 163; <sup>†</sup>Unigene build 202.

**Table 3.** GO Annotations of the Cross-Species Conserved Genes

Cellular function	Direction	Genes
Cell cycle	Up	<i>CCND1, CCNA2, CKS2*, CEP55</i>
DNA replication	Up	<i>RRM2, RFC3, PUS7*, POLE2, RPA1, NAP1L1</i>
DNA repair	Up	<i>XRN2*, PUS7*, POLD3, PARP1, RAD51AP1</i>
Apoptosis	Up	<i>DLG5, BIRC5</i>
	Down	<i>BAD, IRF2*, TNFSF10*, UNC5B, PIM1</i>
RNA and protein biogenesis, processing and transport	Up	<i>RPS4X, NOLA2, CCT5, ILF3, NCBP2, TCOF1, MKI67IP, THOC1, EIF3S9, EIF3S1, POLR2B, SYNCRIP, IARS, SNRPB2, RPS24, NOLA5A, HNRPU, XRN2*, POLR1C, SFRS1, PPIG, CCT4</i>
	Down	<i>ZDHHC7, GOSR2, GALNT1, TRAK1</i>
TGFβ	Up	<i>TGFBR2, SMAD6</i>
	Down	<i>BMP2</i>
Chromatin remodeling	Up	<i>CBX3, SMARCA5, DNMT1</i>
Cytoskeleton organization	Up	<i>LLGL1, KRT18, CTTNBP2NL</i>
	Down	<i>ARHGEF18, KLC4, WASPIP*, ESPN*</i>
Genome integrity (mitotic checkpoint and telomere maintenance)	Up	<i>STMN1, ZWILCH, BUB3, CKS2*, PRC1, BIRC5*, PARP1*, PRKDC</i>
	Down	<i>ESPN*</i>
Cell adhesion and migration	Up	<i>SEMA4D, JUB, CD44, TRIP6, DLG5, MAP2K5</i>
	Down	<i>NPTN, PVRL2, TSPAN7, WASPIP*</i>
Transcription factors	Up	<i>SOX4, RUNX1, YAP1, MTDH, ITGB3BP, ZFP451, RFP, RNF12</i>
	Down	<i>MLX, MXI1, GATA4, IRF2</i>
G protein signaling	Up	<i>PRKAR1A</i>
	Down	<i>OPN3, PRKCD, GNA11</i>
Immune response	Up	<i>ANXA1</i>
	Down	<i>IRF2*, TNFSF10*, IL10RB, HLA-DMA, BSG, SELS</i>
Chromatin remodeling	Up	<i>CBX3, SMARCA5, DNMT1</i>
Metabolism	Up	<i>SLC7A5, MTHFD2, GGH, AYT2, MGEA5, PCK2</i>
	Down	<i>DHRS1, GSTM1, DGAT1, SLC27A4, NAGS, HDHD3, GPD2, SLC7A9, OGDH</i>
Proteolysis	Up	<i>ENC1, PSMC2, MMP7</i>
	Down	<i>DPP4, ACE, RNF167</i>

Functional annotations were retrieved from GO and the scientific literature. Genes belonging to more than one functional category are marked with\*. Gene symbols refer to the human annotation.



# Cross-Species Comparison of Human and Mouse Intestinal Polyps Reveals Conserved Mechanisms in Adenomatous Polyposis Coli (*Apc*)-Driven Tumorigenesis

Conserved Mechanisms in *APC*-Mutant Tumors 1373  
AJP May 2008, Vol. 172, No. 5

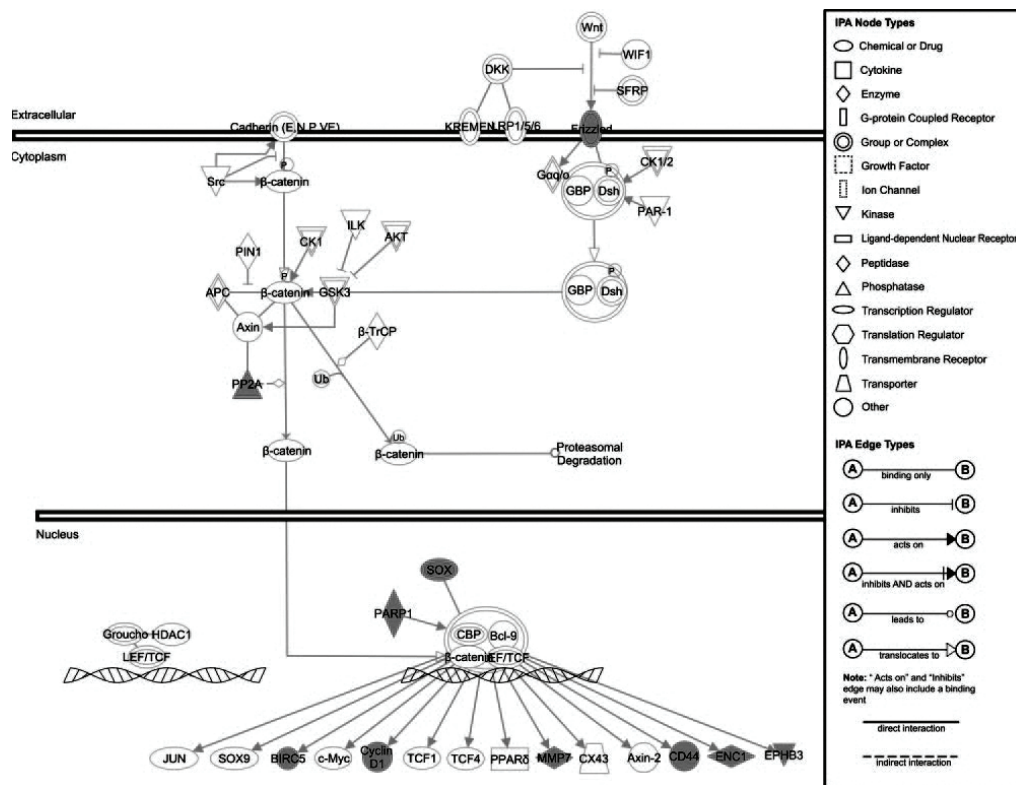


**Figure 2.** IPA of the genes encompassed by the conserved 166 signatures and belonging to the Wnt signal transduction pathway. The canonical Wnt pathway from the IPA database was slightly modified to accommodate additional Wnt target genes.<sup>11,12</sup> The signaling network is represented graphically as nodes (symbols representing genes) and lines/arrows (biological relationship between the genes according to the legend). Red and green gene symbols denote up- and down-regulated genes, respectively. White symbols denote genes not differentially expressed in the conserved signature.

tive of mitogenic stimulation as previously reported.<sup>41</sup> Also, annexin A1 expression appears not to be confined to the intestinal epithelium, but also to extend to the stromal compartment<sup>42</sup> (Figure 3, a–d).

Cyclin A2 (*CCNA2*) is a ubiquitously expressed regulator of cell cycle progression known to promote G<sub>1</sub>/S and G<sub>2</sub>/M transitions.<sup>43</sup> In normal mouse (upper GI) and human (colon) intestinal mucosa, *CCNA2* IHC analysis shows nuclear expression mainly restricted to the crypts (Figure 3, e–h). *CCNA2* up-regulation in both mouse and human intestinal adenomas (Table 1) is reflected by an increase in the relative number of cells with nuclear *CCNA2* staining spread throughout the tumors. The latter is indicative of enhanced cell proliferation of *APC*-mutant tumor cells, as was also confirmed by the GO analysis of the conserved gene list (Table 3).

To date, the function of Marks-like protein 1 (*MARCKSL1*) is not fully elucidated, although evidence in the literature indicates that it might be involved in the regulation of intracellular Ca<sup>2+</sup> levels under the control of protein kinase C.<sup>44</sup> Up-regulation of this protein has been previously reported in prostate cancer,<sup>45</sup> and is here

found in both FAP and *Apc*<sup>+/1638N</sup> adenomas (Table 1). Similar to what was observed for *CCNA2*, *MARCKSL1* expression is limited to a specific subset of cells within the normal human (colon) and mouse (upper GI) intestinal crypts. Likewise, a pronounced increase in cytoplasmic expression is observed in the vast majority of tumor cells (Figure 3, i–l). Overall, the above IHC results validate the cross-species expression profiling data for genes belonging to distinct GO and functional categories.

## The Conserved Cross-Species Signature As a Tool to Differentiate Hereditary Polyposis Syndromes

Apart from its implications for the understanding of the molecular and cellular mechanisms underlying *APC*-driven colorectal tumorigenesis, the conserved cross-species signature may represent a useful tool to discriminate among adenomas from hereditary patients with different genetic syndromes, namely *APC*- and *MYH*-as-

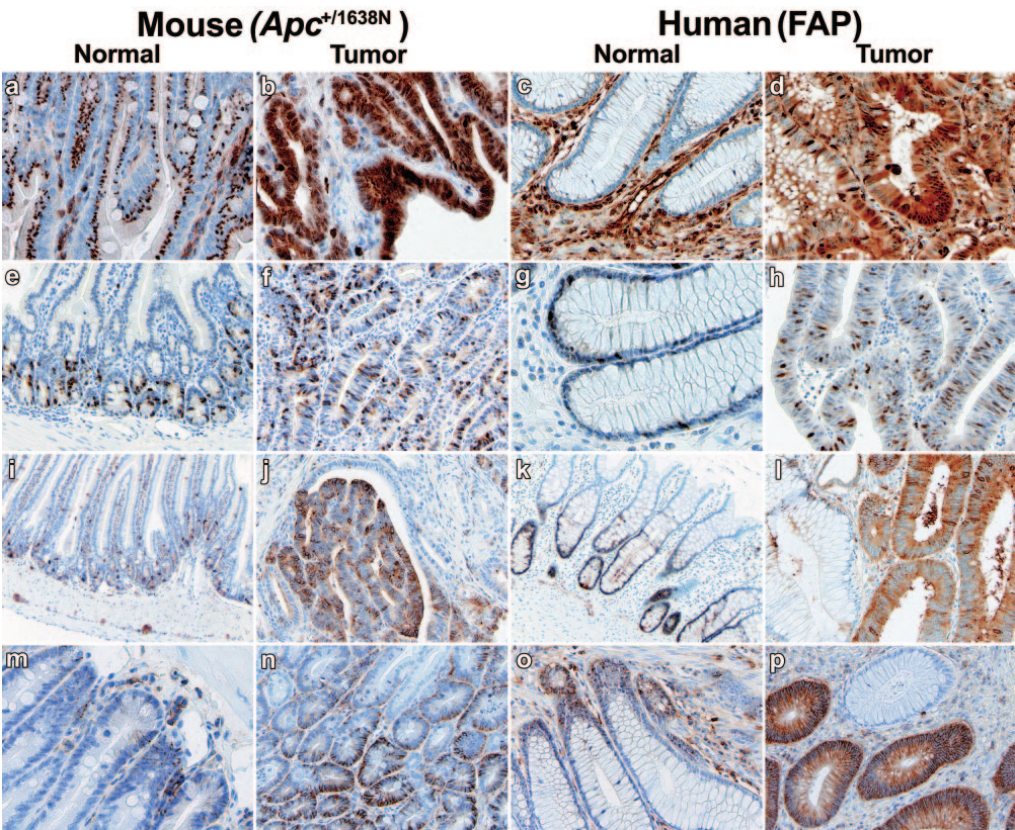


**Figure 3.** Immunohistochemistry validation analysis of cross-species conserved genes. Human (colorectal polyps and normal mucosa from FAP patients carrying germline *APC* mutations) and mouse (duodenal adenomas and normal mucosa from inbred C57BL/6/J *Apc*<sup>+/1638N</sup> and *Apc*<sup>+/+</sup> mice) tissue sections were analyzed with specific antibodies (see Materials and Methods) for expression of the following proteins: ANXA1 (a–d), CCNA2 (e–h), MARCKSL1 (i–l), and CD44 (m–p).

sociated polyposis. To this aim, an additional 14 adenomas have been obtained from five unrelated patients with pathologically confirmed polyposis of the colon and carrying biallelic *MYH* germline mutations.<sup>23</sup> As for the *APC*-mutant polyps, RNA was extracted from the microdissected MAP adenomas and subsequently used for expression profiling. First, unsupervised hierarchical clustering was applied to all 56 profiles (from both the *APC*- and *MYH*-mutant patients) without any prior filtering to generate an overview of the global gene expression differences among all samples. Overall, we could not observe any clear association with mutation status (data not shown). The mixed-effects regression model<sup>34</sup> was again applied, this time fitted to consider mutation (*APC* and *MYH* germline mutation carriers) as having a fixed effect and patient as having a random effect. With an FDR set to 0.5%, we were able to select 49 genes differentially expressed between FAP and MAP adenomas (Table 4). To investigate further whether the 49-gene signature as a whole can predict the underlying *APC* or *MYH* gene defect, we applied the previously described globaltest

for the analysis of microarray data.<sup>32</sup> This test assesses whether the global expression pattern of a group of genes is significantly related to any given parameter. It should be noted that, when applying the globaltest, the patient effect cannot be regarded as random and therefore be controlled by its inclusion in the model as a confounder, as it would also represent the genotype effect (all samples from a patient belong to the same genotype). We circumvented this problem by first selecting at random one sample at a time from each patient and then applying the globaltest. After repeating this process for 1000 random combinations of patients' samples, 57% of the computed *P* values were found to be below the 0.05 threshold, whereas the maximum value is close to 0.5 (Figure 4a). Next, we repeated this procedure with the conserved 166-gene signature. In sharp contrast with the previous result, 99.4% of the computed *P* values are below the 0.05 threshold with a maximum of 0.06 (Figure 4b). Accordingly, two-dimensional hierarchical clustering analysis of the expression profiles obtained from all of the FAP and MAP polyps with the



# Cross-Species Comparison of Human and Mouse Intestinal Polyps Reveals Conserved Mechanisms in Adenomatous Polyposis Coli (*Apc*)-Driven Tumorigenesis

Conserved Mechanisms in *APC*-Mutant Tumors 1375  
*AJP* May 2008, Vol. 172, No. 5

**Table 4.** The 49-Gene Signature Based on Statistically Significant Differences (FDR = 0.5%) Between Expression Profiles of FAP- and MAP-Derived Adenomatous Polyps, After Implementation of the Mixed-Effect Regression Model<sup>24</sup> Fitted Considering Mutation (*APC* vs. *MYH*) as Having Fixed Effect and Patient as Having a Random Effect

GenBank	Gene symbol	Gene description
H41285	<i>GDPD2</i>	Glycerophosphodiester phosphodiesterase domain containing 2
T46878	<i>EIF3S1</i>	Eukaryotic translation initiation factor 3, subunit 1 alpha
AA479795	<i>ISG20</i>	Interferon-stimulated exonuclease gene
AA151214	<i>G3BP2</i>	Ras-GTPase activating protein SH3 domain-binding protein 2
H28091	<i>PMP22</i>	Peripheral myelin protein 22
N59330	<i>NUP35</i>	Nucleoporin
H19333	<i>LOC285550</i>	Hypothetical protein LOC285550
AA449688	<i>FLJ32065</i>	Hypothetical protein FLJ32065
N/A	N/A	—
AA977417	<i>AA977417</i>	—
N50636	<i>RAP1GDS1</i>	RAP1, GTP-GDP dissociation stimulator 1
T61866	<i>IPO7</i>	Importin 7
AA453435	<i>LTV1</i>	LTV1 homolog ( <i>S. cerevisiae</i> )
N91962	<i>EEF1E1</i>	Eukaryotic translation elongation factor 1 epsilon 1
H77636	<i>CD68</i>	CD68 antigen
AI308916	<i>PRSS3</i>	Protease, serine, 3 (mesotrypsin)
AA478589	<i>APOE</i>	Apolipoprotein E
AA459401	<i>KLK10</i>	Kallikrein 10
AA625765	<i>DDA1</i>	DDA1
AA205665	<i>SET</i>	SET translocation (myeloid leukemia-associated)
AA707453	<i>FLJ43855</i>	Similar to sodium- and chloride-dependent creatine transporter
AA464147	<i>CARS</i>	CysteinyI-tRNA synthetase
AA456630	<i>ARHGEF18</i>	Rho/rac guanine nucleotide exchange factor (GEF) 18
N20475	<i>CTSD</i>	Similar to RIKEN cDNA 6330512M04 gene (mouse)
N31935	<i>ANGPTL1</i>	Angiopoietin-like 1
R77512	<i>PCDH1</i>	Protocadherin 1 (cadherin-like 1)
N31492	<i>FMO4</i>	Topoisomerase (DNA) I pseudogene 1
N45236	<i>KIAA0114</i>	KIAA0114 gene product
H60549	<i>CD59</i>	CD59 antigen, complement regulatory protein
AA907626	<i>KIF26B</i>	Kinesin family member 26B
AA917374	<i>TIMP2</i>	TIMP metalloproteinase inhibitor 2
AA983530	<i>VNN1</i>	Vanin 1
N90109	<i>NCL</i>	U23 small nucleolar RNA
H15431	<i>POLR2D</i>	Polymerase (RNA) II (DNA directed) polypeptide D
H52673	<i>BAK1</i>	BCL2-antagonist/killer 1
T72259	<i>CYP2A6</i>	Cytochrome P450, family 2, subfamily A, polypeptide 6
AA455910	<i>F2R</i>	Coagulation factor II (thrombin) receptor
AA775840	<i>C9orf123</i>	Chromosome 9 open reading frame 123
AA464566	<i>LRP1</i>	Low density lipoprotein-related protein 1
AA489640	<i>IFT1</i>	Interferon-induced protein with tetratricopeptide repeats 1
AA962541	<i>LOC286167</i>	Hypothetical protein LOC286167
AA464421	<i>PCGF2</i>	Polycomb group ring finger 2
H25761 AI668603	—	—
AA447748	<i>DLD</i>	Dihydrolipoamide dehydrogenase
AA278755	<i>CEP27</i>	Centrosomal protein
AI261833	<i>SLC7A9</i>	Solute carrier family 7 (cationic amino acid transporter, y+ system) member 9
H72802	<i>ESPN</i>	Espin
AA608713	<i>C1QDC1</i>	C1q domain containing 1
AA047465	<i>SLC6A8</i>	Solute carrier family 6 (neurotransmitter transporter, creatine), member 8

107

49- and 166-gene signatures confirms that the latter is considerably more discriminative than the former in resolving tumors from carriers of *APC* germline mutations from those derived from MAP patients (Figure 4, c and d).

### Discussion

Expression profiling by oligonucleotide and cDNA microarray platforms has rapidly become a commonly used tool for the qualitative and quantitative evaluation of the genome-wide transcriptional activity of human cancers. However, the outcomes of expression profiling of cancers

are often very complex as they reflect the heterogeneity of cell types and biological activities present within the neoplastic mass, thus making their functional interpretation a difficult task. This is certainly the case for the expression (and genomic) profiles obtained to date from colorectal cancers. Although several studies have been published in the scientific literature, the degree of overlap between independent data sets is limited, possibly also as a consequence of differences in patient cohorts and methodologies used.<sup>16</sup> Cross-species comparison of cancer profiling data represents a valuable approach to i) decrease the complexity of omics signatures, ii) pinpoint

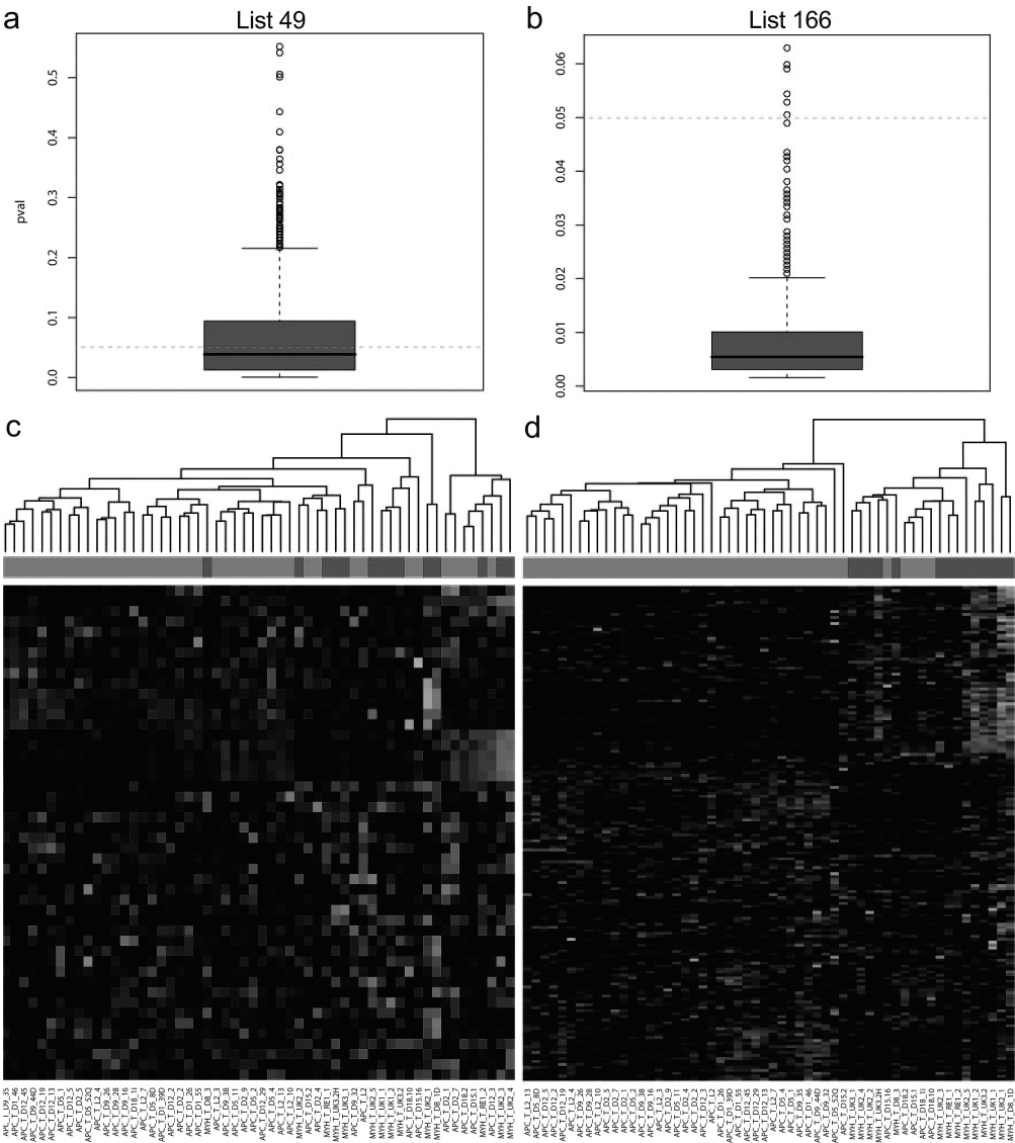


**Figure 4.** Analysis of the cross-species conserved signature as a tool to separate hereditary polypoid syndromes due to *APC* (FAP) or *MYH* (MAP) germline mutations. The globaltest<sup>32</sup> was performed with the 49 (a)- and 166 (b)-gene signature and graphically represented by box plots of the *P* values generated after 1000 iterations in which only one random sample from each patient was used at a time. Box plots were generated using the standard settings present in R2.4.1. The filled blue boxes encompass the range of *P* values representative of 50% of the data points, whereas the central line represents the median. two-dimensional hierarchical clustering analysis was performed with the 49 (c)- and 166 (d)-gene signature, respectively, on the expression profiles obtained from all 56 colorectal adenomas (42 from *APC* and 14 from *MYH* gene mutation carriers). The colored bar above the heat map represents the mutation status of the corresponding polyp samples: red, polyps from patients carrying germline *APC* mutations; blue, polyps from patients carrying bi-allelic germline *MYH* mutations.

conserved target genes more likely to play rate-limiting functional roles in tumor initiation and progression to malignancy, and iii) accelerate the development of tailor-made anticancer therapies.<sup>46,47</sup>

Notwithstanding the above-mentioned heterogeneity, colorectal cancer represents, at least from a genetic perspective, a relatively homogeneous disease as the vast majority of the sporadic cases is known to be trig-

# Cross-Species Comparison of Human and Mouse Intestinal Polyps Reveals Conserved Mechanisms in Adenomatous Polyposis Coli (*Apc*)-Driven Tumorigenesis

Conserved Mechanisms in *APC*-Mutant Tumors 1377  
*AJP* May 2008, Vol. 172, No. 5

gered by somatic mutations at the *APC* or *CTNNB1* ( $\beta$ -catenin) genes, leading to the constitutive activation of the canonical Wnt signaling pathway.<sup>10</sup> These mutations are known to initiate the formation of aberrant crypt foci and adenomatous polyps, the earliest benign precursors of the adenoma-carcinoma sequence. Also, germline *APC* mutations underlie FAP, an autosomal dominant predisposition to the development of multiple adenomatous polyps throughout the colon-rectum.<sup>48</sup> The availability of a unique collection of adenomatous polyps obtained from FAP patients carrying germline *APC* mutations and from a mouse model, *Apc*<sup>+/-1638N</sup>, carrying a targeted mutation in the endogenous *Apc* gene allowed us to perform the cross-species computational comparison of their gene expression profiles and derive a conserved 166-gene signature. It should be noted that whereas FAP patients mainly develop polyps in the colon-rectum, *Apc* mouse models are characterized by adenomas clustering in the upper gastrointestinal tract, mainly in the duodenum. This anatomical difference between the mouse and human adenomas used for the cross-species comparison may exert a confounding effect in our computational analysis as duodenum and colon-rectum represent distinct organs. However, it may also confer an additional advantage to our approach as tissue-specific differences between the two GI tracts are likely to be filtered out, thus retaining only those conserved differentially expressed genes more likely to play functional roles in intestinal tumor formation, regardless of anatomical sub-location. The same holds true for our methodological approach: different microarray platforms were used to derive the human (cDNA arrays) and mouse (oligonucleotide arrays) gene profiles. In both cases, laser-guided microdissection was used to enrich in tumor cells without the confounding effects of contaminating stromal cells. Overall, our IHC analysis of a subset of proteins encoded by the conserved genes confirmed their differential expression between normal tissue and adenomas in both species (Figure 3), thus validating our methodological strategy.

The significance thresholds used to generate the differentially expressed lists of genes for the human (approximately 10% of the represented genes, with FDR = 0.5%) and mouse (approximately 18% of the represented genes, with FDR = 5%) studies are admittedly arbitrary. They were chosen using two generic criteria: i) the gene lists would be representative of the differential signature without encompassing an excessive percentage of false positives, and ii) the resulting conserved list of differentially expressed genes would be sufficiently large to enable pathway analysis. The presence in our cross-species signature of several genes known to be differentially expressed in sporadic colorectal cancers<sup>16</sup> also represents an indirect confirmation of the general validity of our computational approach.

GO-based functional analysis of the 166 conserved genes reveals a general increase in cell division as shown by the up-regulation of genes related to DNA replication and repair, cell cycle regulation, and the maintenance of genomic integrity (Table 3). Notably, exclusively up-regulated genes were encompassed within

these categories, indicative of the increased proliferation rate of tumor cells when compared with normal ones. Genes belonging to the transcriptional and translational machinery were also up-regulated when compared with normal tissues. These included genes involved in ribosome biogenesis, mRNA synthesis and maturation, and protein synthesis and folding (Table 3).

As expected from our selection of adenomas from *APC*-mutant patients and mouse models, several members of the Wnt signal transduction pathway are included among the conserved 166 differentially expressed genes (Figure 2). These included the Frizzled receptor homolog *FZD6*, the protein phosphatase type 2A (*PP2A*), the HMG box transcription factor *SOX4*,<sup>49</sup> and several Wnt downstream transcriptional targets, namely, the matrix metalloproteinase matrilysin (*MMP7*),<sup>36,37,50</sup> *CD44*,<sup>36</sup> *ENC1* (ectodermal-neural cortex 1),<sup>51</sup> ephrin receptor B3 (*EPHB3*),<sup>52</sup> cyclin D1 (*CCND1*),<sup>53,54</sup> and the apoptosis inhibitor survivin (*BIRC5*)<sup>55,56</sup> (Figure 2). However, *AXIN2*, a well known downstream Wnt target gene, is not included in this list simply because its probe is not encompassed by the human cDNA array. Other known Wnt target genes such as *EPHB2*, *SOX9*, and *MYC* were excluded because of the high stringency of the statistical thresholds used or to their absence in one of the platforms. Recently, an "intestinal Wnt/TCF4 signature" was obtained by integrating expression profiling data from CRC cell lines engineered with an inducible block of Wnt signaling and from sporadic human adenomas and carcinomas.<sup>11</sup> Comparison of this 208-gene Wnt/TCF gene signature with our cross-species conserved list revealed 10 common entries, 4 of which belong to the Wnt/ $\beta$ -catenin signaling pathway (*CD44*, *ENC1*, *EPHB3*, and *SOX4*). The latter is not surprising in view of the different computational approaches and tumor cohorts used. Moreover, the use of CRC cell lines with dominant negative *TCF4* constructs does not necessarily mimic the initial and rate-limiting loss of *APC* function characteristic of the mouse and human adenomas used in our cross-species analysis. Of more interest is the comparison with the study by Kaiser et al<sup>57</sup> in which a cross-species comparison was performed among human and mouse intestinal tumors together with mouse embryonic stages of intestinal development. As depicted in Supplemental Table S5 (see <http://ajp.amjpathol.org>), the overlap between the two studies is high, with 46 of 166 differentially expressed genes shared between the data sets. Notably, the overlap is considerably higher with genes showing similar behavior in intestinal tumorigenesis and embryonic development.

Apoptosis inhibition in the adenomas, as suggested by *BIRC5* up-regulation, is also strengthened by the conserved down-regulation of the *BAD* gene, encoding for a potent pro-apoptotic protein. *BAD* forms heterodimers with *BCL2* and *BCL-XL*, thus repressing their anti-apoptotic function.<sup>58,59</sup>

Two members of the TGF- $\beta$  signaling pathways are up-regulated among the cross-species conserved genes, namely *SMAD6* and *TGFBR2*. The TGF- $\beta$  ligand mediates its effects through the transmembrane type I (TGFBR1) and type II receptor subunits (TGFBR2), and in

the cytoplasm through stimulatory and inhibitory SMADs. The up-regulation of the *TGFB2* gene encoding for the type II receptor is remarkable in view of its frequent mutational inactivation in a substantial proportion of sporadic colon cancers.<sup>60</sup> The *SMAD6* gene encodes for an inhibitory SMAD protein that becomes up-regulated as the result of a negative feedback loop. SMAD6 is thought to represent a key component in the integration of signals from different pathways and was shown to exert BMP inhibitory activity.<sup>61</sup> Down-regulation of the bone morphogenetic *BMP2* gene apparently confirms the inhibition of this TGF- $\beta$ -related pathway. Although its role in tumorigenesis is yet unclear, SMAD6 up-regulation has been reported in other tumor types.<sup>62</sup> Overall, the conserved gene signature is indicative of the activation of TGF- $\beta$  and inhibition of BMP signaling at early stages of intestinal tumorigenesis. However, this observation needs to be validated by additional expression and reporter assays.

Among the many genes encompassed by the cross-species conserved signature, the up-regulation of *ANXA1* is of interest in view of its phospholipase A2 (PPA2) inhibitory activity, an enzyme involved in the synthesis of prostaglandins during inflammation.<sup>42</sup> Antibodies against annexin A1 have been found in patients with inflammatory bowel disorders.<sup>38</sup> Also, its up-regulation was shown to occur in mitogenically stimulated cells in a PKC phosphorylation-dependent fashion, accompanied by its translocation from the cytoplasm to the nucleus.<sup>41</sup> Notably, changes in *ANXA1* subcellular localization were also observed in our IHC validation analysis (Figure 3).

Apart from its implications for the understanding and elucidation of the molecular and cellular mechanisms underlying APC-driven intestinal tumor formation, the cross-species conserved gene signature may also represent a useful tool to discriminate among hereditary polyposis patients with distinct genetic defects. Expression profiling analysis of the additional set of 14 colorectal adenomas obtained from patients carrying bi-allelic mutations at the *MYH* gene showed a high degree of similarity with the APC profiles. This could be explained by previous observations, according to which the APC gene is a preferential target for somatic mutations in colorectal adenomas from carriers of bi-allelic *MYH* germline mutations.<sup>63</sup> The observed high degree of similarity between expression profiles from FAP and MAP polyps could then be explained provided that the somatic APC mutation does represent the initiating event in *MYH*-associated polyp formation. Alternatively, human adenoma profiles may be similar notwithstanding the initiating genetic defect, as indicated by our own most recent results with the expression analysis of three polyposis patients of unknown genetic basis (and no germline mutations found after sequencing of the *MYH* and *APC* genes). Also in these cases, the resulting profiles were virtually indistinguishable from those derived from *MYH*- and *APC*-mutant polyps (data not shown).

Nevertheless, by applying an FDR threshold of 0.5%, we could generate a 49-gene signature based on differences between *MYH*- and *APC*-mutant human polyps. Yet, both globaltest and two-dimensional hierarchical clustering analyses showed that the conserved 166-sig-

nature clusters more accurately the expression profile data from FAP and MAP patients than does the 49-gene signature (Figure 4).

In conclusion, cross-species comparison of expression profiles of intestinal adenomas obtained from hereditary polyposis patients and mouse models carrying germline APC mutations resulted in a signature of 166 differentially expressed genes. Functional annotation of the conserved genes indicates an overall increase in cell division and the up-regulation of the Wnt/ $\beta$ -catenin signaling pathway. These main cellular and molecular changes are accompanied by a plethora of gene-specific changes yet to be tested by functional assays to determine their relative contribution to intestinal tumor formation. Additional validation on independent polyp cohorts and further fine-tuning of the conserved gene signature are needed toward the development of an expression-based assay to classify hereditary polyposis syndromes.

### Acknowledgments

We thank Dr. Guido Jenster and Dr. Don de Lange for granting access and helping with the Sequence Retrieval System (SRS), and for fruitful discussions; Dr. Bruce J. Aronow for providing the detailed list of genes from his group's microarray results used here for a comparison; and Mr. Frank van der Panne for his assistance with the artwork.

### References

- de la Chapelle A: Genetic predisposition to colorectal cancer. *Nat Rev Cancer* 2004, 4:769–780
- Kinzler KW, Vogelstein B: Lessons from hereditary colorectal cancer. *Cell* 1996, 87:159–170
- Groden J, Thliveris A, Samowitz W, Carlson M, Gelbert L, Albertsen H, Joslyn G, Stevens J, Spirio L, Robertson M, Sargeant L, Krapcho K, Wolff E, Burt R, Hughes J, Warrington J, McPherson J, Wasmuth J, LePaslier D, Abderrahim H, Cohen D, Leppert M, White R: Identification and characterization of the familial adenomatous polyposis coli gene. *Cell* 1991, 66:589–600
- Joslyn G, Carlson M, Thliveris A, Albertsen H, Gelbert L, Samowitz W, Groden J, Stevens J, Spirio L, Robertson M, Sargeant L, Krapcho K, Wolff E, Burt R, Hughes JP, Warrington J, McPherson J, Wasmuth J, LePaslier D, Abderrahim H, Cohen D, Leppert M, White R: Identification of deletion mutations and three new genes at the familial polyposis locus. *Cell* 1991, 66:601–613
- Kinzler KW, Nilbert MC, Vogelstein B, Bryan TM, Levy DB, Smith KJ, Preisinger AC, Hamilton SR, Hedge P, Markham A, Carlson M, Joslyn G, Groden J, White R, Miki Y, Miyoshi Y, Nishisho I, Nakamura Y: Identification of a gene located at chromosome 5q21 that is mutated in colorectal cancers. *Science* 1991, 251:1366–1370
- Nishisho I, Nakamura Y, Miyoshi Y, Miki Y, Ando H, Horii A, Koyama K, Utsunomiya J, Baba S, Hedge P: Mutations of chromosome 5q21 genes in FAP and colorectal cancer patients. *Science* 1991, 253:665–669
- Smith KJ, Johnson KA, Bryan TM, Hill DE, Markowitz S, Willson JK, Paraskeva C, Petersen GM, Hamilton SR, Vogelstein B, Kinzler KW: The APC gene product in normal and tumor cells. *Proc Natl Acad Sci USA* 1993, 90:2846–2850
- Powell SM, Zilz N, Beazer-Barclay Y, Bryan TM, Hamilton SR, Thibodeau SN, Vogelstein B, Kinzler KW: APC mutations occur early during colorectal tumorigenesis. *Nature* 1992, 359:235–237
- Miyoshi Y, Nagase H, Ando H, Horii A, Ichii S, Nakatsuru S, Aoki T, Miki Y, Mori T, Nakamura Y: Somatic mutations of the APC gene in

# Cross-Species Comparison of Human and Mouse Intestinal Polyps Reveals Conserved Mechanisms in Adenomatous Polyposis Coli (*Apc*)-Driven Tumorigenesis

Conserved Mechanisms in *APC*-Mutant Tumors 1379  
*AJP May 2008, Vol. 172, No. 5*

- colorectal tumors: mutation cluster region in the APC gene. *Hum Mol Genet* 1992, 1:229–233
10. Fodde R, Smits R, Clevers H: APC, signal transduction and genetic instability in colorectal cancer. *Nat Rev Cancer* 2001, 1:55–67
11. Van der Flier LG, Sabates-Bellver J, Oving I, Haegebarth A, De Palo M, Anti M, Van Gijn ME, Suijkerbuijk S, Van de Wetering M, Marra G, Clevers H: The intestinal Wnt/TCF signature. *Gastroenterology* 2007, 132:628–632
12. Vlad A, Rohrs S, Klein-Hitpass L, Muller O: The first five years of the Wnt targetome. *Cell Signal* 2008, 20:795–802
13. Lipton L, Tomlinson I: The genetics of FAP and FAP-like syndromes. *Fam Cancer* 2006, 5:221–226
14. Cheadle JP, Sampson JR: Exposing the MYTH about base excision repair and human inherited disease. *Hum Mol Genet* 2003, 12 Spec No 2:R159–R165
15. Fodde R, Smits R: Disease model: familial adenomatous polyposis. *Trends Mol Med* 2001, 7:369–373
16. Cardoso J, Boer J, Morreau H, Fodde R: Expression and genomic profiling of colorectal cancer. *Biochim Biophys Acta* 2007, 1775:103–137
17. Sweet-Cordero A, Mukherjee S, Subramanian A, You H, Roix JJ, Ladd-Acosta C, Mesirov J, Golub TR, Jacks T: An oncogenic KRAS2 expression signature identified by cross-species gene-expression analysis. *Nat Genet* 2005, 37:48–55
18. Ellwood-Yen K, Graeber TG, Wongvipat J, Iruela-Arispe ML, Zhang J, Matusik R, Thomas GV, Sawyers CL: Myc-driven murine prostate cancer shares molecular features with human prostate tumors. *Cancer Cell* 2003, 4:223–238
19. Lee JS, Chu IS, Mikaelian A, Calvisi DF, Heo J, Reddy JK, Thorgeirsson SS: Application of comparative functional genomics to identify best-fit mouse models to study human cancer. *Nat Genet* 2004, 36:1306–1311
20. Lee JS, Grisham JW, Thorgeirsson SS: Comparative functional genomics for identifying models of human cancer. *Carcinogenesis* 2005, 26:1013–1020
21. Fodde R, Edelmann W, Yang K, van Leeuwen C, Carlson C, Renault B, Breukel C, Alt E, Lipkin M, Khan PM, Kucherlapati R: A targeted chain-termination mutation in the mouse *Apc* gene results in multiple intestinal tumors. *Proc Natl Acad Sci USA* 1994, 91:8969–8973
22. Smits R, van der Hoven van Oordt W, Luz A, Zurcher C, Jagmohan-Changur S, Breukel C, Khan PM, Fodde R: *Apc1638N*: a mouse model for familial adenomatous polyposis-associated desmoid tumors and cutaneous cysts. *Gastroenterology* 1998, 114:275–283
23. Cardoso J, Molenaar L, de Menezes RX, van Leerdam M, Rosenberg C, Moslein G, Sampson J, Morreau H, Boer JM, Fodde R: Chromosomal instability in MYH- and APC-mutant adenomatous polyps. *Cancer Res* 2006, 66:2514–2519
24. Cardoso J, Molenaar L, de Menezes RX, Rosenberg C, Morreau H, Moslein G, Fodde R, Boer JM: Genomic profiling by DNA amplification of laser capture microdissected tissues and array CGH. *Nucleic Acids Res* 2004, 32:e146
25. Ihaka R, Gentleman R: R: A Language for Data Analysis and Graphics. *Journal of Computational and Graphical Statistics* 1996, Vol 5, No 3, 299–314
26. Huber W, von Heydebreck A, Sultmann H, Poustka A, Vingron M: Variance stabilization applied to microarray data calibration and to the quantification of differential expression. *Bioinformatics* 2002, 18(Suppl 1):S96–S104
27. Wu H, Kerr MK, Cui X, Garry A: MAANOVA: A Software Package for the Analysis of Spotted cDNA Microarray Experiments. 2005, New York, Churchill, p 314–341
28. Benjamini Y, Hochberg Y: Controlling the false discovery rate—a practical and powerful approach to multiple testing. *J R Stat Soc B Met* 1995, 289–300
29. Gautier L, Cope L, Bolstad BM, Irizarry RA: affy-analysis of Affymetrix GeneChip data at the probe level. *Bioinformatics* 2004, 20:307–315
30. Smyth GK: Linear models and empirical Bayes methods for assessing differential expression in microarray experiments. *Stat Appl Genet Mol Biol* 2004, 3:Article 3
31. Smyth GK: Limma: linear models for microarray data. *Bioinformatics and Computational Biology Solutions using R and Bioconductor*. Edited by R Gentleman, V Carey, S Dudoit, R Irizarry, W Huber. New York, Springer, 2005, pp 397–420
32. Goeman JJ, van de Geer SA, de Kort F, van Houwelingen HC: A global test for groups of genes: testing association with a clinical outcome. *Bioinformatics* 2004, 20:93–99
33. Veldhoven A, de Lange D, Smid M, de Jager V, Kors JA, Jenster G: Storing, linking, and mining microarray databases using SRS. *BMC Bioinformatics* 2005, 6:192
34. Kerr MK, Martin M, Churchill GA: Analysis of variance for gene expression microarray data. *J Comput Biol* 2000, 7:819–837
35. Dennis G, Jr., Sherman BT, Hosack DA, Yang J, Gao W, Lane HC, Lempicki RA: DAVID: database for annotation, visualization, and integrated discovery. *Genome Biol* 2003, 4:P3
36. Abbasi AM, Chester KA, Talbot IC, Macpherson AS, Boxer G, Forbes A, Malcolm AD, Begent RH: CD44 is associated with proliferation in normal and neoplastic human colorectal epithelial cells. *Eur J Cancer* 1993, 29A:1995–2002
37. Wielenga VJ, Smits R, Korinek V, Smit L, Kielman M, Fodde R, Clevers H, Pals ST: Expression of CD44 in *Apc* and *Tcf* mutant mice implies regulation by the WNT pathway. *Am J Pathol* 1999, 154:515–523
38. Perretti M, Gavins FN: Annexin 1: an endogenous anti-inflammatory protein. *News Physiol Sci* 2003, 18:60–64
39. Vergnolle N, Pages P, Guimbaud R, Chaussade S, Bueno L, Escourrou J, Comera C: Annexin 1 is secreted in situ during ulcerative colitis in humans. *Inflamm Bowel Dis* 2004, 10:584–592
40. Vergnolle N, Comera C, Bueno L: Annexin 1 is overexpressed and specifically secreted during experimentally induced colitis in rats. *Eur J Biochem* 1995, 232:603–610
41. Kim YS, Ko J, Kim IS, Jang SW, Sung HJ, Lee HJ, Lee SY, Kim Y, Na DS: PKCdelta-dependent cleavage and nuclear translocation of annexin A1 by phorbol 12-myristate 13-acetate. *Eur J Biochem* 2003, 270:4089–4094
42. Pepinsky RB, Sinclair LK, Browning JL, Mattaliano RJ, Smart JE, Chow EP, Falbel T, Ribolini A, Garwin JL, Walner BP: Purification and partial sequence analysis of a 37-kDa protein that inhibits phospholipase A2 activity from rat peritoneal exudates. *J Biol Chem* 1986, 261:4239–4246
43. Pagano M, Pepperkok R, Verde F, Ansorge W, Draetta G: Cyclin A is required at two points in the human cell cycle. *EMBO J* 1992, 11:961–971
44. Raufman JP, Malhotra R, Xie Q, Raffaniello RD: Expression and phosphorylation of a MARCKS-like protein in gastric chief cells: further evidence for modulation of pepsinogen secretion by interaction of Ca<sup>2+</sup>/calmodulin with protein kinase C. *J Cell Biochem* 1997, 64:514–523
45. Chaib H, Cockrell EK, Rubin MA, Macoska JA: Profiling and verification of gene expression patterns in normal and malignant human prostate tissues by cDNA microarray analysis. *Neoplasia* 2001, 3:43–52
46. Graeber TG, Sawyers CL: Cross-species comparisons of cancer signaling. *Nat Genet* 2005, 37:7–8
47. Peeper D, Berns A: Cross-species oncogenomics in cancer gene identification. *Cell* 2006, 125:1230–1233
48. Fodde R, Khan PM: Genotype-phenotype correlations at the adenomatous polyposis coli (APC) gene. *Crit Rev Oncog* 1995, 6:291–303
49. Reichling T, Goss KH, Carson DJ, Holdcraft RW, Ley-Ebert C, Witte D, Aronow BJ, Groden J: Transcriptional profiles of intestinal tumors in *Apc(Min)* mice are unique from those of embryonic intestine and identify novel gene targets dysregulated in human colorectal tumors. *Cancer Res* 2005, 65:166–176
50. Crawford HC, Fingleton BM, Rudolph-Owen LA, Goss KJ, Rubinfeld B, Polakis P, Matrisian LM: The metalloproteinase matrilysin is a target of beta-catenin transactivation in intestinal tumors. *Oncogene* 1999, 18:2883–2891
51. Fujita M, Furukawa Y, Tsunoda T, Tanaka T, Ogawa M, Nakamura Y: Up-regulation of the ectodermal-neural cortex 1 (ENC1) gene, a downstream target of the beta-catenin/T-cell factor complex, in colorectal carcinomas. *Cancer Res* 2001, 61:7722–7726
52. Battle E, Henderson JT, Beghtel H, van den Born MM, Sancho E, Huls G, Meeldijk J, Robertson J, van de Wetering M, Pawson T, Clevers H: Beta-catenin and TCF mediate cell positioning in the intestinal epithelium by controlling the expression of EphB/ephrinB. *Cell* 2002, 111:251–263
53. Tetsu O, McCormick F: Beta-catenin regulates expression of cyclin D1 in colon carcinoma cells. *Nature* 1999, 398:422–426
54. Shutman M, Zhurinsky J, Simcha I, Albanese C, D'Amico M, Pestell

1380 Gaspar et al  
*AJP May 2008, Vol. 172, No. 5*

- R, Ben-Ze'ev A: The cyclin D1 gene is a target of the beta-catenin/LEF-1 pathway. *Proc Natl Acad Sci USA* 1999, 96:5522–5527
55. Zhang T, Fields JZ, Ehrlich SM, Boman BM: The chemopreventive agent sulindac attenuates expression of the antiapoptotic protein survivin in colorectal carcinoma cells. *J Pharmacol Exp Ther* 2004, 308:434–437
  56. Zhu HX, Zhang G, Wang YH, Zhou CQ, Bai JF, Xu NZ: [Indomethacin induces apoptosis through inhibition of survivin regulated by beta-catenin/TCF4 in human colorectal cancer cells]. *Ai Zheng* 2004, 23:737–741
  57. Kaiser S, Park YK, Franklin JL, Halberg RB, Yu M, Jessen WJ, Freudenberg J, Chen X, Haigis K, Jegga AG, Kong S, Sakthivel B, Xu H, Reichling T, Azhar M, Boivin GP, Roberts RB, Bissahoyo AC, Gonzales F, Bloom GC, Eschrich S, Carter SL, Aronow JE, Kleimeyer J, Kleimeyer M, Ramaswamy V, Settle SH, Boone B, Levy S, Graff JM, Doetschman T, Groden J, Dove WF, Threadgill DW, Yeatman TJ, Coffey RJ Jr, Aronow BJ: Transcriptional recapitulation and subversion of embryonic colon development by mouse colon tumor models and human colon cancer. *Genome Biol* 2007, 8:R131
  58. Kelekar A, Chang BS, Harlan JE, Fesik SW, Thompson CB: Bad is a BH3 domain-containing protein that forms an inactivating dimer with Bcl-XL. *Mol Cell Biol* 1997, 17:7040–7046
  59. Yang E, Zha J, Jockel J, Boise LH, Thompson CB, Korsmeyer SJ: Bad, a heterodimeric partner for Bcl-XL and Bcl-2, displaces Bax and promotes cell death. *Cell* 1995, 80:285–291
  60. Markowitz S, Wang J, Myeroff L, Parsons R, Sun L, Lutterbaugh J, Fan RS, Zborowska E, Kinzler KW, Vogelstein B, Brattain M, Willson JKV: Inactivation of the type II TGF-beta receptor in colon cancer cells with microsatellite instability. *Science* 1995, 268:1336–1338
  61. Hata A, Lagna G, Massague J, Hemmati-Brivanlou A: Smad6 inhibits BMP/Smad1 signaling by specifically competing with the Smad4 tumor suppressor. *Genes Dev* 1998, 12:186–197
  62. Park SH: Fine tuning and cross-talking of TGF-beta signal by inhibitory Smads. *J Biochem Mol Biol* 2005, 38:9–16
  63. Al-Tassan N, Chmiel NH, Maynard J, Fleming N, Livingston AL, Williams GT, Hodges AK, Davies DR, David SS, Sampson JR, Cheadle JP: Inherited variants of MYH associated with somatic G:C→T:A mutations in colorectal tumors. *Nat Genet* 2002, 30:227–232



***Smad4* haploinsufficiency:  
a matter of dosage**

# Chapter 6

Paola Alberici, Claudia Gaspar, Patrick Franken, Marcin M Gorski,  
Ingrid de Vries, Rodney J Scott, Ari Ristimäki, Lauri A Aaltonen and  
Riccardo Fodde





Research

Open Access

## ***Smad4* haploinsufficiency: a matter of dosage**

Paola Alberici<sup>1,7</sup>, Claudia Gaspar<sup>1</sup>, Patrick Franken<sup>1</sup>, Marcin M Gorski<sup>2,8</sup>, Ingrid de Vries<sup>1</sup>, Rodney J Scott<sup>3</sup>, Ari Ristimäki<sup>4,6</sup>, Lauri A Aaltonen<sup>5,6</sup> and Riccardo Fodde<sup>\*1</sup>

Address: <sup>1</sup>Department of Pathology, Josephine Nefkens Institute, Erasmus MC, Rotterdam, The Netherlands, <sup>2</sup>Department of Biochemistry, Erasmus MC, Rotterdam, The Netherlands, <sup>3</sup>Newcastle Bowel Cancer Research Collaborative, Hunter Medical Research Institute, John Hunter Hospital and The University of Newcastle, Newcastle, Australia, <sup>4</sup>Division of Pathology HUSLAB and Haartman Institute, Helsinki University Central Hospital, Helsinki, Finland, <sup>5</sup>Department of Medical Genetics, HUSLAB and Haartman Institute, Helsinki University Central Hospital, Helsinki, Finland, <sup>6</sup>Genome Scale Pathology Program, Biomedicum Helsinki, University of Helsinki, Helsinki, Finland, <sup>7</sup>Current address: IFOM -The FIRG Institute of Molecular Oncology, IFOM-IEO Campus, Milano, Italy and <sup>8</sup>Current address: Department of Experimental Oncology, European Institute of Oncology (IEO), IFOM-IEO Campus, Milano, Italy

Email: Paola Alberici - [paola.alberici@ifom-ieo-campus.it](mailto:paola.alberici@ifom-ieo-campus.it); Claudia Gaspar - [c.gaspar@erasmusmc.nl](mailto:c.gaspar@erasmusmc.nl); Patrick Franken - [p.f.franken@erasmusmc.nl](mailto:p.f.franken@erasmusmc.nl); Marcin M Gorski - [marcin.gorski@ifom-ieo-campus.it](mailto:marcin.gorski@ifom-ieo-campus.it); Ingrid de Vries - [i.devries.1@erasmusmc.nl](mailto:i.devries.1@erasmusmc.nl); Rodney J Scott - [rodney.scott@newcastle.edu.au](mailto:rodney.scott@newcastle.edu.au); Ari Ristimäki - [ari.ristimaki@helsinki.fi](mailto:ari.ristimaki@helsinki.fi); Lauri A Aaltonen - [Lauri.Aaltonen@Helsinki.Fi](mailto:Lauri.Aaltonen@Helsinki.Fi); Riccardo Fodde\* - [r.fodde@erasmusmc.nl](mailto:r.fodde@erasmusmc.nl)

\* Corresponding author

Published: 3 November 2008

Received: 3 July 2008

PathoGenetics 2008, 1:2 doi:10.1186/1755-8417-1-2

Accepted: 3 November 2008

This article is available from: <http://www.pathogenetics.com/content/1/1/2>

© 2008 Alberici et al; licensee BioMed Central Ltd.

This is an Open Access article distributed under the terms of the Creative Commons Attribution License (<http://creativecommons.org/licenses/by/2.0>), which permits unrestricted use, distribution, and reproduction in any medium, provided the original work is properly cited.

### **Abstract**

**Background:** The inactivation of tumor suppressor genes follows Alfred Knudson's 'two-hit' model: both alleles need to be inactivated by independent mutation events to trigger tumor formation. However, in a minority of tumor suppressor genes a single hit is sufficient to initiate tumorigenesis notwithstanding the presence of the wild-type allele, a condition known as haploinsufficiency. The *SMAD4* gene is an intracellular mediator of the TGF- $\beta$  and BMP signal transduction pathways and a tumor suppressor involved in pancreatic and colorectal tumorigenesis. In *Smad4*-mutant mouse models, haploinsufficiency characterizes the development of gastrointestinal polyps with initial retention of the wild-type allele and protein expression within the nascent tumors and in their direct microenvironment. Similarly, germline *SMAD4* mutations are responsible for a subset of patients affected by juvenile polyposis syndrome, an autosomal dominant intestinal cancer syndrome. To date, the molecular and cellular consequences of *SMAD4* haploinsufficiency on TGF- $\beta$  and BMP signaling and on genome-wide gene expression have not been investigated.

**Results:** Here we show that, similar to previous observations in *Smad4*-mutant mouse models, haploinsufficiency characterizes a substantial fraction of the juvenile polyps arising in patients with germline *SMAD4* mutations. Also, mouse embryonic and intestinal cells heterozygous for a targeted *Smad4* null mutation are characterized by a corresponding 50% reduction of the *Smad4* protein levels. Reporter assays revealed that mouse *Smad4*<sup>+/-</sup> cells exert intermediate inhibitory effects on both TGF- $\beta$  and BMP signaling. Genome-wide expression profiling analysis of *Smad4*<sup>+/-</sup> and *Smad4*<sup>-/-</sup> cells pinpointed a subset of dosage-dependent transcriptional target genes encompassing, among others, members of the TGF- $\beta$  and Wnt signaling pathways. These *SMAD4* dosage-dependent

transcriptional changes were confirmed and validated in a subset of target genes in intestinal tissues from juvenile polyposis syndrome patients.

**Conclusion:** *Smad4* haploinsufficiency is sufficient to significantly inhibit both TGF- $\beta$  and BMP signal transduction and results in the differential expression of a broad subset of target genes likely to underlie tumor formation both from the mesenchymal and epithelial compartments. The results of our study, performed in normal rather than tumor cells where additional (epi-) genetic alterations may confound the analysis, are relevant for our understanding and elucidation of the initial steps underlying *SMAD4*-driven intestinal tumorigenesis.

## Background

Haploinsufficiency is defined as the condition where mutation or loss of a single allele is sufficient to alter the phenotype of a diploid cell [1]. Haploinsufficiency at a tumor suppressor locus may overcome the need for somatic loss or mutation of its wild-type allele, predicted as the rate-limiting event for tumor development by the Knudson's 'two-hit' model [2]. To date, experimental evidence for haploinsufficiency in cancer predispositions comes from the analysis of tumors obtained from mouse models or hereditary cancer patients carrying heterozygous *null* mutations at known tumor suppressor genes [3]. The absence of the second hit in a subset of these tumors has been attributed to many causes, including inactivation of the remaining allele by alternative mechanisms such as epigenetic silencing, mutations in non-coding sequences, or to limited sensitivity of the employed mutation detection protocol. However, *bona fide* haploinsufficiency has been demonstrated for a subset of tumor suppressor loci including *SMAD4* [4-6], an intracellular mediator of the TGF- $\beta$  and BMP signal transduction pathways [7,8]. Upon TGF- $\beta$  or BMP signaling, *SMAD4* binds to the receptor-activated *SMADs* and translocates to the nucleus where it modulates the transcription of a broad spectrum of target genes involved in cell growth inhibition, apoptosis, differentiation, and matrix production [7-9]. Somatic *SMAD4* gene mutations are found in only a fraction of advanced sporadic colorectal cancers (CRCs) [10], whereas germline *SMAD4* mutations are responsible for a subset of patients affected by juvenile polyposis syndrome (JPS; Online Mendelian Inheritance in Man 174900) [4], an autosomal dominant intestinal cancer syndrome. Although the original report showing that *SMAD4* germline mutations are responsible for JPS also contained preliminary data indicating that loss of heterozygosity (LOH) of the wild-type allele occurred in a minority of the polyps examined [4], the most convincing evidence for haploinsufficiency at this locus came from the analysis of mouse models for juvenile polyposis. We and others showed that mice carrying targeted *Smad4* mutations develop gastrointestinal (GI) polyps with initial retention of the wild-type *Smad4* allele; complete functional loss only occurs at later stages of tumor progression within the epithelial compartment [5,6]. Nota-

bly, loss of a single *Smad4* allele in the T-cell compartment and not in the intestinal epithelium resulted in mice characterized by hyperplasia and polyp formation in the GI tract, similar to the animals with constitutive *Smad4* mutations [11]. These data indicate that *Smad4* haploinsufficiency is likely to play a causative role in GI tumor formation by exerting a 'landscaping' effect from within the microenvironment as originally proposed by Kinzler and Vogelstein [12], and its complete loss of function in the epithelial cells at later tumor stages accompanies progression towards malignancy [5,6]. Whether *SMAD4* causes polyp formation through haploinsufficiency has been challenged by two studies showing that the majority of tumors from JPS patients carrying germline mutations do show LOH at the wild-type locus [13,14]. These somatic events occurred both in the epithelial and stromal components of JPS polyps but not in the infiltrating lymphocytes [13].

Here, we have analyzed a cohort of juvenile polyps from patients with germline *SMAD4* mutations for the retention of protein expression and confirmed that haploinsufficiency characterizes early stages of polyp formation in a substantial proportion of the cases. Moreover, we attempted the elucidation of the molecular basis of *Smad4* haploinsufficiency by studying signal transduction and global gene expression in otherwise normal *Smad4*<sup>+/-</sup> cells.

## Results

### *SMAD4* haploinsufficiency underlies human juvenile polyposis

Although haploinsufficiency has been thoroughly characterized in mouse models carrying targeted mutations in the *Smad4* gene [5,6], two reports have shown that in the majority of tumors from JPS patients carrying *SMAD4* germline mutations LOH could be detected at the wild-type allele [13,14]. To clarify this apparent discordance between mouse and man, and to establish whether *SMAD4* behaves as a classical tumor suppressor gene or if, analogous to the *Smad4* mouse models, haploinsufficiency underlies early stages of tumor formation in man, we performed *SMAD4* immunohistochemistry (IHC) analysis of juvenile polyps from six unrelated JPS patients with known *SMAD4* germline mutations (Table 1). Out of

**Table 1: Results of the immunohistochemical analysis of intestinal polyps from Juvenile Polyposis syndrome patients carrying established SMAD4 germline mutations.**

	SMAD4 Germline Mutation Nucleotide [ref.]	Amino Acid	Epithelial SMAD4 expression	Stromal SMAD4 expression
<b>JPS case #1</b>				
polyp A	nt 1042–43, 2 bp del, TTGTTA-TTTA [4]	FS 350X	-	+
polyp B	nt 1042–43, 2 bp del, TTGTTA-TTTA [4]	FS 350X	-	-
<b>JPS case #2</b>				
polyp A	nt 424+1, intron 2 TTGg-TTGa	splice defect	+/-	+
<b>JPS case #3</b>				
polyp A	nt 1058 TAC-TCC [40]	Tyr353Ser	+/-	+
polyp B	nt 1058 TAC-TCC [40]	Tyr353Ser	+	+
polyp C	nt 1058 TAC-TCC [40]	Tyr353Ser	+	+
<b>JPS case #4</b>				
polyp A	nt 533 TCA-TGA [40]	Ser178X	+/-	+
polyp B	nt 533 TCA-TGA [40]	Ser178X	+	+
<b>JPS case #5</b>				
polyp A	nt 687–692, 1 bp ins, TGGGGGGC-TGGGGGGC [4]	FS 235X	+	+
polyp B	nt 687–692, 1 bp ins, TGGGGGGC-TGGGGGGC [4]	FS 235X	-	-
polyp C	nt 687–692, 1 bp ins, TGGGGGGC-TGGGGGGC [4]	FS 235X	+/-	+/-
<b>JPS case #6</b>				
polyp A	nt 1244–47, 4 bp del, AGACAGAG-AGAG [4]	FS 434X	+/-	+
polyp B	nt 1244–47, 4 bp del, AGACAGAG-AGAG [4]	FS 434X	+/-	+

In the last two columns, +, +/-, and - indicate homogeneously positive, patchy, and homogeneously negative nuclear SMAD4 staining, respectively (for examples of the various staining patterns, see Figure 1).

117

13 polyps analyzed, three (23%) revealed a homogeneously negative staining of the epithelial tumor cells, thus indicating functional loss of the wild-type SMAD4 allele (Figure 1g and 1h). In the remaining cases, SMAD4 expression was either patchy with groups of negative glands scattered among positive ones ( $n = 6$ , 46%; Figure 1c to 1f), or showed clear retention of SMAD4 expression ( $n = 4$ , 31%; Figure 1a and 1b). As far as the tumor-associated stroma is concerned, different mesenchymal cell types, for example stromal fibroblasts and infiltrating lymphocytes, showed in almost all cases SMAD4 nuclear reactivity amidst a variable number of negative cells (Figure 1). However, no relationship could be established between the percentage of SMAD4-positive stromal cells and the loss/retention of expression in the adjacent epithelial glands. Also, although the total number of tumors analyzed is admittedly small, no correlation could be found between polyp size and loss/retention of SMAD4 expression.

Overall, the IHC results confirm that in a substantial proportion of the polyps here analyzed from JPS patients with SMAD4 germline mutations, tumor onset does not follow Knudson's two-hit model as SMAD4 expression is retained in either all or in a considerable proportion of the epithelial tumor cells. In these cases, as previously shown

in the *Smad4*<sup>+/-E6sad</sup> mouse model [6], haploinsufficiency is likely to underlie juvenile polyp onset, whereas later stages of tumor progression are accompanied by loss of the wild-type allele.

#### **Smad4 haploinsufficiency results in partial inhibition of TGF- $\beta$ and BMP signaling**

In order to study the transcriptional and signal transduction defects arising from haploinsufficiency at the *Smad4* tumor suppressor gene, we employed mouse embryonic stem (ES) cells where a null mutation, namely a single nucleotide deletion in the exon 6 splice acceptor site resulting in an unstable mRNA, is present in the endogenous locus [6,15]. The choice of ES cells as a cellular model to study *Smad4* haploinsufficiency was made mainly based on observations that different components of the parenchymal and microenvironmental compartments are likely to contribute to polyp initiation and progression to malignancy [5,6,11], as described above. ES cells represent the inner cell mass of the pre-implantation blastocyst and thus precede the differentiation of the three main germ layers. Moreover, the employment of normal rather than neoplastic cells allows bypassing of confounders caused by the altered cellular physiology characteristic of tumor cells and focuses on the primary molecular and cellular consequences of *Smad4* haploinsufficiency. The



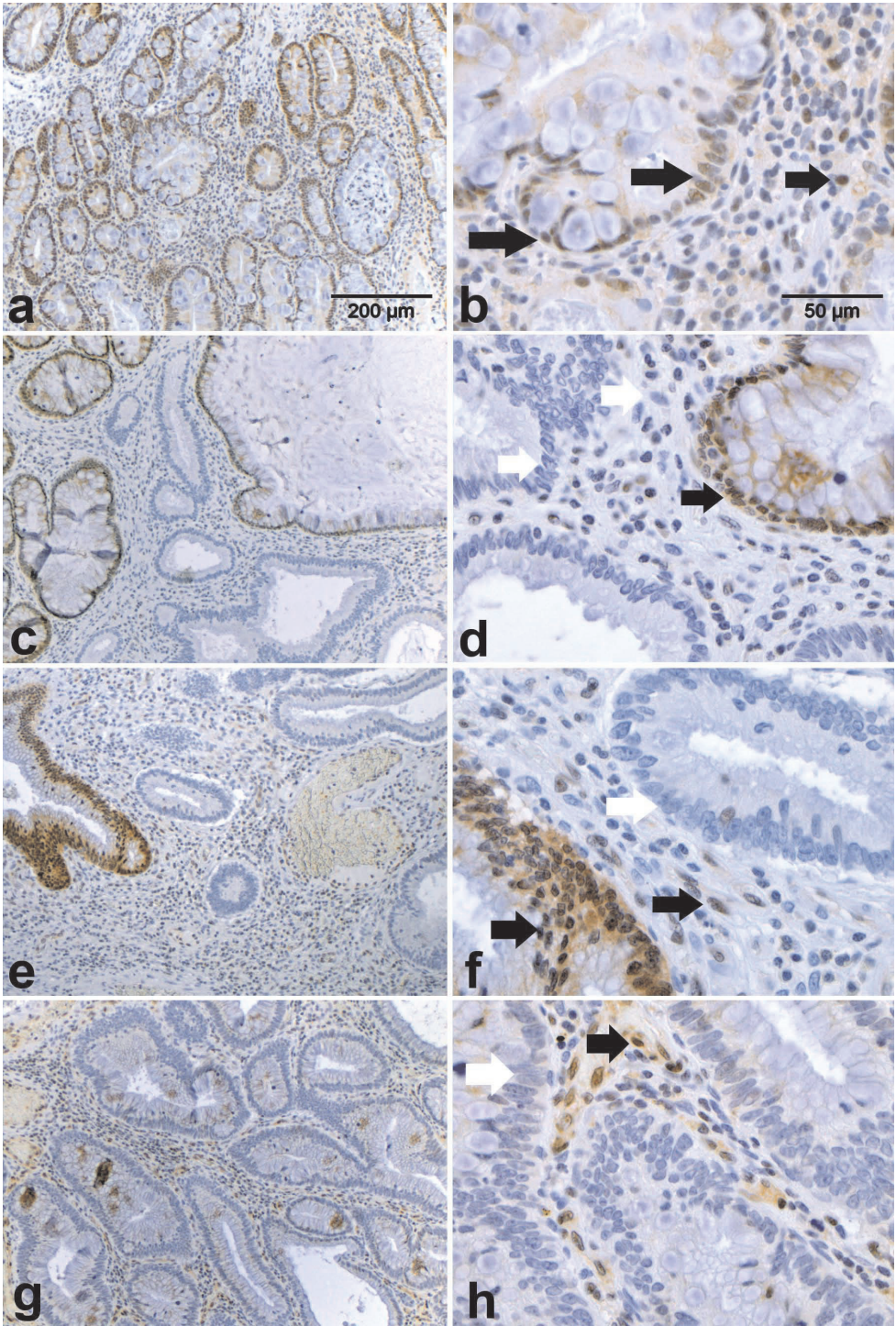


**Figure I** (see legend on next page)

**Figure 1** (see previous page)

**Immunohistochemical analysis of SMAD4 protein expression in juvenile polyps from patients carrying SMAD4 germline mutations.** SMAD4 immunohistochemical analysis of hamartomatous polyps obtained from unrelated Juvenile Polyposis syndrome patients with established SMAD4 germline mutations (see Table 1). Images were taken at 10× (a, c, e, g,) and 40× (b, d, f, h). Filled (black) arrows indicate cells scored as positive, whereas white arrows point to negatives. **a-b.** Example of a polyp positive for SMAD4 nuclear staining in both the epithelial and stromal compartment (scored as double positive in Table 1). **c-d.** Polyp with heterogeneous SMAD4 expression pattern with patches of positively and negatively staining epithelial glands. Most of the stromal cells appear negative with few exceptions. This tumor was scored as +/- (epithelial) and - (stromal) in Table 1. **e-f.** Example of a juvenile polyp with heterogeneous SMAD4 expression in the epithelial compartment but with a more pronounced positive staining of the stromal tumor microenvironment. This tumor was scored as +/- (epithelial) and + (stromal) in Table 1. **g-h.** Example of a juvenile polyp characterized by negative SMAD4 staining throughout the epithelial cells. In the stromal compartment however, several positively staining cells are present. This tumor was scored as - (epithelial) and + (stromal) in Table 1.

alternative use of mouse embryonic fibroblasts (MEFs) was made impossible by the early *in utero* lethality characteristic of the *Smad4*<sup>E66sad/E66sad</sup> embryos which precludes MEFs isolation with this genotype [15].

First, we evaluated Smad4 protein expression in wild-type (*Smad4*<sup>+/+</sup>), heterozygous (*Smad4*<sup>+/-E66sad</sup>), and homozygous (*Smad4*<sup>E66sad/E66sad</sup>) ES cells obtained from pre-implantation blastocysts of interbred C57Bl6/J *Smad4*<sup>+/-E66sad</sup> mice. To this aim, two independent hetero- and homozygous ES clones were analyzed by western blot. As shown in Figure 2 (upper panel), *Smad4*<sup>E66sad/E66sad</sup> cells did not reveal any protein expression thus confirming the null nature of this mutation, whereas heterozygous ES lines showed a consistent reduction in protein expression when compared with wild-type ES cells, indicative of their haploinsufficiency at the protein level. Moreover, western analysis of intestinal cells from *Smad4*<sup>+/-E66sad</sup> mice validated the protein haploinsufficiency in adult tissues (Figure 2, lower panel).

To determine whether the observed reduction of Smad4 expression in mouse *Smad4*<sup>+/-E66sad</sup> ES and intestinal cells impairs TGF-β and BMP signaling, we measured the levels of the Smads transcriptional complex by a TGF-β reporter assay system [16]. Due to the insufficient expression levels of the type II TGF-β receptor (TBR2) in ES cells (data not shown), TGF-β reporter assay constructs were co-transfected with an expression vector (pCMV5-TBR2) encoding for the TBR2 receptor [17]. A dose-response assay was subsequently performed which indicated that a TGFβ 1 concentration of 50 pmol provides the highest response in the TBR2-transfected cells (data not shown). As depicted in Figure 3A, *Smad4*<sup>E66sad/E66sad</sup> ES cells demonstrated a dramatic decrease in TGF-β signaling activity when compared with the wild-type controls. Notably, decreased TGF-β activity is already apparent in *Smad4*<sup>+/-E66sad</sup> ES clones, characterized by an intermediate yet highly significant ( $p < 0.001$ ) level of luciferase activity between wild-type and homozygous cells. The difference between

*Smad4*<sup>+/+</sup> and *Smad4*<sup>+/-E66sad</sup> ES cells was not significant when untransfected cells were employed.

Similar results were obtained by analyzing the *Smad4*-mutant ES cells for BMP signaling levels by the BRE-luc reporter assay transfected together with a constitutively active ActR-I receptor (Alk-2) [18]: while *Smad4*<sup>E66sad/E66sad</sup> ES cells showed a marked decrease in BMP signaling, haploinsufficient cells revealed an intermediate though significant ( $p = 0.0024$ ) level between wild-type and *Smad4*-deficient ES cells (Figure 3B). Also, rescue of homozygous *Smad4*<sup>E66sad/E66sad</sup> ES cells by transfection with a human SMAD4 expression vector [9] fully restored TGF-β signaling (Figure 3C).

#### **Smad4 affects genome-wide gene expression in a dosage-dependent fashion**

In order to further characterize the effects of Smad4 haploinsufficiency on gene transcription, expression profiling analysis of total RNA samples from wild-type, *Smad4*<sup>+/-E66sad</sup>, and *Smad4*<sup>E66sad/E66sad</sup> ES cells was performed using the Affymetrix MOE430 2.0 array. Two independent clones for each genotype were employed for the analysis. Two individual lists of differentially expressed genes were generated by applying a p-value threshold of  $p < 0.01$  and  $p < 0.05$  for the homo- and heterozygous cells, respectively. Comparison of these two data sets led to the identification of a signature of 79 differentially expressed genes (31 up- and 48 down-regulated respectively) common to *Smad4* hetero- and homozygous cells, 64 of which (24 up- and 40 down) represent functionally annotated genes (Additional file 1).

Among the differentially expressed entries, a broad spectrum of functional categories is represented: members of known signal transduction pathways (for example, *Mdm2*, *Axin2*, *Smad7*, *Zak*), growth factors (*Fgf5*, *Fgf8*, *Igf1bp3*, *Lefty2*), immunity related genes (*Irgm*, *Il23a*, *Cxcl14*), and transcription factors (*Nrip1*, *Eomes*, *Stat3*, *Cnot6*, *T* brachyury homolog) (Additional file 1). This is

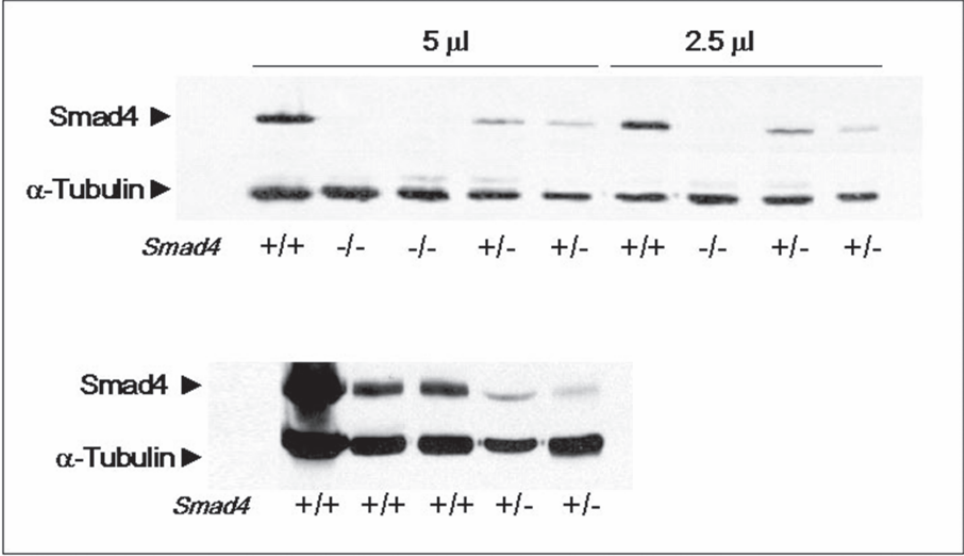


**Figure 2**  
**Western analysis of *Smad4*-mutant embryonic stem cell lines.** SMAD4 western blot analysis demonstrates haploinsufficiency in embryonic stem (ES) and adult intestinal cells from *Smad4*<sup>+/-E6sad</sup> mice. **Upper panel:** ES cell lysates loaded at two different protein amounts; **lower panel:** normal intestinal tissue lysates from wild-type and *Smad4*<sup>+/-E6sad</sup> mice.

also confirmed by Ingenuity Pathway analysis performed on the 64 gene signature (Additional file 2). The presence of *Smad4* itself within the list of differentially expressed genes serves as an internal confirmation of the validity of our approach. Notably, when the fold changes levels relative to these 79 genes are plotted in a trend analysis according to the *Smad4* genotypes, the *Smad4* dosage-dependent gradient of transcriptional response becomes apparent (Figure 4).

In order to validate the observed *Smad4* dosage-dependent effect on the transcriptional regulation of a subset of target genes, we performed quantitative real-time RT-PCR on laser-capture microdissected (LCM) normal intestinal cells obtained from two wild-type and three *Smad4*<sup>+/-E6sad</sup> animals. From the list of 64 genes differentially expressed upon *Smad4* haploinsufficiency, we selected six known to be expressed in the GI tract and characterized by at least a two-fold change in the ES cell expression profiling data (log2>1). As an internal reference standard, we employed the *Cryz1* (crystallin zeta quinone reductase-like 1) gene, which retains constant expression levels between all ES

and adult intestinal cells (data not shown). Similar to the ES cells expression profiling results, both up- (*Prkar1b* and *Tgb1*) and down-regulated (*Smad7*, *Irgm*, *Arts-1* and *Igfbp1*) genes showed consistent changes in gene expression levels in *Smad4*<sup>+/-E6sad</sup> normal intestinal cells when compared with intestinal epithelia from wild-type (*Smad4*<sup>+/+</sup>) animals (Figure 5), thus validating the microarray expression profiling results.

**Discussion**

Over the last few years it has become clear that in a subset of tumor suppressor genes the somatic inactivation or mutation of the wild-type allele (the second hit) does not invariably represent the rate-limiting tumor formation step [1,3,19]. It is generally thought that haploinsufficiency may affect normal cell function and homeostasis, possibly in a synergistic manner with other genetic or epigenetic somatic hits at unrelated cancer genes. Both JPS patients and mouse models carrying loss of function mutations at the *SMAD4* tumor suppressor gene represent illustrative examples of haploinsufficiency in GI tract tumorigenesis. In partial disagreement with Knudson's two-



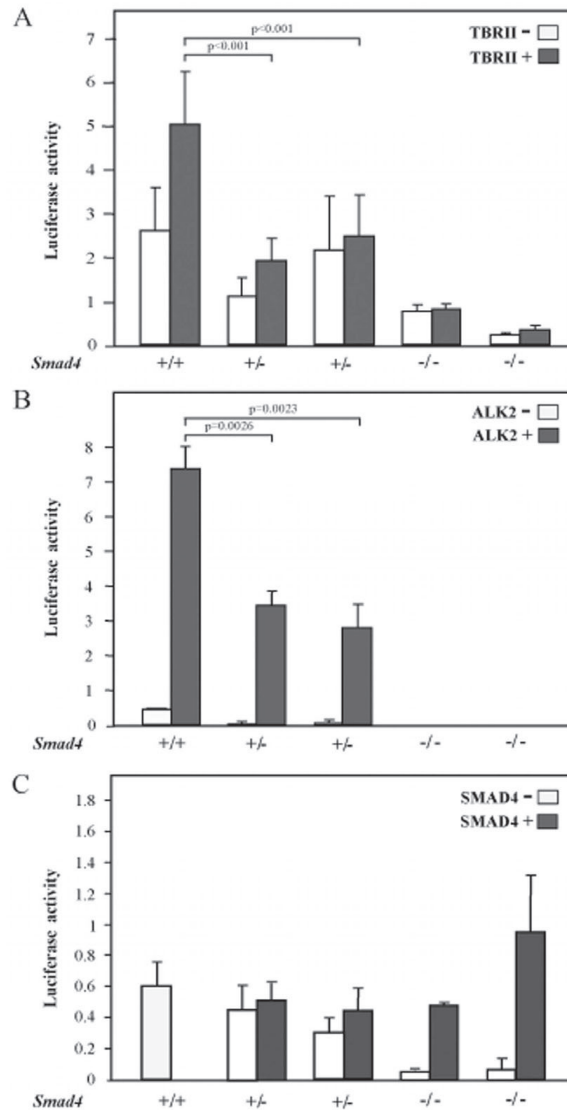


**Figure 3**

**TGF- $\beta$  and BMP reporter assay analysis of *Smad4*-mutant embryonic stem cell lines.** TGF- $\beta$  and BMP reporter assay analysis of *Smad4*-mutant embryonic stem (ES) cell lines. **A.** TGF- $\beta$  (CAGA12-MLP-luciferase) and **B.** BMP (BRE-luciferase) reporter assays were carried out in wild-type (+/+), *Smad4*<sup>+/-E6s</sup> (+/-), and *Smad4*<sup>E6s/E6s</sup> (-/-) ES cell lines. Normalized CAGA-luc and BRE-luc levels are indicated for each cell line. For each genotype reporter activities are shown for cells transfected (TBR11+ and ALK2+) and non transfected (TBR11- and ALK2-) with the corresponding receptor-expressing vector. In **C.** the TGF- $\beta$  reporter assays analysis was carried out after transfection with a *SMAD4*-expressing vector. Each bar represents the average of three independent experiments, and the error bars represent the standard deviation. For the CAGA12-MLP-luciferase assay, three independent ES wild-type clones have been employed. The WT bar represents the average of the luciferase activities measured in two independent experiments. p values were calculated by the statistical two samples t-test (two tails).

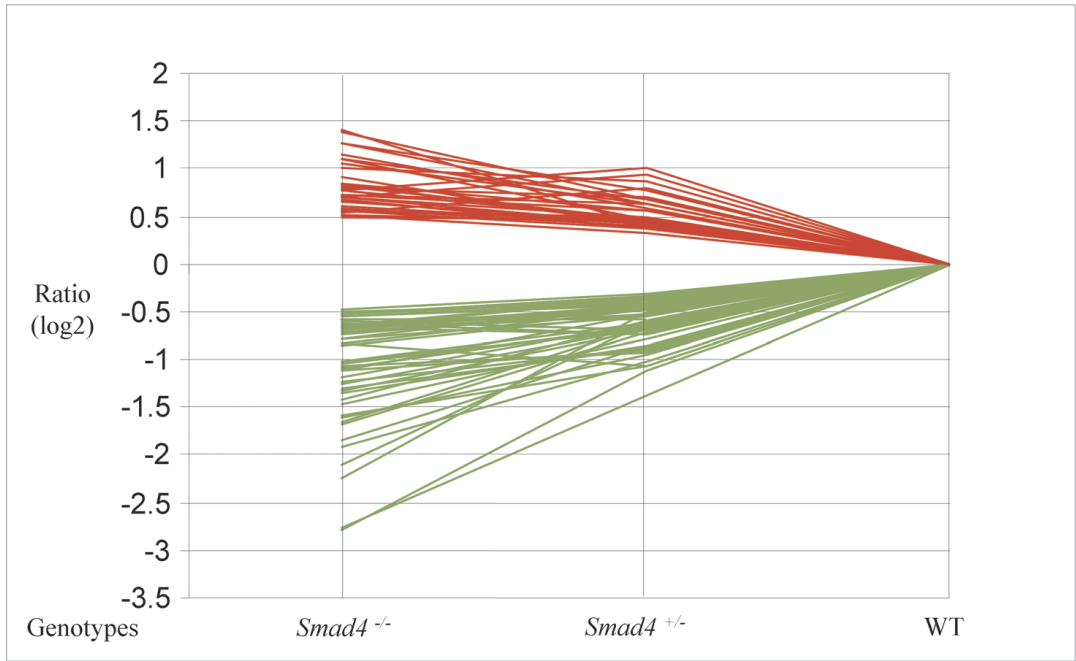


**Figure 4**  
**Trend analysis of *Smad4* dosage-dependent transcriptional targets.** Trend analysis of the 79 genes found to be differentially expressed in both *Smad4*<sup>+/-E6sad</sup> and *Smad4*<sup>E6sad/E6sad</sup> embryonic stem cells. The fold changes are represented as (log2) ratio values and plotted as red and green lines for up- and down-regulated genes, respectively.

hit model, somatic loss of the wild-type allele is not a rate-limiting event in intestinal polyp formation in *Smad4*-mutant mouse models [5,6]. Accordingly, as shown in our study, the majority of polyps from JPS patients carrying *SMAD4* germline mutations retain *SMAD4* expression both in epithelial tumor cells and in their stromal micro-environment, thus indicating haploinsufficiency. Previously, Howe et al showed that juvenile polyps from *SMAD4* mutation carriers reveal loss of the wild-type allele in only 9% (1/11) of their cases [4]. However, the analysis was done by an exon-specific PCR assay unable to detect more subtle somatic hits such as point mutations and epigenetic silencing. Notably, two subsequent and more thorough reports have shown by LOH, fluorescence in situ hybridization, and IHC analysis that loss of the wild-type allele could be detected in the majority of tumors from JPS patients carrying *SMAD4* germline muta-

tions [13,14]. Moreover, *SMAD4* loss was observed in both epithelial and some of the stromal cells, which was interpreted by the authors as an indication of the clonal origin of these lesions, and of the fact that *SMAD4* represents a classical 'gatekeeper' tumor suppressor rather than a 'landscaper' as originally proposed [12,13]. How can the apparent discordance between the present study and the reports by Woodford-Richens and colleagues be solved? From the IHC analysis depicted in Figure 1 it should be clear that a high degree of heterogeneity in *SMAD4* expression characterizes juvenile polyps both in the epithelial and mesenchymal compartments. This heterogeneity, when reduced to more quantitative values as in the case of PCR-based LOH analysis of whole tumor specimens comprehensive of both parenchymal and microenvironmental cells, may result in loss of accuracy. Also, differences in interpretation of IHC images may partly underlie this dis-

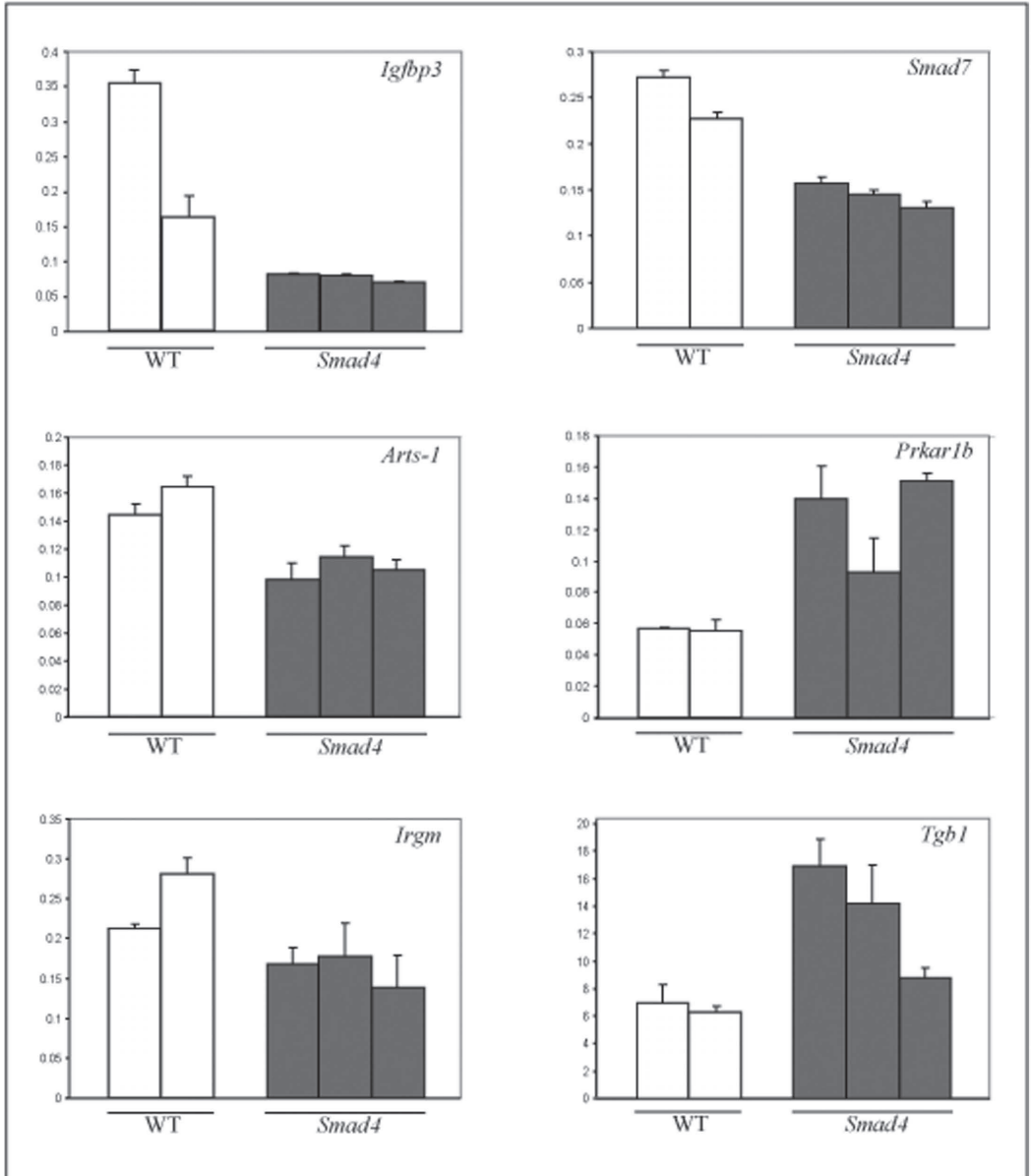


**Figure 5**  
**qPCR validation of the expression profiling results.** Quantitative PCR analysis of a selection of six genes differentially regulated in *Smad4*<sup>+/-E6sad</sup> cells. Gene expression was quantified in normal intestinal tissues from two wild-type (WT) and three *Smad4*<sup>+/-E6sad</sup> (*Smad4*) animals and is plotted as ratio over the reference gene (see Materials and Methods). Each bar represents the average of three independent experiments.

crepancy. In their IHC analysis of juvenile polyps from *SMAD4*-mutant JPS patients [14], Woodford-Richens et al present an example where, similar to observations in our study, a heterogeneous staining pattern is observed with positive epithelial glands amidst negative ones. Last but not least, both the two-hit and haploinsufficiency models appear to hold true for *SMAD4*-driven tumorigenesis, and this may depend on the molecular nature and pathogenicity of the first hit, namely the germline mutation. As predicted by the 'just right' model for the *APC* tumor suppressor gene [20,21], the molecular nature of the first hit at a tumor suppressor locus affects the type of second-hit mutation at the wild-type allele. It is plausible to think that while some *SMAD4* mutations require functional inactivation of the wild-type allele to trigger tumor formation, others can result in juvenile polyp onset without this otherwise rate-limiting somatic step.

A second important aspect is relative to the role of the *SMAD4* in tumor formation either as an epithelial 'gatekeeper' or as a 'landscaper', that is, acting from within the microenvironment to affect epithelial homeostasis [12]. Recently, it was shown that selective loss of *Smad4* in the mouse T-cell compartment results in intestinal adenomas reminiscent of JPS polyps [11]. Notably, loss of a single *Smad4* allele in T-cells also resulted in hyperplasia and polyp formation in the intestinal epithelial layer, thus indicating that *Smad4* haploinsufficiency plays a causative role in GI tumor formation by exerting a 'landscaping' effect from within the stromal compartment [11]. Conversely, our own observation, according to which more advanced lesions of the *Smad4*<sup>+/E6<sup>smad</sup> mouse model show complete loss of *Smad4* expression [6], is indicative of an additional role for the complete loss of *Smad4* function in the epithelial compartment at later tumor progression stages. Whether the same holds true for *SMAD4*-driven juvenile polyp formation in man is still debatable. From our own IHC analysis (Figure 1), it should be evident that the *SMAD4* expression pattern in the tumor microenvironment appears rather heterogeneous, with a mixture of positive and negative stromal fibroblasts and infiltrating lymphocytes. However, these results are inconclusive in discriminating between the 'gatekeeper' versus 'landscaper' scenarios. In fact, there is little doubt about the active role played by the tumor microenvironment, especially in the presence of a TGF- $\beta$  signaling defect. Previous reports have shown that loss of function mutations at the *TBR1* gene can both trigger epithelial tumorigenesis from the stromal layer [22] and underlie malignant transformation when induced in the parenchymal cells of intestinal adenomas initiated by *Apc* mutations [23]. Similar observations were made for the *LKB1* gene (also known as *STK11*), responsible for Peutz-Jeghers syndrome (JPS; OMIM 175200), an autosomal dominant predisposition to hamartomas (polyps of the GI tract with a pronounced</sup>

mesenchymal component, very similar to those characteristic of JPS). *Lkb1*<sup>+/−</sup> mice develop intestinal polyps which often retain the wild type allele [24]. Accordingly, LOH is not an obligate step in polyps from JPS patients with germline *LKB1* mutations [25]. Notably, monoallelic loss of murine *Lkb1* in the smooth muscle compartment results in GI polyps indistinguishable from those observed in mice and in JPS patients with a constitutive mutation, thus confirming the 'landscaping' role of *Lkb1* haploinsufficiency [26]. Further molecular analysis of these mice revealed that the partial loss of *Lkb1* function results in a TGF- $\beta$  signaling defect within the stromal compartment likely to contribute to polyp formation by generating a permissive microenvironment for the malignant transformation of the epithelium [26]. Given the heterogeneous composition of the tumor microenvironment comprising not only stromal fibroblasts but also smooth muscle cells and various cellular types of immune origin, it is plausible to think that haploinsufficiency at members of the TGF- $\beta$  signaling pathways such as *SMAD4* and *LKB1* affects cell to cell communication in different tissues, thus leading to loss of tissue architecture.

In this study, we have shown that *Smad4* haploinsufficiency results in dosage-dependent inhibition of TGF- $\beta$  and BMP signaling, thus affecting epithelial cell proliferation and differentiation both in the stromal and epithelial compartments and likely to underlie juvenile polyp formation in the intestinal tract. Also, expression profiling of *Smad4* haploinsufficient cells revealed the existence of a subset of target genes whose expression is specifically regulated by decreased dosages of this tumor suppressor, presumably through TGF- $\beta$  and BMP signaling, as also shown by the differential expression of two known downstream targets of the TGF- $\beta$  pathway, namely *Smad7* and *Tgfb1*. *Smad7* is both an inhibitor of TGF- $\beta$  signaling and itself a TGF- $\beta$  downstream target [27]. Hence, *Smad7* down-regulation, as observed in the *Smad4*<sup>+/E6<sup>smad</sup> ES cells, reflects the observed TGF- $\beta$  signaling inhibition. *Tgfb1* is an extracellular protein with only poorly characterized functions, though its significant over-expression, as observed in *Smad4*-mutant ES cell lines, has also been reported in sporadic CRC [28].</sup>

Among the genes shown to be differentially up- or down-regulated in a *Smad4* dosage-dependent fashion, members of other signal transduction pathways were also included (Additional files 1 and 2). *Mdm2* up-regulation, as observed in *Smad4*<sup>+/E6<sup>smad</sup> cells, may favor tumor transformation by inhibiting p53-mediated transactivation [29] and by destabilizing retinoblastoma (RB). The gene encoding for the scaffold protein Axin2 (conductin), down-regulated in *Smad4*<sup>+/E6<sup>smad</sup> cells, has been previously implicated in canonical Wnt signaling and colorectal pathogenesis [30]. The latter is indicative of cross-talking</sup></sup>

between TGF- $\beta$  and Wnt signal transduction already in haploinsufficiency. Down-regulation of the *Igfbp3* gene, encoding for the insulin growth factor binding protein, in *Smad4*<sup>+/E6sad</sup> ES and intestinal cells may also represent a relevant early step in tumor formation. *Igfbp3* has been described as tumor suppressor gene [31], due to its role in the regulation of cell proliferation and apoptosis, and its differential methylation in a substantial fraction of CRC cases [32].

Overall, Smad4 haploinsufficiency affects both TGF- $\beta$  and BMP signaling together with a broad spectrum of transcriptional targets and cellular functions. Future studies will reveal which of these target genes are preferentially affected in a specific cellular compartment, and the paracrine or cell autonomous effect that they exert on epithelial tumorigenesis.

## Conclusion

In this study we have shown that haploinsufficiency at the *SMAD4* tumor suppressor locus underlies polyp formation in a proportion of GI tumors from JPS patients, as previously shown in *Smad4*-mutant mouse models. Moreover, *SMAD4* haploinsufficiency affects both the TGF- $\beta$  and BMP signal transduction pathways together with a broad spectrum of transcriptional targets and cellular functions. These results contribute to our understanding of the cellular and molecular mechanisms underlying intestinal tumorigenesis due to TGF- $\beta$  (and BMP) signaling defects not only in the parenchymal cells but also from within the stromal microenvironment. This is of fundamental but also of clinical relevance as these dosage-specific transcriptional targets may offer novel opportunities in the development of tailor-made therapeutic strategies.

## Methods

### Generation of *Smad4*-mutant ES cell lines

*Smad4*<sup>+/E6sad</sup> mice, available on the inbred C57Bl/6J background, were inter-bred and the resulting blastocysts harvested at 3.5 dpc. Flushed pre-implantation blastocysts were then individually cultured on 96-well dishes coated with MEFs as previously described [33].

All mouse experiments were performed upon approval of the local animal experiment committee (DEC permissions nr. EUR 596, 600, 623 and 730) and according to internationally recognized guidelines (as described by the *Code of Practice Dierproeven in het Kankeronderzoek*).

### *Smad4* western analysis

Equal amounts (40  $\mu$ g) of protein lysates were separated on 12% SDS polyacrylamide gels, and further subjected to immunoblotting according to standard procedures. Several studies have validated the specificity and sensitivity of

the B-8; sc-7966 monoclonal antibody against SMAD4 (Santa Cruz Biotechnology) to detect alterations of protein expression in both mouse and human specimens. The B-8; sc-7966 primary antibody was employed for western analysis at a 1:100 dilution. Peroxidase-conjugated secondary antibodies (Jackson ImmunoResearch) were visualized with an enhanced chemiluminescence system.

### Reporter assay analysis

ES cells grown on tissue culture dishes coated by mitotically inactivated primary MEFs were transfected by Lipofectamine 2000 (Life Technologies) with 250 ng of the reporter plasmid ((CAGA)12-MLP-luciferase for the TGF- $\beta$  signaling or BRE-luciferase for the BMP signaling), 100 ng of receptor-expressing vector (TGFBRII or, for BMP signaling, a constitutively active form of ALK2) [17,18] (all kindly provided by Professor P ten Dijke), and 5 ng of a *Renilla reniformis* luciferase-expressing vector. For the rescue experiments, 100 ng of the *Smad4*-pCMV5 expression vector [9] were transfected together with (CAGA) 12-MLP-luciferase and TGFBRII. After 24 hours, ES cells transfected with the (CAGA)12-MLP-luciferase were stimulated with recombinant human TGF- $\beta$  (50 pmol) for 1 hour before measuring luciferase activity with the luminometer Fluoroskan Ascent CF (Labsystems) using the Dual Luciferase Reporter Assay system (Promega). Luciferase activities were calculated as a ratio between the specific luciferase-reporter construct and the Renilla luciferase levels, for a total of three different experiments, each carried out in triplicate. For the CAGA12-MLP-luciferase assay, three independent ES wild-type clones were used and the average of their luciferase activities measured in two independent experiments.

### Immunohistochemical analysis

Formalin-fixed, paraffin-embedded intestinal polyps were prepared as 4  $\mu$ m sections and immunostained with the mouse Smad4 B-8; sc-7966 monoclonal antibody directed against Smad4 (Santa Cruz Biotechnology Inc, dilution 1:100). After antigen retrieval treatment (10 min boiling in Tris-EDTA pH 8.0), endogenous peroxidase was inactivated with 1% H<sub>2</sub>O<sub>2</sub>/PBS. A 30 min pre-incubation step in 5% non-fat dry milk in PBS was followed by incubation with the Smad4 antibody overnight at 4°C in pre-incubation buffer. Sections were then stained with the Envision HRP-ChemMate kit (DAKO). Smad4 IHC staining was evaluated after brief hematoxylin counterstaining of the slides.

### Expression profiling analysis

Total RNA was labeled using the GeneChip One-Cycle Target Labeling and Control Reagents kit, and hybridized to MOE430 2.0 Affymetrix oligonucleotide arrays, according to the manufacturers' instructions. Raw signal intensities were extracted and summarized from cel-files,

Table 2: Primers used in real-time RT-PCR analysis

Gene	Forward Primer	Reverse Primer
<i>Cryz1l</i>	5'-AGCTGCTGGCGTCATCCG-3'	5'-CTGTGGTGGGCTAACTGAATGG-3'
<i>Smad4</i>	5'-GTGACTGTGGATGGCTATGTGG-3'	5'-GCAACCTCGCTCTCTCAATCG-3'
<i>Arts-1</i>	5'-GCAGACTTGGACAGATGAAGG-3'	5'-TGACTTCCACTCTCTGAAATAGC-3'
<i>Smad7</i>	5'-TGCCTCGGACAGCTCAATTTCG-3'	5'-CCCACAGGCCATCCACTTCC-3'
<i>Prkar1b</i>	5'-GCCCGAATCCTGTGCCCTTG-3'	5'-TGCTGGCTCATATCACACTCC-3'
<i>Irgm</i>	5'-ACAGGCTCCAGCAGTTACC-3'	5'-TTGCCACAGTCTCCTTGATTCC-3'
<i>Tgfb1</i>	5'-CAAACAGGCGTCAGCGTATTCC-3'	5'-GGCTCTCTCCTCGGTCTTCC-3'
<i>Igfbp1</i>	5'-CCCAGAGGCGTCCACATCC-3'	5'-GTCCACACACCAGCAGAAGC-3'

followed by normalization using the robust multi-array average expression measure implemented in the Bioconductor package affyGUI [34]. No filtering was applied to the data. A Bayesian linear regression model was used to detect differentially expressed genes implemented in the Bioconductor package limma [35,36]. All Bioconductor packages were used with R statistical Computing Software v2.2.1 [37].

Quantitative real-time RT-PCR analysis

LCM of intestinal tissues (approx. 6000 cells) was performed as previously described [38]. PCR analysis was carried out in triplicate in 25 µl volumes using 1 µl of cDNA and SYBR® Green Dye (Applied Biosystems) on the MyiQ Single-Color Real-Time PCR Detection System (Bio-Rad). Primers sequences are listed below. Standard curves for the target genes and the reference *Cryz1l* gene were generated and the normalization and ratio were calculated as described [39], (see Table 2).

Competing interests

The authors declare that they have no competing interests.

Authors' contributions

PA was responsible for the immunohistochemistry, reporter assay, western and Q-PCR analyses, and has been involved in drafting the manuscript. CG performed the microarray analysis and the bioinformatic analysis of the resulting data. PF was mainly responsible for the histological processing of the tumor tissues and the SMAD4 immunohistochemistry analysis. MMG contributed to the target validation by quantitative PCR. IdV carried out the TGF-β reporter assays. RJS, AR, and LAA contributed the intestinal polyps from JPS patients with SMAD4 germline mutations. RF designed and supervised the study and wrote the final manuscript. All authors have read and approved the final manuscript.

Additional material

Additional file 1

Supplementary Table 1. List of 64 functionally annotated genes differentially express in Smad4<sup>+/E6sad</sup> and Smad4<sup>E6sad/E6sad</sup> ES cell lines. Expression profiling values are expressed as absolute fold change values when compared to Smad4<sup>+/+</sup> ES cells.

Click here for file  
[http://www.biomedcentral.com/content/supplementary/1755-8417-1-2-S1.doc]

Additional file 2

Supplementary Table 2. Ingenuity Pathway Analysis of the 64 functionally annotated genes differentially expressed (denoted as "focus molecules" in bold) in Smad4<sup>+/E6sad</sup> and Smad4<sup>E6sad/E6sad</sup> ES cell lines. The column denoted as "Top Functions" describe the gene ontology groups to which the genes encompassed in a given Ingenuity Network belong. Only the top 4 networks with the most significant scores are included.

Click here for file  
[http://www.biomedcentral.com/content/supplementary/1755-8417-1-2-S2.doc]

Acknowledgements

Supported was obtained from the Dutch Cancer Society (EMCR 2001-2482), the Dutch Research Council (NWO/Vici 016.036.636), the 'Besluit Subsidies Investeren Kennisinfrastructuur' program of the Dutch Government (BSIK 03038), Dutch Research Council (NWO-Vici), EU FP6 (MCSCs; nr. 037297) EU FP7 (TuMIC; nr. 201662), and the 'Maag Lever Darm Stichting' (MWO 04-21). The authors are very grateful to Professor P ten Dijke for his kind donation of the reporter constructs, to S Marttinen for the Finnish JPS patient material, to Dr NH Le for critically reading the manuscript, and to Mr F van der Panne for his help with the artwork.

References

1. Payne SR, Kemp CJ: **Tumor suppressor genetics.** *Carcinogenesis* 2005, **26**:2031-2045.  
2. Knudson AG Jr: **Mutation and cancer: statistical study of retinoblastoma.** *Proc Natl Acad Sci USA* 1971, **68**:820-823.  
3. Fodde R, Smits R: **Cancer biology. A matter of dosage.** *Science* 2002, **298**:761-763.  
4. Howe JR, Roth S, Ringold JC, Summers RW, Jarvinen HJ, Sistonen P, Tomlinson IP, Houlston RS, Bevan S, Mitros FA, Stone EM, Aaltonen LA: **Mutations in the SMAD4/DPC4 gene in juvenile polyposis.** *Science* 1998, **280**:1086-1088.  
5. Xu X, Brodie SG, Yang X, Im YH, Parks WT, Chen L, Zhou YX, Weinstein M, Kim SJ, Deng CX: **Haploid loss of the tumor suppressor Smad4/Dpc4 initiates gastric polyposis and cancer in mice.** *Oncogene* 2000, **19**:1868-1874.



6. Alberici P, Jagmohan-Changur S, De Pater E, Valk M Van Der, Smits R, Hohenstein P, Fodde R: **Smad4 haploinsufficiency in mouse models for intestinal cancer.** *Oncogene* 2006, **25**:1841-1851.
7. Heldin CH, Miyazono K, ten Dijke P: **TGF-beta signalling from cell membrane to nucleus through SMAD proteins.** *Nature* 1997, **390**:465-471.
8. Duff EK, Clarke AR: **Smad4 (DPC4) – a potent tumour suppressor?** *Br J Cancer* 1998, **78**:1615-1619.
9. Nakao A, Imamura T, Souchelnytskyi S, Kawabata M, Ishisaki A, Oeda E, Tamaki K, Hanai J, Heldin CH, Miyazono K, ten Dijke P: **TGF-beta receptor-mediated signalling through Smad2, Smad3 and Smad4.** *Embo J* 1997, **16**:5353-5362.
10. Salovaara R, Roth S, Loukola A, Launonen V, Sistonen P, Avizienyte E, Kristo P, Jarvinen H, Souchelnytskyi S, Sarlomo-Rikala M, Aaltonen LA: **Frequent loss of SMAD4/DPC4 protein in colorectal cancers.** *Gut* 2002, **51**:56-59.
11. Kim BG, Li C, Qiao W, Mamura M, Kasprzak B, Anver M, Wolfrum L, Hong S, Mushinski E, Potter M, Kim SJ, Fu XY, Deng C, Letterio JJ: **Smad4 signalling in T cells is required for suppression of gastrointestinal cancer.** *Nature* 2006, **441**:1015-1019.
12. Kinzler KW, Vogelstein B: **Landscaping the cancer terrain.** *Science* 1998, **280**:1036-1037.
13. Woodford-Richens K, Williamson J, Bevan S, Young J, Leggett B, Frayling I, Thway Y, Hodgson S, Kim JC, Iwama T, Novelli M, Sheer D, Poulson R, Wright N, Houlston R, Tomlinson I: **Allelic loss at SMAD4 in polyps from juvenile polyposis patients and use of fluorescence in situ hybridization to demonstrate clonal origin of the epithelium.** *Cancer Res* 2000, **60**:2477-2482.
14. Woodford-Richens KL, Rowan AJ, Poulson R, Bevan S, Salovaara R, Aaltonen LA, Houlston RS, Wright NA, Tomlinson IP: **Comprehensive analysis of SMAD4 mutations and protein expression in juvenile polyposis: evidence for a distinct genetic pathway and polyp morphology in SMAD4 mutation carriers.** *Am J Pathol* 2001, **159**:1293-1300.
15. Hohenstein P, Molenaar L, Elsinga J, Morreau H, Klift H van der, Struijk A, Jagmohan-Changur S, Smits R, van Kranen H, van Ommen GJ, Cornelisse C, Devilee P, Fodde R: **Serrated adenomas and mixed polyposis caused by a splice acceptor deletion in the mouse Smad4 gene.** *Genes Chromosomes Cancer* 2003, **36**:273-282.
16. Denner S, Itoh S, Vivien D, ten Dijke P, Huet S, Gauthier JM: **Direct binding of Smad3 and Smad4 to critical TGF beta-inducible elements in the promoter of human plasminogen activator inhibitor-type 1 gene.** *Embo J* 1998, **17**:3091-3100.
17. Wrana JL, Attisano L, Carcamo J, Zentella A, Doody J, Laiho M, Wang XF, Massague J: **TGF beta signals through a heteromeric protein kinase receptor complex.** *Cell* 1992, **71**:1003-1014.
18. Korchynski O, ten Dijke P: **Identification and functional characterization of distinct critically important bone morphogenetic protein-specific response elements in the Id1 promoter.** *J Biol Chem* 2002, **277**:4883-4891.
19. Santarosa M, Ashworth A: **Haploinsufficiency for tumour suppressor genes: when you don't need to go all the way.** *Biochim Biophys Acta* 2004, **1654**:105-122.
20. Lamlum H, Ilyas M, Rowan A, Clark S, Johnson V, Bell J, Frayling I, Efstathiou J, Pack K, Payne S, Roylance R, Gorman P, Sheer D, Neale K, Phillips R, Talbot I, Bodmer W, Tomlinson I: **The type of somatic mutation at APC in familial adenomatous polyposis is determined by the site of the germline mutation: a new facet to Knudson's 'two-hit' hypothesis.** *Nat Med* 1999, **5**:1071-1075.
21. Albuquerque C, Breukel C, Luijt R van der, Fidalgo P, Lage P, Slors FJ, Leita CN, Fodde R, Smits R: **The 'just-right' signaling model: APC somatic mutations are selected based on a specific level of activation of the beta-catenin signaling cascade.** *Hum Mol Genet* 2002, **11**:1549-1560.
22. Bhowmick NA, Chytil A, Plith D, Gorska AE, Dumont N, Shappell S, Washington MK, Neilson EG, Moses HL: **TGF-beta signaling in fibroblasts modulates the oncogenic potential of adjacent epithelia.** *Science* 2004, **303**:848-851.
23. Munoz NM, Upton M, Rojas A, Washington MK, Lin L, Chytil A, Sozmen EG, Madison BB, Pozzi A, Moon RT, Moses HL, Grady WM: **Transforming growth factor beta receptor type II inactivation induces the malignant transformation of intestinal neoplasms initiated by Apc mutation.** *Cancer Res* 2006, **66**:9837-9844.
24. Bardeesy N, Sinha M, Hezel AF, Signoretti S, Hathaway NA, Sharpless NE, Loda M, Carrasco DR, DePinho RA: **Loss of the Lkb1 tumour suppressor provokes intestinal polyposis but resistance to transformation.** *Nature* 2002, **419**:162-167.
25. Hernan I, Roig I, Martin B, Gamundi MJ, Martinez-Gimeno M, Carballo M: **De novo germline mutation in the serine-threonine kinase STK11/LKB1 gene associated with Peutz-Jeghers syndrome.** *Clin Genet* 2004, **66**:58-62.
26. Katajisto P, Vaahtomeri K, Ekman N, Ventela E, Ristimaki A, Bardeesy N, Feil R, DePinho RA, Makela TP: **LKB1 signaling in mesenchymal cells required for suppression of gastrointestinal polyposis.** *Nat Genet* 2008, **40**:455-459.
27. Nakao A, Afrakhte M, Moren A, Nakayama T, Christian JL, Heuchel R, Itoh S, Kawabata M, Heldin NE, Heldin CH, ten Dijke P: **Identification of Smad7, a TGFbeta-inducible antagonist of TGF-beta signalling.** *Nature* 1997, **389**:631-635.
28. Buchhaults P, Rago C, St Croix B, Romans KE, Saha S, Zhang L, Vogelstein B, Kinzler KW: **Secreted and cell surface genes expressed in benign and malignant colorectal tumors.** *Cancer Res* 2001, **61**:6996-7001.
29. Sdek P, Ying H, Chang DL, Qiu W, Zheng H, Tuitou R, Allday MJ, Xiao ZX: **MDM2 promotes proteasome-dependent ubiquitin-independent degradation of retinoblastoma protein.** *Mol Cell* 2005, **20**:699-708.
30. Liu W, Dong X, Mai M, Seelan RS, Taniguchi K, Krishnadath KK, Halling KC, Cunningham JM, Qian C, Christensen E, Roche PC, Smith DI, Thibodeau SN: **Mutations in AXIN2 cause colorectal cancer with defective mismatch repair by activating beta-catenin/TCF signalling.** *Nat Genet* 2000, **26**:146-147.
31. Xi Y, Nakajima G, Hamil T, Fodstad O, Riker A, Ju J: **Association of insulin-like growth factor binding protein-3 expression with melanoma progression.** *Mol Cancer Ther* 2006, **5**:3078-3084.
32. Tomii K, Tsukuda K, Toyooka S, Dote H, Hanafusa T, Asano H, Naitou M, Doihara H, Kisimoto T, Katayama H, Pass HI, Date H, Shimizu N: **Aberrant promoter methylation of insulin-like growth factor binding protein-3 gene in human cancers.** *Int J Cancer* 2007, **120**:566-573.
33. Helms AW, Matise MP, Joyner AL: **Establishing new ES lines.** In *Gene Targeting, A Practical Approach* Edited by: Joyner AL. Oxford: Oxford University Press; 2000:129-131.
34. Wettenhall JM, Smyth GK: **limmaGUI: a graphical user interface for linear modeling of microarray data.** *Bioinformatics* 2004, **20**:3705-3706.
35. Smyth GK: **Limma: linear models for microarray data.** In *Bioinformatics and Computational Biology Solutions using R and Bioconductor* Edited by: Gentleman VCR, Dudoit S, Irizarry R, Huber W. New York: Springer; 2005:397-420.
36. Smyth GK: **Linear models and empirical bayes methods for assessing differential expression in microarray experiments.** *Stat Appl Genet Mol Biol* 2004, **3**:Article 3.
37. R Development Core Team: **A language and environment for statistical computing.** Vienna: R Foundation for Statistical Computing; 2005.
38. Alberici P, de Pater E, Cardoso J, Bevelander M, Molenaar L, Jonkers J, Fodde R: **Aneuploidy arises at early stages of apc-driven intestinal tumorigenesis and pinpoints conserved chromosomal loci of allelic imbalance between mouse and human.** *Am J Pathol* 2007, **170**:377-387.
39. Pfaffl MW: **A new mathematical model for relative quantification in real-time RT-PCR.** *Nucleic Acids Res* 2001, **29**:e45.
40. Roth S, Sistonen P, Salovaara R, Hemminki A, Loukola A, Johansson M, Avizienyte E, Cleary KA, Lynch P, Amos CI, Kristo P, Mecklin JP, Kellokumpu I, Jarvinen H, Aaltonen LA: **SMAD genes in juvenile polyposis.** *Genes Chromosomes Cancer* 1999, **26**:54-61.

Chapter▷6

**Supplementary Table 1.** List of 64 functionally annotated genes differentially express in *Smad4*<sup>+/E6sad</sup> and *Smad4*<sup>E6sad/E6sad</sup> ES cell lines. Expression profiling values are expressed as absolute fold change values when compared to *Smad4*<sup>+/+</sup> ES cells.

Gene Symbol and Name	Unigene	Fold Change <i>Smad4</i> <sup>E6sad/E6sad</sup> *	Fold Change <i>Smad4</i> <sup>+/E6sad</sup> *
<b>IMMUNITY RESPONSE</b>			
ARTS-1 (type 1 tumor necrosis factor receptor shedding aminopeptidase regulator)	Mm.83526	-2.8	-1.7
CXCL14 (chemokine (C-X-C motif) ligand 14)	Mm.30211	1.7	-1.9
GBP6 (guanylate binding protein family, member 6)	Mm.45740	-2.3	-1.8
IL23A (interleukin 23, alpha subunit p19)	Mm.125482	1.5	1.3
IRGM (immunity-related GTPase family, M)	Mm.29938	-3.8	-2
TAPBP (TAP binding protein ,tapasin)	Mm.392082	-1.7	-1.4
<b>MOLECULAR TRANSPORT</b>			
ATP11A (ATPase, Class VI, type 11A)	Mm. 257837*	1.8	1.5
LMAN1 (lectin, mannose-binding, 1)	Mm.290857	-2.5	-1.9
SERPINH1 (serpin peptidase inhibitor, clade H (heat shock protein 47), member 1)	Mm.22708	1.8	1.4
STEAP1(six transmembrane epithelial antigen of the prostate 1)	Mm.85429	1.7	1.6
CYP26A1 (cytochrome P450, family 26, subfamily A, polypeptide 1)	Mm.42230	-1.5	-2
<b>SIGNAL TRANSDUCTION</b>			
AXIN2 (axin 2, conductin, axil)	Mm.71710	-1.5	-1.7
COMMD3 (COMM domain containing 3)	Mm.249586	2.2	1.6
FGF5 (fibroblast growth factor 5)	Mm.5055	-6.8	-2.6
FGF8 (fibroblast growth factor 8,androgen-induced)	Mm.4012	-2.5	-1.6
GPR124 (G protein-coupled receptor 124)	Mm.87046	2	1.8
IGFBP3 (insulin-like growth factor binding protein 3)	Mm.29254	-3.1	-1.9
MDM2 (Mdm2, transformed 3T3 cell double minute 2, p53 binding protein)	Mm.22670	1.5	1.3
PARD6G (par-6 partitioning defective 6 homolog gamma)	Mm.24678	1.7	1.4
PRKAR1B (protein kinase, cAMP-dependent, regulatory, type I, beta)	Mm.306163	2.6	1.6
PTDSR (phosphatidylserine receptor)	Mm.383423	-1.6	-1.3
PTPRN2 (protein tyrosine phosphatase, receptor type, N polypeptide 2)	Mm.206054	-1.6	-1.3
RHOF (ras homolog gene family, member F (in filopodia)	Mm.253876	-1.6	-1.3
SH3BP5 (SH3-domain binding protein 5 (BTK-associated)	Mm.383198	1.7	1.5
SMAD4 (SMAD, mothers against DPP homolog 4 (Drosophila)	Mm.100399	-2.7	-1.5
SMAD7 (SMAD, mothers against DPP homolog 7 (Drosophila)	Mm.34407	-3.6	-1.8
STAT3 (signal transducer and activator of transcription 3)	Mm.249934	-1.7	-1.4
TULP4 (tubby like protein 4)	Mm.28251	1.7	1.5
<b>DEVELOPMENT</b>			
T (T, brachyury homolog, in mouse)	Mm.913	-7	-2.2
ODZ4 (odz, odd Oz/ten-m homolog 4 in Drosophila)	Mm.254610	1.4	1.4
ZICS (Zic family member 5 (odd-paired homolog, Drosophila)	Mm.390761	-2	-1.6
<b>TRANSCRIPTION AND TRANSLATION REGULATION</b>			
CNOT6 (CCR4-NOT transcription complex, subunit 6)	Mm.247113	-1.6	-1.4
EIF4E2 (eukaryotic translation initiation factor 4E member 2)	Mm.227183	-1.4	-1.3

Gene Symbol and Name	Unigene	Fold Change Smad4 <sup>E6sad/E6sad</sup>	Fold Change Smad4 <sup>+/E6sad</sup>
EOMES (eomesodermin homolog, in <i>Xenopus laevis</i> )	Mm.200692	-2.1	-1.9
NRIP1 (nuclear receptor interacting protein 1)	Mm.390915	1.5	1.4
RARA (retinoic acid receptor, alpha)	Mm.103336	-1.5	-1.3
ZFP28 (zinc finger protein 28 homolog, in mouse)	Mm.127014	1.5	-1.3
ZNF524 (zinc finger protein 524)	Mm.19974	-1.4	-1.3
ZNRF3 (zinc and ring finger 3)	Mm.216313	-1.6	-1.7
<b>METABOLISM</b>			
PSMB8 (proteasome (prosome, macropain) subunit, beta type, 8)	Mm.180191	-3.1	-1.6
RPL17 (ribosomal protein L17)	Mm.276337	-4.7	-1.4
TRIM12 (tripartite motif protein 12)	Mm.327033	-2.1	-1.6
CYP26A1 (cytochrome P450, family 26, subfamily A, polypeptide 1)	Mm.42230	-2	-1.5
GALNT10 (UDP-N-acetyl-alpha-D-galactosamine:polypeptide N-acetylgalactosaminyltransferase 10)	Mm.271670	-1.7	-1.5
SEPP1 (selenoprotein P, plasma, 1)	Mm.392203	-1.5	1.3
ENPP3 (ectonucleotide pyrophosphatase/phosphodiesterase 3)	Mm.338425	-1.5	1.3
HERC5 (hect domain and RLD)	Mm. 297393	-3	-2.1
<b>BLOOD COAGULATION</b>			
ANXA8 (annexin A8)	Mm.3267	1.4	1.7
<b>CELL PROLIFERATION</b>			
DERL2 (Der1-like domain family, member 2)	Mm.28131	-1.4	-1.2
LEFTY2 (left-right determination factor 2)	Mm.87078	-4.3	-1.5
PEG10 (paternally expressed 10)	Mm.320575	1.4	1.3
<b>CELL ADHESION</b>			
CYR61 (cysteine-rich, angiogenic inducer, 61)	Mm.1231	-1.8	-2.1
TGFB1 (transforming growth factor, beta-induced, 68kDa)	Mm.14455	2.2	1.4
<b>CELL CYCLE</b>			
PMP22 (peripheral myelin protein 22)	Mm.1237	2.6	1.3
ZAK (sterile alpha motif and leucine zipper containing kinase AZK)		1.6	1.4
<b>CYTOSKELETON</b>			
ENC1 (ectodermal-neural cortex (with BTB-like domain)	Mm.241073	-1.4	-1.3
<b>UNKNOWN</b>			
DDIT4L (DNA-damage-inducible transcript 4-like)	Mm.250841	2.4	1.6
DENND1C (DENN/MADD domain containing 1C)	Mm.284447	-1.5	-1.6
GBP4 (guanylate binding protein 4)	Mm. 45740	-2.2	-1.4
KIAA0738 (KIAA0738 gene product)	Mm.24652	1.6	1.3
KLHL26 (kelch-like 26 , in <i>Drosophila</i> )	Mm.187090	1.8	1.3
NOPE (likely ortholog of mouse neighbor of Punc E11)	Mm.209041	1.7	2
PHF19 (PHD finger protein 19)	Mm.65691	-2.1	-1.6
PLEKHG2 (pleckstrin homology domain containing, family G member 2)	Mm.235700	-1.6	-1.4
PSORS1C2 (psoriasis susceptibility 1 candidate 2)	Mm.34201	-2.3	-1.5

**Supplementary Table 2.** Ingenuity Pathway Analysis of the 64 functionally annotated genes differentially expressed (denoted as “focus molecules” in bold) in Smad4+/E6sad and Smad4E6sad/E6sad ES cell lines. The column denoted as “Top Functions” describes the gene ontology groups to which the genes encompassed in a given Ingenuity Network belong. Only the top 4 networks with the most significant scores are included.

ID	Molecules in Network	Score	Focus Molecules	Top Functions
1	BCL2L1, <b>C14ORF46</b> , <b>DDIT4L</b> , ELA2, <b>EOMES</b> , EPAS1, ERBB2, EZH2, FOXA2, FRAP1, <b>GALNT10</b> , <b>GBP6</b> , IGFBP1, <b>IGFBP3</b> , IGFBP4, IGFBP5, IL4, IL6, <b>IL23A</b> , IL6R, INHBA, <b>LEFTY2</b> , MMP7, <b>NRIP1</b> , <b>PHF19</b> , <b>PSMB8</b> , PSME1, PSME2, <b>PTDSR</b> , <b>RARA</b> , <b>RHOF</b> , <b>STAT3</b> , TF, TNFRSF1A, VHL	26	15	Cancer, Cellular Growth and Proliferation, Cell Death
2	<b>ANXA8</b> , BAX, BGLAP, COL2A1, <b>CYR61</b> , ERBB2, <b>GBP4</b> , IFNG, <b>IGFBP3</b> , IGFBP4, INHBA, <b>IRGM</b> , KLF3, KLF4, KLF6, MMP2, MMP3, MYCN, NF 2, NFATC2, <b>PARD6G</b> , <b>PLEKHG2</b> , <b>PRKAR1B</b> , RAC1, <b>SEPP1</b> , <b>SERPINH1</b> , SFTPC, SMARCA4, SPP1, <b>TAPBP</b> , <b>TGFB1</b> , TGFB1, THBS1, TNFRSF1A, TP53	19	12	Cancer, Tumor Morphology, Cellular Movement
3	ACTA2, ANXA2, <b>ARTS-1</b> , <b>AXIN2</b> , CASP8, CD44, CDH3, CTNNB1, <b>ENC1</b> , ERBB2, FGF3, <b>FGF8</b> , FZD8, <b>HERC5</b> , IL6R, INHBA, LDB1, MMP7, MSX1, MYC, MYCN, NFYB, <b>NOPE</b> , PAX5, <b>PEG10</b> , PLAT, RB1, <b>RPL17</b> , T, TGFB1, TGFB2, THBS1, VPS39, <b>ZAK</b> , <b>ZNF524</b>	17	11	Developmental Disorder, Cancer, Tumor Morphology
4	BGLAP, CLEC11A, COL2A1, COL7A1, <b>COMMD3</b> , <b>CXCL14</b> , <b>CYP26A1</b> , EGR2, ERBB2, FGF2, <b>FGF5</b> , FSHR, HOXC8, IGFBP1, <b>IGFBP3</b> , IGFBP4, IGFBP5, KLKB1, <b>LMAN1</b> , <b>MDM2</b> , MPZ, MYCN, NFKB1, PLAT, <b>PMP22</b> , PRKACA, <b>PTPRN2</b> , RUNX1, SAT, <b>SMAD4</b> , <b>SMAD7</b> , SP1, STAMPB, TF, WT1	17	11	Cancer, Cellular Growth and Proliferation, Cell Death

**Discussion**

# Chapter 7





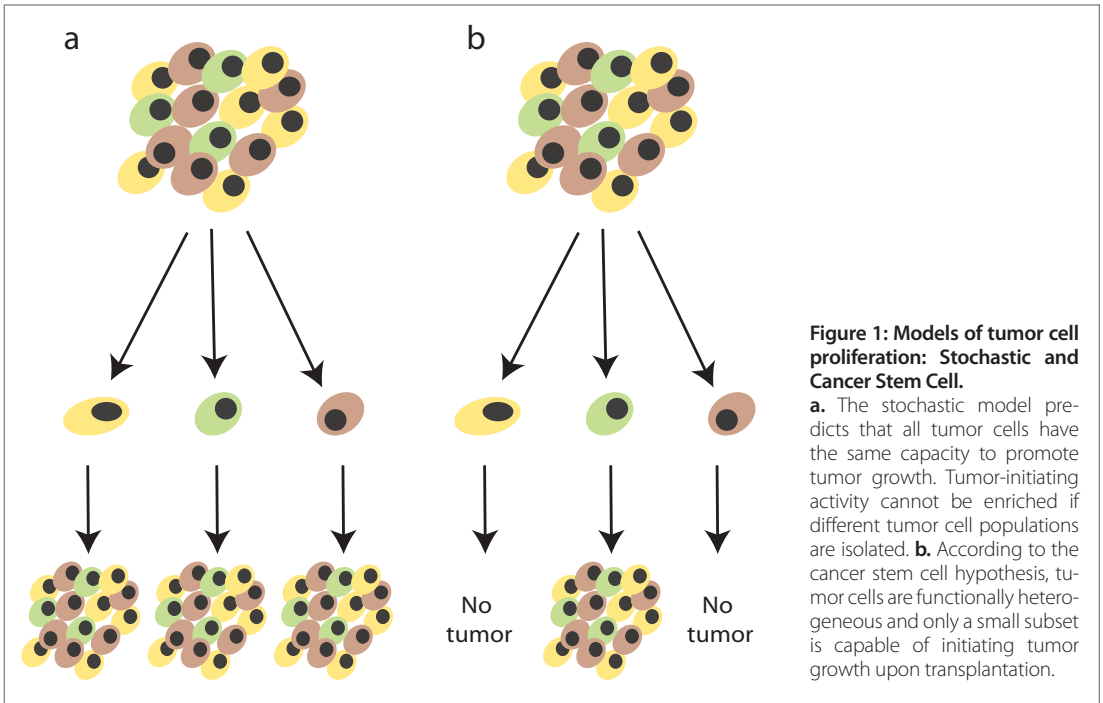
# DISCUSSION

In adult higher organisms, tissues and organs with a high cellular turnover like skin, the gut lining and blood need a constant supply of cells to exert their function or to respond to tissue damage. To date, the best characterized adult stem cell compartment is the haematopoietic niche localized in the bone marrow. Here, a hierarchical organization of the different blood lineages each characterized by a set of cell surface markers has been elucidated. At the very top of this hierarchy, a small population of pluripotent stem cells divides asymmetrically giving rise to a stem cell (with self-renewal capacity) and a partly committed progenitor cell. Progenitor cells have a more restricted differentiation potential and divide further to produce non-dividing, terminally differentiated cells. Homeostasis is achieved through a finely tuned equilibrium between self-renewal and differentiation. Accordingly, transplantation of purified stem cells into irradiated NOD/SCID animals results in the complete reconstitution of normal hematopoiesis whereas transplantation of more differentiated cells

does not. Stem cells generally exist in two different proliferative states: quiescent stem cells divide very infrequently and are thought to serve as a reservoir or back-up in those cases of extreme tissue damage. However, more cycling stem cell populations have been described, probably responsible for the daily turnover that characterize each niche. Examples of this “stem cell dichotomy” with the co-existence of more dormant and cycling subpopulations within the same niche, have been shown in the skin/hair follicle and in the haematopoietic compartment<sup>1-11</sup>. In fact, it has been shown that in the hair follicle two different levels of Wnt signaling regulate the transition between stem cell quiescence and conversion to proliferating transit amplifying (TA) progeny<sup>10</sup>. To date, a notable exception to this dichotomy is the intestinal crypt where, only cycling stem cells, earmarked by expression of the Wnt downstream target *Lgr5*, have been characterized<sup>12,13</sup>.

It is widely accepted that cancer is a multi-step disease that occurs through the accumulation of multi-

133



ple genetic hits<sup>14,15</sup>. These mutations are thought to confer selective advantage to a subset of tumor cells which will clonally expand. However, tumors are known to be very heterogeneous in their histology and to encompass different degrees of differentiation and cellular lineages, thus resembling the hierarchical organization characteristic of normal stem cell niches. Pathologists have taken advantage of this morphologic heterogeneity as a tool to classify tumors as well- or poorly-differentiated and to correlate it with prognosis. Moreover, this morphologic diversity is often reflected by functional heterogeneity as shown by the observation according to which individual cells from the same tumor have different tumorigenic potential both *in vivo* and *in vitro*. According to the original observation by Southam and Brunschwig in the early 60's<sup>16</sup>, human cancer cells were only able to recapitulate tumor formation when subcutaneously autotransplanted (i.e. in the same patient where the tumors were originally derived from!!) at a  $>1 \times 10^6$  multiplicity, thus suggesting that not all cells in the tumor are equally tumorigenic. The development of clonogenic assays provided scientists with an improved tool to test different tumor populations for their tumorigenic ability. In 1963 the first report by Bruce et al.<sup>17</sup> showed that only 1-4% of lymphoma cells were able to proliferate *in vivo* when transplanted into mice. Subsequently, similar results were reported with different tumor types including myeloma<sup>18</sup>, leukaemia<sup>19,20</sup> and solid tumors<sup>21</sup>. Collectively, these observations are supportive of the existence of a hierarchy within tumor masses similar to that observed in adult stem cell niches.

Two models have been proposed to explain the evolution of somatic cells into a tumor mass: the stochastic and the cancer stem cell (CSC) model<sup>22</sup>. The two models are essentially different in addressing which cells possess tumor-initiating and propagating capacities. The stochastic model postulates that most cells within a tumor result from a clonal expansion of a progenitor cell that has accumulated a sufficient number of advantageous (epi)genetic mutations, and are therefore able to sustain neoplastic growth. The CSC model instead, postulates that only a minority of the tumor cells has the ability to recapitulate tumor formation when for example

transplanted in an immuno-deprived experimental animal (Figure 1). This tumor-initiating characteristic results from their ability to both self-renew and differentiate, meaning that, upon cell division, CSCs can give rise to new stem cells but also to more committed cells programmed to differentiate and eventually undergo programmed cell death (terminal differentiation). This also implies that, by sorting different subpopulations of tumor cells (e.g. by FACS, fluorescence activated cell sorting), one could assess their individual tumor initiating capacity and eventually prospectively isolate a small group of cells highly enriched in CSCs<sup>22</sup>. The existence of functionally distinct cells within a tumor mass also accounts for the observed tumor heterogeneity and is reminiscent of the hierarchical structure of normal stem cell niches<sup>22</sup>.

The work of Bonnet et al. on human leukemia has provided experimental evidence in favor of the CSC model<sup>23</sup>. SL-IC cells (SCID leukemia – inducing cells), characterized by the surface markers  $CD34^{++}CD38^{-}$ , were transplanted into NOD/SCID animals at limiting dilutions and compared with  $CD34^{+}CD38^{+}$  cells. As few as  $5 \times 10^3$   $CD34^{++}CD38^{-}$  cells produced leukemic growth whereas as many as  $5 \times 10^5$   $CD34^{+}CD38^{+}$  cells did not<sup>23</sup>. Serial transplantation of SL-IC cells demonstrated that these cells were capable of self-renewal. Furthermore, the normal hierarchical organization of the haematopoietic compartment was to a certain degree maintained, where a small number of leukemia stem cells sustain cellular heterogeneity<sup>23</sup>. For the first time, there was compelling evidence in favor of the cancer stem cell hypothesis.

The CSC hypothesis accommodates several of the characteristics of tumor cells and of the tumorigenic process itself. The fact that they are long-lived cells explains how tumors accumulate several key mutations over a considerably large time span, typical of the tumorigenic process. The hierarchical organization, maintained to a certain extent within tumors, allows the transmission of the mutation along the ontogeny in agreement with the observation that tumors have a clonal origin and are histologically heterogeneous<sup>22</sup>.

Whether the first hit is at the stem cell itself or in a more restricted progenitor that re-acquires self-renewal capacity is still a matter of debate. Haematopoietic and intestinal malignancies provided more

**Table 1:** CSC-specific cell surface antigen markers.

TUMOR TYPE	CSC-SPECIFIC MARKERS	REFERENCE
<b>Leukemia</b>	CD34 <sup>+</sup> /CD38 <sup>+</sup>	Nat Med 3:730, 1997
<b>Breast</b>	CD44 <sup>+</sup> /CD24 <sup>low</sup> ALDH1 <sup>+</sup>	PNAS 100:3983, 2003 Cell Stem Cell 1:555, 2007
<b>Brain</b>	CD133 <sup>+</sup>	Nature 432:396, 2004
<b>Myeloma</b>	CD138 <sup>-</sup>	Blood 103:2332, 2004
<b>Prostate</b>	CD44 <sup>+</sup> /α <sub>v</sub> β <sub>1</sub> <sup>hi</sup> /CD133 <sup>+</sup>	Cancer Res 65:10946, 2005
<b>Lung</b>	Sca1 <sup>+</sup> /CD45 <sup>+</sup> /Pecam <sup>-</sup> CD133 <sup>+</sup>	Cell 121:823, 2005 Cell Death Diff 15:504, 2008
<b>Pancreas</b>	CD44 <sup>+</sup> /CD24 <sup>+</sup> /ESA <sup>+</sup> CD133 <sup>+</sup>	Cancer Res 67:1030, 2007 Cell Stem Cell 1:313, 2007
<b>Melanoma</b>	ABC85 <sup>+</sup>	Nature 451:345, 2008
<b>Liver</b>	CD90 <sup>+</sup>	Cancer Cell 13:153, 2008
<b>Colon</b>	CD133 <sup>+</sup> CD44 <sup>+</sup> /CD166 <sup>+</sup> /EpCAM <sup>+</sup>	Nature 445:106, 2007 Nature 445:111, 2007 PNAS 104:10158, 2007

135

convincing evidence for this controversy<sup>22</sup>. Recently, it has been shown that in chronic myeloid leukemia (CML) oncogene expression in the stem cell compartment is sufficient to trigger and recapitulate disease<sup>24</sup>. Accordingly, inactivation of the tumor suppressor gene *APC* in intestinal stem cells (earmarked by *Lgr5* expression) leads to tumor formation, whereas introduction of the same mutation in transient amplifying (TA) cells does not<sup>25</sup>. Both studies point to the stem cell as the cell of origin in cancer.

The key features of cancer stem cells are the same as those of normal stem cells: self-renewal, differentiation capacity, telomerase expression, active DNA repair mechanisms, anti-apoptotic pathways, and anchorage independence among others<sup>22,26</sup>. In fact, to date CSCs can only be 'operationally' defined, namely by their ability to recapitulate tumor formation upon transplantation into NOD/SCID recipient mice. However, this operational definition implies that

CSCs are cell-autonomous, i.e. do not depend on the surrounding microenvironment. This is highly unlikely given the prominent role played by the niche in the maintenance of stem cell homeostasis (reviewed by Moore et al)<sup>27</sup>. Immuno-compromised animals have for long been used to assay self-renewal and propagation of stem cells to bypass rejection. However, the absence of an immune response is also not reflective of the natural physiological conditions in which the tumor develops.

Although most of the groundbreaking work on CSCs has been done in the haematopoietic niche, recent studies reported the prospective isolation of cancer stem cells from a broad spectrum of solid tumors by applying similar FACS and transplantation strategies (Table 1). The vast majority of solid tumors is of epithelial origin and follows a multistep progression from benign adenomas to malignant carcinomas from which metastases in distant organs

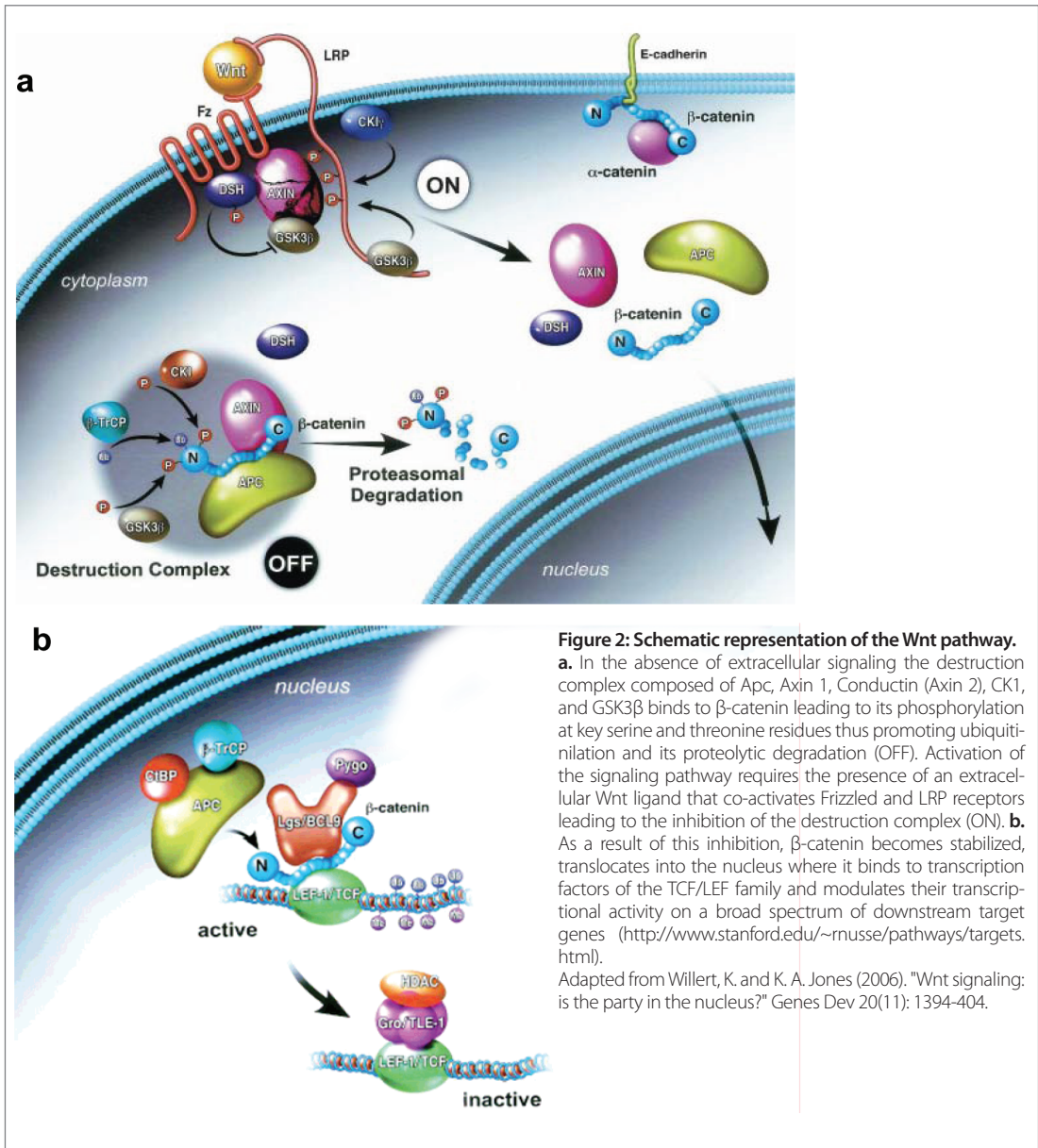
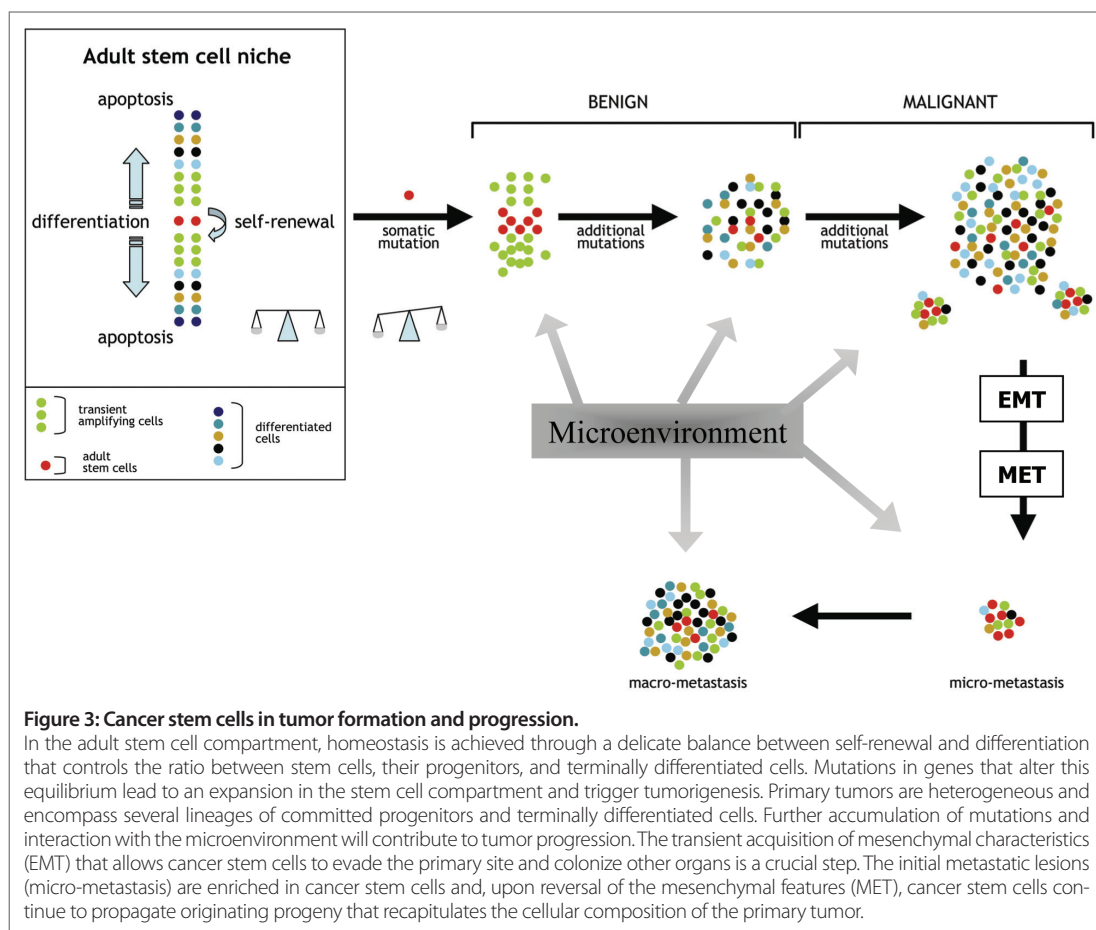


**Figure 2: Schematic representation of the Wnt pathway.**  
**a.** In the absence of extracellular signaling the destruction complex composed of Apc, Axin 1, Conductin (Axin 2), CK1, and GSK3β binds to β-catenin leading to its phosphorylation at key serine and threonine residues thus promoting ubiquitination and its proteolytic degradation (OFF). Activation of the signaling pathway requires the presence of an extracellular Wnt ligand that co-activates Frizzled and LRP receptors leading to the inhibition of the destruction complex (ON). **b.** As a result of this inhibition, β-catenin becomes stabilized, translocates into the nucleus where it binds to transcription factors of the TCF/LEF family and modulates their transcriptional activity on a broad spectrum of downstream target genes (<http://www.stanford.edu/~rnusse/pathways/targets.html>).  
Adapted from Willert, K. and K. A. Jones (2006). "Wnt signaling: is the party in the nucleus?" *Genes Dev* 20(11): 1394-404.

are originated<sup>14</sup>. The invasive process has been associated with the loss of epithelial identity and the acquisition of mesenchymal characteristics through a process denominated epithelial to mesenchymal transition (EMT). Accordingly, EMT enhances tumor cell dissemination throughout the body<sup>28</sup> and is correlated with prognosis and survival<sup>29,30</sup>. Cells undergoing EMT are characterized by the loss of

E-cadherin expression at the cell membrane and the expression of mesenchymal proteins such as fibronectin and vimentin<sup>31</sup>. Several molecular pathways have been involved in this mechanism reviewed elsewhere<sup>32,33</sup>.  
Colorectal cancer (CRC) still represents the best characterized model of tumor initiation and progression where a well-defined series of histopathological



changes are accompanied and result from specific genetic “hits” at a number of oncogenes and tumor suppressor genes<sup>34</sup>. Mutations in the *APC* gene have been found in the vast majority of sporadic colorectal tumors regardless of the histological stage and are therefore regarded as the rate-limiting initiation step<sup>35</sup>. Accordingly, germline *APC* mutations lead to an hereditary predisposition to colorectal cancer, familial adenomatous polyposis (FAP)<sup>36</sup>. Notwithstanding its multi-functionality, the main tumor suppressor activity of *APC* is thought to reside in its ability to bind to and downregulate  $\beta$ -catenin; loss of APC function results in the constitutive activation of the Wnt pathway<sup>37</sup>. Figure 2 illustrates the different components of the Wnt pathway in the absence and presence of the extracellular ligand.

Wnt activity has been associated with a wide variety

of cellular responses among which the induction of EMT. Nuclear  $\beta$ -catenin localization has been associated with activation of EMT through upregulation of *SLUG* a transcriptional factor that represses expression of E-cadherin<sup>38,39</sup>. Accordingly, CRC cells located at the invasive front of primary tumors have been shown to loose E-cadherin expression<sup>31</sup> and acquire mesenchymal markers such as fibronectin<sup>40</sup>.

The genetic model of the Wnt signaling pathway predicts that every single cell in colorectal tumors initiated by *APC* loss of function mutations should be earmarked by nuclear  $\beta$ -catenin accumulation. However,  $\beta$ -catenin immunohistochemical analysis of the majority of CRCs reveals a highly heterogeneous staining pattern: differentiated cells within the tumor show normal membrane expression whereas cells with nuclear localization are predominantly

found at the invasive front and in disseminated cells in the stromal compartment<sup>41</sup>. How can this paradoxical, non-random distribution of  $\beta$ -catenin be explained? Apparently, loss of *APC* mutation is insufficient (though necessary) to fully activate the Wnt/ $\beta$ -catenin signaling and requires additional synergistic factors to enhance Wnt activity in a dosage-dependent fashion<sup>42</sup>. Both cell-autonomous factors such as additional genetic “hits” and autocrine signaling loops<sup>43</sup> are likely to synergize with *APC* mutation and enhance Wnt signaling, as demonstrated for *KRAS* mutations<sup>44</sup>. Even more importantly, paracrine factors such as growth factors and cytokines produced by the stromal compartment are likely to explain the non-random distribution of tumor cells with nuclear  $\beta$ -catenin accumulation<sup>45</sup>.

By using CRC as a model, Brabletz et al. have established an association between  $\beta$ -catenin heterogeneity, EMT, and malignancy, and proposed the migrating cancer stem cell model (Figure 3). It postulates the existence of two types of cancer stem cells: the stationary (SCS) and the mobile cancer stem (MCS) cells<sup>46</sup>. The SCS cells are present throughout the tumor mass and can already be found in the initial stages of tumor progression displaying a normal pattern of  $\beta$ -catenin localization, namely at the cytoplasmatic membrane. The MCS cells can be found at the invasive front of tumors where tumor-stroma interactions, enhance Wnt signaling thus triggering nuclear  $\beta$ -catenin translocation. Consequently, EMT is induced thus facilitating detachment and migration of MCS cells from the primary site to distant organs<sup>45,46</sup>. Accordingly, *in vitro* experiments have shown that induction of the EMT program generates cells with mesenchymal characteristics and possibly underlies cancer stemness<sup>47</sup>. The model also predicts that the activation of the mesenchymal program is transient and reversible through mesenchymal to epithelial transition (MET) when cells home into distant organs. The latter is also in agreement with the capacity of the metastasis to recapitulate the primary tumor<sup>46</sup>.

The observation according to which Wnt acts in response to a dynamic range of signaling activity (discussed in **Chapter 1**) has led to the formulation of the “just-right” signaling hypothesis<sup>48</sup>. According to this hypothetical model, complete inactivation of

Wnt signaling is not advantageous to tumorigenesis and its over stimulation could lead to conflicting transcriptional responses that ultimately activate apoptosis<sup>48</sup>. Thus, residual activity is needed to promote tumorigenesis. Moreover, each tissue-specific stem cell niche is thought to be characterized by different, “just-right”, signaling levels that regulate cell proliferation, differentiation and apoptosis to maintain homeostasis (as further discussed in **Chapter 1** and later on in the Discussion).

The main goal of the work presented in this PhD thesis is to demonstrate the role played by different signaling dosages in self-renewal and differentiation. In particular, I am interested in elucidating how such changes can affect homeostasis of specific adult stem cell compartments and lead to tumorigenesis.

## Wnt signaling and cell fate determination in embryonic stem cells

In **Chapter 1** we have summarized the functional domains present in APC and how different mutations and transcriptional levels modulate the half-life of  $\beta$ -catenin and therefore Wnt activity. **Chapters 2, 3** and **4** address the question of how different Wnt signaling dosages affect cell differentiation by employing a unique series of embryonic stem (ES) cell lines carrying homozygous or compound heterozygous hypomorphic mutations at the endogenous *Apc* gene. Since ES cells are pluripotent, the effects of the different Wnt signaling dosages on cell fate determination and differentiation could be addressed by *in vivo* (teratoma assay) and *in vitro* differentiation assays. Several differentiation patterns were observed depending on the signaling activity of the respective mutant. Figure 4 summarizes the results obtained in these studies. Wnt signaling activity was found to correlate in a dosage-dependent fashion with the ability of ES cells to differentiate. Moreover, we demonstrated that this differentiation defect is cell autonomous since cell-to-cell contact or growth factor supplementation does not affect cell fate determination. These observations underlie the role of Wnt signaling in the maintenance of a stem cell phenotype and support the cancer stem cell hypothesis discussed later in the discussion.



Notably, genome-wide transcriptional analysis confirmed the dosage-dependent correlation between levels of Wnt activity and the expression of a wide variety of target genes. One could argue however, that the generated signatures mainly reflect the cellular composition of the different teratomas and are not the direct consequence of the Wnt dosage-dependent transcriptional effect. In **Chapter 3**, expression profiling of undifferentiated ES cells, a more homogeneous and undifferentiated cellular population than the teratomas, revealed that the transcriptional program is already altered before differentiation is triggered. As for the teratomas, the level of expression of the different target genes directly correlates with the level of Wnt activity. Although lower levels of Wnt signaling activity are already able to affect transcription when compared with wild type ES cells, measurable phenotypic effects on differentiation are only observed when higher magnitude of Wnt activation is induced.

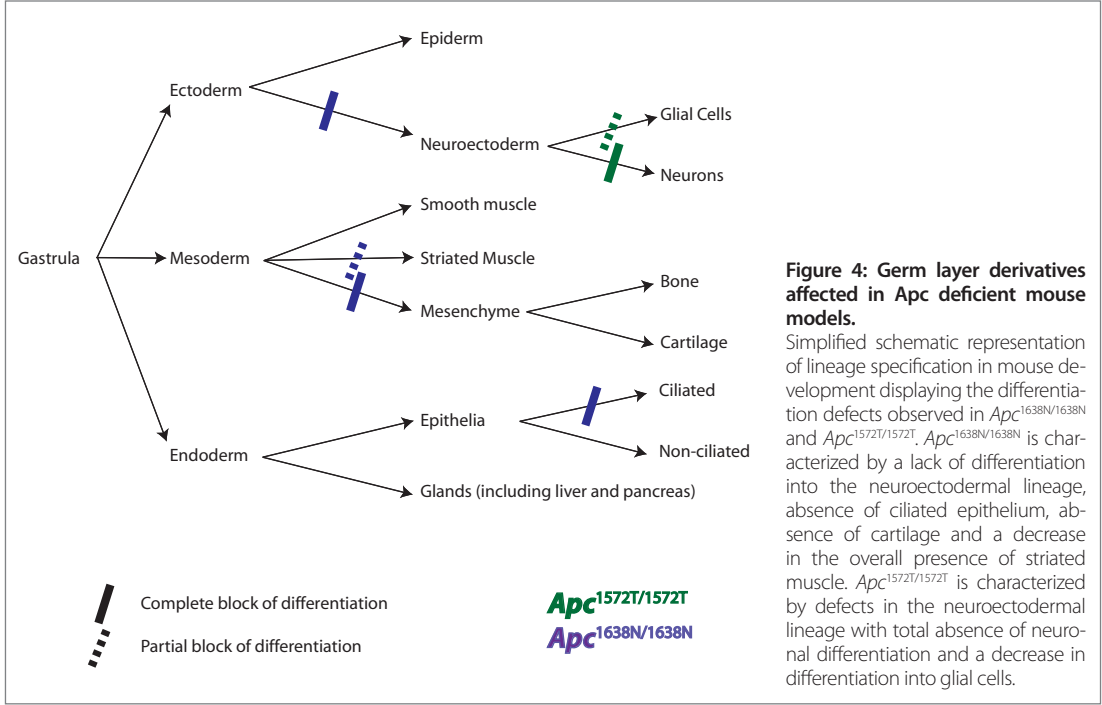
In general, it is believed that Wnt signaling activity results in the transcriptional upregulation of a broad spectrum of target genes through the nuclear interaction between  $\beta$ -catenin and Tcf's. However, in ES cells and to a lesser degree also in teratomas, the majority of the genes differentially expressed upon loss of *Apc* function appears to be downregulated (**Chapter 3**). Since the experimental design did not allow the discrimination between primary and secondary targets, the induction of transcriptional repressors cannot be excluded. Furthermore,  $\beta$ -catenin has been found to bind to several other nuclear partners besides TCF/LEF transcription factors, whose downstream effectors are still largely unknown<sup>49</sup>. Recently, *Tcf3*, the highest expressed member of the Tcf/Lef family of transcription factors in ES cells, has been implicated in self-renewal. Tcf3 binds to the same genomic areas as Nanog and Oct4 and acts mainly as a transcriptional repressor through its Groucho interaction domain<sup>50,53</sup>. Tcf3 inhibits expression of Nanog, making cells responsive to differentiation cues<sup>52</sup>. On the other hand, Nanog and Oct4 are necessary for the proper expression of Tcf3 creating a finely tuned equilibrium between Nanog and Tcf3 activities in self-renewal and differentiation, respectively<sup>53</sup>. Moreover, *Tcf3*<sup>-/-</sup> ES cells show delayed differentiation and maintain self-renewal markers even in Lif-free culturing conditions<sup>52,53</sup>.

The observation that *Tcf3* is highly downregulated in *Apc*<sup>1638N/1638N</sup> ES cells may provide a molecular explanation as to why *Apc*-mutant ES cells have differentiation defects. To validate this hypothesis further experiments are needed where expression of *Tcf3* is re-established to rescue at least part of the observed defects. Although, increased Nanog expression has been reported in *Tcf3*<sup>-/-</sup> ES cells, our expression profiling data did not confirm such effect. However, *Tcf3* expression is not totally abolished in *Apc*-mutant ES cells as in *Tcf3*<sup>-/-</sup> ES cells and residual *Tcf3* activity may suffice to control Nanog expression. Overall, the relationship between *Tcf3* downregulation and Wnt activity is not yet clear. Is *Tcf3* a direct or a secondary target of Wnt? Further experiments are needed to clarify which molecular mechanism lies behind the repression of *Tcf3* in *Apc*-mutant ES cells.

## Wnt, adult stem cell niches and cancer

Although the rate-limiting role of Wnt/ $\beta$ -catenin signaling is well established for a broad spectrum of cancers<sup>54</sup>, it is yet unclear whether it causes a generalized proliferation increase throughout the whole tumor mass or if it differentially affects self renewal and differentiation rates in stem and/or progenitor cells thus triggering cancer stem cell onset and/or modulating their invasive behavior.

In **Chapter 4** we describe a new mouse model, *Apc*<sup>+ /1572T</sup>, characterized by the development of mammary tumors with a penetrance of 80-100% in females, depending on the genetic background, and of 30% among males. Furthermore, a considerable proportion of these tumors were found to spontaneously metastasize to the lung. In the male mouse embryo, the development of the mammary gland is stopped at day E15 when testosterone induces the mesenchymal cells surrounding the mammary bud to trigger epithelial cell death<sup>55,56</sup>. The appearance of mammary tumors in male *Apc*<sup>+ /1572T</sup> animals suggests that this process is inhibited during embryonic development. Possibly, Wnt activity increases progenitor's tolerance to the apoptotic signals coming from the surrounding mesenchyme. In concordance, ectopic expression of *Wnt1*<sup>57</sup> and *Wnt10b*<sup>58</sup> have also been reported to induce mammary tumor



formation and the Wnt pathway has therefore been suggested to play a role in sexual dimorphism<sup>58</sup>. In our mouse model, it is unlikely that at this point in development the second hit at the wild-type *Apc* locus has occurred, suggestive of a haploinsufficient effect of the *Apc* locus.

In all the analyzed tumors, ontogeny of the mammary gland was recapitulated as both epithelial and myoepithelial cellular lineages are present in the primary lesions thus the mutation must affect the stem cell itself or a very early bipotent progenitor. Notably, these lesions were metaplastic with large areas of squamous differentiation of skin and hair follicle type. During embryonic development, between days E10.5 and E11<sup>59</sup>, cells from the ectodermal germ layer migrate and invade the underlying mesenchyme where epithelial-stromal interactions give rise to mammary rudiments denominated placodes<sup>59,60</sup>. Moreover, the ectodermal germ layer is also involved in the formation of skin and hair follicles. The observed metaplasia encompassing closely related cellular lineages derived from the same multipotent progenitor cell is in agreement with a role for the Wnt pathway in cell fate determination<sup>61</sup>.

Another type of heterogeneity within the mammary tumors of *Apc*<sup>+/1572T</sup> mice was found at the level of expression and subcellular localization of  $\beta$ -catenin. Areas with clear nuclear staining were interspersed within larger fields characterized by slight cytoplasmatic accumulation and membranous staining pattern (see Figure3i-j, **Chapter 4**). This heterogeneous pattern is reminiscent of the already mentioned heterogeneity of  $\beta$ -catenin intracellular localization observed in CRC<sup>41</sup> and offers an unique opportunity to test and validate the CSC model and the hypothesis according to which intracellular  $\beta$ -catenin accumulation represents a functional determinant of cancer stemness in epithelial tumors<sup>45</sup>. Do the mammary tumor cells earmarked by intracellular  $\beta$ -catenin accumulation represent *bona fide* CSCs? Do they also lead to the formation of distant metastases? In **Chapter 4**, by using Lin<sup>-</sup>CD29<sup>hi</sup>CD24<sup>+</sup> cell surface markers, previously employed to isolate normal mammary stem cells (MaSCs)<sup>62</sup>, we showed that this population of tumor cells are highly enriched in cancer stem cells and are earmarked by intracellular  $\beta$ -catenin accumulation.

The CSC hypothesis postulates that these cells are not only responsible for initiation of the primary lesions but also for the formation of distant metastasis. In fact, the pulmonary metastases in *Apc*<sup>1572T</sup> mice fully recapitulated the differentiation pattern observed in the primary tumors, thus suggesting the involvement of CSCs in tumor dissemination and homing. Accordingly, nascent pulmonary micrometastases displayed a relative enrichment for cells earmarked by intracellular  $\beta$ -catenin accumulation and a generalized low level of (myo)epithelial differentiation. Thus,  $\beta$ -catenin intracellular accumulation apparently underlies not only tumor initiation at the primary site but also invasion and metastasis formation at distant sites.

Although CSCs earmarked by intracellular  $\beta$ -catenin accumulation are predicted to activate an EMT program, expression profiling failed to show differential upregulation of EMT genes like *Slug*, *Twist*, and *Zeb1*. It is plausible to think that, in the mouse model here described, EMT is not the mechanism underlying evasion and that other Wnt target genes can cooperate to promote malignancy.

The central question becomes how normal adult stem cells differ from cancer stem cells. In **Chapter 4**, we show that in mouse mammary gland these populations differ by less than 400 genes. Wnt, TGF- $\beta$ , Notch and Sonic Hedgehog (Shh) are key signaling pathways involved in stem cell self-renewal and differentiation. Of these, only Shh could clearly discriminate between normal and cancer stem cells while the remaining had very similar degrees of signaling activities between the two populations. Shh appears clearly upregulated in tumor cells, as shown by the increased expression of *Gli1*, the main effector of the pathway.

Also of note, a substantial upregulation of the Wnt pathway is already observed in the normal mammary stem cells when compared to the more differentiated progeny, reinforcing Wnt's role in adult stem cell homeostasis. The underlying cause of the observed Wnt signaling activation in MaSCs is the downregulation of *Apc* gene expression to levels comparable to tumor where a targeted mutation and the somatic loss of the wild type have occurred, probably due to epigenetic silencing. Differentiated epithelial cells did show normal *Apc* expression levels, thus indicat-

ing the transient nature of the gene-silencing event in mammary stem cells.

Although, the overall level of signaling activation in CSCs does not dramatically differ from that of normal mammary stem cells, specific differences in the transcriptional activation of some Wnt target genes (*Axin2*, *Cd44*, *CyclinD1*, *Birc5*) could be found. This is even more surprising when considering that CSCs are characterized by a distinct pattern of intracellular  $\beta$ -catenin accumulation whereas normal mammary stem cells show normal  $\beta$ -catenin subcellular localization. This observation is reminiscent of the recent report where colorectal cancer cells located at the invasive front and earmarked by nuclear  $\beta$ -catenin were shown to express known Wnt target genes in a similar fashion as cells from within the tumor center with membrane-bound  $\beta$ -catenin localization<sup>63</sup>. Hence, the presence of  $\beta$ -catenin in the nucleus of Lin<sup>+</sup>CD29<sup>hi</sup>CD24<sup>+</sup> cells from *Apc*<sup>+/1572T</sup> mammary adenocarcinomas suggests its interaction with yet unknown binding partners and transcription factors other than the known members of the TCF/LEF family<sup>49</sup>.

A delicate balance between self-renewal and differentiation maintains homeostasis in adult stem cell niches. Such balance is deregulated in cancer and, if specifically targeted, could represent an attractive therapeutical option: upon specific CSCs ablation, loss of self-renewal capacity and accumulation of committed lineages programmed to terminally differentiate, would eventually lead to the eradication of the tumor mass. However, as also shown in **Chapter 4**, adult stem cells and CSC share similar expression signatures<sup>22,26</sup> which cast some doubts on the possibility of implementing CSC-targeted therapy.

Breast cancer is still one of the major causes of mortality among women. A role for several Wnt pathway components has been identified in a large fraction of breast cancer cases and correlated with a poorer prognosis. These include the overexpression of Cyclin D1<sup>64</sup>, methylation of SFRP1<sup>65</sup>, expression of DKK1<sup>66</sup>, and overexpression and nuclear localization of  $\beta$ -catenin<sup>67</sup>. A minority of studies also reported a relatively small (6-18%) percentage of *APC* mutations<sup>68-70</sup>. However, a larger percentage (42-52%) of breast cancers was shown to be charac-

terized by methylation of the *APC* promoter<sup>71-73</sup>.

Overall, 18 histological breast cancer subtypes have been described. Among these, metaplastic carcinoma of the squamous type, responsible for 1 to 5% of the total breast cancer burden, most closely resembles the mammary adenocarcinomas observed in *Apc*<sup>1572T</sup><sup>74,75</sup>. Breast metaplastic carcinoma in man are typically ER, PgR and HER2 negative, and therefore unresponsive to conventional therapies<sup>75-79</sup>. A recent paper by Hayes et al. attributes a significant role to the Wnt pathway in metaplastic breast cancer<sup>69</sup>. Approximately 92% of the tumors analyzed displayed aberrant expression of  $\beta$ -catenin, 41% of which with mutations in *APC*, *CTNNB1* ( $\beta$ -catenin) and *WISP3*, three key Wnt signaling molecules<sup>69</sup>. Hence, the *Apc*<sup>1572T</sup> mouse model could prove extremely valuable for the study of the molecular mechanism underlying tumorigenesis in this subgroup of breast cancers and as a tool for the screening of possible therapeutic compounds given the current lack of an effective treatment for these patients.

## Wnt signaling: is tissue specificity dosage-dependent?

In familial adenomatous polyposis (FAP), germline mutations in *APC* do not exclusively lead to gastro-intestinal tumorigenesis but are also associated with other extra-colonic manifestations as described in **Chapter 1**. Phenotypic variability occurs in the multiplicity of colonic tumors and in the type of extra-colonic manifestations observed<sup>42,80</sup>. The same phenotypic variability is observed among *Apc*-mutant mouse models and has been correlated with Wnt signaling activity<sup>42</sup>. Intestinal tumorigenesis is favored when mutations in *Apc* lead to high Wnt activity. Hypomorphic *Apc* alleles with some residual  $\beta$ -catenin downregulating activity are associated with decreased numbers of intestinal tumors though with an increase in the incidence and type of extra-intestinal manifestations. Accordingly, the newly characterized *Apc*<sup>1572T</sup> hypomorphic allele (**Chapter 4**), encodes for intermediate Wnt signaling activity and results in a very high incidence of extra-intestinal manifestations such as mammary and liver tumors, desmoids and epidermal cysts with no predisposition to intestinal tumors. The intermediate signaling

activity of *Apc*<sup>1572T</sup> was achieved by removal of the last Axin 2 (conductin) binding domain still encompassed by the *Apc*<sup>1638T</sup> truncated protein, previously shown to efficiently downregulate  $\beta$ -catenin even when compared to wild type cells (**Chapter 4**). These results underline the importance of the axin binding domain (SAMP) for APC's tumor suppressing function and suggest the existence of a threshold of Wnt signaling activity above which neoplastic transformation occurs.

The specific level of Wnt activity encoded by the *Apc*<sup>1572T</sup> allele appears to be "just-right" to trigger tumorigenesis in the mammary gland but not in other adult stem cell niches as the intestinal crypt. According to the results presented in **Chapter 4** and here previously discussed, tumorigenesis occurs due to an imbalance in the delicate equilibrium between self-renewal and differentiation in adult stem cell compartments. According to the "just-right" signaling model, the level of Wnt activity encoded by *Apc*<sup>1572T</sup> is particularly suited to outbalance self-renewal and differentiation in the mammary gland but too low to for the intestinal stem cell compartment. This implies that these two niches are very different in their susceptibility to Wnt induced tumorigenesis. Although with very low incidence, two additional *Apc* mouse models have been reported to spontaneously develop mammary tumors: *Apc*<sup>+/<sup>Min</sup> and *Apc*<sup>+/<sup>1638N</sup><sup>81-83</sup>. In both cases, intestinal tumors are found suggesting that the encoded alleles are able to produce higher Wnt signaling activity as confirmed by TOP-FLASH reporter assays<sup>61</sup>. The fact that these mouse models also develop mammary tumors although with a very low frequency might reflect the inadequacy of these alleles to generate the "just-right" level of Wnt activity to promote tumorigenesis in the mammary gland. It would be interesting to address the type of secondary hits in *Apc* in these tumors, they could be mainly point mutations that still allow residual control of Wnt signaling. Another possibility would be the accumulation of mutations in other tumor suppressor genes that change that could cause the level of susceptibility to Wnt induced tumorigenesis to change.</sup></sup>

As previously mentioned, mutations in *APC* are scarce in sporadic breast cancer especially when compared with the high percentage of loss of het-

erozygosity (38%) and of promoter methylation events (50%)<sup>68-73</sup>. Such high percentage of methylation events, leading to lower *APC* expression, allow some residual control over the Wnt pathway signaling, and is supportive of the “just-right” signaling hypothesis.

## Haploinsufficiency and gene dosage

Knudson’s two hit hypothesis postulates that both alleles of a tumor suppressor gene have to be somatically inactivated in order to trigger tumorigenesis<sup>84</sup>. For a long time cancer research has been based on this model and proven valid for a wide range of tumor suppressor genes and types of cancer. However, in the last decade several genes which do not follow the Knudson’s model have been identified where the loss of only one allele is sufficient to trigger a cellular phenotype (for a comprehensive list of genes proven to be haploinsufficient see Payne et al<sup>85</sup>). Hence, haploinsufficiency can be seen as a mechanism underlying changes in gene dosage levels.

As for *APC*, it has been reported that, in a minority of cases, loss of only one allele could by itself initiate the tumorigenic process<sup>86,87</sup>, possibly through enhanced stem cell survival<sup>88</sup>. Furthermore, cells heterozygous for *APC* mutations have been reported to show different phenotypes including altered actin localization and microtubule dynamics<sup>89,90</sup>; decreased cellular migration<sup>90,91</sup>; increased EGFR signaling<sup>92</sup>; decreased apoptotic response and increased oxidative stress response<sup>93</sup>. In the N-terminus of APC an oligomerization domain is believed to be necessary for proper formation of functional dimeric complexes. In cells where one of the *APC* alleles is truncated by mutation, heterodimers are possibly functionality impaired. This dominant negative effect leads also to a dosage phenomenon of functional homodimers that in the heterozygous cell would be lower than in the wild type situation and insufficient to exert its normal function. In **Chapter 3**, by using different *Apc* mutant alleles which encode for the same truncated protein but express it at different levels (2%; 50% and 100%), we have shown dosage-dependent effects on the transcriptional levels of Wnt target genes.

The TGF- $\beta$  pathway is also commonly altered in cancer and its normal activity results in the inhibition of proliferation through the induction of differentiation. In the early tumorigenic process, inactivation of this pathway is often due to loss of function of its intracellular components or mutations at cell membrane receptors. Intriguingly, in advanced stages of tumor progression, the TGF- $\beta$  pathway is often activated to induce malignant behavior<sup>94-99</sup>. *Smad4* is a key molecule where signals from both TGF- $\beta$  and BMP pathways seem to converge to be then conveyed into the nucleus. Thus, loss of *Smad4* function is predicted to affect both signaling pathways by eliminating their transcriptional response. Haploinsufficiency at the *SMAD4* locus underlies juvenile polyposis syndrome (JPS) in man<sup>100</sup> (**Chapter 6**) and the formation of stromal gastrointestinal polyps in *Smad4* targeted mouse models with retention of the wild type allele in the early stages of tumor progression<sup>101-103</sup>. Loss of the wild type allele seems to be associated with tumor progression as it is observed only in later stages of the adenoma-carcinoma sequence<sup>103</sup>. Although most of the tumors analyzed from JPS patients retained expression of the full-length protein, some lesions did not thus suggesting that both haploinsufficiency and the classical two hit hypothesis are valid for *SMAD4*-driven tumorigenesis. This dual behavior is likely to reflect the pathogenic nature of the germline mutation, depending on the severity of the TGF- $\beta$  and/or BMP signaling defect it encodes. In view of the latter hypothesis, it would be interesting to identify in a larger cohort of patients with multiple polyps the type of second hits at the *SMAD4* locus that are selected for tumorigenesis. This could prove the existence of interdependency between the first and second hit in triggering tumorigenesis, just as it was shown for the *APC* tumor suppressor gene. One can also envisage that haploinsufficiency provides the “just-right” level of signaling activity to trigger tumorigenesis. However, in this specific case, in the presence of a germline mutation one would expect every cell to undergo neoplastic transformation which is obviously not the case. A somatic rate-limiting event must therefore be postulated. The accumulation of genetic and/or epigenetic mutation events could act synergistically with haploinsufficiency to trigger tumor formation. In *Apc*<sup>+/M<sup>fin</sup></sup> animals, intestinal and mammary tumor



burden is largely increased when animals receive pro-inflammatory T cells and the effect can be abolished by the co-transfer of anti-inflammatory regulatory lymphocytes<sup>104</sup>. Thus, a non cell-autonomous factor such as inflammation can also contribute to tumorigenesis and modulate cellular behavior and provide the “just-right” signaling activity.

Since cellular context and microenvironment play a crucial role in the pathway's response, ES cells were employed as a model system for the elucidation of the molecular mechanisms underlying haploinsufficiency. We established a dosage dependent effect of *Smad4* in the TGF- $\beta$  and BMP signaling pathways and consequently on the transcriptional activity. Haploinsufficiency for *Apc* (**Chapter 2**) and *Smad4* (**Chapter 6**) lead to intermediate levels of the Wnt and TGF- $\beta$ /BMP pathways, respectively. In both cases, a dosage-dependent effect on the transcriptional signature could be detected by expression profiling.

Overall, the results presented in my PhD thesis underscore the importance of protein expression levels in the cell and how their fluctuation can affect cellular homeostasis and contribute to tumorigenesis.

## References

- <sup>1</sup> Cotsarelis, G., Sun, T. T., and Lavker, R. M. Label-retaining cells reside in the bulge area of pilosebaceous unit: implications for follicular stem cells, hair cycle, and skin carcinogenesis. *Cell* 61 (7), 1329 (1990).
- <sup>2</sup> Tumber, T., Guasch, G., Greco, V., Blanpain, C., Lowry, W. E., Rendl, M., and Fuchs, E. Defining the epithelial stem cell niche in skin. *Science* 303 (5656), 359 (2004).
- <sup>3</sup> Morris, R. J., Liu, Y., Marles, L., Yang, Z., Trempus, C., Li, S., Lin, J. S., Sawicki, J. A., and Cotsarelis, G. Capturing and profiling adult hair follicle stem cells. *Nat Biotechnol* 22 (4), 411 (2004).
- <sup>4</sup> Blanpain, C., Lowry, W. E., Geoghegan, A., Polak, L., and Fuchs, E. Self-renewal, multipotency, and the existence of two cell populations within an epithelial stem cell niche. *Cell* 118 (5), 635 (2004).
- <sup>5</sup> Panteleyev, A. A., Jahoda, C. A., and Christiano, A. M. Hair follicle predetermination. *Journal of cell science* 114 (Pt 19), 3419 (2001).
- <sup>6</sup> Oshima, H., Rochat, A., Kedzia, C., Kobayashi, K., and Barrandon, Y. Morphogenesis and renewal of hair follicles from adult multipotent stem cells. *Cell* 104 (2), 233 (2001).
- <sup>7</sup> Taylor, G., Lehrer, M. S., Jensen, P. J., Sun, T. T., and Lavker, R. M. Involvement of follicular stem cells in forming not only the

follicle but also the epidermis. *Cell* 102 (4), 451 (2000).

- <sup>8</sup> Wilson, A., Laurenti, E., Oser, G., van der Wath, R. C., Blanco-Bose, W., Jaworski, M., Offner, S., Dunant, C. F., Eshkind, L., Bockamp, E., Lio, P., Macdonald, H. R., and Trumpp, A. Hematopoietic stem cells reversibly switch from dormancy to self-renewal during homeostasis and repair. *Cell* 135 (6), 1118 (2008).
- <sup>9</sup> Nguyen, H., Rendl, M., and Fuchs, E. Tcf3 governs stem cell features and represses cell fate determination in skin. *Cell* 127 (1), 171 (2006).
- <sup>10</sup> Lowry, W. E., Blanpain, C., Nowak, J. A., Guasch, G., Lewis, L., and Fuchs, E. Defining the impact of beta-catenin/Tcf transactivation on epithelial stem cells. *Genes Dev* 19 (13), 1596 (2005).
- <sup>11</sup> Foudi, A., Hochedlinger, K., Van Buren, D., Schindler, J. W., Jaenisch, R., Carey, V., and Hock, H. Analysis of histone 2B-GFP retention reveals slowly cycling hematopoietic stem cells. *Nat Biotechnol* (2008).
- <sup>12</sup> Barker, N., van Es, J. H., Jaks, V., Kasper, M., Snippert, H., Toftgard, R., and Clevers, H. Very Long-term Self-renewal of Small Intestine, Colon, and Hair Follicles from Cycling Lgr5+ve Stem Cells. *Cold Spring Harbor symposia on quantitative biology* (2008).
- <sup>13</sup> Jaks, V., Barker, N., Kasper, M., van Es, J. H., Snippert, H. J., Clevers, H., and Toftgard, R. Lgr5 marks cycling, yet long-lived, hair follicle stem cells. *Nat Genet* 40 (11), 1291 (2008).
- <sup>14</sup> Vogelstein, B., Fearon, E. R., Hamilton, S. R., Kern, S. E., Preisinger, A. C., Leppert, M., Nakamura, Y., White, R., Smits, A. M., and Bos, J. L. Genetic alterations during colorectal-tumor development. *N Engl J Med* 319 (9), 525 (1988).
- <sup>15</sup> Hanahan, D. and Weinberg, R. A. The hallmarks of cancer. *Cell* 100 (1), 57 (2000).
- <sup>16</sup> Southam, C. & Brunschwig, A. Quantitative studies of autotransplantation of human cancer preliminary report. *Cancer* 14, 971 (1961).
- <sup>17</sup> Bruce, W. R. and Van Der Gaag, H. A Quantitative Assay for the Number of Murine Lymphoma Cells Capable of Proliferation in Vivo. *Nature* 199, 79 (1963).
- <sup>18</sup> Park, C. H., Bergsagel, D. E., and McCulloch, E. A. Mouse myeloma tumor stem cells: a primary cell culture assay. *Journal of the National Cancer Institute* 46 (2), 411 (1971).
- <sup>19</sup> Sabbath, K. D., Ball, E. D., Larcom, P., Davis, R. B., and Griffin, J. D. Heterogeneity of clonogenic cells in acute myeloblastic leukemia. *The Journal of clinical investigation* 75 (2), 746 (1985).
- <sup>20</sup> Sabbath, K. D. and Griffin, J. D. Clonogenic cells in acute myeloblastic leukaemia. *Scandinavian journal of haematology* 35 (3), 251 (1985).



- <sup>21</sup> Hamburger, A. W. and Salmon, S. E. Primary bioassay of human tumor stem cells. *Science* 197 (4302), 461 (1977).
- <sup>22</sup> Reya, T., Morrison, S. J., Clarke, M. F., and Weissman, I. L. Stem cells, cancer, and cancer stem cells. *Nature* 414 (6859), 105 (2001).
- <sup>23</sup> Bonnet, D. and Dick, J. E. Human acute myeloid leukemia is organized as a hierarchy that originates from a primitive hematopoietic cell. *Nat Med* 3 (7), 730 (1997).
- <sup>24</sup> Perez-Caro, M., Cobaleda, C., Gonzalez-Herrero, I., Vicente-Duenas, C., Bermejo-Rodriguez, C., Sanchez-Beato, M., Orfao, A., Pintado, B., Flores, T., Sanchez-Martin, M., Jimenez, R., Piri, M. A., and Sanchez-Garcia, I. Cancer induction by restriction of oncogene expression to the stem cell compartment. *Embo J* (2008).
- <sup>25</sup> Barker, N., Ridgway, R. A., van Es, J. H., van de Wetering, M., Begthel, H., van den Born, M., Danenberg, E., Clarke, A. R., Sansom, O. J., and Clevers, H. Crypt stem cells as the cells-of-origin of intestinal cancer. *Nature* (2008).
- <sup>26</sup> Wicha, M. S., Liu, S., and Dontu, G. Cancer stem cells: an old idea—a paradigm shift. *Cancer Res* 66 (4), 1883 (2006).
- <sup>27</sup> Moore, K. A. and Lemischka, I. R. Stem cells and their niches. *Science* 311 (5769), 1880 (2006).
- <sup>28</sup> Xue, C., Plieth, D., Venkov, C., Xu, C., and Neilson, E. G. The gatekeeper effect of epithelial-mesenchymal transition regulates the frequency of breast cancer metastasis. *Cancer Res* 63 (12), 3386 (2003).
- <sup>29</sup> Ueno, H., Murphy, J., Jass, J. R., Mochizuki, H., and Talbot, I. C. Tumour 'budding' as an index to estimate the potential of aggressiveness in rectal cancer. *Histopathology* 40 (2), 127 (2002).
- <sup>30</sup> Jass, J. R., Barker, M., Fraser, L., Walsh, M. D., Whitehall, V. L., Gabrielli, B., Young, J., and Leggett, B. A. APC mutation and tumour budding in colorectal cancer. *Journal of clinical pathology* 56 (1), 69 (2003).
- <sup>31</sup> Brabletz, T., Jung, A., Reu, S., Porzner, M., Hlubek, F., Kunz-Schughart, L. A., Knuechel, R., and Kirchner, T. Variable beta-catenin expression in colorectal cancers indicates tumor progression driven by the tumor environment. *Proc Natl Acad Sci U S A* 98 (18), 10356 (2001).
- <sup>32</sup> Thiery, J. P. and Sleeman, J. P. Complex networks orchestrate epithelial-mesenchymal transitions. *Nature reviews* 7 (2), 131 (2006).
- <sup>33</sup> Huber, M. A., Kraut, N., and Beug, H. Molecular requirements for epithelial-mesenchymal transition during tumor progression. *Curr Opin Cell Biol* 17 (5), 548 (2005).
- <sup>34</sup> Fodde, R. The APC gene in colorectal cancer. *Eur J Cancer* 38 (7), 867 (2002).
- <sup>35</sup> Powell, S. M., Zilz, N., Beazer-Barclay, Y., Bryan, T. M., Hamilton, S. R., Thibodeau, S. N., Vogelstein, B., and Kinzler, K. W. APC mutations occur early during colorectal tumorigenesis. *Nature* 359 (6392), 235 (1992).
- <sup>36</sup> Kinzler, K. W. and Vogelstein, B. Lessons from hereditary colorectal cancer. *Cell* 87 (2), 159 (1996).
- <sup>37</sup> Fodde, R., Smits, R., and Clevers, H. APC, signal transduction and genetic instability in colorectal cancer. *Nat Rev Cancer* 1 (1), 55 (2001).
- <sup>38</sup> Hajra, K. M., Chen, D. Y., and Fearon, E. R. The SLUG zinc-finger protein represses E-cadherin in breast cancer. *Cancer Res* 62 (6), 1613 (2002).
- <sup>39</sup> Conacci-Sorrell, M., Simcha, I., Ben-Yedidia, T., Blehman, J., Savagner, P., and Ben-Ze'ev, A. Autoregulation of E-cadherin expression by cadherin-cadherin interactions: the roles of beta-catenin signaling, Slug, and MAPK. *J Cell Biol* 163 (4), 847 (2003).
- <sup>40</sup> Kirchner, T. and Brabletz, T. Patterning and nuclear beta-catenin expression in the colonic adenoma-carcinoma sequence. Analogies with embryonic gastrulation. *Am J Pathol* 157 (4), 1113 (2000).
- <sup>41</sup> Brabletz, T., Jung, A., Hermann, K., Gunther, K., Hohenberger, W., and Kirchner, T. Nuclear overexpression of the oncoprotein beta-catenin in colorectal cancer is localized predominantly at the invasion front. *Pathology, research and practice* 194 (10), 701 (1998).
- <sup>42</sup> Gaspar, C. and Fodde, R. APC dosage effects in tumorigenesis and stem cell differentiation. *Int J Dev Biol* 48 (5-6), 377 (2004).
- <sup>43</sup> Bafico, A., Liu, G., Goldin, L., Harris, V., and Aaronson, S. A. An autocrine mechanism for constitutive Wnt pathway activation in human cancer cells. *Cancer Cell* 6 (5), 497 (2004).
- <sup>44</sup> Janssen, K. P., Alberici, P., Fsihi, H., Gaspar, C., Breukel, C., Franken, P., Rosty, C., Abal, M., El Marjou, F., Smits, R., Louvard, D., Fodde, R., and Robine, S. APC and oncogenic KRAS are synergistic in enhancing Wnt signaling in intestinal tumor formation and progression. *Gastroenterology* 131 (4), 1096 (2006).
- <sup>45</sup> Fodde, R. and Brabletz, T. Wnt/beta-catenin signaling in cancer stemness and malignant behavior. *Curr Opin Cell Biol* 19 (2), 150 (2007).
- <sup>46</sup> Jung, A., Brabletz, T., and Kirchner, T. The migrating cancer stem cells model—a conceptual explanation of malignant tumour progression. *Ernst Schering Foundation symposium proceedings* (5), 109 (2006).
- <sup>47</sup> Mani, S. A., Guo, W., Liao, M. J., Eaton, E. N., Ayyanan, A., Zhou, A. Y., Brooks, M., Reinhard, F., Zhang, C. C., Shipitsin, M., Campbell, L. L., Polyak, K., Briskin, C., Yang, J., and Weinberg, R. A. The epithelial-mesenchymal transition generates

- cells with properties of stem cells. *Cell* 133 (4), 704 (2008).
- <sup>48</sup> Albuquerque, C., Breukel, C., van der Luijt, R., Fidalgo, P., Lage, P., Slors, F. J., Leïtao, C. N., Fodde, R., and Smits, R. The 'just-right' signaling model: APC somatic mutations are selected based on a specific level of activation of the beta-catenin signaling cascade. *Hum Mol Genet* 11 (13), 1549 (2002).
  - <sup>49</sup> Le, N. H., Franken, P., and Fodde, R. Tumour-stroma interactions in colorectal cancer: converging on beta-catenin activation and cancer stemness. *Br J Cancer* 98 (12), 1886 (2008).
  - <sup>50</sup> Cole, M. F., Johnstone, S. E., Newman, J. J., Kagey, M. H., and Young, R. A. Tcf3 is an integral component of the core regulatory circuitry of embryonic stem cells. *Genes Dev* 22 (6), 746 (2008).
  - <sup>51</sup> Boyer, L. A., Lee, T. I., Cole, M. F., Johnstone, S. E., Levine, S. S., Zucker, J. P., Guenther, M. G., Kumar, R. M., Murray, H. L., Jenner, R. G., Gifford, D. K., Melton, D. A., Jaenisch, R., and Young, R. A. Core transcriptional regulatory circuitry in human embryonic stem cells. *Cell* 122 (6), 947 (2005).
  - <sup>52</sup> Pereira, L., Yi, F., and Merrill, B. J. Repression of Nanog gene transcription by Tcf3 limits embryonic stem cell self-renewal. *Mol Cell Biol* 26 (20), 7479 (2006).
  - <sup>53</sup> Yi, F., Pereira, L., and Merrill, B. J. Tcf3 functions as a steady-state limiter of transcriptional programs of mouse embryonic stem cell self-renewal. *Stem cells (Dayton, Ohio)* 26 (8), 1951 (2008).
  - <sup>54</sup> Reya, T. and Clevers, H. Wnt signalling in stem cells and cancer. *Nature* 434 (7035), 843 (2005).
  - <sup>55</sup> Kratochwil, K. In vitro analysis of the hormonal basis for the sexual dimorphism in the embryonic development of the mouse mammary gland. *Journal of embryology and experimental morphology* 25 (1), 141 (1971).
  - <sup>56</sup> Kratochwil, K. and Schwartz, P. Tissue interaction in androgen response of embryonic mammary rudiment of mouse: identification of target tissue for testosterone. *Proc Natl Acad Sci U S A* 73 (11), 4041 (1976).
  - <sup>57</sup> Tsukamoto, A. S., Grosschedl, R., Guzman, R. C., Parslow, T., and Varmus, H. E. Expression of the int-1 gene in transgenic mice is associated with mammary gland hyperplasia and adenocarcinomas in male and female mice. *Cell* 55 (4), 619 (1988).
  - <sup>58</sup> Lane, T. F. and Leder, P. Wnt-10b directs hypermorphic development and transformation in mammary glands of male and female mice. *Oncogene* 15 (18), 2133 (1997).
  - <sup>59</sup> Balinsky, B. I. On the prenatal growth of the mammary gland rudiment in the mouse. *Journal of anatomy* 84 (3), 227 (1950).
  - <sup>60</sup> Hennighausen, L. and Robinson, G. W. Think globally, act locally: the making of a mouse mammary gland. *Genes Dev* 12 (4), 449 (1998).
  - <sup>61</sup> Kielman, M. F., Rindapaa, M., Gaspar, C., van Poppel, N., Breukel, C., van Leeuwen, S., Taketo, M. M., Roberts, S., Smits, R., and Fodde, R. Apc modulates embryonic stem-cell differentiation by controlling the dosage of beta-catenin signaling. *Nat Genet* 32 (4), 594 (2002).
  - <sup>62</sup> Shackleton, M., Vaillant, F., Simpson, K. J., Stingl, J., Smyth, G. K., Asselin-Labat, M. L., Wu, L., Lindeman, G. J., and Visvader, J. E. Generation of a functional mammary gland from a single stem cell. *Nature* 439 (7072), 84 (2006).
  - <sup>63</sup> Hlubek, F., Brabletz, T., Budczies, J., Pfeiffer, S., Jung, A., and Kirchner, T. Heterogeneous expression of Wnt/beta-catenin target genes within colorectal cancer. *Int J Cancer* 121 (9), 1941 (2007).
  - <sup>64</sup> Lin, S. Y., Xia, W., Wang, J. C., Kwong, K. Y., Spohn, B., Wen, Y., Pestell, R. G., and Hung, M. C. Beta-catenin, a novel prognostic marker for breast cancer: its roles in cyclin D1 expression and cancer progression. *Proc Natl Acad Sci U S A* 97 (8), 4262 (2000).
  - <sup>65</sup> Klopocki, E., Kristiansen, G., Wild, P. J., Klamann, I., Castanos-Velez, E., Singer, G., Stohr, R., Simon, R., Sauter, G., Leibiger, H., Essers, L., Weber, B., Hermann, K., Rosenthal, A., Hartmann, A., and Dahl, E. Loss of SFRP1 is associated with breast cancer progression and poor prognosis in early stage tumors. *International journal of oncology* 25 (3), 641 (2004).
  - <sup>66</sup> Forget, M. A., Turcotte, S., Beauseigle, D., Godin-Ethier, J., Pelletier, S., Martin, J., Tanguay, S., and Lapointe, R. The Wnt pathway regulator DKK1 is preferentially expressed in hormone-resistant breast tumours and in some common cancer types. *Br J Cancer* 96 (4), 646 (2007).
  - <sup>67</sup> Nakopoulou, L., Mylona, E., Papadaki, I., Kavantzis, N., Giannopoulou, I., Markaki, S., and Keramopoulos, A. Study of phospho-beta-catenin subcellular distribution in invasive breast carcinomas in relation to their phenotype and the clinical outcome. *Mod Pathol* 19 (4), 556 (2006).
  - <sup>68</sup> Furuuchi, K., Tada, M., Yamada, H., Kataoka, A., Furuuchi, N., Hamada, J., Takahashi, M., Todo, S., and Moriuchi, T. Somatic mutations of the APC gene in primary breast cancers. *Am J Pathol* 156 (6), 1997 (2000).
  - <sup>69</sup> Hayes, M. J., Thomas, D., Emmons, A., Giordano, T. J., and Kleer, C. G. Genetic changes of Wnt pathway genes are common events in metaplastic carcinomas of the breast. *Clin Cancer Res* 14 (13), 4038 (2008).
  - <sup>70</sup> Kashiwaba, M., Tamura, G., and Ishida, M. Aberrations of the APC gene in primary breast carcinoma. *J Cancer Res Clin Oncol* 120 (12), 727 (1994).
  - <sup>71</sup> Lee, A., Kim, Y., Han, K., Kang, C. S., Jeon, H. M., and Shim, S. I. Detection of Tumor Markers Including Carcinoembryonic

- Antigen, APC, and Cyclin D2 in Fine-Needle Aspiration Fluid of Breast. *Archives of pathology & laboratory medicine* 128 (11), 1251 (2004).
- <sup>72</sup> Sarrio, D., Moreno-Bueno, G., Hardisson, D., Sanchez-Estevéz, C., Guo, M., Herman, J. G., Gamallo, C., Esteller, M., and Palacios, J. Epigenetic and genetic alterations of APC and CDH1 genes in lobular breast cancer: relationships with abnormal E-cadherin and catenin expression and microsatellite instability. *Int J Cancer* 106 (2), 208 (2003).
- <sup>73</sup> Virmani, A. K., Rath, A., Sathyanarayana, U. G., Padar, A., Huang, C. X., Cunningham, H. T., Farinas, A. J., Milchgrub, S., Euhus, D. M., Gilcrease, M., Herman, J., Minna, J. D., and Gazdar, A. F. Aberrant methylation of the adenomatous polyposis coli (APC) gene promoter 1A in breast and lung carcinomas. *Clin Cancer Res* 7 (7), 1998 (2001).
- <sup>74</sup> Rosen, P. P. and Ernster, D. Low-grade adenosquamous carcinoma. A variant of metaplastic mammary carcinoma. *The American journal of surgical pathology* 11 (5), 351 (1987).
- <sup>75</sup> Weigelt, B., Kreike, B., and Reis-Filho, J. S. Metaplastic breast carcinomas are basal-like breast cancers: a genomic profiling analysis. *Breast cancer research and treatment* (2008).
- <sup>76</sup> Hennessy, B. T., Giordano, S., Broglio, K., Duan, Z., Trent, J., Buchholz, T. A., Babiera, G., Hortobagyi, G. N., and Valero, V. Biphasic metaplastic sarcomatoid carcinoma of the breast. *Ann Oncol* 17 (4), 605 (2006).
- <sup>77</sup> Hennessy, B. T., Krishnamurthy, S., Giordano, S., Buchholz, T. A., Kau, S. W., Duan, Z., Valero, V., and Hortobagyi, G. N. Squamous cell carcinoma of the breast. *J Clin Oncol* 23 (31), 7827 (2005).
- <sup>78</sup> Leibl, S. and Moirand, F. Metaplastic breast carcinomas are negative for Her-2 but frequently express EGFR (Her-1): potential relevance to adjuvant treatment with EGFR tyrosine kinase inhibitors? *Journal of clinical pathology* 58 (7), 700 (2005).
- <sup>79</sup> Reis-Filho, J. S., Milanezi, F., Carvalho, S., Simpson, P. T., Steele, D., Savage, K., Lambros, M. B., Pereira, E. M., Nesland, J. M., Lakhani, S. R., and Schmitt, F. C. Metaplastic breast carcinomas exhibit EGFR, but not HER2, gene amplification and overexpression: immunohistochemical and chromogenic in situ hybridization analysis. *Breast Cancer Res* 7 (6), R1028 (2005).
- <sup>80</sup> Fodde, R. and Khan, P. M. Genotype-phenotype correlations at the adenomatous polyposis coli (APC) gene. *Crit Rev Oncog* 6 (3-6), 291 (1995).
- <sup>81</sup> Moser, A. R., Mattes, E. M., Dove, W. F., Lindstrom, M. J., Haag, J. D., and Gould, M. N. ApcMin, a mutation in the murine Apc gene, predisposes to mammary carcinomas and focal alveolar hyperplasias. *Proc Natl Acad Sci U S A* 90 (19), 8977 (1993).
- <sup>82</sup> van der Houven van Oordt, C. W., Smits, R., Schouten, T. G., Houwing-Duistermaat, J. J., Williamson, S. L., Luz, A., Meera Khan, P., van der Eb, A. J., Breuer, M. L., and Fodde, R. The genetic background modifies the spontaneous and X-ray-induced tumor spectrum in the Apc1638N mouse model. *Genes Chromosomes Cancer* 24 (3), 191 (1999).
- <sup>83</sup> van der Houven van Oordt, C. W., Smits, R., Williamson, S. L., Luz, A., Khan, P. M., Fodde, R., van der Eb, A. J., and Breuer, M. L. Intestinal and extra-intestinal tumor multiplicities in the Apc1638N mouse model after exposure to X-rays. *Carcinogenesis* 18 (11), 2197 (1997).
- <sup>84</sup> Knudson, A. G., Jr. Mutation and cancer: statistical study of retinoblastoma. *Proc Natl Acad Sci U S A* 68 (4), 820 (1971).
- <sup>85</sup> Payne, S. R. and Kemp, C. J. Tumor suppressor genetics. *Carcinogenesis* 26 (12), 2031 (2005).
- <sup>86</sup> Venesio, T., Balsamo, A., Rondo-Spaudo, M., Varesco, L., Riso, M., and Ranzani, G. N. APC haploinsufficiency, but not CTNNB1 or CDH1 gene mutations, accounts for a fraction of familial adenomatous polyposis patients without APC truncating mutations. *Laboratory investigation; a journal of technical methods and pathology* 83 (12), 1859 (2003).
- <sup>87</sup> Sieber, O. M., Lammler, H., Crabtree, M. D., Rowan, A. J., Barclay, E., Lipton, L., Hodgson, S., Thomas, H. J., Neale, K., Phillips, R. K., Farrington, S. M., Dunlop, M. G., Mueller, H. J., Bisgaard, M. L., Bulow, S., Fidalgo, P., Albuquerque, C., Scarano, M. I., Bodmer, W., Tomlinson, I. P., and Heinemann, K. Whole-gene APC deletions cause classical familial adenomatous polyposis, but not attenuated polyposis or "multiple" colorectal adenomas. *Proc Natl Acad Sci U S A* 99 (5), 2954 (2002).
- <sup>88</sup> Kim, K. M., Calabrese, P., Tavaré, S., and Shibata, D. Enhanced stem cell survival in familial adenomatous polyposis. *Am J Pathol* 164 (4), 1369 (2004).
- <sup>89</sup> Kopelovich, L., Conlon, S., and Pollack, R. Defective organization of actin in cultured skin fibroblasts from patients with inherited adenocarcinoma. *Proc Natl Acad Sci U S A* 74 (7), 3019 (1977).
- <sup>90</sup> Hughes, S. A., Carothers, A. M., Hunt, D. H., Moran, A. E., Mueller, J. D., and Bertagnoli, M. M. Adenomatous polyposis coli truncation alters cytoskeletal structure and microtubule stability in early intestinal tumorigenesis. *J Gastrointest Surg* 6 (6), 868 (2002).
- <sup>91</sup> Carothers, A. M., Melstrom, K. A., Jr., Mueller, J. D., Weyant, M. J., and Bertagnoli, M. M. Progressive changes in adherens junction structure during intestinal adenoma formation in Apc mutant mice. *J Biol Chem* 276 (42), 39094 (2001).
- <sup>92</sup> Moran, A. E., Hunt, D. H., Javid, S. H., Redston, M., Carothers, A. M., and Bertagnoli, M. M. Apc deficiency is associated with increased Egfr activity in the intestinal enterocytes and

- adenomas of C57BL/6J-Min/+ mice. *J Biol Chem* 279 (41), 43261 (2004).
- <sup>93</sup> Yeung, A. T., Patel, B. B., Li, X. M., Seeholzer, S. H., Coudry, R. A., Cooper, H. S., Bellacosa, A., Boman, B. M., Zhang, T., Litwin, S., Ross, E. A., Conrad, P., Crowell, J. A., Kopelovich, L., and Knudson, A. One-hit effects in cancer: altered proteome of morphologically normal colon crypts in familial adenomatous polyposis. *Cancer Res* 68 (18), 7579 (2008).
- <sup>94</sup> Massague, J. How cells read TGF-beta signals. *Nature reviews* 1 (3), 169 (2000).
- <sup>95</sup> Massague, J., Blain, S. W., and Lo, R. S. TGFbeta signaling in growth control, cancer, and heritable disorders. *Cell* 103 (2), 295 (2000).
- <sup>96</sup> Massague, J. and Chen, Y. G. Controlling TGF-beta signaling. *Genes Dev* 14 (6), 627 (2000).
- <sup>97</sup> Massague, J. and Wotton, D. Transcriptional control by the TGF-beta/Smad signaling system. *Embo J* 19 (8), 1745 (2000).
- <sup>98</sup> Blobe, G. C., Schieman, W. P., and Lodish, H. F. Role of transforming growth factor beta in human disease. *N Engl J Med* 342 (18), 1350 (2000).
- <sup>99</sup> Bachman, K. E. and Park, B. H. Duel nature of TGF-beta signaling: tumor suppressor vs. tumor promoter. *Current opinion in oncology* 17 (1), 49 (2005).
- <sup>100</sup> Alberici, P., Gaspar, C., Franken, P., Gorski, M. M., de Vries, I., Scott, R. J., Ristimaki, A., Aaltonen, L. A., and Fodde, R. Smad4 haploinsufficiency: a matter of dosage. *PathoGenetics* 1 (1), 2 (2008).
- <sup>101</sup> Howe, J. R., Roth, S., Ringold, J. C., Summers, R. W., Jarvinen, H. J., Sistonen, P., Tomlinson, I. P., Houlston, R. S., Bevan, S., Mitros, F. A., Stone, E. M., and Aaltonen, L. A. Mutations in the SMAD4/DPC4 gene in juvenile polyposis. *Science* 280 (5366), 1086 (1998).
- <sup>102</sup> Xu, X., Brodie, S. G., Yang, X., Im, Y. H., Parks, W. T., Chen, L., Zhou, Y. X., Weinstein, M., Kim, S. J., and Deng, C. X. Haploid loss of the tumor suppressor Smad4/Dpc4 initiates gastric polyposis and cancer in mice. *Oncogene* 19 (15), 1868 (2000).
- <sup>103</sup> Alberici, P., Jagmohan-Changur, S., De Pater, E., Van Der Valk, M., Smits, R., Hohenstein, P., and Fodde, R. Smad4 haploinsufficiency in mouse models for intestinal cancer. *Oncogene* 25 (13), 1841 (2006).
- <sup>104</sup> Rao, V. P., Poutahidis, T., Ge, Z., Nambiar, P. R., Horwitz, B. H., Fox, J. G., and Erdman, S. E. Proinflammatory CD4+ CD45RB(hi) lymphocytes promote mammary and intestinal carcinogenesis in Apc(Min/+) mice. *Cancer Res* 66 (1), 57 (2006).

# Summary and Samenvatting

## Summary

The Wnt pathway is a well-known signaling transduction pathway playing pivotal roles during embryonic development, cell cycle control, self-renewal and differentiation in adult tissues. Many of its components are involved in the etiology of a wide variety of neoplasias. Germline mutations in the *APC* tumor suppressor gene have been found in patients with familial adenomatous polyposis (FAP), a condition associated with the presence of hundreds of polyps in the colon. APC is a key regulatory component of the Wnt signaling pathway and its main tumor suppressor activity resides in its ability to bind to and downregulate  $\beta$ -catenin. Several mouse models for *Apc* have been developed to date that resemble the human disease. In **Chapter 1** we present a review on how different *APC* mutations encode different Wnt signaling activities, trigger different cellular differentiation patterns and account for the phenotypic variability observed in human kindreds and mouse models.

There is compelling evidence on the role of the Wnt pathway in cellular fate determination but the dosage effects of its signaling activity have not been addressed. The possibility of generating different levels of Wnt activity through hypomorphic mutations in the *Apc* gene gave us the opportunity to study signaling dosage effects on cell differentiation, as reported in **Chapter 2**. A series of embryonic stem (ES) cell lines carrying homozygous or compound heterozygous hypomorphic mutations in the endogenous locus were used to address differentiation capacity both *in vivo* (teratoma differentiation assay) and *in vitro*. We showed that Wnt signaling activity correlates in a dosage-dependent fashion with the ability of the ES cells to differentiate. Hypomorphic *Apc* mutants presented milder differentiation defects when compared to more severe defects where complete differentiation blockage in specific lineages is observed. Both in undifferentiated ES cells and in teratomas, genome-wide transcriptional analysis confirmed the dosage-dependent correlation between level of Wnt activity and the expression of a wide variety of target genes

(**Chapters 2 and 3**). The results pinpoint a role for Wnt signaling in maintaining stem cell properties in a dosage dependent manner and thus relevant for understanding the pleiotropic nature of the tumorigenic process.

In sporadic and FAP-associated colorectal tumors, most of the *APC* mutations are found within the mutation cluster region leaving intact three of the  $\beta$ -catenin binding domains. A similar protein encoded by the mouse *Apc*<sup>Δ638T</sup> allele encompasses three  $\beta$ -catenin binding and one Axin binding domains and does not predispose heterozygous animals to tumorigenesis. To study the functional role of the remaining Axin domain in the tumorigenic process we have generated a new mouse model, *Apc*<sup>Δ572T</sup>, encompassing only three  $\beta$ -catenin binding domains as often observed in human tumors. ES cell lines homozygous for the *Apc*<sup>Δ572T</sup> mutation displayed intermediate Wnt signaling levels when compared to other previously published *Apc* mutant alleles, which is also reflected by their milder differentiation defect. Mice heterozygous for this mutation were not prone to intestinal tumorigenesis but developed mammary adenocarcinomas that spontaneously formed metastases in the lung. Furthermore, intracellular  $\beta$ -catenin accumulation underlies cancer stemness and metastatic behavior in the mammary gland underlining the importance of specific dosages of Wnt signaling in conferring predisposition to organ-specific tumorigenesis.

Colorectal cancer still represents one of the leading causes of mortality in the Western societies but also one of the most studied types of neoplasia. Reports on genome-wide transcriptional analysis have tried to elucidate the molecular mechanisms underlying this tumorigenic process. However, the high-complexity of the lists of genes differentially expressed in CRC is overwhelming and makes their functional interpretation difficult. To overcome this problem, we have looked for evolutionary conserved target genes by comparing human intestinal polyps from FAP patients with mouse intestinal tumors from



*Apc*<sup>+/1638N</sup>, **Chapter 5**. This cross-species comparison yielded a list of 166 conserved genes involved in APC-driven tumor initiation including several of the already described targets of the Wnt pathway. In the same study, we report a high similarity between genome-wide expression profiles derived from APC and MYH associated polyps where only 49 genes are found to be differentially expressed. An improved discriminative ability of the cross-species conserved genes highlights the added value of this approach as a tool to identify more functionally relevant genes from complex microarray profiling data sets.

Haploinsufficiency can be seen as a mechanism that underlies changes in gene dosage levels. The tumor suppressor gene *SMAD4*, a signaling component of the TGF- $\beta$  and BMP pathways, has been shown to initiate tumor formation in juvenile polyposis syndrome (JPS) without the loss of the wild type allele (Chapter 6). In ES cell lines carrying targeted *Smad4*-mutant alleles, Smad4 protein expression was directly correlated with the gene copy number: *Smad4*<sup>+/+</sup>=100%; *Smad4*<sup>+/Sad</sup>=50%; and *Smad4*<sup>Sad/Sad</sup>=0%. By using reporter assays for TGF- $\beta$  and BMP pathways, we showed that progressively decreased Smad4 protein

levels affect accordingly the signaling activity intensities of both pathways. The transcriptional effects elicited by haploinsufficiency have been evaluated by genome-wide expression analysis and revealed a set of dosage-dependent target genes. This expression signature was validated for a subset of targets by real-time PCR on mouse intestinal tissues from *Smad4*<sup>+/Sad</sup>. Our study provides information on the molecular mechanisms underlying haploinsufficiency for *Smad4* (and *Apc*, see **Chapter 3**), thus contributing to our understanding on how gene dosage can contribute to tumorigenesis.

In conclusion, the work presented in this PhD thesis is in agreement with our initial hypothesis (**Chapter 1**) where we postulated that adult stem cell niches are regulated and finely tuned by specific doses of signaling activity. Altered signaling levels lead to the expansion of the stem cell compartment by enhancing self-renewal or by inhibiting and re-wiring of the differentiation program. The next challenge will be to understand, at the molecular level, how the specific levels generated either via haploinsufficiency or hypomorphic mutations contribute to tumorigenesis.

## Samenvatting

Het Wnt-pathway is een bekend signaal transductie pad welke een centrale rol speelt bij de embryonale ontwikkeling, de controle op celdeling en de zelfvernieuwing en differentiatie van stamcellen in volwassen weefsels. Veel van de componenten van dit pad zijn betrokken bij het ontstaan van een breed spectrum aan type tumoren. Bovendien, kiembaan mutaties in het APC-gen, een essentieel onderdeel van het Wnt pad, veroorzaken familiale adenomateuze polyposis (FAP): een erfelijke aanleg voor darmkanker. De belangrijkste tumoronderdrukkende activiteit van APC ligt in het vermogen om zich te binden aan  $\beta$ -catenine, het centrale signaleiwit van het Wnt pad, en dit zodoende te reguleren. APC-mutaties leiden tot een ongecontroleerde opstapeling van  $\beta$ -catenine in de cel en tot de constitutieve activatie van het Wnt pathway. Ons laboratorium heeft tot nu toe verschillende muismodellen voor *Apc* ontwikkeld, die de ziekte kunnen weergeven zoals die verloopt in de mens. In **Hoofdstuk 1** presenteren we een review over hoe de verschillende *APC*-mutaties tot verschillende Wnt-signaleringsactiviteiten leiden, die de fenotypische variabiliteit (in muis en mens) kunnen verklaren.

Over de rol van Wnt in het bepalen van het differentiatievermogen van stamcellen bestaat overweldigend bewijs. Maar het effect van verschillende doseringen van de signaleringsactiviteit van Wnt is nog niet onderzocht. De mogelijkheid om verschillende niveaus van Wnt-activiteit op te wekken door specifieke mutaties in het *Apc*-gen gaf ons de kans om de effecten van deze signaaldosering op celdifferentiatie te onderzoeken. Dit onderzoek is weergegeven in **Hoofdstuk 2**. Er is gebruik gemaakt van een reeks embryonale stamcel (ES) lijnen die drager zijn van verschillende *Apc*-mutaties zodat de capaciteit tot differentiatie, zowel *in vivo* als *in vitro*, kan worden bekeken. We hebben aangetoond dat de Wnt-signaleringsactiviteit het vermogen van de ES cellen om te differentiëren op een doseringsafhankelijke manier kan reguleren. *Apc*-mutaties die tot een subtieler Wnt-defect leiden, vertoonden mildere effecten op het differentiatievermogen van ES cellen in vergelij-

king met ernstigere mutaties waarbij een complete differentiatie blokkade werd waargenomen. De doseringsafhankelijke relatie tussen het niveau van de Wnt-activiteit en het differentiatievermogen van stamcellen werd bevestigd door middel van “expression profiling” analyse van beide *Apc*-mutante ES cellen en hun gedifferentieerde equivalent (**Hoofdstuk 2 en 3**). Deze resultaten zijn van belang om de pleiotropie van het proces van tumorvorming te kunnen begrijpen.

In sporadische en in FAP-gerelateerde darmtumoren worden de meeste *APC*-mutaties gevonden binnen de zgn. “mutatie-cluster-regio”. Deze mutaties leiden tot getrunceerde *APC*-eiwitten die nog steeds in staat zijn om aan  $\beta$ -catenine te binden. In het *Apc*<sup>1638T</sup> muismodel komt een wat langer eiwit tot expressie, wat niet tot een predispositie voor tumorvorming bij heterozygote dieren leidt. Om de functionele rol van het overblijvende (Axin-binding) domein van het *APC*-eiwit in tumorvorming te kunnen bestuderen hebben we een nieuw muismodel gemaakt: *Apc*<sup>1572T</sup>. Dit model bevat een mutatie, die resulteert in een getrunceerd *Apc*-eiwit, zoals dat ook vaak wordt gezien in humane tumoren (dwz met  $\beta$ -catenine bindende activiteit maar zonder het Axin domein). ES cellijnen die homozygoot zijn voor de *Apc*<sup>1572T</sup>-mutatie vertoonden gemiddelde Wnt-signaleringsniveaus in vergelijking met andere, eerder gepubliceerde *Apc*-mutante allelen, wat ook wordt weerspiegeld in hun mildere differentiatie defect. Opvallend, muizen die heterozygoot zijn voor deze mutatie waren niet vatbaar voor darmtumoren, maar ontwikkelden wel borst-adenocarcinomen die zich spontaan uitzaaiden in de long. Bovendien ligt intercellulaire opstapeling van  $\beta$ -catenine aan de basis van het ontstaan van kankerstemcellen en metastatisch gedrag in de borstklier, wat het belang van specifieke dosering van Wnt-signaleringsactiviteit bij aanleg voor orgaanspecifieke tumorgenese onderstreept.

Darmkanker is nog steeds een van de belangrijkste doodsoorzaken in westerse maatschappijen, maar het is ook een van de meest bestudeerde vormen van neoplasmen. Met behulp van expression profil-

ing analyse is geprobeerd de moleculaire mechanismen, die aan de basis liggen van het tumorvormende proces, op te helderen. Helaas is de complexiteit van de lijst van genen, die differentieel tot expressie in darmkanker komen, overweldigend hetgeen een functionele interpretatie zeer moeilijk maakt. Om dit probleem te omzeilen hebben we gekeken naar evolutionair geconserveerde targetgenen door darmtumoren van FAP-patiënten (d.w.z. dragers van kiembaan APC-mutaties) te vergelijken met *Apc*<sup>+/1638N</sup> darmtumoren van de muis (**Hoofdstuk 5**). Deze vergelijking tussen twee species leverde een lijst van 166 geconserveerde genen op die betrokken zijn bij tumorvorming. In deze lijst komen verscheidene targets van het Wnt-pathway voor, die al eerder zijn beschreven. In hetzelfde onderzoek melden we een grote overeenkomst tussen de expressie profielen van APC- en MYH-mutante poliepen. Slechts 49 genen blijken differentieel tot expressie te komen. Deze genen hebben een verbeterd onderscheidend vermogen om de twee soorten patiënten te classificeren, hetgeen de toegevoegde waarde van deze aanpak, als een instrument om de meer functioneel relevante genen uit complexe microarray profiling data te kunnen identificeren, benadrukt.

Haploinsufficiëntie kan gezien worden als een mechanisme dat aan de basis ligt van veranderingen in de dosering van genexpressie. Het is aangetoond dat het tumorsuppressorgen *SMAD4*, een belangrijke component van de TGF- $\beta$  en BMP paden, tumorformatie initieert in een tweede vorm van

erfelijke darmkanker, juvenile polyposis syndrome (JPS), zonder dat hierbij het wildtype allel verloren gaat (**Hoofdstuk 6**). In ES cellijnen, waarin targeted *Smad4*-mutante allelen voorkomen, was de expressie van het Smad4-eiwit direct gecorreleerd met het gen copy nummer. Middels reporter assays voor de TGF- $\beta$  en BMP paden hebben we aangetoond dat progressief toegenomen Smad4-eiwitniveaus de intensiteit van de signaleringsactiviteit van beide paden beïnvloeden. De door haploinsufficiëntie uitgelokte gentranscriptie effecten werden met behulp van expression profiling geëvalueerd waarbij een set van doseringsafhankelijke targetgenen aan het licht kwam. Ons onderzoek geeft informatie over de moleculaire mechanismen die aan de basis liggen van *Smad4* (en *Apc*, zie **Hoofdstuk 3**) haploinsufficiëntie en draagt zodoende bij aan een beter begrip van de invloed van gendoseringen op tumorvorming.

Concluderend, het werk dat in dit proefschrift wordt gepresenteerd komt overeen met onze oorspronkelijke hypothese (**Hoofdstuk 1**) waarin wij stellen dat de volwassen stamcel niches door specifieke dosering van signaleringsactiviteit worden gereguleerd en afgestemd. Veranderingen in het niveau van signalering leidt tot expansie van het stamcel compartiment door vermeerdering van zelfvernieuwing of door het onderdrukken en herschakelen van het differentiëringsprogramma. De volgende uitdaging is te komen tot een beter begrip van de wijze waarop specifieke verlaagde genexpressie niveaus bijdragen aan tumorontwikkeling.



# Acknowledgements

*Friends should be forever but not always that happens and distance surely puts friendships to the test. My great friends: Ana Afonso, Teresa and Ana Henriques who have managed to put up with my short visits and have always managed to find sometime to catch up with me: It is great to have friends like you. Luis, I know I have been a pain in the last weeks, in between a 1000 sms and phone calls we managed to do the layout of the thesis. Thank you for your help!*

*Within the nine years I spent in Holland many people have crossed my path and acknowledging everyone's contribution and friendship is a daunting task. The work here described could not have been performed if it wasn't for the help of my colleagues and collaborators throughout these years. To all the collaborators: Iris Nagtegaal, Jan de Boer, Ram Siddappa, Jonathan Coxhead, Martin van der Valk Henk van Kranen and Yavuz Ariyurek it was a pleasure to work with you. Marco and Alex your stay in Holland was short but fun! Next time we should meet in Portugal, I'm sure there is a Witte Aap alike somewhere in town ;-)*

*The Leiden group: Juul, Ada, Shantie, Heleen and Paul we have shared many laughs during the coffee breaks and your friendly smile has always made me feel welcome in Holland. I do miss all the time we spent together outside of the lab skating, sailing, karting and skiing. It was great fun. Menno you have guided me in the very first months in the lab, discussing with you was always a challenge. Ron, you have been a very patient teacher who introduced me to the mouse work/world. More than that, you have also been a friend wondering through the streets of Leiden on Friday nights looking for a restaurant that would still serve a meal. Peter after knowing you, mess had a different meaning for me ;-)* If only I knew that a bet would have been enough to make you keep everything clean we could have avoided all the avalanches from your desk onto mine. Maybe we should have another bet so that I will come to Edinburgh to visit you ;-)

*The Rotterdam group: Ingrid, Jos, Lau, Petra, Brechtje, Yaser, Hang, Rubina, Mieke, Andrea, Ivana and Celia thank you for your help and for making work in the lab a daily pleasure. I will miss you all. Marieke, thanks for your extra effort in these last months to make sure that I comply with all the PhD rules. Mehrnaz, you have been great, Lady I owe you big time. Do you think I can have Blacky back, now?*

*Paola and Joana we have spent wonderful years together. In the lab we formed a great team, they could start a new TV series: "Desperate LCMwives". If it wasn't for our small support group, I don't know how we would have maintained our mental sanity ;-)* I have had the opportunity to work, learn and exchange ideas with both of you but the thing I will forever remember is all the time spent together outside of the lab.



*Paolinha, you have always been there for the good and bad moments with a friendly smile. My greatest adventure was to go with you on a sailing holiday. Me, you and a bunch of Italians in a boat having fun, sailing together with dolphins, enjoying a glass of wine at sunset, looking at the stars, listening to the same music for a week. I'm glad that we took this journey together because I got to know the "non-German" side of Paola ;-) Your departure from Holland was difficult to handle... I will miss you.*

*Joana, we were off to a rough start but I believe that without that period our friendship wouldn't have become as solid as it is now. I'm glad we could forgive and forget because behind that tough appearance lies a great friend. I will forever remember the day little David was born. Now that we are again living in the same city I'm sure we will see each other much more often, and laugh about the period we spent together in Holland.*

*Lia, you have been a great help in the accomplishment of this thesis. In between all the IP's, FACS, Affy experiments and many other things we still managed to have a good time. You, Joris and Jasper have been also part of my little "Ducth family" and I hope you return soon to Portugal, I'm sure Jasper would like to see it from a different perspective;-)*

*Delila, if I have to think of anything good that happened during that week in November is that I finally realised how great you are. You stood by me in one of the most difficult days of my life. I wish we could have been friends for a longer time.* 157

*Joana and Sabrina, the Grey's Anatomy Club was just another excuse for us to spend more time together, have some good laughs and enjoy nice food. Sabrina, I will miss your friendly smile and the "Hey Lady" every morning in the office. It was nice to have someone else also complaining about things in the lab ;-)*

*Joana, you have been my best pal for the last years. Dinners, coffees, apple strudels, Coupling episodes, cinema sessions are just a glimpse of how much we have done together. I have really enjoyed your company and my only wish is that you come back to Lisbon quickly (Sorry, Riccardo!!). I also want to thank you for all your devotion to the project, the late hours and weekends that we worked together to accomplish this goal. You have made a great contribution for the completion of this thesis.*

*Renée, you might not believe me but I will miss the Friday afternoons I have spent with you discussing statistics. I have learnt a lot but most importantly, you have helped me to overcome the "fear" and scepticism I had about statistics. I'm sorry for all the afternoons I made you explain ten times in a row the same thing. Fortunately, what started as a work relationship has quickly become a good friendship.*

*An extra word to both Joanas, Sabrina, Renée and Delila. As good friends, you have been there for me and Tommy when we most needed you. I have no words to*

*express my gratitude for your support during those weeks.*

*My paranymphs, Cor and Patrick, I'm sorry for having given to you this extra burden ;-). Cor, it has now been five years since we worked together and I still haven't found someone with as sharp comments as yours in the lab ;-). I do miss you, not only because I liked working with you but I also miss our conversations. Patrick, we started in the lab more or less at the same time and quickly became friends. I lost track on how many hours we have spent behind the microscope together. Without your hard work and willingness to help, my PhD would really not have been the same. Thank you for being there and for being who you are!*

*After nine years working in the Netherlands many people have crossed my path and have contributed to make my years abroad richer and I will forever remember you. To all of you I have only one request: "Keep in touch!"*

*Riccardo, you have welcomed me the very first night I arrived in Holland. Throughout these years you have been more than The Boss, you've been a friend and in many ways part of my family. You, Monique, Marco and Iosto have hosted and welcomed me into your house, I will be forever grateful to all of you for the months I could live with you. Your enthusiasm and passion for science have been an inspiration, working with you was a privilege but above all I will miss your friendship.*

*Miguel, all these years in Holland would have not been the same without your virtual support ;-). (phone companies have made a fortune with us). You have never tried to stop me from chasing this dream even when four years turned into nine years. Although, sometimes you felt otherwise you have always encouraged me to do my best no matter how much longer it would take. Thank you for all your love and understanding.*

*Finally, a few words to my parents who have always stood by me and fully supported my decisions...*

*Acima de tudo quero agradecer aos meus pais, que sempre me incentivaram a querer ver e aprender coisas novas e a enfrentar os desafios da vida. Do dia em que parti de Portugal recordarei para sempre as vossas palavras de incentivo e conforto. Mesmo nos últimos anos, em que a vida nem sempre vos sorriu, o vosso apoio, carinho e compreensão esteve sempre presente. Muito obrigado por tudo o que fizeram por mim, todos os pais deveriam ser assim.*



# *Curriculum vitae*



## Personal data

**Name:** Cláudia Sofia Cardoso Gaspar  
**Birth date:** 27/03/1974  
**Nationality:** Portuguese

## Academic Degree

**September 1997** Faculty of Sciences, University of Lisbon. Degree in Biology, Microbiology and Genetics.

## Professional Experience

**November 2003 to present** Post-doc position at the Josephine Nefkens Institute, Erasmus University Rotterdam. Scientific supervisor: Prof. Riccardo Fodde.

**November 1999 to October 2003** PhD student at Leiden University Medical Center, Human Genetics Department. Project: "Identification of downstream target genes of the wnt pathway and their role in tumorigenesis". Scientific supervisor: Prof. Riccardo Fodde.

**September 1997 to October 1999** Instituto Portugues de Oncologia de Francisco Gentil, Lisbon, Portugal. Project: "Hereditary colorectal carcinoma in the south of Portugal". Scientific supervisor: Dr. Marília Cravo, M.D.

## Awards

**2002** AACR Scholar in training award.  
**1997** Rhône Poulenc Rorer award in Oncology - P Lage, M Cravo, C Albuquerque, T Gomes, I Claro, P Chaves, C Gaspar, P Fidalgo, J Soares, F Costa Mira, C Nobre Leitão. "Instabilidade de microssatélites em carcinomas do cólon e recto esporádicos: valor na detecção de novos casos de síndromes hereditários."

## List of Publications

1. Alberici P, **Gaspar C**, Franken P, Gorski MM, de Vries I, Scott RJ, Ristimäki A, Aaltonen LA, Fodde R. Smad4 haploinsufficiency: a matter of dosage. *Pathogenetics*. 2008 Nov 3;1(1):2.
2. Siddappa R, Martens A, Doorn J, Leusink A, Olivo C, Licht R, van Rijn L, **Gaspar C**, Fodde R, Janssen F, van Blitterswijk C, de Boer J. cAMP/PKA pathway activation in human mesenchymal stem cells in vitro results in robust bone formation in vivo. *Proc Natl Acad Sci U S A*. 2008 May 20;105(20):7281-6.
3. **Gaspar C**, Cardoso J, Franken P, Molenaar L, Morreau H, Möslin G, Sampson J, Boer JM, Menezes R, Fodde R. Cross-species comparison of human and mouse intestinal polyps reveals conserved mechanisms in adenomatous polyposis coli (*APC*)-driven tumorigenesis. *Am J Pathol*. 2008 May;172(5):1363-80.
4. Janssen KP, Alberici P, Fsihi H, **Gaspar C**, Breukel C, Franken P, Rosty C, Abal M, El Marjou F, Smits R, Louvard D, Fodde R, Robine S. APC and oncogenic KRAS are synergistic in enhancing Wnt signaling in intestinal tumor formation and progression. *Gastroenterology*. 2006 Oct;131(4):1096-109.
5. Nagtegaal ID, **Gaspar CG**, Peltenburg LT, Marijnen CA, Kapiteijn E, van de Velde CJ, Fodde R, van Krieken JH. Radiation induces different changes in expression profiles of normal rectal tissue compared with rectal carcinoma. *Virchows Arch*. 2005 Feb;446(2):127-35.
6. Nagtegaal I, **Gaspar C**, Marijnen C, Van De Velde C, Fodde R, Van Krieken H. Morphological changes in tumour type after radiotherapy are accompanied by changes in gene expression profile but not in clinical behaviour. *J Pathol*. 2004 Oct;204(2):183-92.
7. **Gaspar C**, Fodde R. APC dosage effects in tumorigenesis and stem cell differentiation. *Int J Dev Biol*. 2004;48(5-6):377-86.
8. de Boer J, Siddappa R, **Gaspar C**, van Apeldoorn A, Fodde R, van Blitterswijk C. Wnt signaling inhibits osteogenic differentiation of human mesenchymal stem cells. *Bone*. 2004 May;34(5):818-26.
9. Kielman MF, Rindapaa M, **Gaspar C**, van Poppel N, Breukel C, van Leeuwen S, Taketo MM, Roberts S, Smits R, Fodde R. Apc modulates embryonic stem-cell differentiation by controlling the dosage of beta-catenin signaling. *Nat Genet*. 2002 Dec;32(4):594-605.



10. Fodde R, Kuipers J, Rosenberg C, Smits R, Kielman M, **Gaspar C**, van Es JH, Breukel C, Wiegant J, Giles RH, Clevers H. Mutations in the APC tumour suppressor gene cause chromosomal instability. *Nat Cell Biol.* 2001 Apr;3(4):433-8.
11. Fidalgo P, Almeida MR, West S, **Gaspar C**, Maia L, Wijnen J, Albuquerque C, Curtis A, Cravo M, Fodde R, Leitao CN, Burn J. Detection of mutations in mismatch repair genes in Portuguese families with hereditary non-polyposis colorectal cancer (HNPCC) by a multi-method approach. *Eur J Hum Genet.* 2000 Jan;8(1):49-53.
12. Cravo M, Lage P, Albuquerque C, Chaves P, Claro I, Gomes T, **Gaspar C**, Fidalgo P, Soares J, Nobre-Leitao C. BAT-26 identifies sporadic colorectal cancers with mutator phenotype: a correlative study with clinico-pathological features and mutations in mismatch repair genes. *J Pathol.* 1999 Jul;188(3):252-7.
13. Cravo ML, Fidalgo PO, Lage PA, Albuquerque CM, Chaves PP, Claro I, Gomes T, **Gaspar C**, Soares JO, Nobre-Leitao C. Validation and simplification of Bethesda guidelines for identifying apparently sporadic forms of colorectal carcinoma with microsatellite instability. *Cancer.* 1999 Feb 15;85(4):779-85.
14. Claro I, Cravo M, Gloria L, **Gaspar C**, Albuquerque C, Lage P, Fidalgo P, Ramalho E, Chaves P, Cardoso P, Nobre Leitao C. Colonic cancer in a 34-yr-old woman: should it prompt microsatellite instability studies and mismatch repair gene testing? *Am J Gastroenterol.* 1998 Oct;93(10):1991-2.



# PhD Portfolio



## PhD Portfolio Summary

### Summary of PhD training and teaching activities

<b>Name PhD student:</b> Claudia Sofia Cardoso Gaspar <b>Erasmus MC Department:</b> Pathology <b>Research School:</b> Medisch-Genetisch Centrum Zuid-West Nederland (MGC) and Erasmus Postgraduate School Molecular Medicine (MolMed).	<b>PhD period:</b> November 1999 to February 2009 <b>Promotor(s):</b> Prof.dr. Riccardo Fodde <b>Supervisor:</b> Prof.dr. Riccardo Fodde	
<b>1. PhD training</b>		
	<b>Year</b>	<b>Workload (Hours/ECTS)</b>
<b>General academic skills</b> - Laboratory animal science	2000	80h
<b>Research skills</b> - Statistics, Leiden	2003	20h
<b>In-depth courses (e.g. Research school, Medical Training)</b> - In vivo imaging; from cell to organism. - Course Ensembl. - Transgenesis, Gene targeting and gene therapy. - Oncogenesis and tumor biology. - Signal Transduction.	2004 2004 2001 2000 2000	31h 8h 40h 30h 40h
<b>Presentations</b> - “MaSCs vs. MaCSCs similarities and differences”. BSIK. Rotterdam, Netherlands. - “Apc1572T: a mouse model encoding for Wnt/b-catenin signalling dosages affecting mammary but not intestinal stem cell homeostasis and malignancy”. International Workshop on Cancer Stem Cells 2 <sup>nd</sup> edition. Milan, Italy. - “Wnt activated stem cells in colon and breast cancer”. BSIK. Rotterdam, Netherlands. - “Wnt/b-catenin signalling dosages and organ specific tumorigenesis: a cancer stem cell effect?”. Keystone Symposia: “Molecular Regulation of Stem Cells”. Banff, Canada. - “Generation and characterization of two new mouse models for FAP: Apc1572T and Apc1572N”. 4 <sup>th</sup> Joint Meeting Leeds Castle Polyposis Group and International Collaborative Group Hereditary Non-Polyposis Colorectal Cancer. Cleveland, Ohio, USA. - “Dosage effects of Apc mutations on $\beta$ -catenin signal transduction measured by expression profiling”. AACR – 93 <sup>rd</sup> Annual meeting. San Francisco, California. - “Identification of the downstream targets of the APC/ $\beta$ -catenin signal transduction pathway”. 3 <sup>rd</sup> Joint Meeting Leeds Castle Polyposis Group and International Collaborative Group Hereditary Non-Polyposis Colorectal Cancer. Venice, Italy.	2008 2007 2006 2005 2003 2002 2001	24h 24h 24h 24h 24h 24h 24h

<b>International conferences</b>		
- Stem Cells, Development and Regulation, Amsterdam.	2008	
- International Workshop on Cancer Stem Cells 2 <sup>nd</sup> edition. Milan, Italy.	2007	
- Keystone Symposia: "Molecular Regulation of Stem Cells". Banff, Canada.	2005	
- 4 <sup>th</sup> Joint Meeting Leeds Castle Polyposis Group and International Collaborative Group Hereditary Non-Polyposis Colorectal Cancer. Cleveland, Ohio, USA.	2003	
- AACR – 93 <sup>rd</sup> Annual meeting. San Francisco, California.		
- Wnt signalling in development and cancer, Amsterdam.	2002	
- 3 <sup>rd</sup> Joint Meeting Leeds Castle Polyposis Group and International Collaborative Group Hereditary Non-Polyposis Colorectal Cancer. Venice, Italy.	2002	
	2001	
<b>Seminars and workshops</b>		
- ICRF-MGC Graduate student workshop, Oxford, UK	2000	24
- 2 <sup>nd</sup> joint ICRF-MGC Graduate student Colloquium, Bruges, Belgium	2001	24
<b>2. Teaching activities</b>		
	<b>Year</b>	<b>Workload (Hours/ECTS)</b>
<b>Lecturing</b>		
- Euroconference on Animal Models of Human Diseases. Sesimbra, Portugal: "Expression profiling in cancer research".	2001	48h
- ErasmusMC Molecular Medicine Master of Science: "Apc dosage effects in differentiation"	2005	24h
<b>Supervising practicals and excursions</b>		
- Practical supervision on mutational analysis. Leiden University	2002	4h
- Practical supervision on the use of the bioinformatic tool: RasMol.	2002	150h

